

Contrails

Unclassified

SECURITY CLASSIFICATION OF THIS PAGE (When Data Entered)

REPORT DOCUMENTATION PAGE		READ INSTRUCTIONS BEFORE COMPLETING FORM
1. REPORT NUMBER AFFDL-TR-79-3069 Volume I	2. GOVT ACCESSION NO.	3. RECIPIENT'S CATALOG NUMBER
4. TITLE (and Subtitle) New Remotely Piloted Vehicle Launch and Recovery Concepts - Analysis, Preliminary Design and Performance/Cost Trade Studies	5. TYPE OF REPORT & PERIOD COVERED Technical - Final March 1978- March 1979	
	6. PERFORMING ORG. REPORT NUMBER	
7. AUTHOR(s) S. J. Baumgartner R. F. Yurczyk J. G. Brister V. K. Rajpaul	8. CONTRACT OR GRANT NUMBER(s) F33615-78-C-3404	
9. PERFORMING ORGANIZATION NAME AND ADDRESS Boeing Aerospace Company P. O. Box 3999 Seattle, Washington 98124	10. PROGRAM ELEMENT, PROJECT, TASK AREA & WORK UNIT NUMBERS 2402-01-08	
11. CONTROLLING OFFICE NAME AND ADDRESS Air Force Flight Dynamics Laboratory (FEMB) Wright-Patterson AF Base, Ohio 45433	12. REPORT DATE June 1979	
	13. NUMBER OF PAGES 236	
14. MONITORING AGENCY NAME & ADDRESS (if different from Controlling Office)	15. SECURITY CLASS. (of this report) Unclassified	
	15a. DECLASSIFICATION/DOWNGRADING SCHEDULE	
16. DISTRIBUTION STATEMENT (of this Report) Approved for public release; distribution unlimited		
17. DISTRIBUTION STATEMENT (of the abstract entered in Block 20, if different from Report)		
18. SUPPLEMENTARY NOTES		
19. KEY WORDS (Continue on reverse side if necessary and identify by block number) Air Cushion Landing System Dynamic Analysis Air Bag Skid Launch EASY Program Recovery RPV		
20. ABSTRACT (Continue on reverse side if necessary and identify by block number) Dynamic analysis, preliminary design, and performance/cost trade studies of air bag skid and air cushion concepts for launch and recovery of Boeing and Rockwell advanced RFV concepts have been conducted. Dynamic analysis was performed using the six degree-of-freedom computer program EASY. Dynamic simulations included perturbations to steady state flight, landing, and takeoff simulations. Launch and recovery concepts investigated were air bag skid system, air cushion recovery systems, integrated air cushion system, and air cushion launch platform. Performance/cost trade study factors investigated were complexity, fuel require-		

DD FORM 1 JAN 73 1473 EDITION OF 1 NOV 65 IS OBSOLETE

SECURITY CLASSIFICATION OF THIS PAGE (When Data Entered)

Approved for Public Release

ABSTRACT (Continued)

ments, adverse weather capability, ground equipment and facility requirements, survivability/vulnerability, reliability and maintainability, and system acquisition and life cycle costs. Results of the study indicated that an air cushion system is a feasible means of recovery of an RPV such as the Boeing and Rockwell ARPV concepts. An air bag skid with an arrestor system is a feasible approach when minimum field length is a major design factor. Integrated air cushion systems for launch and recovery are greatly affected by engine characteristics. In each case, the launch and recovery systems are shown to be an integral part of the total vehicle design and strongly influences the airframe design.

FOREWORD

This report describes research work performed by The Boeing Company, Boeing Military Airplane Development, Seattle, Washington, for the Air Force Flight Dynamics Laboratory, Air Force Wright Aeronautical Laboratories, Wright-Patterson Air Force Base, Ohio. The program was funded by the Laboratory Director's Fund under Contract F33615-78-C-3404, Project 2402. Project engineers for the contract were Peters Skele and Lt. David L. Fischer, AFFDL/FEM. This research work is part of an effort to obtain new launch and recovery concepts for improving the effectiveness of remotely piloted vehicles. This report is in two volumes:

- I Analysis, Preliminary Design and Performance/Cost Trade Studies
- II Computer Program Listings

The work reported herein was performed during the period 15 March 1978 to 15 March 1979, and the report was submitted 16 April 1979.

Vinod K. Rajpaul served as the program manager. Roger F. Yurczyk was principal investigator for the technical work, assisted by Steven J. Baumgartner and James G. Brister. Other members of the Boeing Military Airplane Development assisting in this investigation included Daniel Tracy, Phil Gotlieb, Peter Milns, Ralph Rankin, John Munnis, Robert Brown, Richard Newton, Theresa Gnagy and Jeanne Owens.

Contrails

TABLE OF CONTENTS

SECTION	PAGE
I INTRODUCTION	1
1. OBJECTIVE	4
2. BACKGROUND	6
3. SCOPE AND GENERAL APPROACH	8
II DYNAMIC SIMULATIONS AND ANALYSIS	12
1. INFLIGHT SIMULATIONS AND ANALYSIS	12
a. Development of Math Models	12
(1) Air Vehicle Configurations	12
(2) Air Vehicle Mass Properties	13
(3) Aerodynamic Characteristics	13
(4) Program EASY Air Vehicle Models	21
b. Boeing ARPV Inflight Simulations	21
c. Rockwell ARPV Inflight Simulations	29
d. Conclusions of Inflight Simulations	36
2. LANDING SIMULATIONS AND ANALYSIS	43
a. Development of Math Models	43
(1) Touchdown Conditions	44
(2) Inelastic Air Cushion Recovery Trunk Design	44
(3) Air Bag Skid Design	52
(4) Air Supply System	52
(5) Suction Braking	74
(6) Arrestment Systems	76
(7) Other Characteristics of the Landing Math Models	76
b. Landing Simulation Results	80
(1) Boeing ARPV Landing Simulations	82
(2) Rockwell ARPV (Inelastic) Landing Simulations	116
(3) Rockwell ARPV (Elastic) Landing Simulations	140
c. Landing Simulation Conclusions	147

Contracts

TABLE OF CONTENTS (cont'd.)

SECTION	PAGE
II	
3. TAKEOFF SIMULATIONS AND ANALYSIS	153
a. Development of Math Models	154
(1) Air Supply Systems	154
(2) Air Cushion Takeoff Trunk	155
(3) Launch Platform	157
b. Takeoff Simulation Results	160
(1) Rockwell ARPV with Air Cushion Launch Platform	160
(2) Rockwell ARPV with Inelastic IACS	160
(3) Rockwell ARPV with Elastic IACS	167
c. Takeoff Simulation Conclusions	174
III PRELIMINARY DESIGN	175
1. BOEING ARPV RECOVERY SYSTEM CONCEPTS	175
a. Boeing ABSS Configuration	175
b. Boeing ACRS Configuration	181
2. ROCKWELL ARPV LAUNCH AND RECOVERY SYSTEM CONCEPTS	187
a. Rockwell ACLP (Launch) and ACRS (Recovery)	187
b. Rockwell IACS	199
IV PERFORMANCE/COST ANALYSIS	210
1. ANALYSIS	210
a. Complexity	210
b. Fuel Requirements	214
c. Adverse Weather Capability	217
d. Ground Equipment and Facility Requirements	219
e. Survivability/Vulnerability	219
f. Reliability and Maintainability	227
g. System Acquisition and Life Cycle Costs	230
V CONCLUSIONS	232
VI RECOMMENDATIONS	235
REFERENCES	236

LIST OF ILLUSTRATIONS

FIGURE		PAGE
1	Boeing ARPV Baseline Recovery System	2
2	Rockwell ARPV Baseline Recovery System	3
3	Configuration Combinations Evaluated	10
4	Rockwell Baseline ARPV	14
5	Rockwell ARPV Air Cushion Trunk Installation	15
6	Boeing Baseline Vehicle	16
7	Block Diagram of Program EASY Math Models for Boeing and Rockwell ARPVs	22
8	Root Locus Plot Showing Lateral and Longitudinal Modes for the Boeing ARPV without SAS	24
9	Program EASY Optimal Controller Characteristics	28
10	Boeing ARPV with ACRS Deployed at Landing Approach, Response of Optimal Controller to 15 Ft/Sec Sharp Edged Gust at 5 Seconds	30
11	Boeing ARPV with ACRS Deployed at Landing Approach, Response of Optimal Controller to 15 Ft/Sec Sharp Edged Gust at 5 Seconds	31
12	Boeing ARPV with ACRS Deployed, Landing Approach Trim with No Crosswind, Air Vehicle Attitude vs. Sink Rate	32
13	Boeing ARPV with ACRS Deployed, Landing Approach Trim with 20 Ft/Sec Crosswind, Air Vehicle Attitude vs. Sink Rate	33
14	Boeing ARPV with ABSS Deployed, Landing Approach Trim with No Crosswind, Air Vehicle Attitude vs. Sink Rate	34
15	Root Locus Plot Showing Lateral and Longitudinal Modes for the Rockwell ARPV without SAS	35
16	Rockwell ARPV with ACRS Deployed at Landing Approach, Response of Optimal Controller to Displacement From Glide Path, Flight Spoiler Position vs. Time	37

LIST OF ILLUSTRATIONS (cont'd.)

FIGURE		PAGE
17	Rockwell ARPV with ACRS Deployed at Landing Approach, Response of Optimal Controller to Displacement From Glide Path, Roll Angle vs. Time	38
18	Rockwell ARPV with ACRS Deployed at Landing Approach, Response of Optimal Controller to Displacement From Glide Path, Pitch Angle vs. Time	39
19	Rockwell ARPV with ACRS Deployed at Landing Approach, Response of Optimal Controller to Displacement From Glide Path, Yaw Angle vs. Time	40
20	Rockwell ARPV with ACRS Deployed at Landing Approach, Response of Optimal Controller to Displacement From Glide Path, Lateral Displacement From Glide Path vs. Time	41
21	Rockwell ARPV with ACRS Deployed, Landing Approach Trim with No Crosswind, Air Vehicle Attitude vs. Sink Rate	42
22	Boeing ARPV with Wide Stance ACRS Installation	47
23	Boeing Vehicle with Baseline Air Cushion Configuration	48
24	Rockwell Vehicle with Baseline Air Cushion Configuration	49
25	Relationship Between Friction Coefficient and Trunk Lubrication Flow	50
26	Boeing Vehicle with Baseline Air Bag Skid Configuration	53
27	Rockwell Vehicle with Baseline Air Bag Skid Configuration	54
28	Teledyne CAE-373 Turbojet Engine for Boeing ARPV	55
29	Boeing ARPV Electrical Load Profile	55
30	CAE-373 Performance with Bleed Air	58
31	Model TD-530 Ejector Nozzle	60
32	Model TD-457 Tip Turbine Fan	61

LIST OF ILLUSTRATIONS (cont'd.)

FIGURE		PAGE
33	Air Augmentation Ratio as a Function of Drive Pressure for Fan and Ejector with Various Back Pressures	62
34	Performance Ratio as a Function of Back Pressure for Fan and Ejector at Various Drive Pressures	63
35	Pressure-Flow Characteristics for Boeing ARPV with ACRS	64
36	Total Air Mass Flow Rate Into Plenum Chamber as a Function of Back Pressure for Various Ejector Drive Pressures	66
37	Inlet and Drive Air Flow Rates as a Function of Ejector Drive Pressure with Ambient Back Pressure	67
38	Basic Engine Assembly for Rockwell ARPV	68
39	Maximum Power Extraction for J85-GE-4 Engine	69
40	Maximum Bleed Air for J85-GE-4 Engine	69
41	J85-GE-4 Performance with Bleed Air	73
42	Fan Pressure-Flow Characteristics	75
43	Schematic Arrangement - Rotary Hydraulic Arresting System	77
44	Water Twister Arresting System	78
45	Baseline Air Bag Model for Boeing ARPV	83
46	Air Bag Geometry	84
47	Air Bag Geometry for Boeing ARPV with Baseline ABSS, Y0 vs. Z0	85
48	Air Bag Geometry for Boeing ARPV with Baseline ABSS, L1 vs. Z0	86
49	Air Bag Geometry for Boeing ARPV with Baseline ABSS, L3 vs. Z0	87
50	Boeing ARPV with ABSS, 3 DOF Landing Simulations, Air Bag Length vs. Acceleration and Clearances	90
51	Boeing ARPV with ABSS, 3 DOF Landing Simulations, Air Bag Diameter vs. Acceleration and Clearances	91
52	Boeing ARPV with ABSS, 3 DOF Landing Simulations, Relief Valve Cracking Pressure vs. Sink Rate	92

Contrails

LIST OF ILLUSTRATIONS (cont'd.)

FIGURE		PAGE
53	Boeing ARPV with ABSS, 3 DOF Landing Simulations, Air Bag Pressure vs. Sink Rate	93
54	Boeing ARPV with ABSS, 3 DOF Landing Simulations, Maximum Acceleration vs. Sink Rate	95
55	Boeing ARPV with ABSS, Landing Trim Conditions and Touchdown Constraints	96
56	Boeing ARPV with ABSS, 6 DOF Landing Simulation without Arrestment, Acceleration vs. Time	99
57	Boeing ARPV with ABSS, 6 DOF Landing Simulation without Arrestment, Roll Angle vs. Time	100
58	Boeing ARPV with ABSS, 6 DOF Landing Simulation without Arrestment, Yaw Angle vs. Time	101
59	Boeing ARPV with ABSS, 6 DOF Landing Simulation with Arrestment, Acceleration vs. Time	102
60	Boeing ARPV with ABSS, 6 DOF Landing Simulation with Arrestment, Yaw Angle vs. Time	103
61	Baseline Air Cushion Model for Boeing ARPV	105
62	Trunk Geometry for Boeing ARPV with Baseline ACRS, Z0 vs. Z0/ZOFS	106
63	Trunk Geometry for Boeing ARPV with Baseline ACRS, Y0 vs. Z0/ZOFS	107
64	Trunk Geometry for Boeing ARPV with Baseline ACRS, L1 vs. Z0/ZOFS	108
65	Trunk Geometry for Boeing ARPV with Baseline ACRS, L3 vs. Z0/ZOFS	109
66	Boeing ARPV with ACRS, 3 DOF Landing Simulations, Maximum Acceleration vs. Sink Rate	111
67	Boeing ARPV with ACRS, Landing Trim Conditions and Touchdown Constraints	112
68	Boeing ARPV with ACRS, 3 DOF Landing Simulations, Clearances vs. Pitch Angle	113

LIST OF ILLUSTRATIONS (cont'd.)

FIGURE		PAGE
69	Boeing ARPV with ACRS, 3 DOF Landing Simulations, Distance Between Trunk C.P. and Vehicle C.G. vs. Acceleration and Clearances	115
70	Landing Runout Distance for Boeing ARPV with ACRS	117
71	Baseline Air Bag Model for Rockwell ARPV	119
72	Air Bag Geometry for Rockwell ARPV with Baseline ABSS, Y0 vs. Z0	120
73	Air Bag Geometry for Rockwell ARPV with Baseline ABSS, L1 vs. Z0	121
74	Air Bag Geometry for Rockwell ARPV with Baseline ABSS, L3 vs. Z0	122
75	Rockwell ARPV with ABSS, 3 DOF Landing Simulations, Air Bag Length vs. Acceleration and Clearances	123
76	Rockwell ARPV with ABSS, 3 DOF Landing Simulations, Air Bag Pressure vs. Sink Rate	124
77	Rockwell ARPV with ABSS, 3 DOF Landing Simulations, Clearances vs. Pitch Angle	126
78	Rockwell ARPV with ABSS, 3 DOF Landing Simulations, Maximum Acceleration vs. Sink Rate	127
79	Rockwell ARPV with ABSS, Landing Trim Conditions and Touchdown Constraints	128
80	Baseline Air Cushion Model for Rockwell ARPV	129
81	Trunk Geometry for Rockwell ARPV with Baseline ACRS, Z0 vs. Z0/ZOFS	130
82	Trunk Geometry for Rockwell ARPV with Baseline ACRS, Y0 vs. Z0/ZOFS	131
83	Trunk Geometry for Rockwell ARPV with Baseline ACRS, L1 vs. Z0/ZOFS	132
84	Trunk Geometry for Rockwell ARPV with Baseline ACRS, L3 vs. Z0/ZOFS	133

LIST OF ILLUSTRATIONS (cont'd.)

FIGURE		PAGE
85	Trunk Meridian Dimensions for Rockwell ARPV with ACRS	135
86	Rockwell ARPV with ACRS, 3 DOF Landing Simulations, Clearances vs. Pitch Angle	136
87	Rockwell ARPV with ACRS, 3 DOF Landing Simulations, Maximum Acceleration vs. Sink Rate	137
88	Rockwell ARPV with ACRS, Landing Trim Conditions and Touchdown Constraints	138
89	Landing Runout Distance for Rockwell ARPV with ACRS	139
90	Elastic IACS Model for Rockwell ARPV	142
91	Elastic Trunk Load/Deflection Curves Used in Dynamic Analysis	143
92	Rockwell ARPV with IACS (Elastic), 3 DOF Landing Simulations, Clearances vs. Pitch Angle	144
93	Rockwell ARPV with IACS (Elastic), 3 DOF Landing Simulations, Maximum Acceleration vs. Sink Rate	145
94	Rockwell ARPV with Elastic IACS, Touchdown Constraints	146
95	Rockwell ARPV with IACS (Elastic), 6 DOF Landing Simulations, Relief Valve Cracking Pressure vs Acceleration and Clearances	148
96	Rockwell ARPV with IACS (Elastic), 6 DOF Landing Simulation with Arrestment, Vehicle Acceleration vs. Time	149
97	Rockwell ARPV with IACS (Elastic), 6 DOF Landing Simulation without Arrestment, Vehicle Acceleration vs. Time	150
98	Rockwell Air Cushion Launch Platform	158
99	Launch Platform Trunk Model for Rockwell ARPV	161
100	Rockwell ARPV with ACLP (Inelastic), 3 DOF Takeoff Simulation, Vehicle Forward Velocity vs. Time	162
101	Rockwell ARPV with ACLP (Inelastic), 3 DOF Takeoff Simulation, Vehicle Pitch Angle vs. Time	163

LIST OF ILLUSTRATIONS (cont'd.)

FIGURE		PAGE
102	Rockwell ARPV with ACLP (Inelastic), 3 DOF Takeoff Simulation, Vehicle C.G. Altitude vs. Time	164
103	Stability Analysis Results for EASY Model of Jindivik with Inelastic Trunk	165
104	Inelastic IACS Model for Rockwell ARPV	166
105	Rockwell ARPV with IACS (Elastic), 6 DOF Takeoff Simulation, Vehicle Forward Velocity vs. Time	168
106	Rockwell ARPV with IACS (Elastic), 6 DOF Takeoff Simulation, Vehicle Pitch Angle vs. Time	169
107	Rockwell ARPV with IACS (Elastic), 6 DOF Takeoff Simulation, Vehicle C.G. Altitude vs. Time	170
108	Rockwell ARPV with IACS (Elastic), 6 DOF Takeoff Simulation, Trunk Pressure vs. Time	171
109	Rockwell ARPV with IACS (Elastic), 6 DOF Takeoff Simulation, Trunk Volume vs. Time	172
110	Rockwell ARPV with IACS (Elastic), 6 DOF Takeoff Simulation, Cushion Pressure vs. Time	173
111	Boeing ARPV with ABSS and Cool Gas Generator	176
112	Boeing ARPV with ABSS and Bleed Air	179
113	Boeing ABSS Assembly Build-up	180
114	Boeing ARPV with ACRS	182
115	Rockwell ARPV with ACRS	188
116	Rockwell ACRS Door Locking Mechanism Detail	189
117	Rockwell ACRS Assembly Build-up	191
118	Rockwell ACRS Dolly Wheel Installation	193
119	Rockwell Air Cushion Launch Platform	194
120	Rockwell ARPV with IACS	200
121	Thrust Vector Control System Concept	206

Contracts

LIST OF TABLES

TABLE		PAGE
1	Rockwell and Boeing ARPV Mass Properties	17
2	Stability Coefficients for Boeing Vehicle and ACRS	19
3	Stability Coefficients for Boeing Vehicle and ABSS	20
4	Stability Coefficients for Rockwell Vehicle and ACRS	25
5	Stability Coefficients for Rockwell Vehicle and ABSS	26
6	Variation of Landing Impact Conditions	45
7	Baseline ACRS Dimensions and Parameters	51
8	Baseline ABSS Dimensions and Parameters	56
9	Model CAE-373 Turbojet Engine Performance	57
10	J85-GE-4 Engine Performance	70
11	Accessory Drive Pad Characteristics for J85-GE-4 Engine	71
12	Arrestment System Parameters	79
13	Airplane to Ground Clearances Calculated by Program EASY During the Landing Simulations	81
14	Alternate Air Bag Skid Dimensions for Boeing ARPV	88
15	Baseline Rockwell IACS Dimensions and Parameters	156
16	Baseline Rockwell ACLP Dimensions and Parameters	159
17	Launch and Recovery System Design Parameters	177
18	Aircraft Installed Equipment for Boeing ARPV with ABSS with Cool Gas Generator	183
19	Aircraft Installed Equipment for Boeing ARPV with ABSS with Bleed Air	184
20	Aircraft Installed Equipment for Boeing ARPV with ACRS	186
21	Aircraft Installed Equipment for Rockwell ARPV with ACRS	195
22	Rockwell ACRS Weight Analysis	196
23	Rockwell ACLP Weight Analysis	198
24	Air Cushion Launch Platform Trade Study Results (4 sheets)	201
25	Aircraft Installed Equipment for Rockwell ARPV with IACS	208
26	Rockwell IACS Weight Analysis	209
27	Results of Complexity Analysis	212

LIST OF TABLES (cont'd.)

TABLE		PAGE
28	Results of Fuel Requirements Analysis	216
29	Launch and Recovery Site Dimensions and Area	220
30	Launch and Recovery Operation Sequence	221
31	Launch and Recovery Operation Sequence	222
32	Launch and Recovery Operation Sequence	223
33	Launch and Recovery Operation Sequence	224
34	Launch and Recovery Operation Sequence	225
35	Launch and Recovery Operation Sequence	226
36	Results of Reliability and Maintainability Analysis	229
37	System Acquisition and Life Cycle Cost	231

LIST OF ABBREVIATIONS AND SYMBOLS

ABSS	Air Bag Skid System
ACLP	Air Cushion Launch Platform
ACLS	Air Cushion Landing System
ACRS	Air Cushion Recovery System
AFFDL	Air Force Flight Dynamics Laboratory
Al	Aluminum
AMST	Advanced Medium STOL
AN/ALE-38	Chaff Dispenser Pod
API	Armor Piercing Incendiary
ARPV	Advanced Remotely Piloted Vehicle
APU	Auxiliary Power Unit
C.G.	Center of Gravity
C.P.	Center of Pressure
DATCOM	Data Compendium
Deg	Degree
Deg F	Degree Fahrenheit
DOF	Degree-of-Freedom
EQMO	Program EASY Subroutine
FEM	Vehicle Equipment Branch
Ft/sec	Feet per Second
GPS	Global Positioning System
HEI	High Explosive Incendiary
Hp	Horsepower
IACS	Integrated Air Cushion System
Kva	Kilovolt Amperes
Kw	Kilowatt
LCC	Life Cycle Cost
LRU	Line Replaceable Unit
MCBF	Mean Cycle Between Failure
Mm	Millimeter
MMH/FH	Maintenance Manhours per Flight Hour

LIST OF ABBREVIATIONS AND SYMBOLS (cont'd.)

MTBF	Mean Time Between Failure
O&S	Operating and Support
R&M	Reliability and Maintainability
RATO	Rocket Assist Takeoff
Rpm	Revolutions per Minute
RPV	Remotely Piloted Vehicle
SAS	Stability Augmentation System
S/C	Stability and Controllability
SPO	System Program Office
USAF	United States Air Force
ϕ	Roll Angle
θ	Pitch Angle
ψ	Yaw Angle
α	Angle of Attack
γ	Glide Slope Angle
μ	Coefficient of Friction
σ	Standard Deviation
\bar{P}	Vehicle Roll Rate
\bar{Q}	Vehicle Pitch Rate
\bar{U}	Vehicle X Axis Velocity
\bar{V}	Vehicle Y Axis Velocity

LIST OF PROGRAM EASY COMPONENTS

OC	Optimal Controller
IO	Inlet-Outlet
OL	Longitudinal Aerodynamic Model
DL	Lateral Aerodynamic Model
VA	Aerodynamic Variables from States
TK	Trunk (inelastic)
TS	Trunk (elastic)
AB	Air Bag Skid
EJ	Ejector
FR	Fan with Surge Analysis
DS	Six Degree-of-Freedom Rigid Body Dynamics
SG	Generalized Six Degree-of-Freedom Rigid Body Dynamics
TT	Two Degree-of-Freedom Rigid Body Dynamics
TL	Three Degree-of-Freedom Rigid Body Dynamics
TA	Tabular Functions of Time (4 outputs)
TB	Tabular Functions of Time (2 outputs)
S3	Sum Forces and Moments (3 sets of inputs)
S4	Sum Forces and Moments (4 sets of inputs)
MA	Multiply and Add
TR	Transform Vectors Body to Earth Axis
FU	Function Generator

SUMMARY

Current concepts of warfare call for remotely piloted vehicles (RPV) to perform certain tasks that have been performed by manned vehicles. The effectiveness of RPVs in performing these tasks depends, in part, on the effectiveness of the launch and recovery techniques employed. In fact, the launch and recovery system operation is a critical link in the total weapons system function.

Boeing and Rockwell, under contracts sponsored by the USAF Aeronautical Systems Division RPV SPO, studied many RPV configurations and launch and recovery system concepts in terms of mission requirements and life cycle costs. Because of multimission requirements, subjective weight factors given to some performance factors, and the degree of which site preparation, logistics, and vulnerability were considered, widely differing launch and recovery concepts were arrived at as being optimum for an advanced RPV system (ARPV). The Rockwell air vehicle is equipped with conventional landing gear which is used for takeoff and landing. The Boeing vehicle is launched from a zero length launcher with RATO and is recovered on air bag skids attached to the air vehicle. Both vehicles use a hook and cable arrestment system for recovery.

In the Boeing ARPV trade study document (Reference 1), it was noted that while the tail hook/arrestor cable and air bag skid system represents an attractive low life cycle cost concept, further investigation of the system dynamics would be required to fully validate the concept.

Another launch and recovery system that has been studied considerably in the past ten years is the air cushion system. Prototype systems have been built and tested for the Australian target drone, the Jindivik, and for the XC-8A Dehavilland Buffalo, a medium size transport. The data and technology from these programs, along with developments in mathematical modeling of air cushion systems, can be used to design air cushion systems for aircraft such as RPVs.

Contrails

The objective of this study effort was to perform dynamic analysis preliminary design, and cost and performance trade studies of the air bag skid system and the air cushion concept. The ARPV trade studies data, air cushion technology and test program data, and computer tools developed for analysis of air cushion systems were used. Two launch systems and three recovery systems were studied. The launch systems are the air cushion launch platform and the integrated air cushion system. The recovery systems are the air bag skid system, the air cushion recovery system, and the integrated air cushion system. Both the Boeing and the Rockwell ARPV concepts were included in the study. The Rockwell vehicle with conventional landing gear was used as the baseline in the cost and performance trades.

The government owned six degree-of-freedom computer program EASY developed by Boeing under contract F33615-77-C-3054 was used for the dynamic analysis. Dynamic simulations included perturbations to steady state flight, landing simulations and takeoff simulations.

Cost and performance trade study factors included complexity, fuel requirements, adverse weather capability, ground equipment and facilities requirements, survivability/vulnerability levels, reliability and maintainability, and system acquisition and life cycle cost.

The results of the inflight analysis show that these vehicles are stable with the air cushion trunk or air bag skids deployed during approach although a stability augmentation system may be required. Stability during trunk retraction after takeoff was also adequate.

Landing simulation results show that the air cushion and air bag skid recovery systems on both the Rockwell and the Boeing ARPV induce high incremental loads at touchdown. These high loads are the result of the relatively high vehicle forward speed coupled with the high vehicle pitch rate induced by the trunk. At higher angles of attack, the aft part of the trunk touches down first creating a large pitching moment. The product of the resultant pitch rate and high forward velocity induce an acceleration force to the vehicle structure. This creates severe

Contrails

restrictions on the vehicle approach conditions if the vehicle allowable load factor is relatively low. It is not severely restrictive for a vehicle such as the Boeing ARPV with short, small wings that can tolerate loads to 8 or 10g with little penalty to the structure. However, it is quite restrictive for the Rockwell vehicle which carries its payload on the wings.

Landing slideout with the air bag skid system required arrestment to stabilize the vehicle. Arrestor hook engagement during touchdown increased the incremental load to the vehicle. Therefore, it is recommended that cable-hook engagement occur after touchdown.

Induced loads at touchdown appear to be higher with a one trunk integrated air cushion system than with a system optimized for recovery only. Thus, the one trunk integrated air cushion system is even more restrictive on the landing approach conditions than is the air cushion recovery system.

Landing simulations of both air vehicles with air cushion recovery system and suction braking demonstrated that this can be an effective, low cost approach to recovery of ARPVs. However, the required runway length is considerably greater than that required for recovery with an arrestment system. For example, the Boeing ARPV with suction braking, landing at 130 knots on a wet surface, requires a stopping distance of 4500 feet. The required stopping distance with arrestment is only 200 feet.

Stopping capability of an integrated air cushion system with friction pads is poor. Required runway lengths are excessive for vehicle touchdown speeds above 100 knots.

The vehicle was unstable in takeoff simulations of the Rockwell ARPV with both the air cushion launch platform and the integrated air cushion system with inelastic trunks. This situation was encountered in earlier simulations of the Jindivik with an inelastic trunk air cushion system. It is not known if this instability is realistic or is due to a problem in the simulation model.

Contrails

Takeoff simulations of the Rockwell ARPV with an elastic trunk integrated air cushion system showed that the vehicle was stable through ground roll, rotation, trunk stowage, and climbout.

Available power for an integrated air cushion system on the Rockwell vehicle is marginal. However, the power requirement for a shaft driven fan air supply system can be met by utilizing the limited duration overload capability of the engine accessory drive pad.

The results of the cost/performance trade studies indicate that the air cushion recovery system with suction braking and RATO launch is the least complex, lowest cost approach to ARPV launch and recovery. However, if available site space is critical, the air bag skid system with arrestment becomes more attractive.

The results of the study may be somewhat distorted because the Rockwell vehicle, which was used as a baseline, did not lend itself to adaptation of air cushion or air bag skid systems. Because of the narrow, rounded shape of the fuselage, added complexity and weight were required for installation of these systems. For optimum system performance, the air vehicle and launch/recovery system must be designed as an integral unit.

Contracts

SECTION I INTRODUCTION

Current concepts of warfare call for remotely piloted vehicles (RPV) to perform certain high risk missions that have, in the past, been performed by piloted aircraft. The capabilities of these vehicles in conventional warfare have been demonstrated in Southeast Asia and the Middle East. As a result of this demonstrated capability and of conceptual studies that have been done, ground based RPV systems are being considered as part of an overall defense capability. The role of the RPV includes weapons delivery, reconnaissance, and electronic countermeasures.

Studies of RPVs in these multimission roles by The Boeing Company and Rockwell International under contracts sponsored by the USAF Aeronautical Systems Division RPV SPO (References 1 and 2) developed potential configurations for an advanced RPV system (ARPV). In this program, many system configurations were investigated in terms of mission requirements and life cycle cost. Because of the multimission requirement, subjective weight factors given to various performance factors, and the degree to which site preparation, logistics, and vulnerability were considered, widely differing systems were presented by the two contractors.

Boeing studies conducted under the ARPV contract (F33615-75-C-0516) resulted in the proposal to use an air bag skid recovery system in conjunction with a ground based arrestor cable device (Reference 1). Similarly, studies conducted by Rockwell on a RPV for the same multimission role (Contract F33615-75-C-0518) evolved a conventional tricycle type landing system, also used in conjunction with a ground based arrestor cable installation for recovery. These systems are shown in Figures 1 and 2.

Meanwhile, the technology of air cushion vehicles has been advancing at a high rate in the past ten years and has been studied as a launch and recovery concept for RPVs as well as for piloted aircraft. Prototype air cushion systems have been built and tested for the Australian target

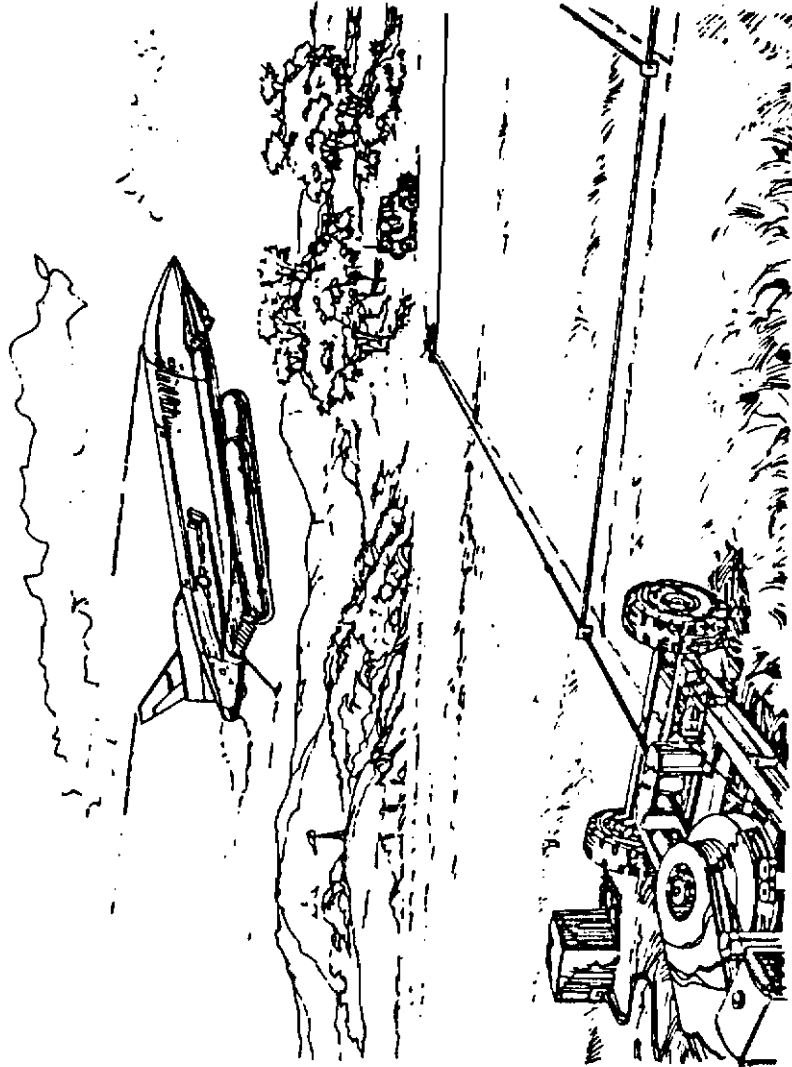


Figure 1 Rockwell ARPV BaseLine Recovery System

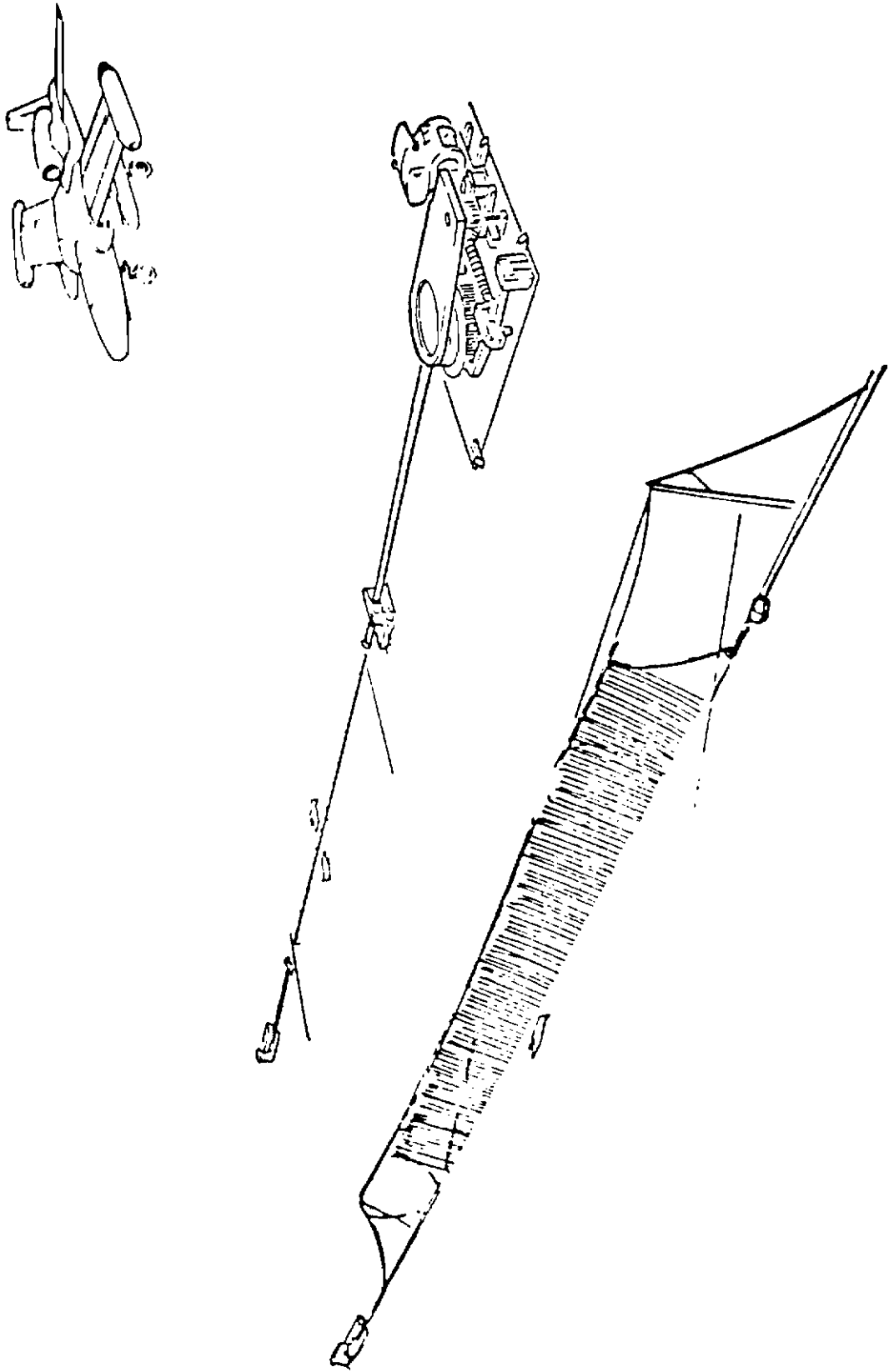


Figure 2 Rockwell ARPV Baseline Recovery System

drone, the Jindivik, and for the XC-8A DeHavilland Buffalo, a medium size (40,000 pound gross weight) turboprop transport.

The launch and recovery systems selected in the ARPV studies were based on limited trade studies and analyses. The dynamics of recovery systems and their deployment were not investigated.

In the Boeing ARPV Trade Study Document (Reference 1) it was noted that while the tail hook/arrestor cable and air skid system represented an attractive low life cycle cost concept, further investigation of the air vehicle/recovery system dynamics would be required to fully validate the concept.

Since the effectiveness of RPVs in performing its missions depends, in part, on the launch and recovery techniques employed, a second look at the factors that determine the rank of these various systems on the ARPV is appropriate.

1. OBJECTIVE

Establishing the effectiveness of these launch and recovery systems was the objective of this study. Specifically, the objective was to perform dynamic analysis, design and cost and performance trade studies of two launch systems and three recovery systems for RPVs. Two generic launch and/or recovery system types were considered. These were the various air cushion systems and the inflatable air bag skid concept. The launch systems include the integrated air cushion system (IACS) which is used for both launch and recovery, and the air cushion launch platform (ACLP). The recovery systems include the air bag skid systems (ABSS), the air cushion recovery system (ACRS), and the IACS.

Recovery of the Boeing ARPV concept was analyzed with the ABSS and the ACRS. The Rockwell ARPV concept was evaluated for launch and/or recovery with the IACS, ACLP, ABSS and ACRS. The Rockwell vehicle concept with conventional landing gear was used as a baseline in cost and performance trade studies of the different systems that were analyzed.

Contrails

Dynamic simulation of the vehicles with the various launch and recovery concepts was made using the EASY Dynamic Analysis Program described in Reference 3. The Basic EASY program was developed by Boeing under Air Force contract F33615-74-C-3041 to provide a means of modeling and analyzing aircraft environmental control systems. The EASY program is a general purpose program for the linear and nonlinear analysis of system dynamics using classical techniques. Through a series of Air Force funded contracts, it has been expanded to model a variety of systems, including environmental control systems, aircraft flight controls and dynamics, space vehicle dynamics, electrical power generation, rapid transit vehicles as well as air cushion landing systems. The program is user oriented and allows the generation of new systems by calling a variety of components from the user library. The special component library developed for the simulation of Air Cushion Landing and Takeoff Systems under contract F33615-77-C-3054 includes a rigid six degree-of-freedom airframe which can be perturbed with all normal aerodynamic forces and moments. The library includes a wind gust model, engine, terrain and an aircraft flight and ground controller. Components for the simulation of a simple aerodynamic control surface system are also included. The air cushion library components include the following:

- o Ducts
- o Flow splits
- o Merges
- o Valves
- o Centrifugal Fan
- o Axial Fan
- o Ejector
- o Inelastic Trunk and Air Cushion
- o Air Bag Skid
- o Elastic Trunk and Air Cushion

An arresting system including a hook, cable and water twister component is also available from the component library. The user can generate

additional components by writing a Fortran subroutine. Program response to execution commands include:

- o Steady State Analysis (Single Point or Scan)
- o Time History Simulation (Linear or Nonlinear)
- o Linear Analysis
- o Stability Matrix
- o Eigenvalues
- o Stability Margin
- o Bode, Nyquist, and Nichols plots

2. BACKGROUND

The Air Bag Skid System is a recovery concept which employs two parallel inflatable membranes or bags along the underside of the fuselage to absorb the aircraft vertical component of kinetic energy, and to provide support during landing slideout and arrestment. The skids are stowed in a collapsed state against the fuselage during flight, and have hard smooth covers or doors to reduce aerodynamic drag and to protect the skid bag material. During landing approach, a control signal activates a cold gas generator which causes the covers or doors to open and the skids to inflate. The covers/doors may drop off or may be retained to provide a wider upper surface for the skids to react against for additional stiffness or roll stability. Each skid has a relief valve to limit peak loads and provide damping upon landing impact. The airframe has a tail hook to engage a cable arresting device installed in the landing area. A rather precise guidance/control system is required in order to ensure hook engagement. An overrun barrier is installed at the end of the recovery area to provide for missed or failed cables. Tow away for turnaround is accomplished by attaching wheels to hard points designed for that purpose.

The skids can be designed as prepacked modules attached to and removed from the fuselage by quick disconnect devices to facilitate vehicle turnaround time. The cold gas generator can be sized to accommodate some bag leakage from damage which may be incurred in flight (battle damage) or during recovery.

Contrails

The Air Cushion Recovery System employs an air cushion designed specifically for landing impact and slideout. The cushion is stowed against the fuselage, with hard covers or doors to reduce drag and protect the cushion. The doors may be used to provide a larger cushion base or to increase roll stiffness. The trunk is usually inflated by diverting air from the compressor section of the thrust engine. The forward one-third of the trunk length has nozzles or holes which serve to provide lubricity in that area, alleviating a "plowing in" tendency. The trunk contact area is covered with an abrasion resistant, high friction material to provide drag to halt the vehicle. Relief valves to reduce impact loads may be employed. The aircraft is towed away for turnaround by a vehicle with an air supply for both the trunk and cushion cavity. No external arresting system is required although one may be employed to reduce the required field length. A final crash barrier may be installed for safety reasons.

The Integrated Air Cushion System is one that provides an air cushion for both the takeoff and landing phases of the aircraft mission. There are two variations, the one trunk concept and the two trunk concept.

The One Trunk Concept employs a single trunk of elastic or inelastic material, to provide both the takeoff and landing functions. Upon rotation, the trunk retracts against the fuselage in the case of the elastic trunk, or is retracted into the fuselage and hard doors close upon it to reduce drag and protect the trunk. Since a large airflow is required for takeoff (compared to landing), a device, such as a tip turbine fan powered by engine bleed air or an auxiliary power unit (APU), is needed to draw in air from the atmosphere for trunk flow. Trunk nozzle configuration is dictated primarily by takeoff requirements resulting in a distribution of nozzles around the entire periphery of the trunk. Landing requirements result in friction pads in some areas of the trunk contact and the capability to reduce cushion pressure after impact to enable friction pad contact. Remote taxi control is a possible design variation if the required thrusters are included. Parking bladders may be included for long term static support.

Contrails

The Two Trunk Concept employs a jettisonable takeoff trunk and a prepacked landing/recovery trunk. The takeoff trunk may have parking bladders and a nozzle pattern similar to the pattern for the one trunk concept. The takeoff trunk is recovered after it is jettisoned and attached to a new aircraft for a subsequent launch. The takeoff trunk configuration and attachment is such that a clean aerodynamic surface is left when it is jettisoned. The stowed landing trunk is now identical to the Air Cushion Recovery System defined earlier, except that excess airflow is available due to takeoff requirements.

The Air Cushion Launch Platform is a launching system that uses a separate air cushion equipped carriage to support the aircraft during takeoff. Upon rotation, the platform is released from the aircraft and is stopped by internal braking or by an external arrestment system. The platform is recovered by either a tow vehicle or by remote control if appropriate thrusters are provided. The platform contains its own air supply and can be designed to carry an additional thrust engine to aid the aircraft engine during takeoff. Parking bladders are incorporated to provide platform and aircraft support while the air supply is turned off.

3. SCOPE AND GENERAL APPROACH

This program consisted of the following:

- o Familiarization with mission requirements and the previous ARPV conceptual studies.
- o Preliminary configuration and assessment of parameters for dynamic modeling of the vehicles with the various launch and recovery concepts.
- o A six degree-of-freedom, rigid body airframe dynamic analysis for each configuration using the EASY dynamic analysis program.
- o Preliminary design to identify system performance and cost factors.
- o Performance and cost trade study.

Contrails

Figure 3 summarizes the combinations of configurations that were studied using the EASY dynamics program. Considering the elastic and inelastic trunk versions of the one trunk integrated air cushion system as separate configurations, a total of eight configurations were evaluated. Four of these were for recovery only, one for launch only, and three for both launch and recovery. In addition, the clean configuration of both the Boeing and Rockwell RPVs were studied to determine basic aerodynamic characteristics.

The dynamic simulation studies included:

- o Vehicle flight stability analysis with the landing system deployed for all launch recovery system combinations. Vehicle parameter adjustments were made as required for most stable flight.

- o Landing simulation, encompassing approach, bag or trunk deployment, flare, touchdown and arrestment or braking for all landing system configurations. The study determined vehicle and landing system parameter adjustments required to achieve satisfactory performance.

- o Takeoff or launch simulation including takeoff roll, rotation, platform or trunk release, and climbout for the integrated air cushion configurations plus the launch platform.

- o Arrestor hook-cable dynamic analysis to define limits of hook properties and aircraft kinematics for proper hook engagement.

Design modifications were made for each airframe/launch/recovery system combination based on the results of the dynamic analysis. The basic airframe designs as described in the conceptual studies for the Boeing and the Rockwell vehicles were used for appropriate modifications to incorporate the results of the dynamic analysis and the requirements of the various launch/recovery systems. Design considerations for each of

LAUNCH/RECOVERY SYSTEM	AIRFRAME		FLIGHT MODE		RECOVERY MODE	
	BOEING	ROCKWELL	LAUNCH	RECOVERY	ARRESTOR	SUCTION BREAKING
AIR BAG SKID (ABSS)	●	●		●	●	
AIR CUSHION RECOVERY (ACRS)	●	●		●	●	●
AIR CUSHION LAUNCH PLATFORM (ACLPL)		●	●		●	●
INTEGRATED AIR CUSHION - ELASTIC (ONE TRUNK) (IACS)		●	●	●	●	●
INTEGRATED AIR CUSHION - INELASTIC (ONE TRUNK) (IACS)		●	●	●		●
INTEGRATED AIR CUSHION - TWO TRUNK (IACS)		●	●	●	● ¹	● ¹

¹ RECOVERY CONFIGURATION SAME AS ACRS ABOVE,

Figure 3 Configuration Combinations Evaluated

Contrails

the concepts included survivability/vulnerability aspects and ground equipment and facilities requirements.

A performance/cost analysis was performed on each airframe/launch/recovery system combination shown to be acceptable by dynamic analyses. Performance/cost increments were made using the Rockwell ARPV design as described in Reference 2 as a baseline.

The following factors were considered in the performance/cost tradeoffs, but only to the extent as they effect or are affected by the launch/recovery systems:

- o Complexity
- o Fuel requirements
- o Adverse weather capability
- o Ground equipment and facility requirements
- o Survivability/vulnerability levels
- o Reliability and maintainability
- o System acquisition and life cycle costs, including those related to site preparation and upkeep.

SECTION II DYNAMIC SIMULATION AND ANALYSIS

Dynamic simulations and various analyses were performed for all of the launch/recovery system/airframe combinations shown in Figure 3 by using program EASY as the principal analysis tool. Three different operating regimes were investigated during these analyses: low speed flight, landing, and takeoff. The two different air vehicles and several different launch/recovery concepts were analyzed during these three operating regimes. This section describes the configurations which were analyzed, the analysis approach which was used, the results obtained, the conclusions made based upon those results, and the configurations recommended for further study.

1. INFLIGHT SIMULATIONS AND ANALYSIS

Deployment of an air cushion recovery system during the landing approach flight phase affects the stability and controllability (S/C) of an air vehicle. The purpose of this portion of the study was to determine the effects of air cushion and air bag systems on the S/C of the Boeing and Rockwell ARPV concepts. Other objectives were to identify any airframe design modifications necessary to achieve acceptable S/C and to determine the trim conditions for both air vehicles during landing approach.

The approach that was followed started with the calculation of S/C coefficients for both air vehicles, with and without the ACRS and ABSS. The next steps involved the development of program EASY models of the air vehicles, linear analysis of these models to identify their dynamic modes, the determination of steady state trim conditions, and the simulation of perturbations about these trim conditions to verify the stability or instability of the air vehicles.

a. Development of Math Models

(1) Air Vehicle Configurations

The air vehicles analyzed included the maximum landing weight configurations for the Boeing and Rockwell designs. Both

configurations were analyzed with both the ACRS and the ABSS. During landing approach, the Boeing ARPV payload was assumed to be one empty AN/ALE-38 chaff dispenser pod carried in the internal weapon bay. This configuration has a maximum landing gross weight of 1600 pounds. The maximum landing gross weight configuration for the Rockwell ARPV, Figure 4, has four empty AN/ALE-38 chaff dispenser pods which results in a gross weight of 4167 pounds when adjustments are made for removal of the baseline wheeled landing gear and installation of the air cushion or air bag skid systems. The baseline Boeing ARPV was initially designed for an air bag skid recovery system so no modifications to the airframe were necessary for the ABSS or ACRS. Several modifications to the Rockwell ARPV were needed to install the ABSS and ACRS. The round fuselage of the baseline Rockwell ARPV does not provide the wide and flat surface needed for an ABSS or ACRS installation. Attaching the bag or trunk directly to the curved fuselage results in excessive trunk volume giving poor roll and pitch stability and damping. Therefore, hinged fairings were proposed which fold out laterally and provide a wide flat surface for attachment of the air cushion trunk or air bag skids, as shown in Figure 5. The fairings are supported by either spring loaded linkages or pressurized bladders.

(2) Air Vehicle Mass Properties

The mass properties for the Boeing and Rockwell ARPVs are listed in Table 1. These values represent the maximum landing gross weight configurations for both air vehicles and include a weight increment for the ABSS or ACRS installations. The ABSS and ACRS installations were assumed to have equal weights for these simulations.

(3) Aerodynamic Characteristics

(a) Boeing ARPV

The baseline Boeing ARPV, Model 1042-15A, is a wing-canard-vertical tail configuration as shown in Figure 6. The elevon control surfaces located on the wing are used for pitch and roll control. Yaw control is provided by a rudder. The canard surface is a double hinged, two position panel; it consists of the canard and a canard flap. During normal flight the surface is not deflected until at landing

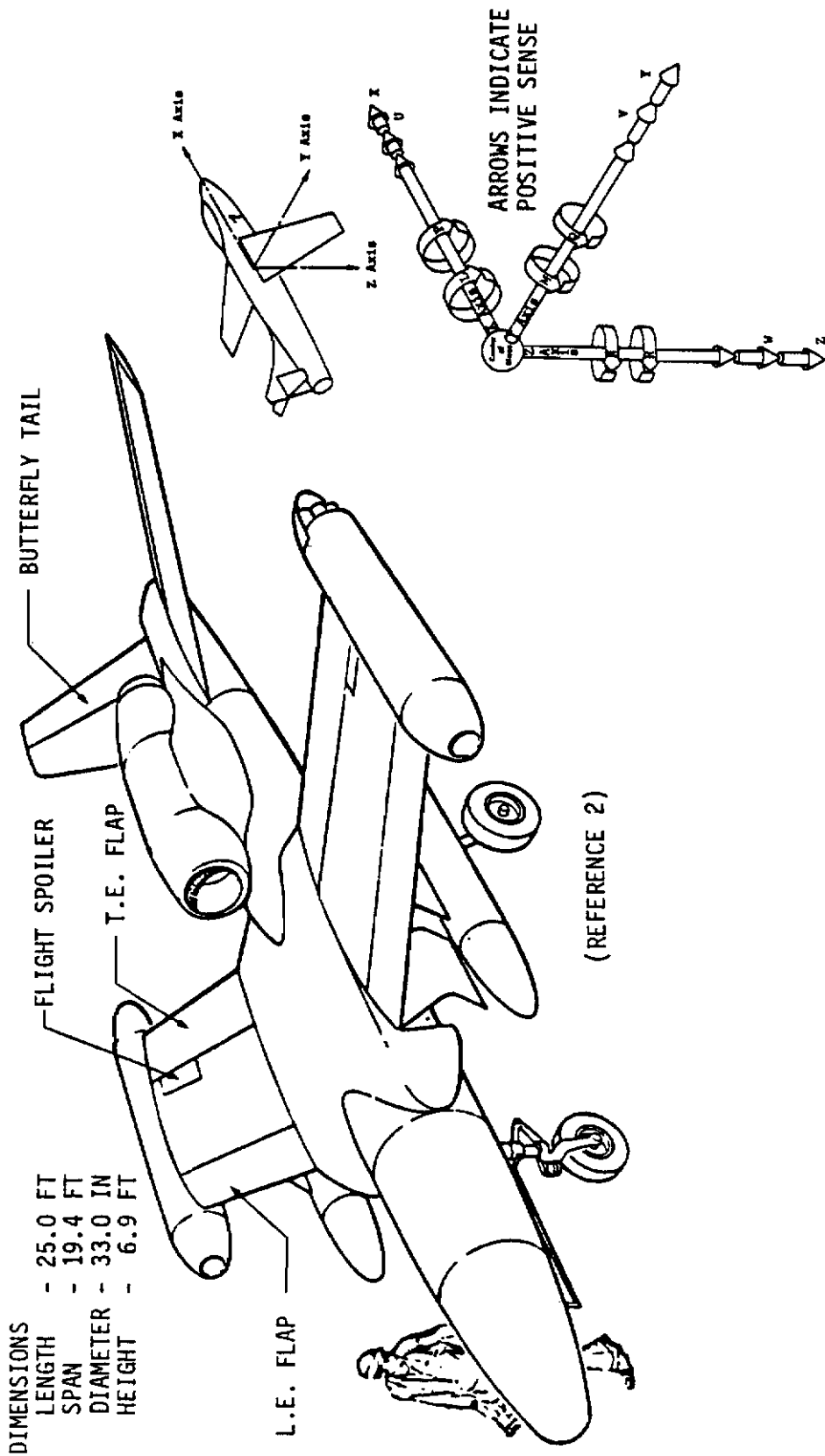


Figure 4 Rockwell Baseline ARPV

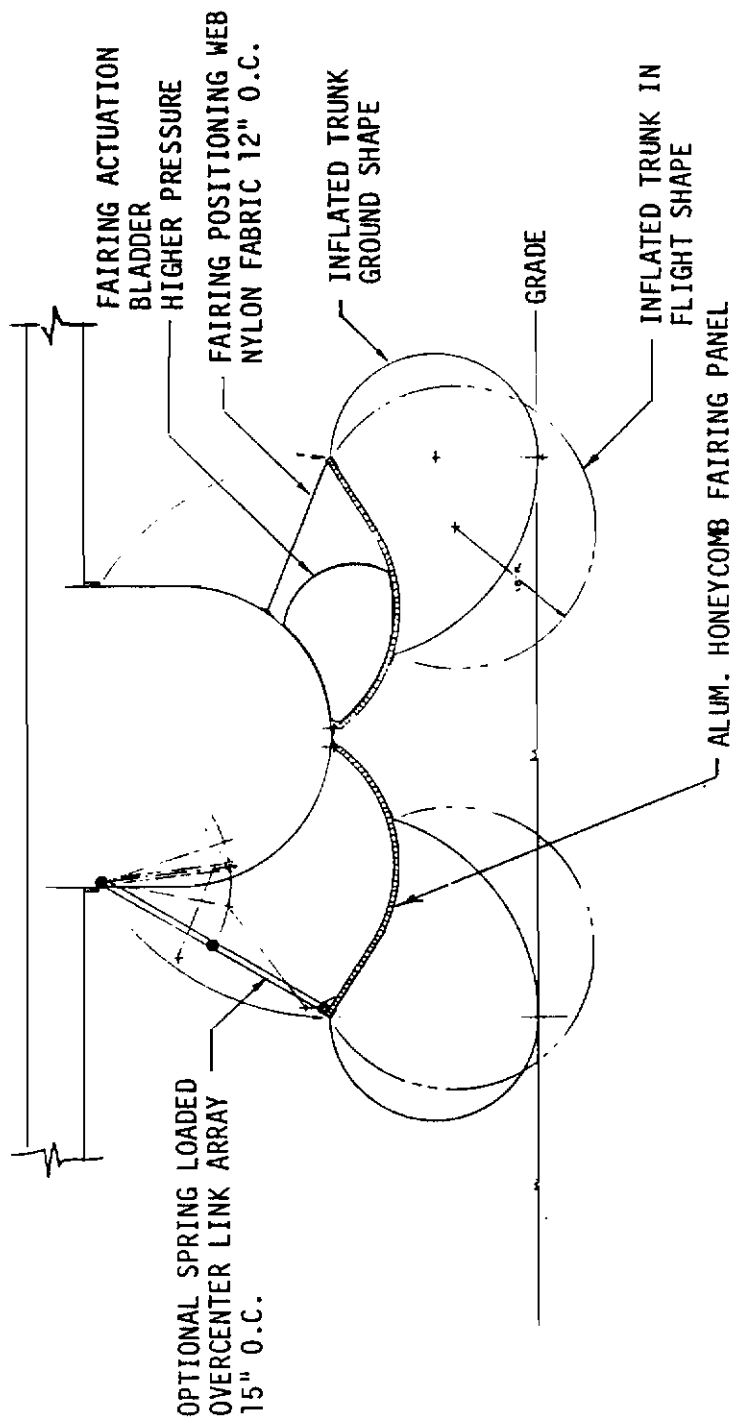
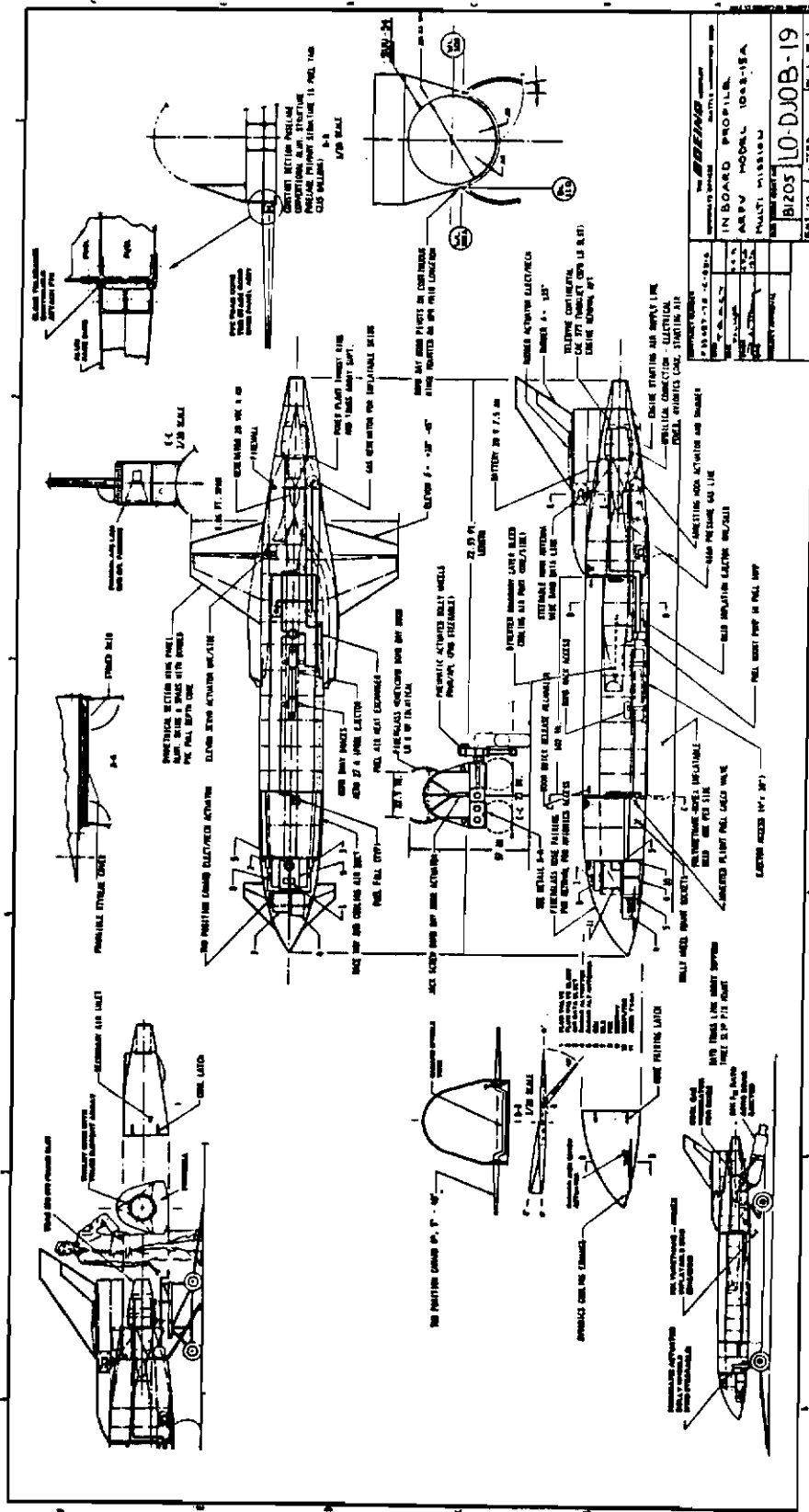


Figure 5 Rockwell ARPV Air Cushion Trunk Installation



IN BOARD PROFILE AIRPV MODEL 1003-15A MULTI-MISSION 10-DJOB-19	
PROJECT NUMBER 10-DJOB-19	DRAWING NUMBER 10-DJOB-19
DATE 10-1-68	SCALE 1/8" = 1'-0"
DESIGNED BY J. W. B.	CHECKED BY J. W. B.
DRAWN BY J. W. B.	APPROVED BY J. W. B.

Figure 6 Boeing Baseline Vehicle

TABLE 1
BOEING AND ROCKWELL ARPV MASS PROPERTIES

	Rockwell ARPV	Boeing ARPV
Vehicle Weight Empty (LB.)	2987	1330
Payload	4 AN/ALE-38's	1 AN/ALE-38
Recovery Weights		
Landing Gross Weight (LB.)	4167	1600
Landing Fuel Weight (LB.)	300	50
Landing Payload Weight (LB.)	880	220
I_{xx} @ Landing GW (Slug-Ft ²)	2860	67
I_{yy} @ Landing GW (Slug-Ft ²)	2680	790
I_{zz} @ Landing GW (Slug-Ft ²)	5120	570
I_{xz} @ Landing GW (Slug-Ft ²)	0	20
Vehicle Center of Gravity	Sta. 168.6, 7.5 in. above airplane CL	Sta. 226 WL 100
Takeoff Weights		
Takeoff Gross Weight (LB.)	7359	3320
Takeoff Fuel Weight (LB.)	2196	1446
Takeoff Payload Weight (LB.)	2176	544
I_{xx} @ TOGW (Slug-Ft ²)	6240	
I_{yy} @ TOGW (Slug-Ft ²)	4840	
I_{zz} @ TOGW (Slug-Ft ²)	10440	
I_{xz} @ TOGW (Slug-Ft ²)	0	
Vehicle Center of Gravity	Sta. 168.6, 7.5 in. above airplane CL	Sta. 226 WL 100

approach, when the canard incidence is 5 degrees and the canard flap is deflected 40 degrees, while the elevons are symmetrically deflected to a nominal position of -30 degrees to trim the air vehicle. All of the flight control surfaces use electromechanical actuators powered by a 4 to 10 kva engine driven alternator.

Preliminary ABSS and ACRS trunk shapes were developed and used to estimate the stability and control coefficients for the air vehicle. It was assumed that the coefficients originally calculated described the dominant S/C characteristics which did not change significantly as the trunk size and shape was modified. Therefore, these coefficients were not updated later as the trunk shapes were modified during the landing simulations. Changes to the ABSS or ACRS designs which could cause undesirable S/C effects were avoided. For instance, an ACLS trunk could interfere with the downwash behind the canard if it was located too far forward and was too wide at its forward end. Also, a trunk which has a very wide aft end could interfere with the wing aerodynamics.

Tables 2 and 3 list the lateral and longitudinal S/C coefficients which were calculated for the Boeing ARPV during landing approach with an ACRS and with an ABSS. The classical notation is listed, along with that used by program EASY. Ground effects were not included in any of the simulations. The coefficients are estimated data based upon methodology presented in the USAF DATCOM (Reference 4). The general trends of the bag deployment data are in agreement with the characteristics of wind tunnel data for the F-8, Buffalo and Jindivik ACLS configurations.

(b) Rockwell ARPV

The baseline Rockwell ARPV is a wing-butterfly tail configuration as shown in Figure 4. Pitch control is achieved by symmetrical deflection of the butterfly tail. Wing outboard spoiler deflection interconnected with differential incidence of the butterfly tail panels produces augmented roll and proverse yaw. Differential deflection of the butterfly tail panels interconnected with outboard spoiler deflection produces augmented yaw and proverse roll. This air vehicle also has leading and trailing edge flaps which are deflected 30

TABLE 2
STABILITY COEFFICIENTS* FOR BOEING VEHICLE AND ACRS

LONGITUDINAL STABILITY AND CONTROL DERIVATIVES: OL

	BIAS	ALPHA	U	ALPHA	Q	δ ELEV	ACRS TRUNK	SPOILERS	GROUND EFFECT	LARGE SIDE SLIP	CANARD & CANARD FLAP	BETA
FX (DRAG)	-0.056	-1.89	0	0	0	0	-0.0276			1.0		
	XO	XA	XU			XDE	XTR	XSP	XGE	KXB		
FZ (LIFT)	-0.765	-3.150	0	0	-2.91	-1.272				1.0	-1.0	
	ZO	ZA	ZU	ZAD	ZQ	ZDE	ZTR	ZSP	ZGE	KZB	ZDS	
TY=M (PITCH)	0.0206	-15 [.50]	0	0	-15.66	-1.805	-0.0147			1.0	2.991	
	MO	MAL	MU	MAD	MQ	MDE	MTR	MSP	MGE	KMB	MDS	MB

LATERAL STABILITY AND CONTROL DERIVATIVES : OL

	BETA	BETA	P	R	δ RUD	δ AIL	ACRS TRUNK	SPOILERS	GROUND EFFECT	LARGE SIDE SLIP	β RUD	AERO ELASTICITY
FY (SIDE)	-1.158	0	0.119	1.44	0.2137	0	-0.332		1.0	1.0	0	1.0
	YB	YBD	YP	YR	YDR	YDA	YTR	YFS	YGE	KYB	YBR	KCY
TX=L (ROLL)	-0.1662	0	-0.235	0.490	0.064	0.1203	-0.0748		1.0	1.0	0	1.0
	LB	LBD	LP	LR	LDR	LDA	LTR	LFS	LGE	KLB	LBR	KCL
TZ=N (YAW)	0.0516	0	0.258	-1.543	0.257	-0.0722	-0.384	NFS	NGE	KNB	NBR	
	NB	NBD	NP	NR	NDR	NDA	NTR	NFS	NGE	KNB	NBR	

NOTE: [] IS VALUE FOR DEPLOYED TRUNK.

*NON-DIMENSIONAL COEFFICIENTS IN THE STABILITY AXIS SYSTEM.

TABLE 3
STABILITY COEFFICIENTS* FOR BOEING VEHICLE AND ABSS

LONGITUDINAL STABILITY AND CONTROL DERIVATIVES: 0L

	BIAS	ALPHA	U	ALPHA	Q	Δ ELEV	ABSS TRUNK	SPOILERS	GROUND EFFECT	LARGE SIDE SLIP	CANARD & CANARD FLAP	BETA
FX (DRAG)	XO -0.056	XA -1.89	XU 0	XDE 0	XTR -0.0156	XSP XGE						
FZ (LIFT)	ZO -0.765	ZA -3.150	ZU 0	ZAD 0	ZQ -2.91	ZDE -1.272	ZTR ZSP		ZGE	KZB 1.0	ZDS -1.0	
TY=M (PITCH)	MO .0206	MAL -.15 [.25]	MU 0	MAD 0	MQ -15.66	MDE -1.805	MTR -0.079	MSP	MGE	KMB 1.0	MDS 2.991	MB

LATERAL STABILITY AND CONTROL DERIVATIVES : DL

	BETA	BETA	P	R	ΔRUD	ΔAIL	ABSS TRUNK	SPOILERS	GROUND EFFECT	LARGE SIDE SLIP	β RUD	AERO ELASTICITY
FY (SIDE)	YB -1.158	YBD 0	YP 0.119	YR 1.44	YDR 0.2137	YDA 0	YTR -0.196	YFS	YGE	KYB 1.0	YBR 0	KCY 1.0
TX=L (ROLL)	LB -0.1662	LBD 0	LP -0.235	LR 0.490	LDR 0.064	LDA 0.1203	LTR -0.079	LFS	LGE	KLB 1.0	LBR 0	KCL 1.0
TZ=N (YAW)	NB .0516	NBD 0	NP 0.258	NR -1.543	NDR 0.257	NDA -0.0722	NTR -0.261	NFS	INGE	KNB 1.0	NBR 0	

NOTE: [] IS VALUE FOR DEPLOYED BAG.

*NON-DIMENSIONAL COEFFICIENTS IN THE STABILITY AXIS SYSTEM.

degrees and 40 degrees respectively during landing approach. Rockwell describes the normal landing approach as a descent at 100 knots on a 5 degree glide slope and 80 knots just prior to touchdown. When landing with a large crosswind, a decrabbing maneuver is also executed just before touchdown. The flight control surfaces use electrically powered actuators.

As with the Boeing ARPV, preliminary ABSS and ACRS trunk shapes were developed and used to estimate the S/C coefficients for the air vehicle with a deployed trunk. Because of the high wing location, aerodynamic interference due to the deployed trunk is not a problem. There is no definite forward constraint to the trunk size and the only rear constraint is the tail hook pivot. The USAF DATCOM methodology was used to estimate those coefficients which were not listed in the Rockwell ARPV report. Rockwell coefficients are listed in Tables 4 and 5.

(4) Program EASY Air Vehicle Models

Figure 7 shows a block diagram of the program EASY math models which were developed for the Boeing and Rockwell vehicles. These math models contain the lateral and longitudinal aerodynamics, the engine thrust, and the air vehicle six degree-of-freedom equations of motion and mass properties.

At an early point during the analysis it became apparent that a math model of the air vehicle stability augmentation system was needed to make the models dynamically stable. A simple model of an SAS was produced by using the EASY optimal controller component. The air vehicle state variables and various error variables are inputs to the controller. Controller outputs are engine thrust setting and flight control surface position commands. More detailed information about each of these components is contained in the program EASY users manual, Reference 3.

b. Boeing ARPV Inflight Simulations

The first analyses to be performed were a series of linear and root locus calculations to identify the lateral and longitudinal modes of the air vehicle with the trunk stowed and deployed. Figure 8 shows the

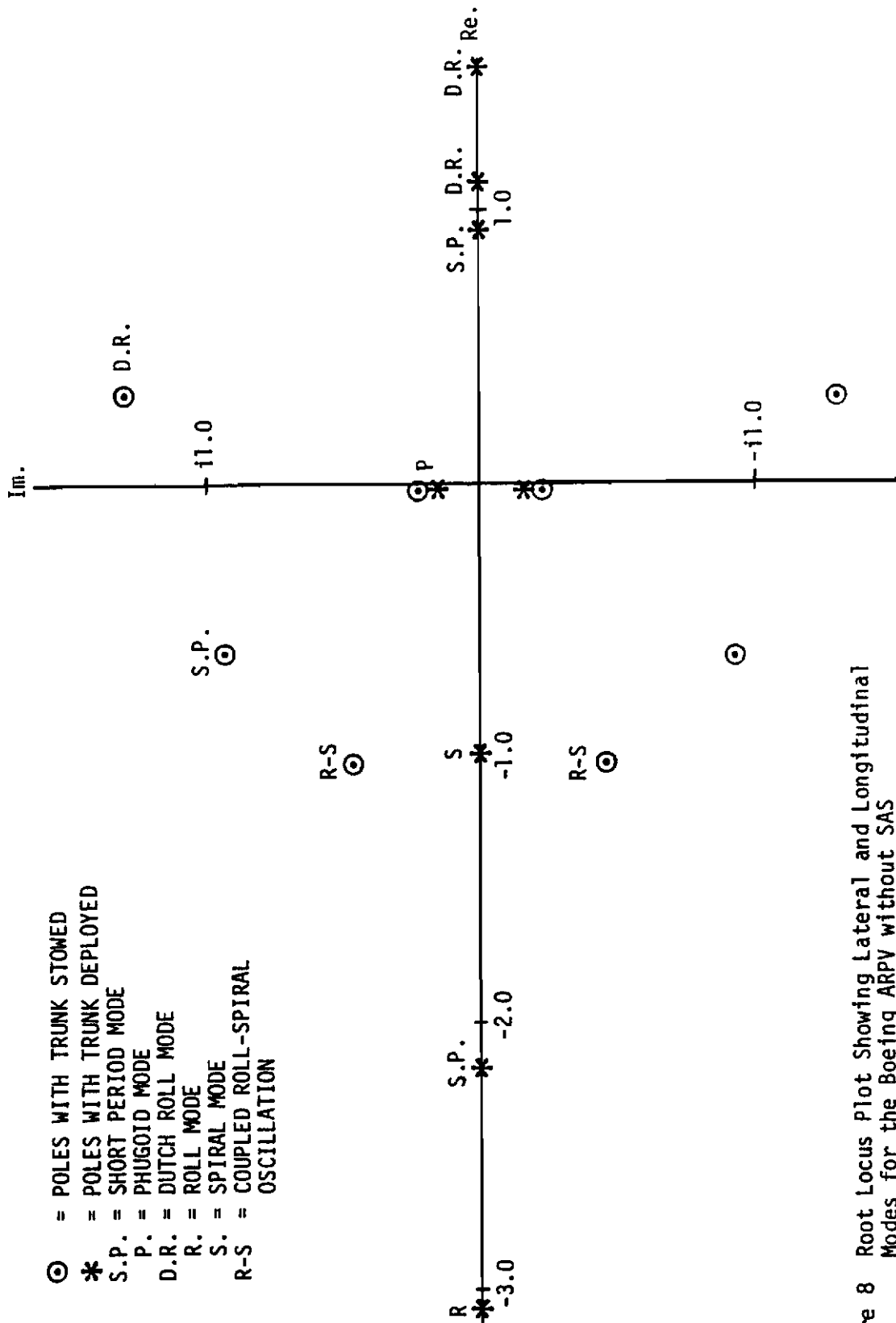


TABLE 4
STABILITY COEFFICIENTS* FOR ROCKWELL VEHICLE AND ACRS

LONGITUDINAL STABILITY AND CONTROL DERIVATIVES: OL

	BIAS	ALPHA	U	ALPHA	Q	δ ELEV	ACRS TRUNK	GROUND SPOILERS	GROUND EFFECT	LARGE SIDESLIP	STABILIZER	BETA
FX (DRAG)	-0.032	(-1.048)	0			0	<-0.0274>	0	0	1.0		
	XO	XA	XU			XDE	XTR	XSP	XGE	KXB		
FZ (LIFT)	(-0.370)	-4.011	0	0		-1.146	0	.25	0	1.0		
	ZO	ZA	ZU	ZAD	ZQ	ZDE	ZTR	ZSP	ZGE	KZB	ZDS	
TY=M (PITCH)	0.0038	-.464	0	-3.50	-6.00	-1.748	-0.008	0	0	1.0		0
	MO	MAL	MU	MAD	MQ	MDE	MTR	MSP	MGE	KMB	MDS	MB

LATERAL STABILITY AND CONTROL DERIVATIVES : DL

	BETA	BETA	P	R	δ RUD	δ AIL	ACRS TRUNK	FLIGHT SPOILERS	GROUND EFFECT	LARGE SIDESLIP	β RUD	AERO ELASTICITY
FY (SIDE)	-0.573	0			0.212		-0.378	0	1.0	1.0	1.0	1.0
	YB	YBD	YP	YR	YDR	YDA	YTR	YFS	YGE	KYB	YBR	KCY
TX=L (ROLL)	-0.264	0	-0.310		-0.084		-0.0811	0.0138	1.0	1.0	1.0	1.0
	LB	LBD	LP	LR	LDR	LDA	LTR	LFS	LGE	KLB	LBR	KCL
TZ=N (YAW)	0.086	0		-0.140	-0.344		-0.0456	0.00525	1.0	1.0	1.0	
	NB	NBD	NP	NR	NDR	NDA	NTR	NFS	NGE	KNB	NBR	NBR

NOTE : () IS VALUE FOR LAUNCH.
< > IS ADDITIONAL DRAG DUE TO ACLP.
[] IS VALUE FOR DEPLOYED TRUNK.

*NON-DIMENSIONAL COEFFICIENTS IN THE STABILITY AXIS SYSTEM.

TABLE 5
STABILITY COEFFICIENTS* FOR ROCKWELL VEHICLE AND ABSS

LONGITUDINAL STABILITY AND CONTROL DERIVATIVES : OL

	BIAS	ALPHA	U	ALPHA	Q	δ ELEV	ABSS TRUNK	GROUND SPOILERS	GROUND EFFECT	LARGE SIDE SLIP	STABILIZER	BETA
FX (DRAG)	-0.032	-1.203	0	0	0	0	-0.00812	0	0	1.0		
	X0	XA	XU	XDE	XSP	XTR	XGE	KXB				
FZ (LIFT)	-0.480	-4.011	0	0	-1.146	0	0	.25	0	1.0		
	Z0	ZA	ZU	ZDE	ZQ	ZTR	ZGE	ZSP	ZDE	KZB	ZDS	
TY-M (PITCH)	0.0038	-464 [-.114]	0	-3.50	-6.00	-1.748	-0.0314	0	0	1.0		0
	M0	MAL	MU	MAD	MQ	MDE	MTR	MSP	MGE	KMB	MDS	MB

LATERAL STABILITY AND CONTROL DERIVATIVES : DL

	BETA	BETA	P	R	δ RUD	δ AIL	ABSS TRUNK	FLIGHT SPOILERS	GROUND EFFECT	LARGE SIDE SLIP	β RUD	AERO ELASTICITY
FY (SIDE)	-.573	0			0.212		-.175	0	1.0	1.0	1.0	1.0
	YB	YBD	YP	YR	YDR	YDA	YTR	YFS	YGE	KYB	YBR	KCY
TX=L (ROLL)	-.264	0	-0.310		-0.084		-.062	0.0138	1.0	1.0	1.0	1.0
	LB	LBD	LP	LR	LDR	LDA	LTR	LFS	LGE	KLB	LBR	KCL
TZ=N (YAW)	.086	0		-0.140	-0.344		-.038	0.00525	1.0	1.0	1.0	
	NB	NBD	NP	NR	NDR	NDA	NTR	NFS	NGE	KNB	NBR	

NOTE : [] IS VALUE FOR DEPLOYED BAG.

*NON-DIMENSIONAL COEFFICIENTS IN THE STABILITY AXIS SYSTEM.

Contrails

results of these analyses for the Boeing ARPV without its stability augmentation system. The dutch roll mode is unstable with the trunk stowed and becomes even more unstable as the trunk is deployed. With the trunk stowed, a coupled roll-spiral oscillation exists but as the trunk is deployed, this oscillatory mode separates into the first order roll subsidence and spiral divergence modes. The longitudinal phugoid mode is stable and changes very little as the trunk is deployed. Large changes occur to the short period mode as the trunk is deployed; the normal stable oscillatory mode changes into two first order modes, one of which moves into the right half plane. Simulation of the free air vehicle response to a small disturbance verified these instabilities.

The existence of the coupled roll spiral oscillation and unstable dutch roll mode when the trunk is stowed shows that a stability augmentation system is needed to increase pitch and yaw damping even without an ACLS. Therefore, the only effect of the ACLS installation on the flight control system will be a change in SAS controller gains.

To investigate the response of the air vehicle to small disturbances during landing approach, it was necessary to include a math model of an SAS in the program EASY air vehicle math model. The optimal controller component was used for this purpose. The optimal controller is designed about a linear model of the nonlinear system at a single operating point. Controller inputs and outputs, the desired operating point, and controller design weights for each of the inputs and outputs must be specified. The controller design weights are used in a cost function which assesses a penalty for system output errors and excessive control power.

Figure 9 shows some of the characteristics of the controller. More detailed information is available in the program EASY users manual, Reference 3.

The optimal controller (OC) component was integrated into the air vehicle math model and several different OC designs were investigated. The OC design factors were determined by a mixture of calculations and qualitative analysis of simulation results.

Contrails

$$\left. \begin{aligned} X &= X_0 + x \\ Y_s &= Y_{s_0} + y_s \\ Y_c &= Y_{c_0} + y_c \end{aligned} \right\}$$

LINEAR MODEL REPRESENTS
PERTURBATION ABOUT OPERATING
POINT

$$J = 1/2 \int_0^{\infty} (y_c' Q y_c + u' R u) dt \quad \text{DESIGN CRITERIA COST FUNCTION}$$

Q = SENSED QUANTITY WEIGHTING MATRIX

R = CONTROL QUANTITY WEIGHTING MATRIX

$$C_d = E (d d')$$

STATE DISTURBANCE COVARIANCE MATRIX

$$C_s = E (v v')$$

SENSOR DISTURBANCE COVARIANCE MATRIX

Figure 9 Program EASY Optimal Controller Characteristics

The response of the air vehicle with SAS to a 15 ft/sec sharp edged gust at 5 seconds was simulated. The simulation also included a math model of the landing approach glide path vector. The optimal controller sensed the position errors which occurred if the air vehicle drifted off the glide path, and then minimized those errors by maneuvering the air vehicle towards the vector by moving the flight control surfaces. The results show that the air vehicle did not become unstable when disturbed by the gust. The optimal controller responded to the gust disturbance by changing the engine thrust setting and moving the flight control surfaces to trim the air vehicle at a pitch angle of 8.5 degrees, a roll angle of 2.25 degrees, and a yaw angle of 1.9 degrees. Figures 10 and 11 show some of the significant results from the simulation. Although the controller is a very simple model of the actual air vehicle SAS and autopilot, it does show that a controller, using reasonable sensors and a limited amount of control power, can stabilize the air vehicle when flying through turbulent conditions with the ACRS trunk deployed during landing approach.

A series of steady state analyses were also performed to define a range of air vehicle trim conditions during landing approach. The results are shown in Figures 12, 13, and 14 and describe the air vehicle attitude when trimmed for various sink rates, glide slope angles and crosswinds for the Boeing ARPV with the ACRS and ABSS. Results showed little difference in control requirements between the vehicle with the ACRS and that with the ABSS.

c. Rockwell ARPV Inflight Simulations

An analysis approach similar to that used for the Boeing ARPV was used to identify the lateral and longitudinal modes for the Rockwell ARPV. Figure 15 shows a root locus plot of the results for the Rockwell ARPV without its stability augmentation system. The phugoid mode is neutrally stable and essentially remains constant as the ACRS trunk is deployed. The short period frequency is reduced by 30% as the trunk is deployed, but its damping ratio increases and it remains stable. No major changes occur to the lateral modes as the trunk is deployed. The

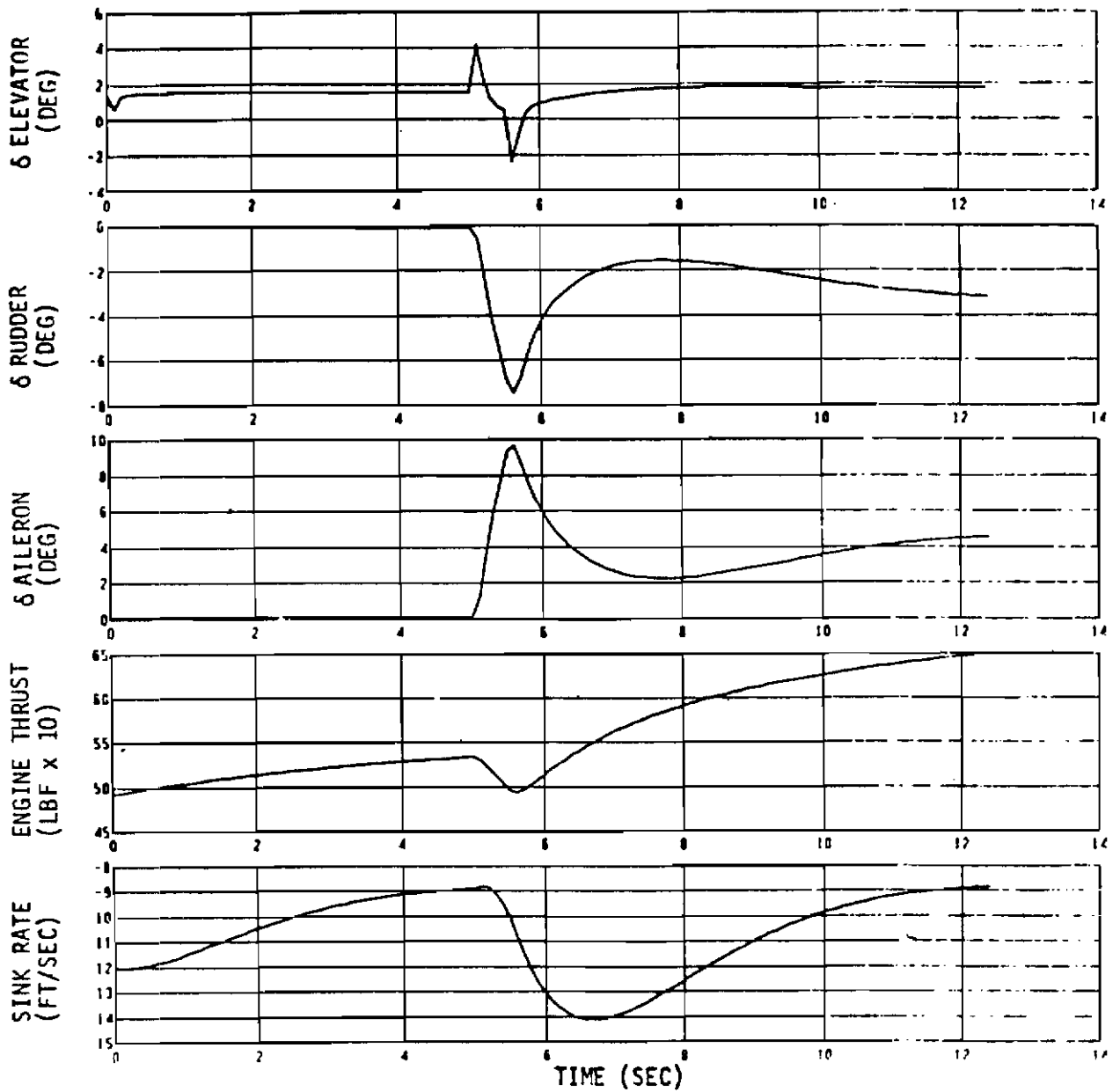


Figure 10 Boeing ARPV with ACRS Deployed at Landing Approach,
Response of Optimal Controller to 15 Ft/Sec Sharp
Edged Gust at 5 Seconds

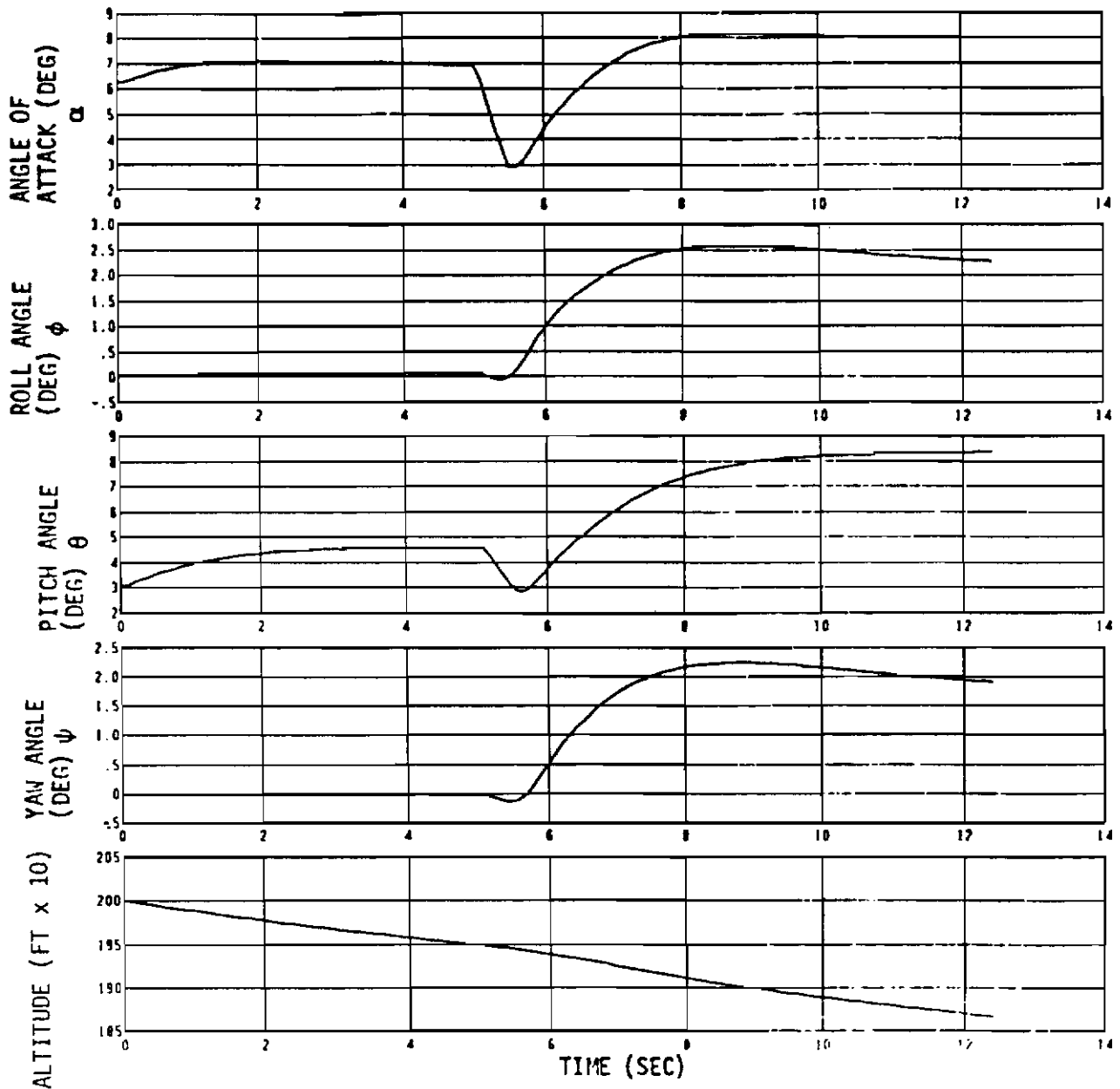


Figure 11 Boeing ARPV with ACSRS Deployed at Landing Approach,
Response of Optimal Controller to 15! Ft/Sec Sharp
Edged Gust at 5 Seconds

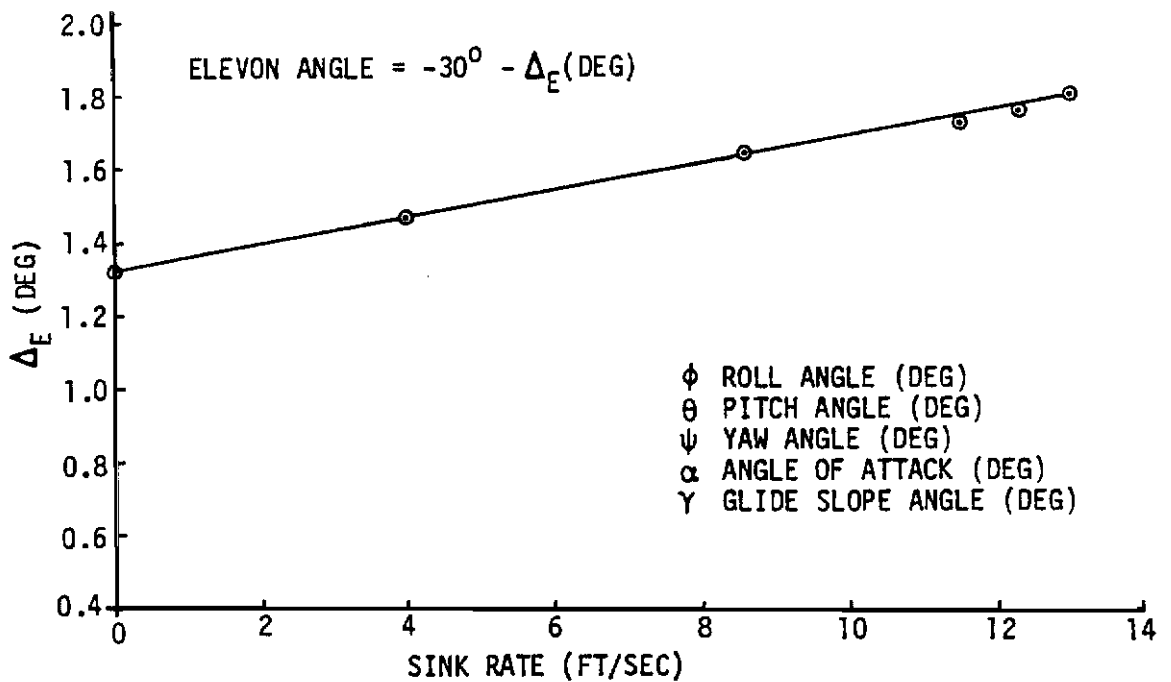
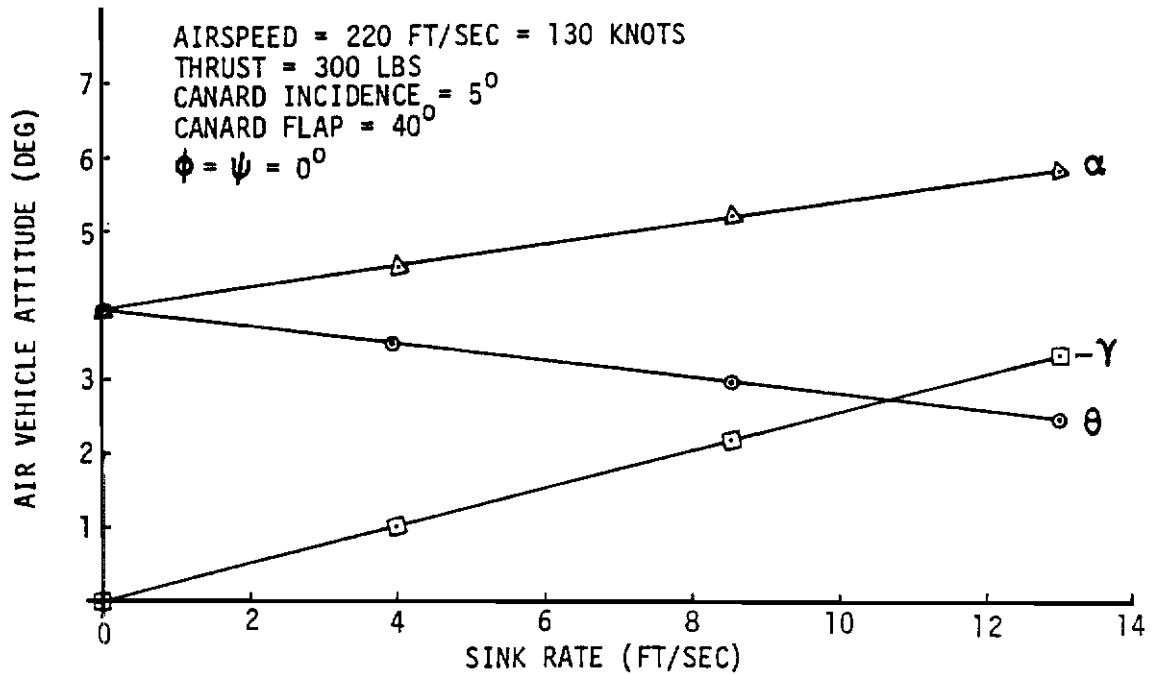


Figure 12 Boeing ARPV with ACRS Deployed, Landing Approach Trim with No Crosswind, Air Vehicle Attitude vs. Sink Rate

Contrails

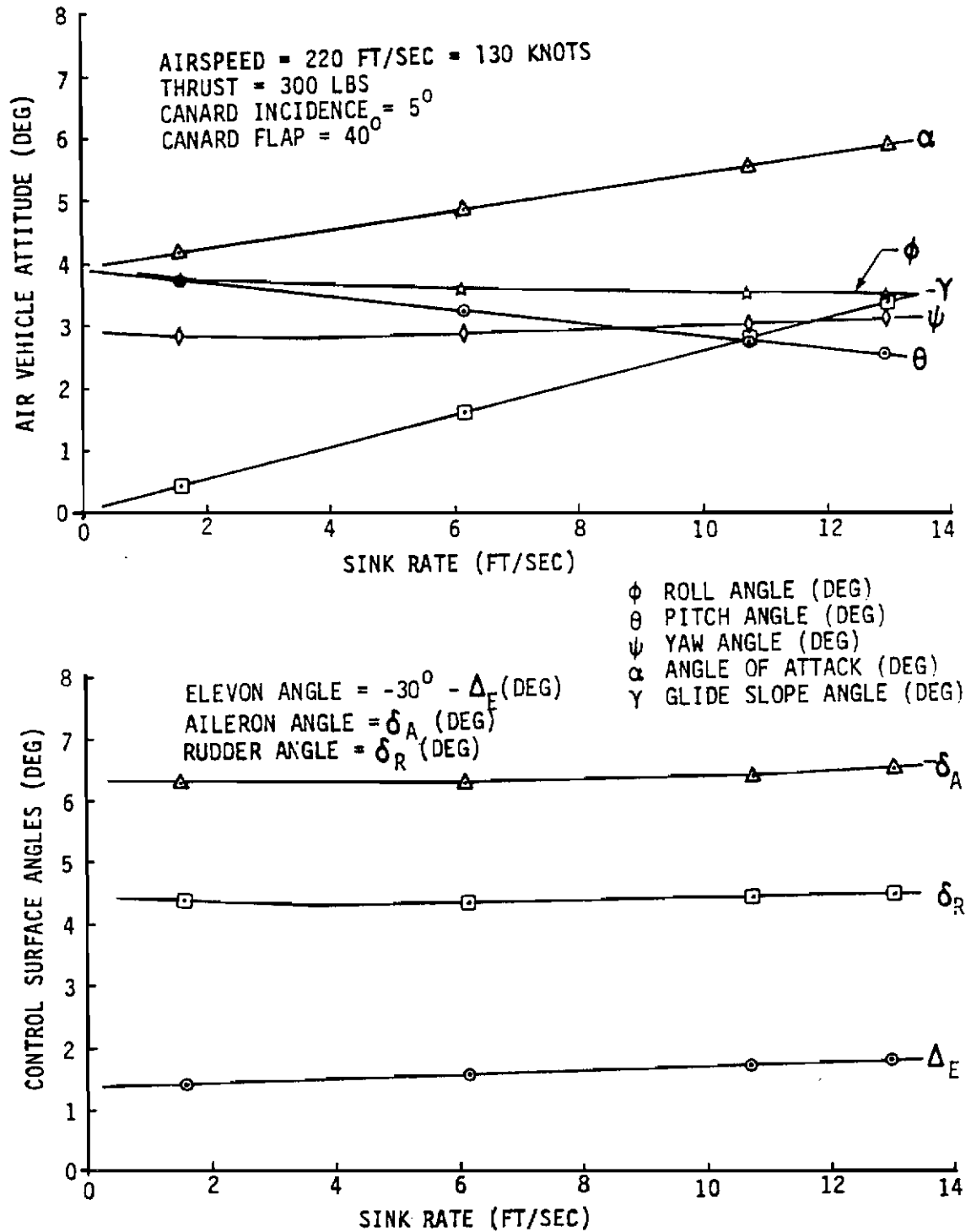


Figure 13 Boeing ARPV with ACSRS Deployed, Landing Approach Trim with 20 Ft/Sec Crosswind, Air Vehicle Attitude vs. Sink Rate

Contrails

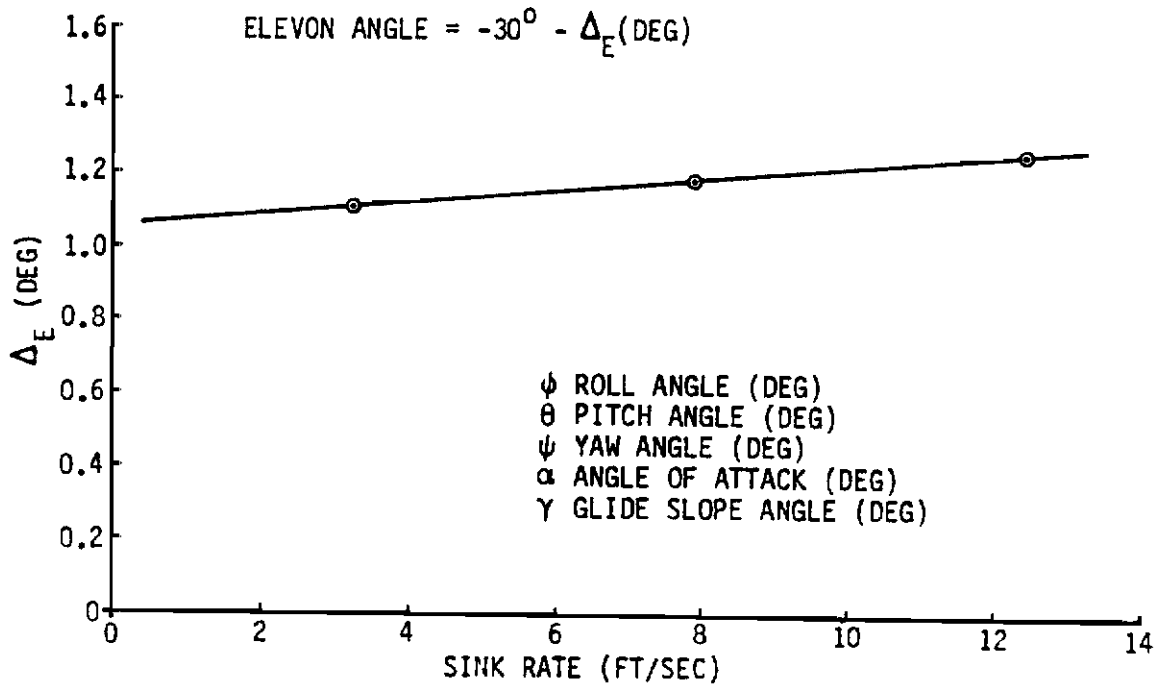
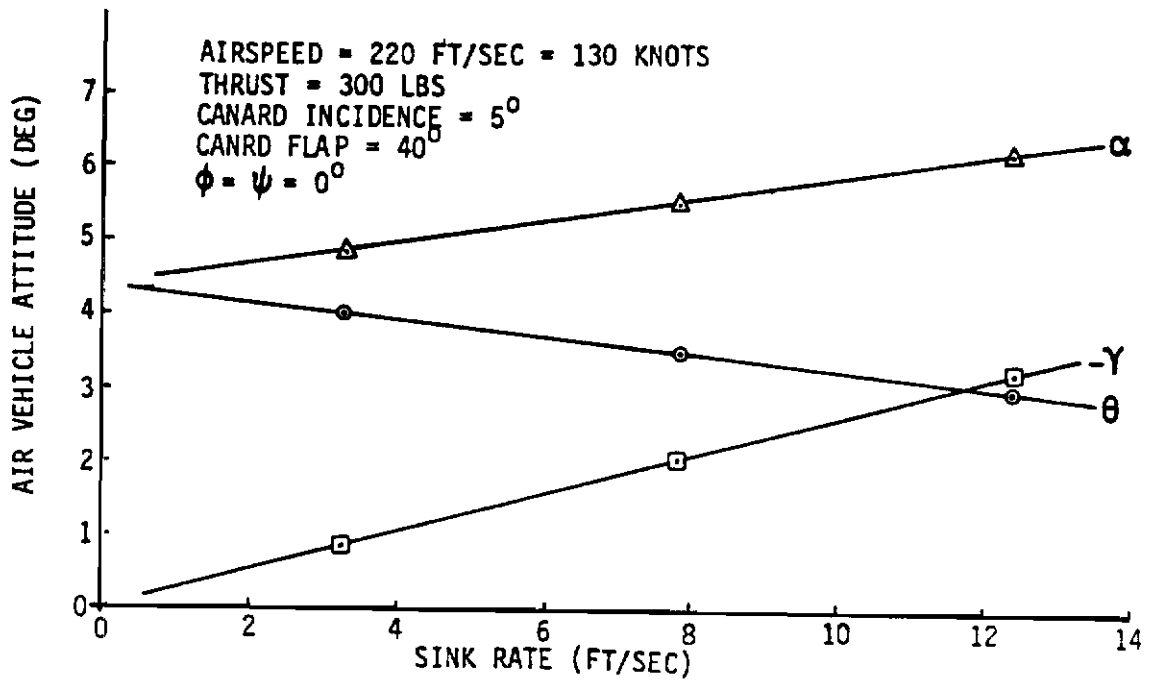


Figure 14 Boeing ARPV with ABSS Deployed, Landing Approach Trim with No Crosswind, Air Vehicle Attitude vs. Sink Rate

Contrails

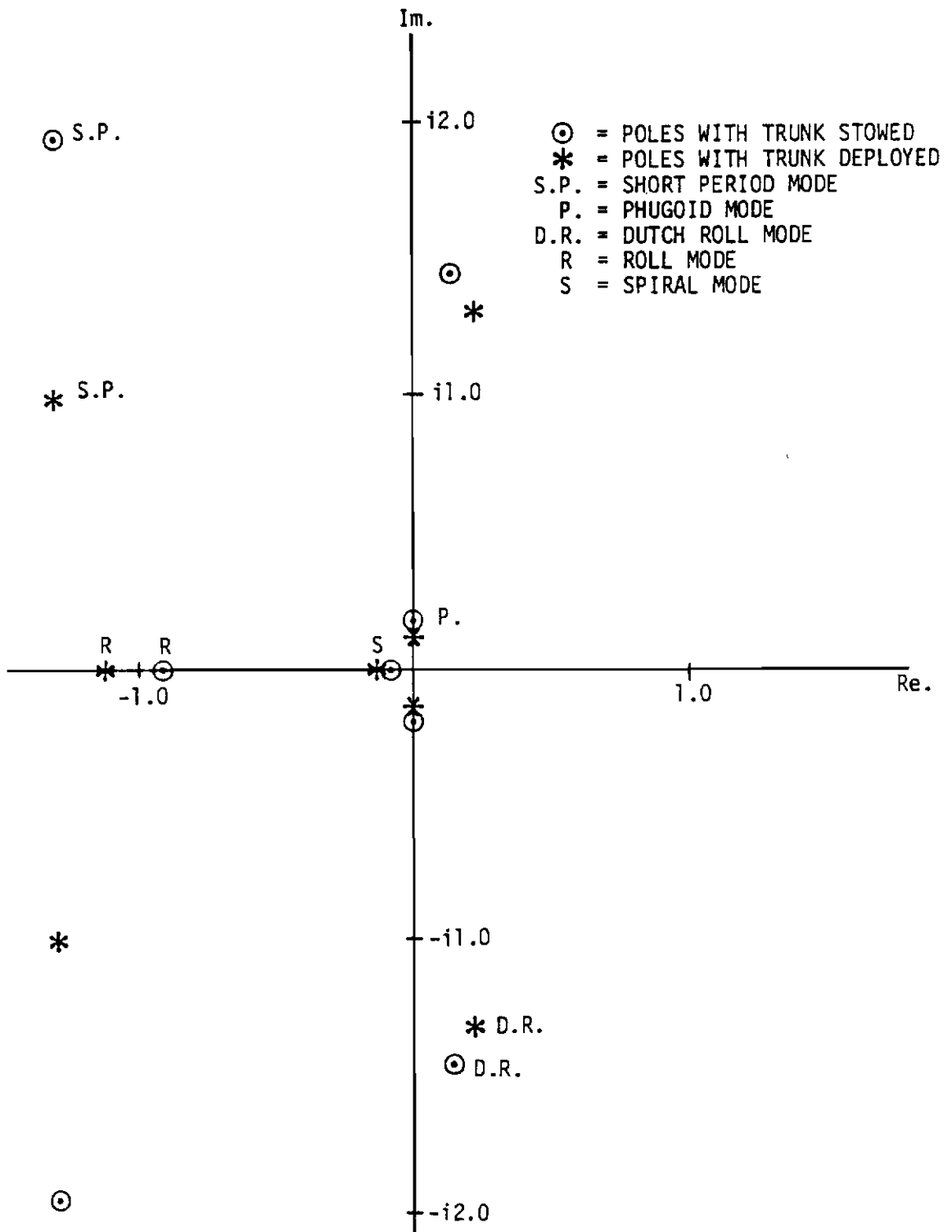


Figure 15 Root Locus Plot Showing Lateral and Longitudinal Modes for the Rockwell ARPV without SAS

roll and spiral mode frequencies increase slightly and remain stable. The dutch roll mode is unstable with the trunk stowed, and becomes slightly more unstable as the trunk is deployed. Because the dutch roll mode is unstable with the trunk stowed, an SAS would be required even without the air cushion recovery system. Therefore, as with the Boeing ARPV, the only air vehicle modification attributable to the ACRS installation is a possible change in the SAS controller gains.

The investigation of the air vehicle response to disturbances during landing approach required the inclusion of an SAS model into the air vehicle math model. As with the Boeing ARPV, the optimal controller component (OC) was used for this purpose. The inputs and outputs for the controller, along with its design approach, were similar to those used for the Boeing ARPV.

A simulation was performed with the Rockwell ARPV displaced from the landing approach glide path vector and simulation results show how the air vehicle responds to this position error and maneuvers to intercept the glide path. Figures 16 through 20 show some of the results. These results show that the air vehicle with a simple SAS model is stable and controllable. Better response could be obtained by making improvements to the optimal controller design, but such an effort was not necessary for this study.

Landing approach trim conditions were also defined by performing a series of steady state analyses. Figure 21 shows the results from this trim analysis. The results show how the air vehicle attitude is related to the glide path angle, sink rate and crosswind.

The analysis approach used for the Rockwell ARPV with the ABSS was very similar to that used for the vehicle with the ACRS. Results were also similar leading to identical conclusions.

d. Conclusions of Inflight Simulation

Program EASY simulation and analysis results have shown that the only impact of the ACRS and ABSS on the Boeing and Rockwell ARPV flight control system is a possible change in SAS and autopilot controller gains.

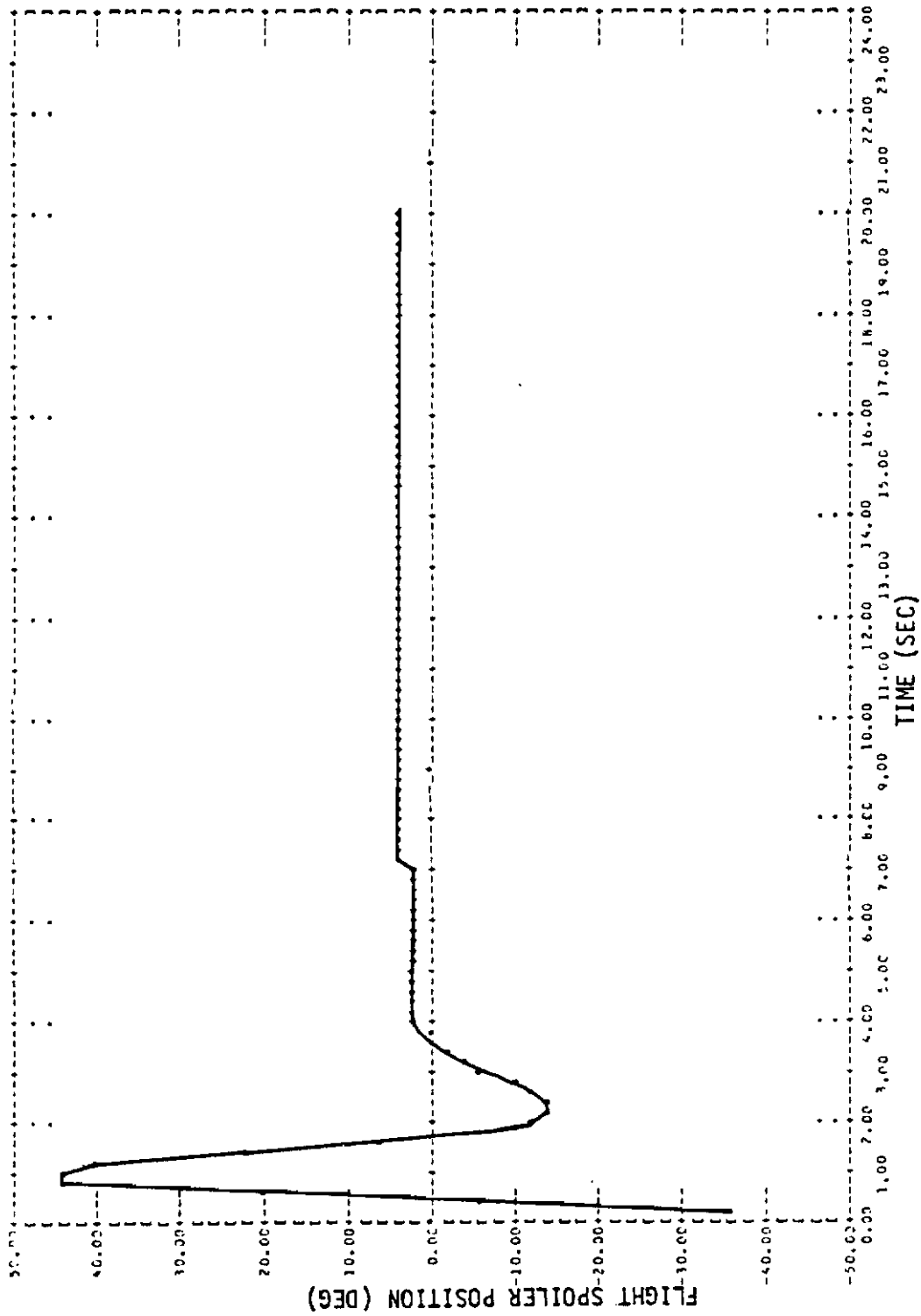


Figure 16 Rockwell ARPV with ACRS Deployed at Landing Approach, Response of Optimal Controller to Displacement From Glide Path, Flight Spoiler Position vs. Time

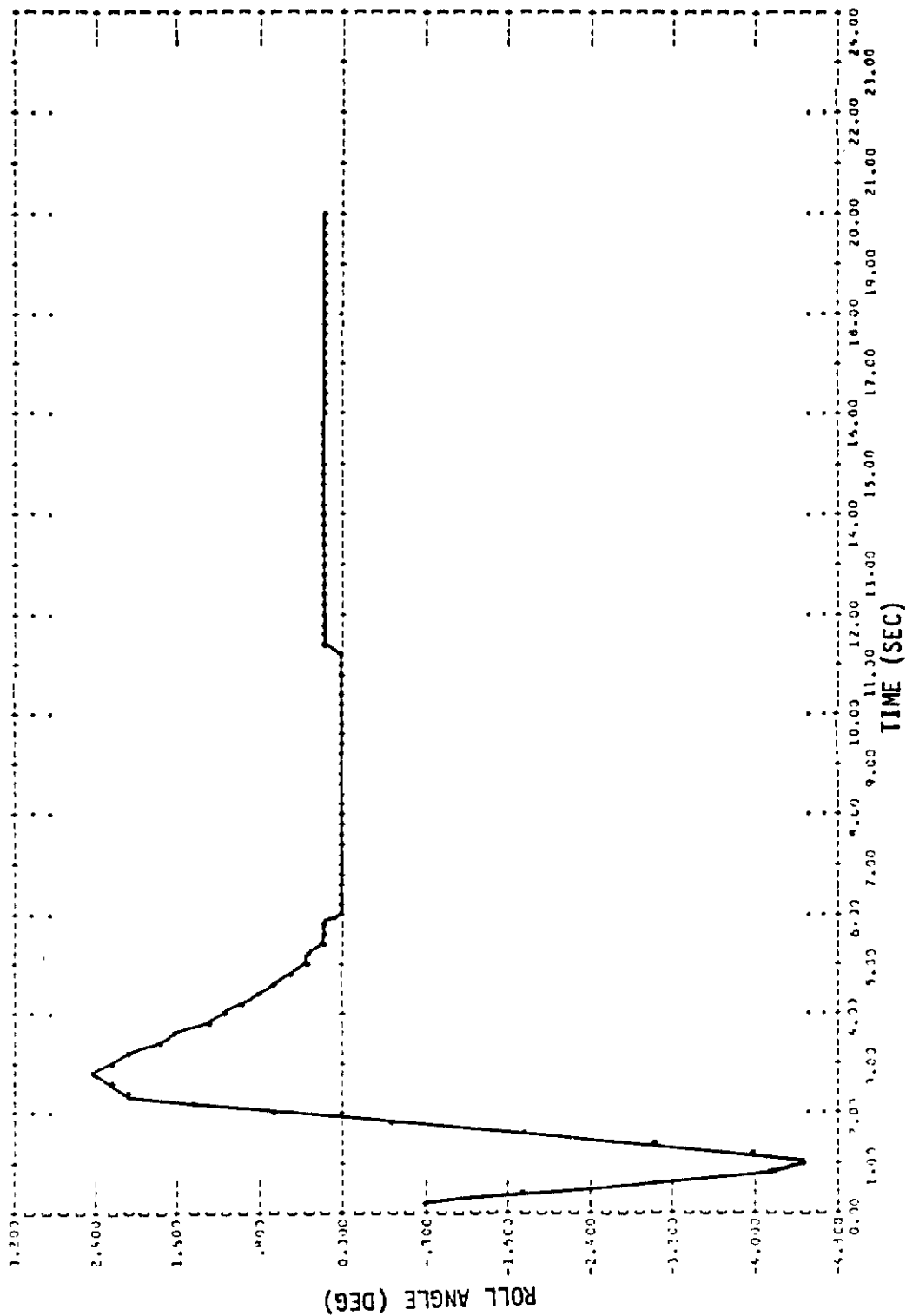


Figure 17 Rockwell ARPV with ACRS Deployed at Landing Approach, Response of Optimal Controller to Displacement From Glide Path, Roll Angle vs. Time

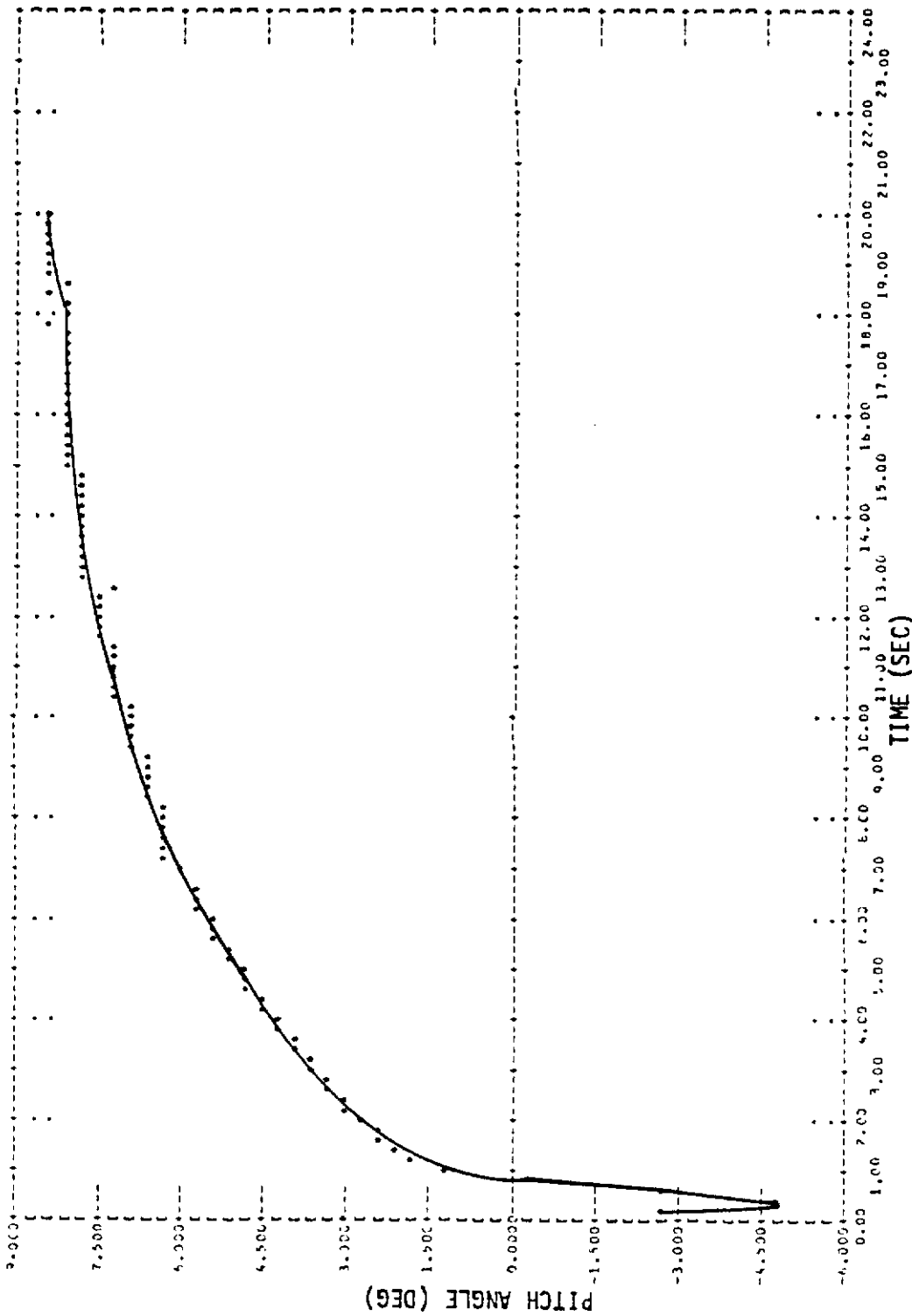


Figure 18 Rockwell ARPV with ACRS Deployed at Landing Approach, Response of Optimal Controller to Displacement From Glide Path, Pitch Angle vs. Time

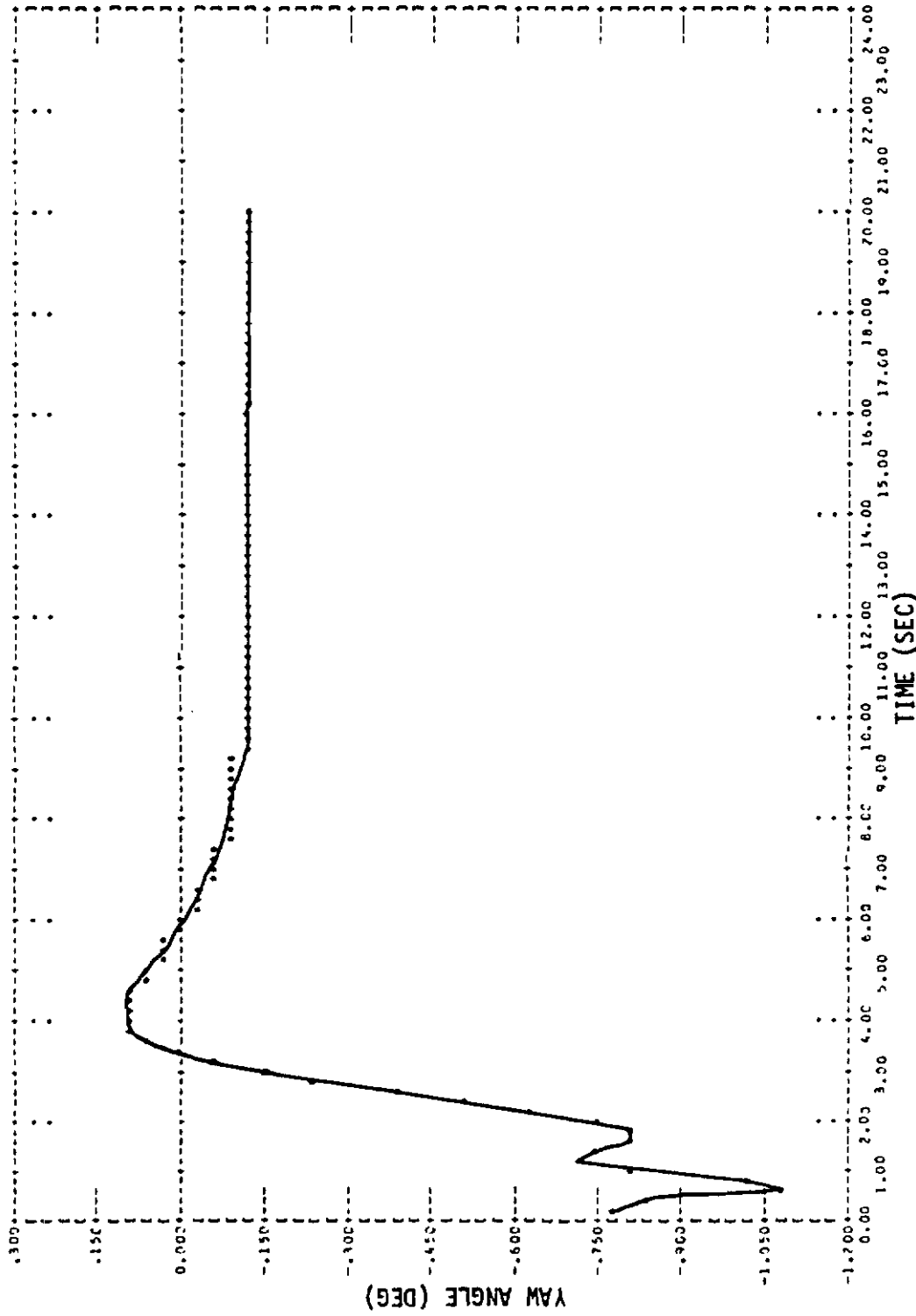


Figure 19 Rockwell ARPV with ACRS Deployed at Landing Approach, Response of Optimal Controller to Displacement From Glide Path, Yaw Angle vs. Time

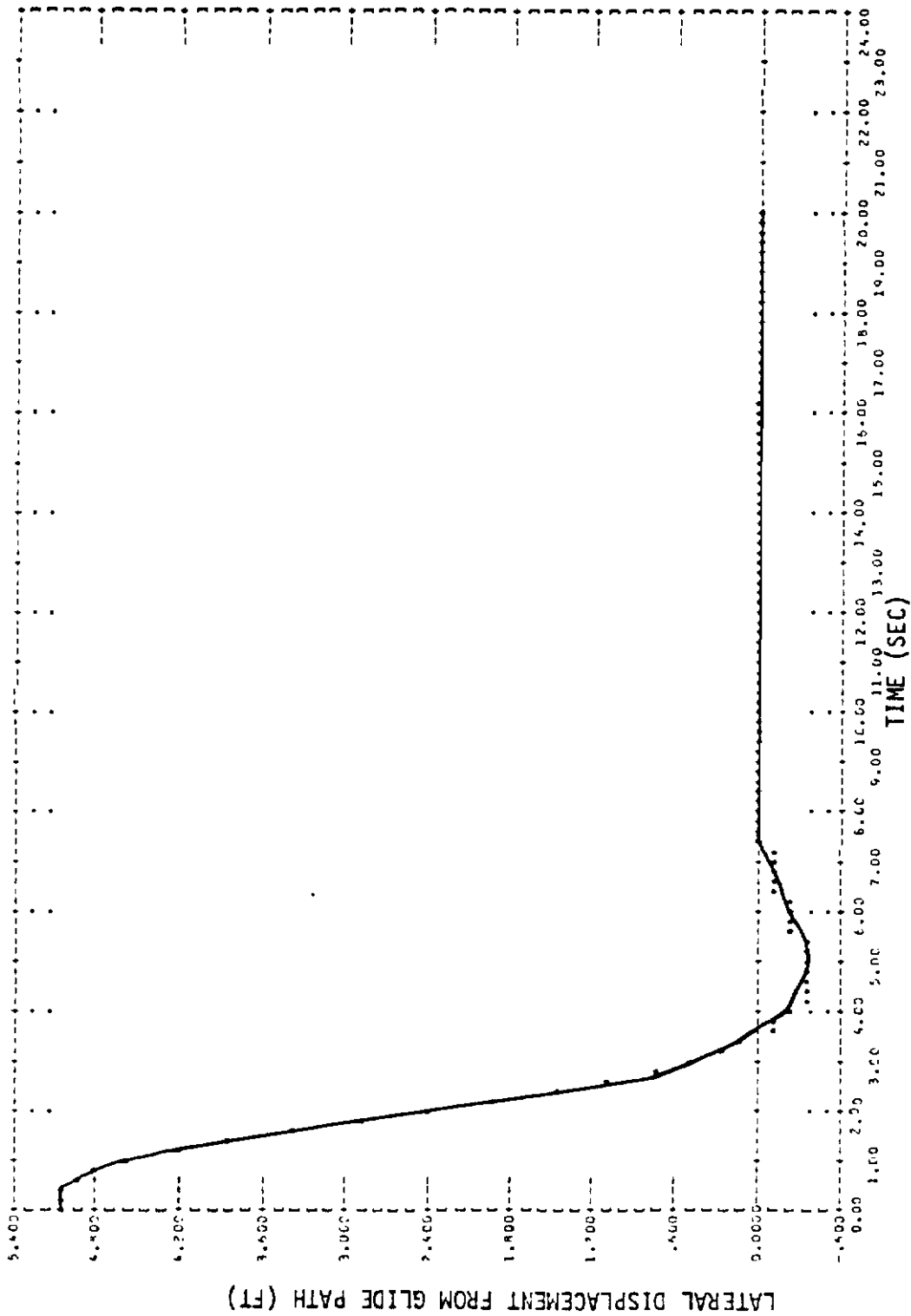


Figure 20 Rockwell ARPV with ACRS Deployed at Landing Approach, Response of Optimal Controller to Displacement From Glide Path, Lateral Displacement From Glide Path vs. Time

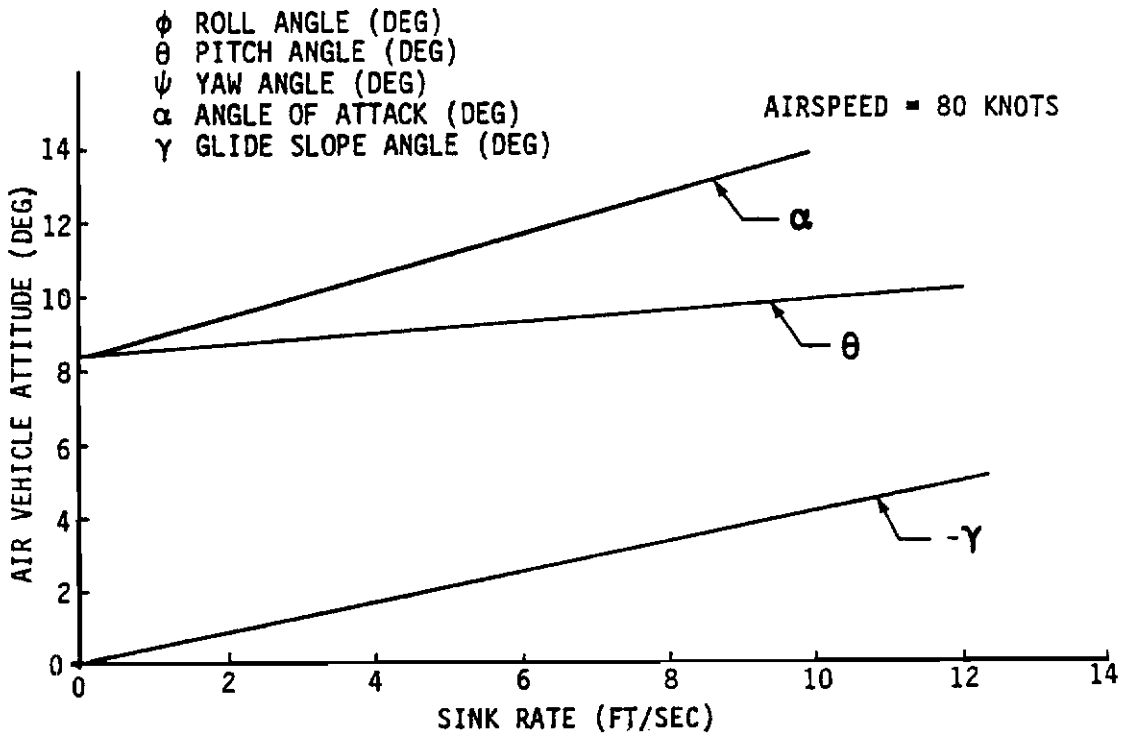
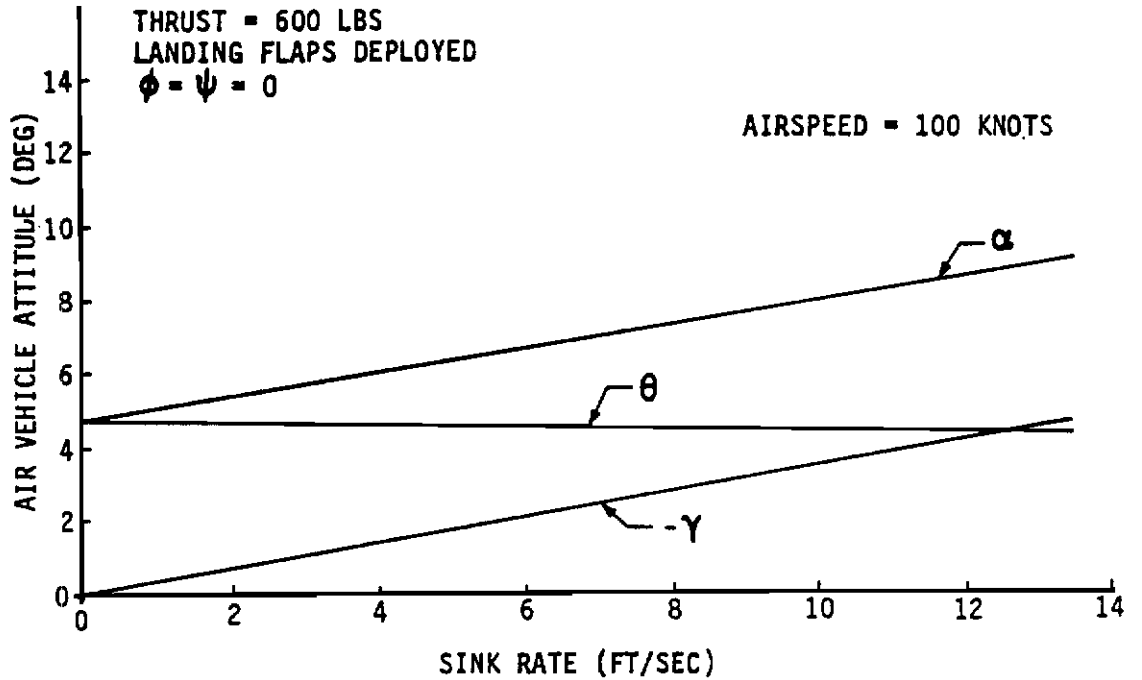


Figure 21 Rockwell ARPV with ACRS Deployed, Landing Approach Trim with No Crosswind, Air Vehicle Attitude vs. Sink Rate

Modifications to the control surfaces or airframe are not necessary if reasonable constraints are imposed on the sizes of the air cushion trunk and air bag skids so they do not cause aerodynamic interference.

2. LANDING SIMULATIONS AND ANALYSIS

The principal objective of this study was to evaluate the performance of several different recovery systems by using program EASY as a design analysis tool. Air bag skid and air cushion trunk recovery systems were investigated for both the Boeing ARPV and Rockwell ARPV. The design variables of each recovery system configuration were investigated to determine their effects on landing dynamics to identify the conditions under which satisfactory performance was achieved, and to arrive at an optimum configuration.

Satisfactory performance meant that several constraints were met. These consisted of load limit constraints, structure-to-ground clearance constraints, and directional stability constraints. Optimum performance meant that all the above constraints were satisfied while the recovery system weight, size, power requirements and complexity were minimized.

The general approach followed was to first construct mathematical models of the landing system components for program EASY by identifying realistic air vehicle attitude and speed conditions at touchdown, and by developing preliminary designs for the recovery trunks and air supply systems. These math models were then used in several three and six degree-of-freedom simulations which showed the effects on system performance of variations to the touchdown initial conditions and the system design parameters. The results of these simulations were used to develop several parametric design curves which relate design parameters and touchdown initial conditions to system performance.

a. Development of Math Models

The air cushion and air bag skid recovery systems consist of several interacting components. The principal components which dominate

the dynamic behavior of the systems were included in the system math models. Standard program EASY subroutines were available for all of these components but input parameters describing each particular piece of hardware had to be defined. This section describes how touchdown initial conditions, the air cushion trunk and air bag skid, air supply components, and arresting gear components were defined for inclusion in program EASY.

(1) Touchdown Conditions

One of the results from the inflight analysis described in Paragraph 1 was the definition of mean air vehicle attitude and thrust conditions when trimmed during landing approach. Disturbances cause the air vehicle to be perturbed about these mean conditions, and the specific perturbations which will occur at landing impact are critical to this study. It was possible to define design envelopes of initial landing conditions which included all the air vehicle attitude and rate variables. Each variable was described by a normal distribution, which was defined by a mean and a standard deviation. The extreme conditions for each envelope were defined by those combinations of variables having a joint likelihood of occurrence equal to a constant. MIL-A-8863A (Reference 5) gives rules and tabulated data for defining these envelopes of landing impact conditions for different types of air vehicle and landing condition. Table 6 was developed from MIL-A-8863A and shows the standard deviations for the air vehicle variables describing landing impact conditions. This table and the MIL-A-8863A rules were used as a guide in defining the worst case landing impact conditions for the Boeing and Rockwell ARPVs.

Nose down (negative pitch angle) landings were not included in the simulations. Landing conditions within two standard deviations (2σ) of the mean landing conditions were used to define the envelope of worst case design conditions. There is a 95.45% probability that these will be the worst case conditions.

(2) Inelastic Air Cushion Recovery Trunk Design

This preliminary design phase consisted of the investigation of those parameters which affect the dynamic characteristics of an air

Table 6

Variation of Landing Impact Conditions

<u>Variable</u>	<u>Standard Deviation (σ)</u>
Approach Speed (knots)	5.0
Horizontal Ground Speed (knots)	8.0
Sinking Speed (ft/sec)	1.33
Air Vehicle Pitch Angle (deg)	2.25
Air Vehicle Roll Angle (deg)	2.5
Air Vehicle Roll Rate (deg/sec)	3.0
Air Vehicle Yaw Angle (deg)	2.5

Contrails

cushion trunk constructed of inelastic materials, the development of design relationships for the trunk, and the specification of those input parameters required by the program EASY trunk model. Design details such as the trunk-to-fuselage attachment method, the trunk material properties, and trunk stowage method are considered in Section III. Three operating conditions were investigated including landing approach with the trunk deployed, landing impact, and landing slideout. The program EASY input parameters for the trunk model include the trunk installation dimensions, dimensions of the lubricated area and its porosity, and coefficients of friction for the lubricated and unlubricated portions of the trunk.

Some of the constraints on air cushion trunk dimensions were outlined in Paragraph 1.a(1). For the Boeing ARPV these constraints included the tailhook pivot at the rear, and the canard at the front. Trunk width is constrained by the fuselage width, unless some type of extendable trunk support structure is used. Figure 22 shows a design variation which increases the width of the deployed trunk. However, this configuration is not practical with the low wing design of the Boeing vehicle. Wing lift would be impaired. The only constraint on the size of the Rockwell ACRS trunk is the rear tailhook pivot. The hinged trunk support fairings could be lengthened or widened to adjust for various trunk sizes and fuselage attachment locations. The initial trunk sizes used in the landing simulations, shown in Figures 23 and 24, were preliminary estimates of the sizes required. These dimensions were later changed when landing simulations made it apparent that modifications were necessary.

Lubrication area, porosity, trunk material, trunk pressure, and runway conditions affect the friction forces acting on the ACRS trunk. Very little test data is available on these subjects, especially data concerning the effectiveness of trunk lubrication. However, some data were found in Reference 6 which was used to define a relationship between the friction coefficient and a lubrication flow coefficient. Figure 25 shows the relationship which was derived and Table 7 lists the baseline trunk dimensions and parameters for the Boeing and Rockwell vehicles.

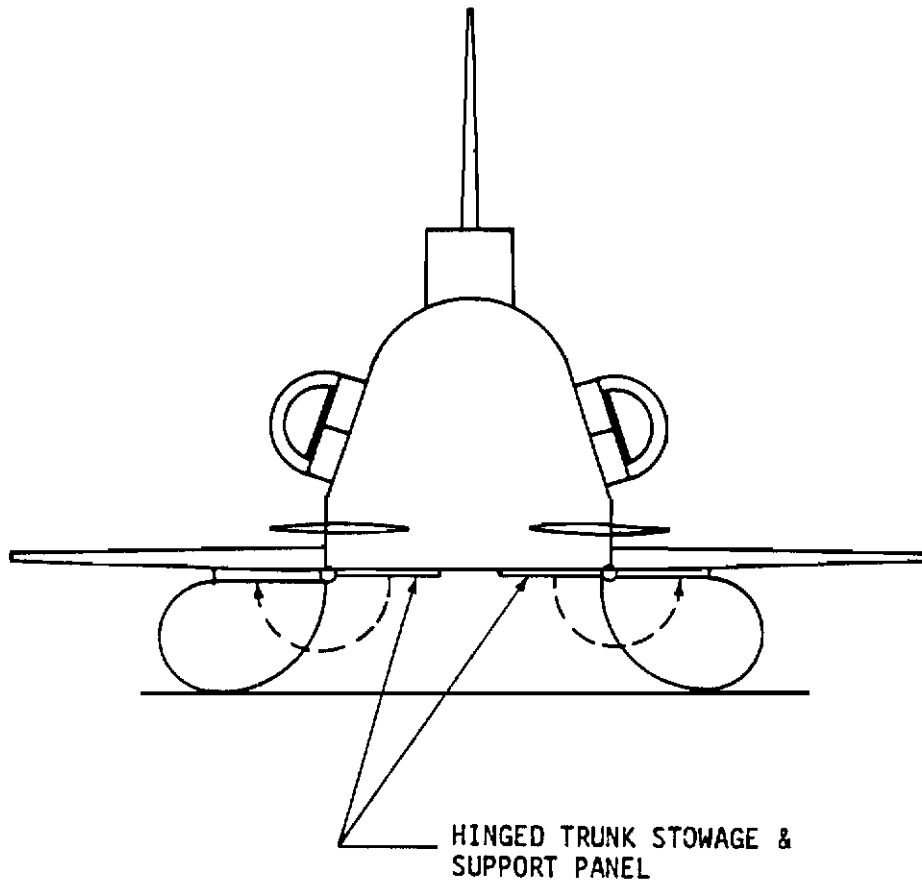


Figure 22 Boeing ARPV with Wide Stance ACRS Installation

NOTE: DIMENSIONS SHOWN WERE ESTIMATES MADE FOR INITIATING SIMULATION

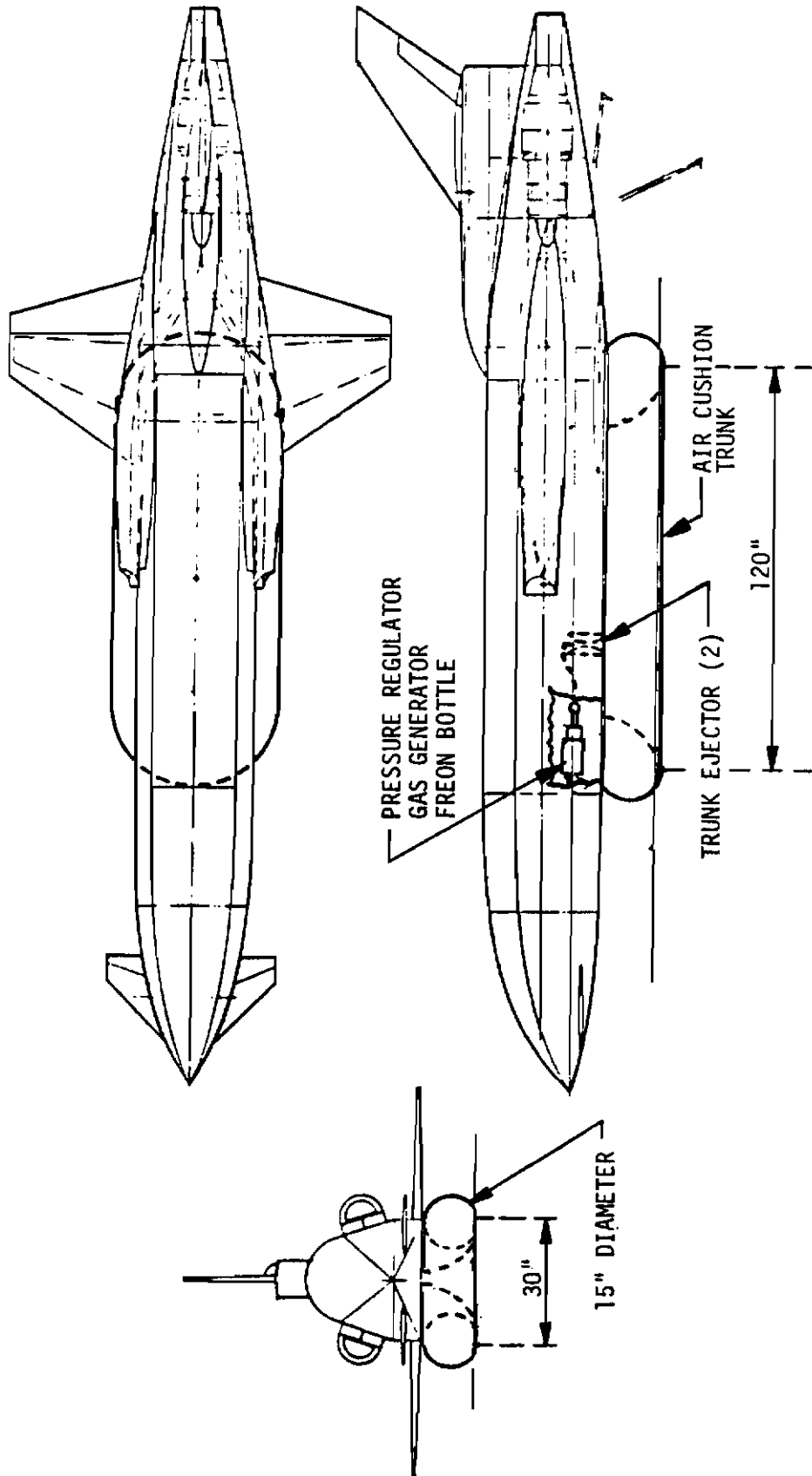


Figure 23 Boeing Vehicle with Baseline Air Cushion Configuration

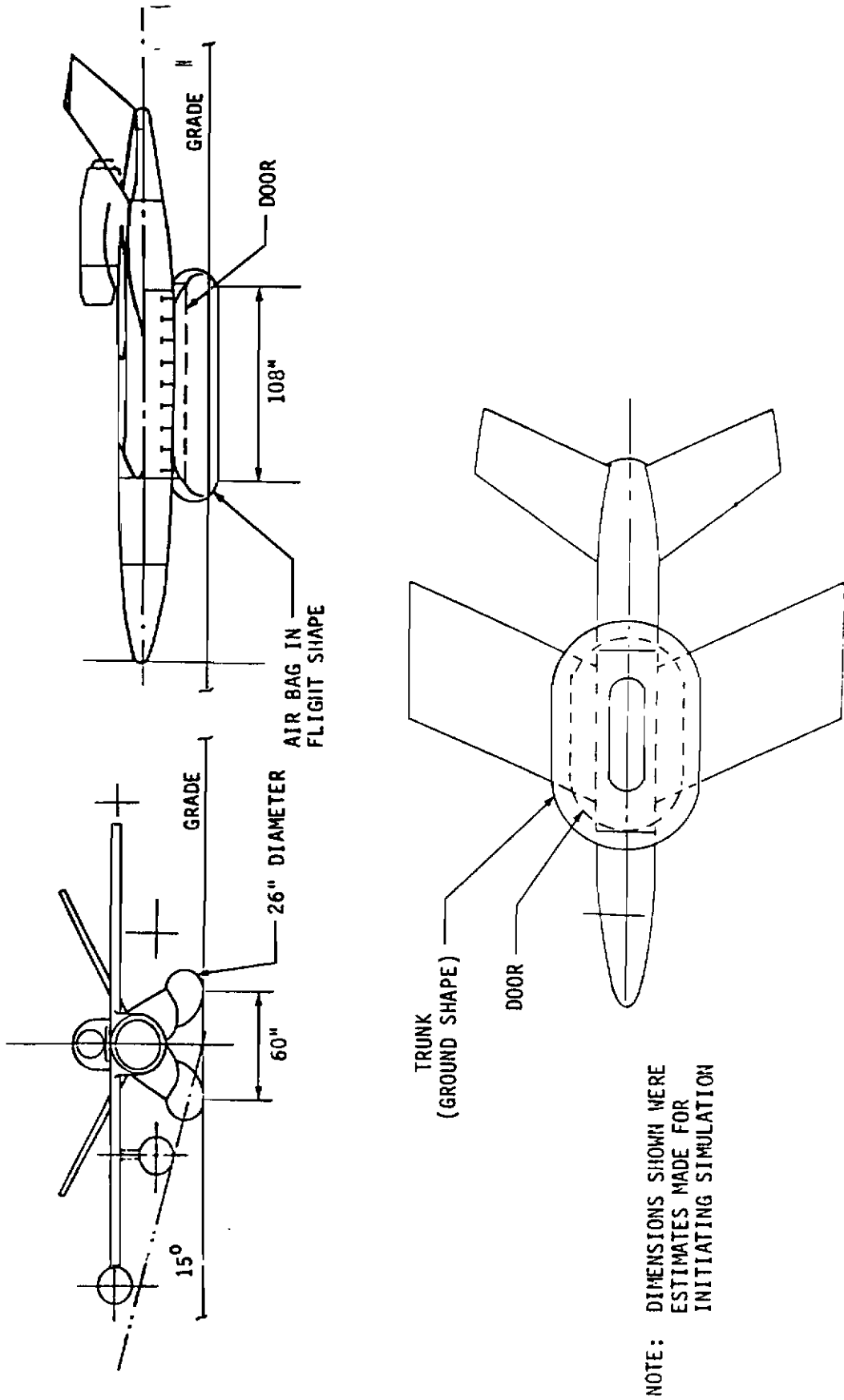


Figure 24 Rockwell Vehicle with Baseline Air Cushion Configuration

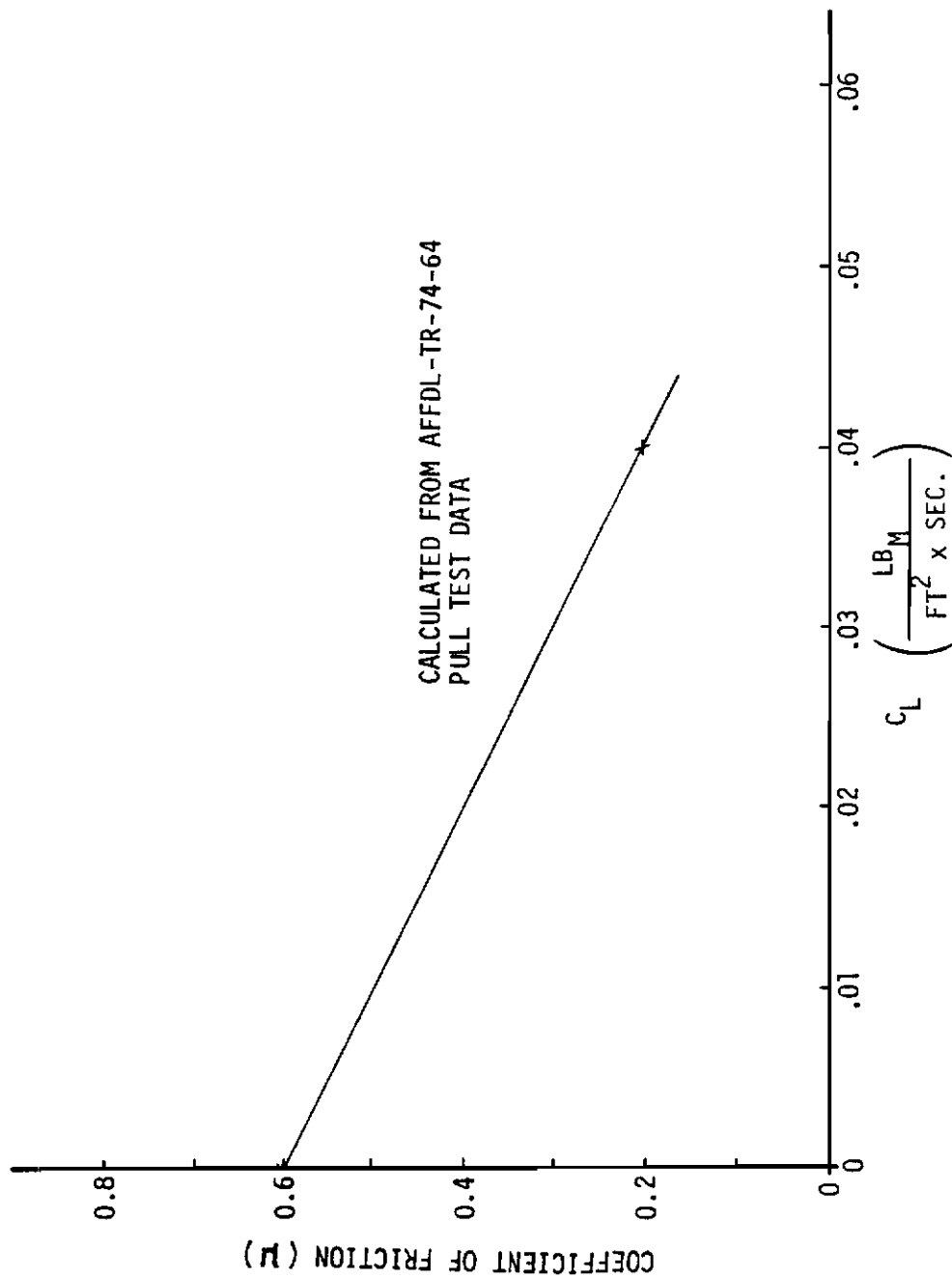


Figure 25 Relationship Between Friction Coefficient and Trunk Lubrication Flow

TABLE 7
BASELINE ACRS DIMENSIONS AND PARAMETERS

<u>Parameters</u>	<u>Boeing ARPV</u>	<u>Rockwell ARPV</u>
Trunk Coefficients of Friction		
Lubricated Surfaces	0.2	0.2
Unlubricated Surfaces (dry runway)	0.7	0.7
Trunk Porosity	.0125	.0125
Area of Trunk Lubrication		
Width of Perforated Area (inches)	20.0	10.0
Length (forward 1/3 of trunk, inches)	97.1	114.2
Flow Discharge Coefficients		
CDGAP (gap between trunk and ground)	0.9	0.9
CD1 (free portion of trunk)	0.6	0.6
CD2 (flattened portion of trunk)	0.2	0.2
CDA (relief valve)	0.9	0.9
Trunk Damping Coefficient (lbf-sec/in ³)	0.02	0.02
Trunk Dimensions		
A (horiz. distance between fuselage attach points, inches)	13	22
B (vert. distance between fuselage attach points, inches)	0	7
LO (trunk meridian length, inches)	40.84	69.1
Number of trunk elements per side	11	8
Distance between trunk center of pressure and vehicle C.G. (inches)	0	0
Overall length (inches)	120	108

(3) Air Bag Skid Design

The initial air bag skid designs used for the Boeing and Rockwell vehicles are shown in Figures 26 and 27. Dimensional constraints for the air bag skids were similar to those for the air cushion recovery trunks. Since the air bag skid recovery configurations will use arrestment systems, lubrication is not necessary for directional stability and was not included in program EASY math models of the air bag skids. Table 8 lists the initial air bag skid dimensions and parameters used in the program EASY math models.

(4) Air Supply System

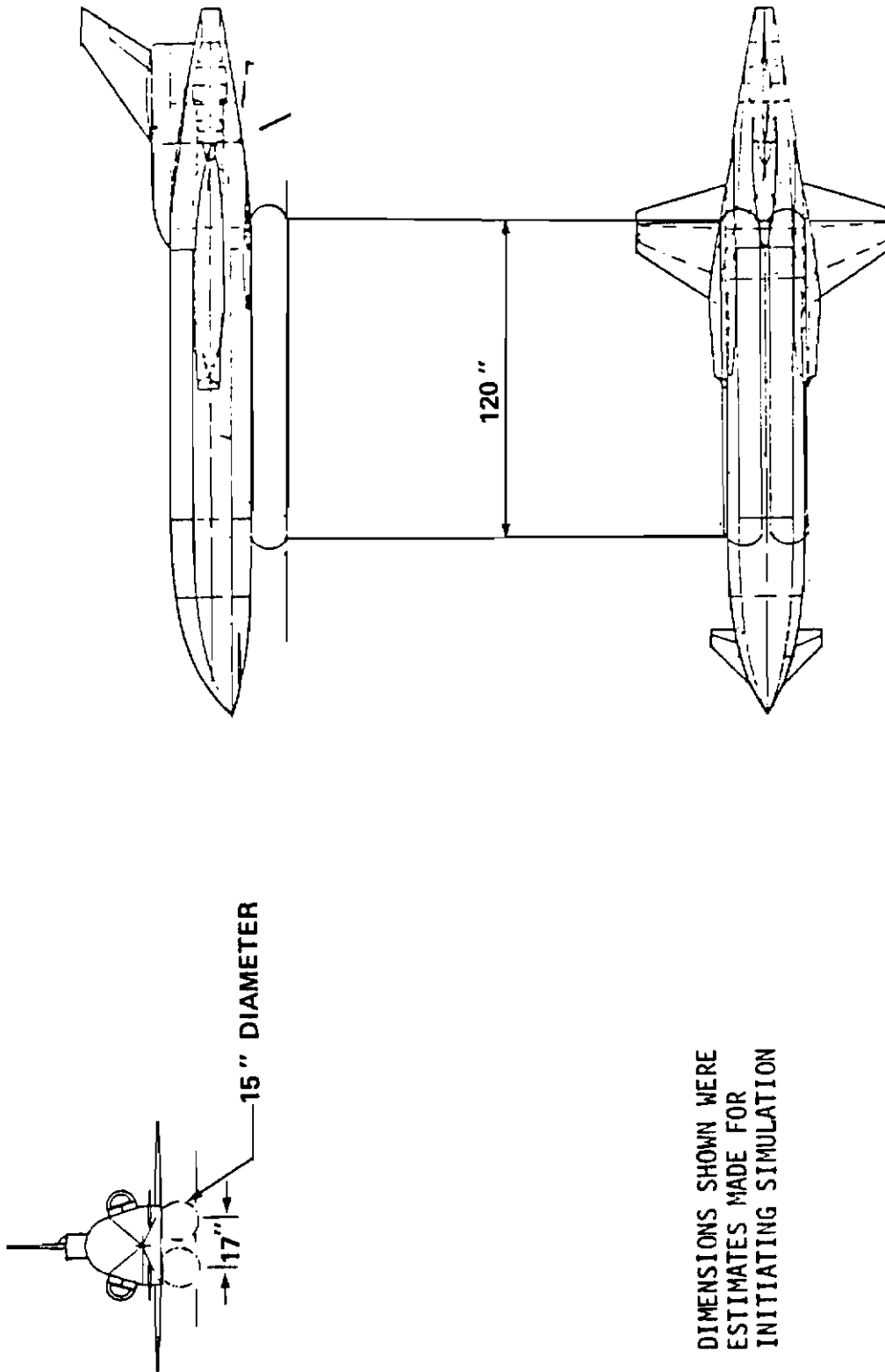
The air supply system for air cushion and air bag skid systems consists of a power source, a flow generator, flow controllers, ducting, relief and backflow check valves, air inlets or ram air scoops and the trunk or air bag. Various power sources and several different flow generators were investigated.

Alternative power sources include engine bleed air, engine drive pad shaft power, cool gas generators, compressed gas bottles, ram air, and auxiliary power units. The baseline Boeing ARPV concept used a cool gas generator as the power source for its air bag skid recovery system. The suitability of this power source was evaluated for both the Boeing air bag skid and the air cushion trunk recovery systems.

Alternative flow generators include shaft driven fans, ejector nozzles, tip turbine fans, and hub turbine fans. The feasibility of these components was investigated for both air vehicles.

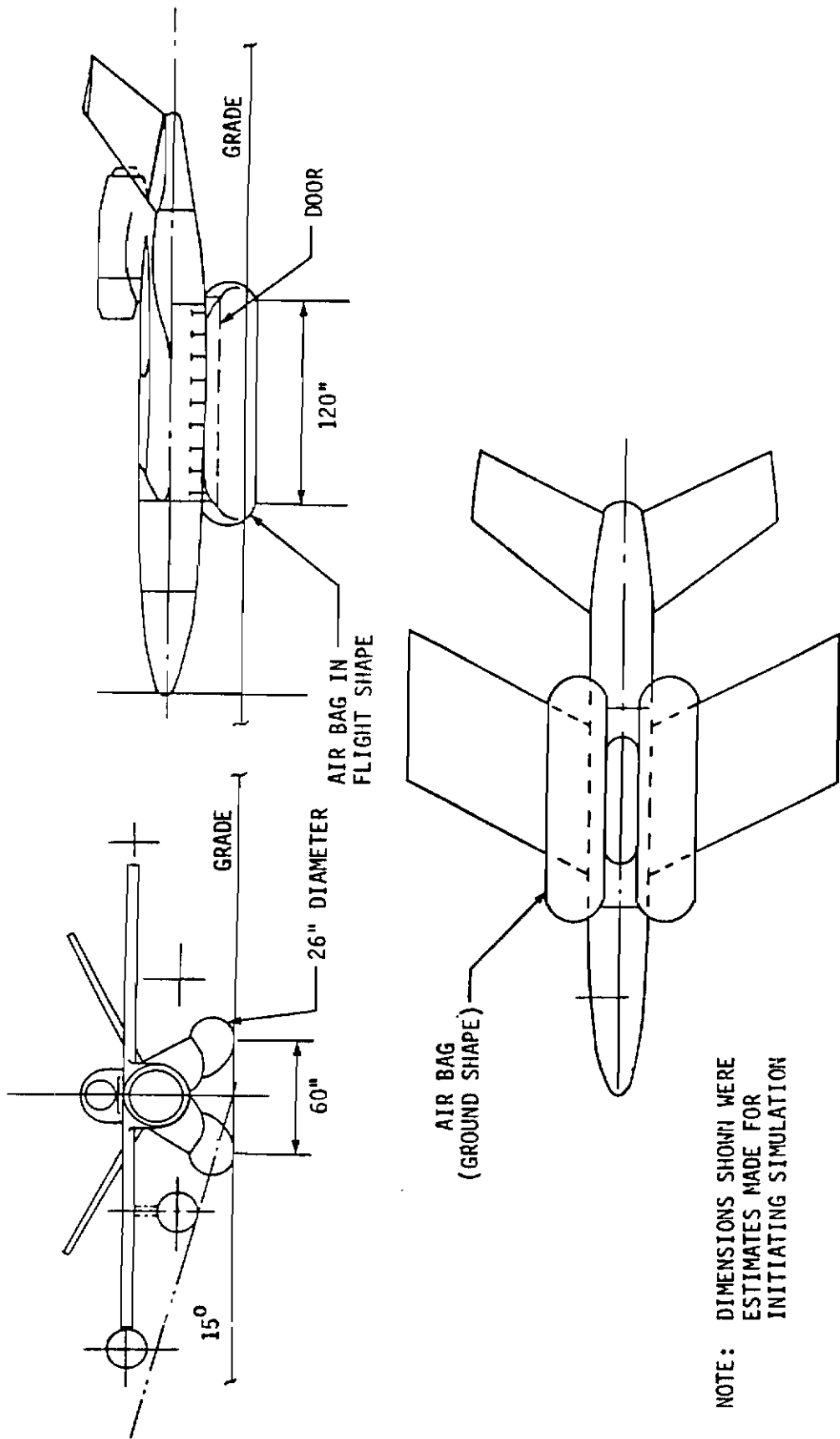
(a) Boeing ARPV

The Boeing ARPV uses the Teledyne Continental CAE-373 engine. Figure 28 shows the engine's basic dimensions and general layout and Table 9 lists engine performance data. This engine has only one pad available for power extraction. This pad is located at the engine inlet where the current concept shows a 4 kw electrical alternator directly coupled to the compressor shaft which has a maximum speed of 42000 rpm. Figure 29 shows the electrical load profile for the air vehicle and



NOTE: DIMENSIONS SHOWN WERE ESTIMATES MADE FOR INITIATING SIMULATION

Figure 26 Boeing Vehicle with Baseline Air Bag Skid Configuration



NOTE: DIMENSIONS SHOWN WERE ESTIMATES MADE FOR INITIATING SIMULATION

Figure 27 Rockwell Vehicle with Baseline Air Bag Skid Configuration

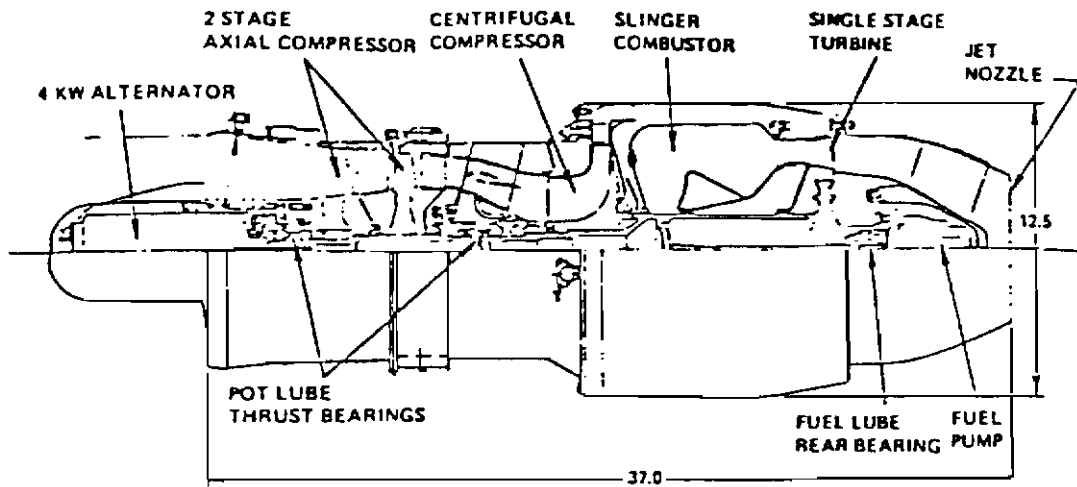


Figure 28 Teledyne CAE-373 Turbojet Engine for Boeing ARPV

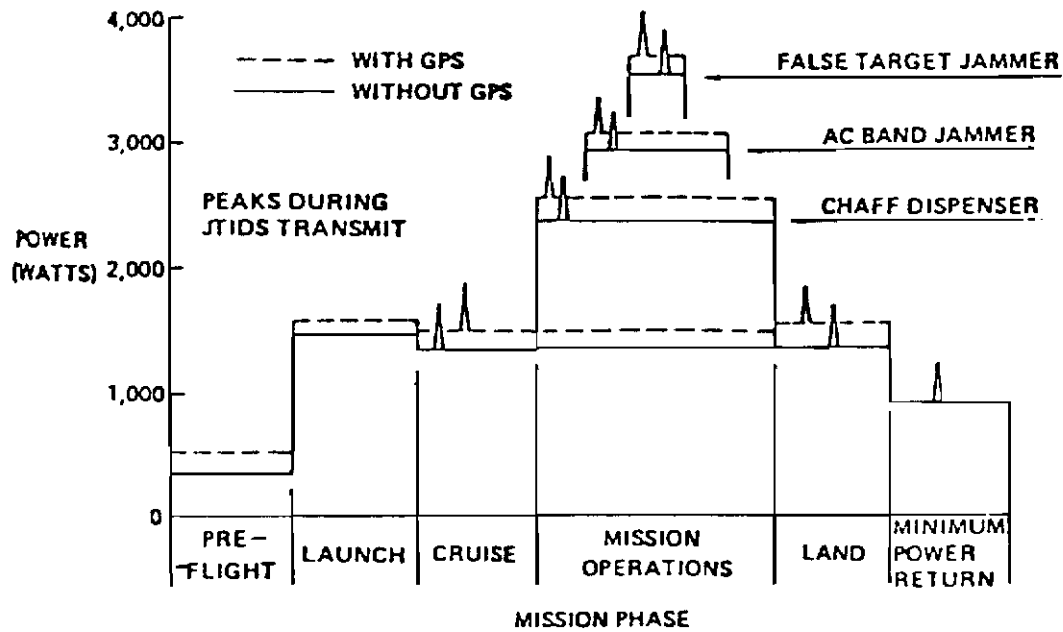


Figure 29 Boeing ARPV Electrical Load Profile

(REFERENCE 1)

TABLE 8
BASELINE ABSS DIMENSIONS AND PARAMETERS

<u>Parameters</u>	<u>Boeing ARPV</u>	<u>Rockwell ARPV</u>
Bag Coefficients of Friction (no lubrication)	0.7	0.7
Flow Discharge Coefficients CDA (relief valve)	0.9	0.9
Bag Damping Coefficient (lbf-sec/in ³)	0.02	0.02
Bag Dimensions		
A (horiz. distance between fuselage attach points, inches)	13	21
B (vert. distance between fuselage attach points, inches)	0	7
L0 (bag meridian length, inches)	31.4	47.6
Number of bag elements per side	6	6
Distance between bag center of pressure and vehicle C.G. (inches)	0	0
Overall length (inches)	120	120

previous studies indicate that a 10 kw alternator is the maximum size that could be installed with current technology.

Table 9
MODEL CAE-373 TURBOJET ENGINE PERFORMANCE

Parameter	S.L.S.	S.L. Mach 0.85	20K Mach 0.85
Thrust - pounds	970	1030	585
SFC -pound/hour/pound	1.04	1.35	1.25
Airflow-pound/second	13.60	19.30	9.97
EGT - deg F	1430	1450	1445

(Reference 1)

A moderate amount of bleed air is also available. The maximum engine high pressure bleed with power extraction is approximately 0.70 pounds mass per second. Figure 30 shows bleed air pressure and temperature, and engine thrust as a function of engine speed. The bleed air temperature is quite high (475 deg F at idle speed), so it would be necessary to mix this bleed air with sufficient cool air to reduce the supply air temperature to less than 200 deg F before it enters the trunk.

Location of the air supply system components is critical because space is very limited on the Boeing ARPV. The baseline air vehicle has the cool gas generator installed below the engine, where the space available limits the generator size. The weapons bay provides an alternate

Contrails

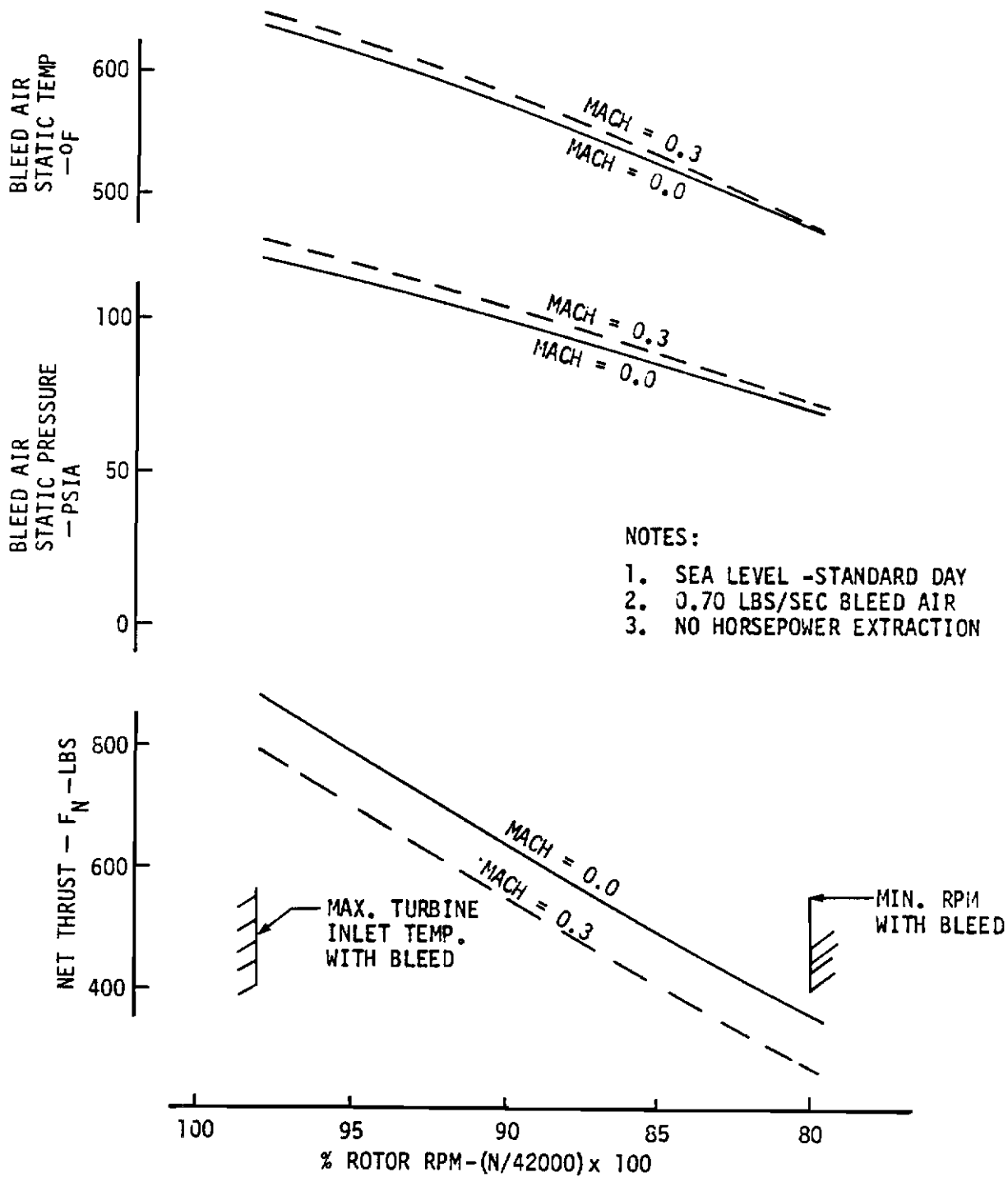
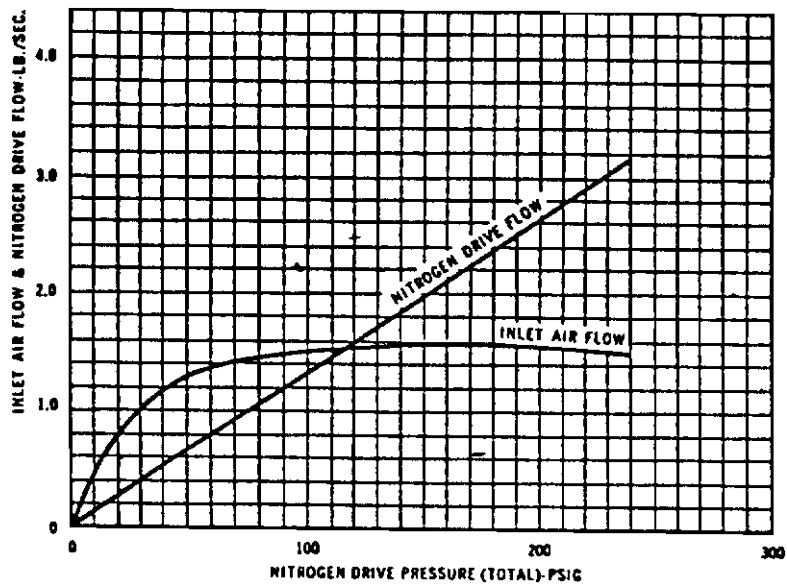


Figure 30 CAE-373 Performance with Bleed Air

location. Space exists on either side of the bomb rack, and since the gas generator must be replaced after every mission, the wide weapons bay doors and extra room may improve serviceability. The gas source for the air cushion trunk which requires a higher flow rate than the air bag skid system will not fit in the weapons bay so it will have to be installed under the weapons bay where fuel is carried. Fuel volume lost is equivalent to the volume of the fan or ejector which is installed.

Another important consideration is the typical pressure-flow characteristic of each component. Reference 7 compares the performance of ejectors and tip turbine fans using a dimensionless "performance ratio" and "augmentation ratio" as comparison parameters. Figures 31 and 32 show the two components which were tested, and Figures 33 and 34 show the augmentation ratio and performance ratio test results. The augmentation ratio is defined as the ratio of pounds mass of secondary flow per pound mass of drive air flow. The test results show that, in general, a tip turbine fan will produce more total flow than an ejector using the same drive air flow. The performance ratio is defined as the ratio of the secondary flow rate at various back pressures to the secondary mass flow rate at ambient back pressure. Figure 33 shows that tip turbine fan flow is much more sensitive than ejector flow to back pressure variations. Because the ejector is the simplest and most reliable device, and because large back pressure variations will occur for an ACLS application, the ejector was chosen to be included in the program EASY model of the Boeing ARPV air cushion and air bag skid recovery systems.

To estimate the size and number of ejectors needed for the landing simulations, the pressure-flow characteristics of the air cushion trunk and air bag skids were analyzed at three operating conditions: landing approach with the trunk deployed, landing impact, and landing slideout. During landing approach, all of the trunk lubrication orifices are exposed to ambient pressure, so trunk outflow is high. During landing slideout however, many of the lubrication orifices are flattened against the ground, so their effective discharge coefficient is decreased thus reducing trunk outflow. Figure 35 summarizes some of the results.



TECH DEVELOPMENT INC.

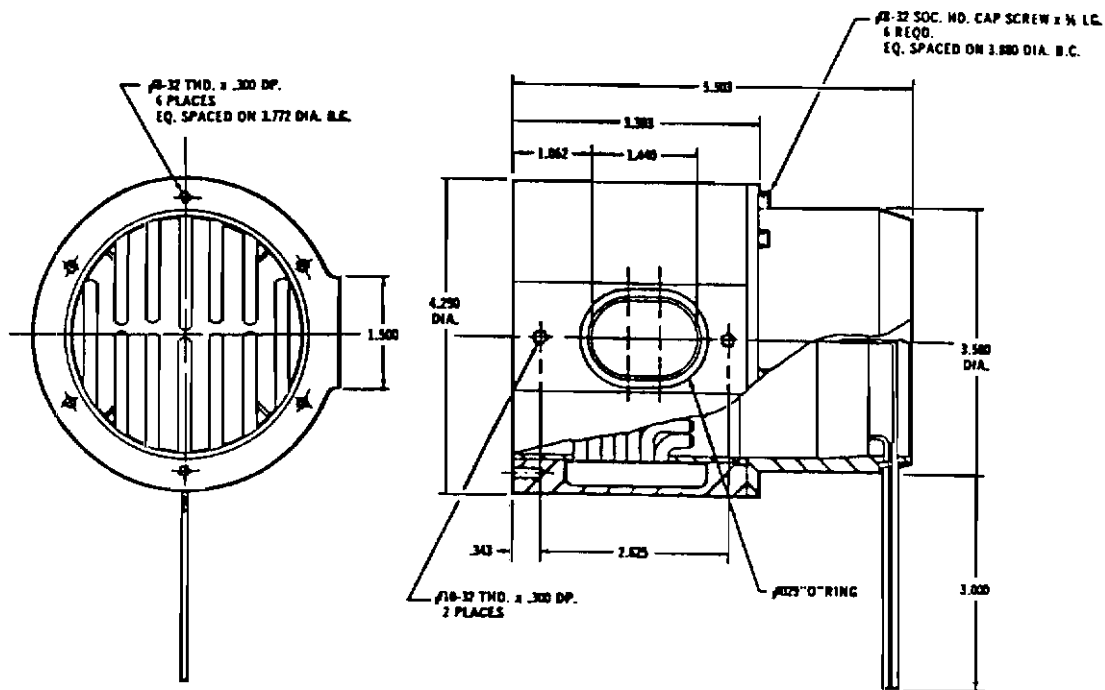
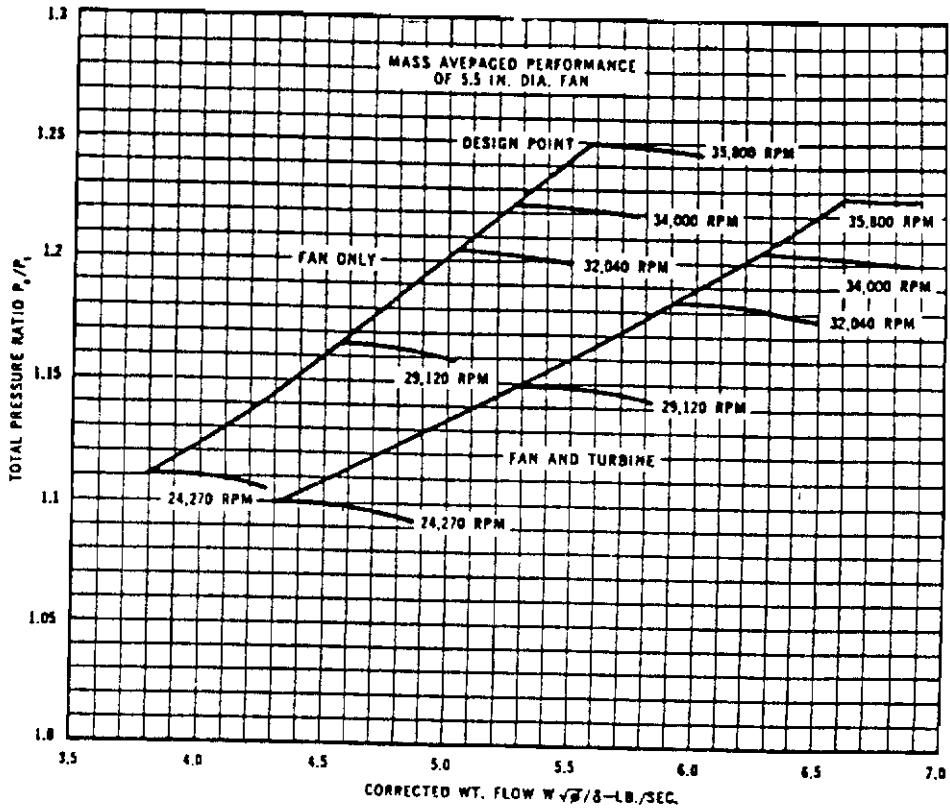


Figure 31 Model TD-530 Ejector Nozzle

(REFERENCE 8)



TECH DEVELOPMENT INC.

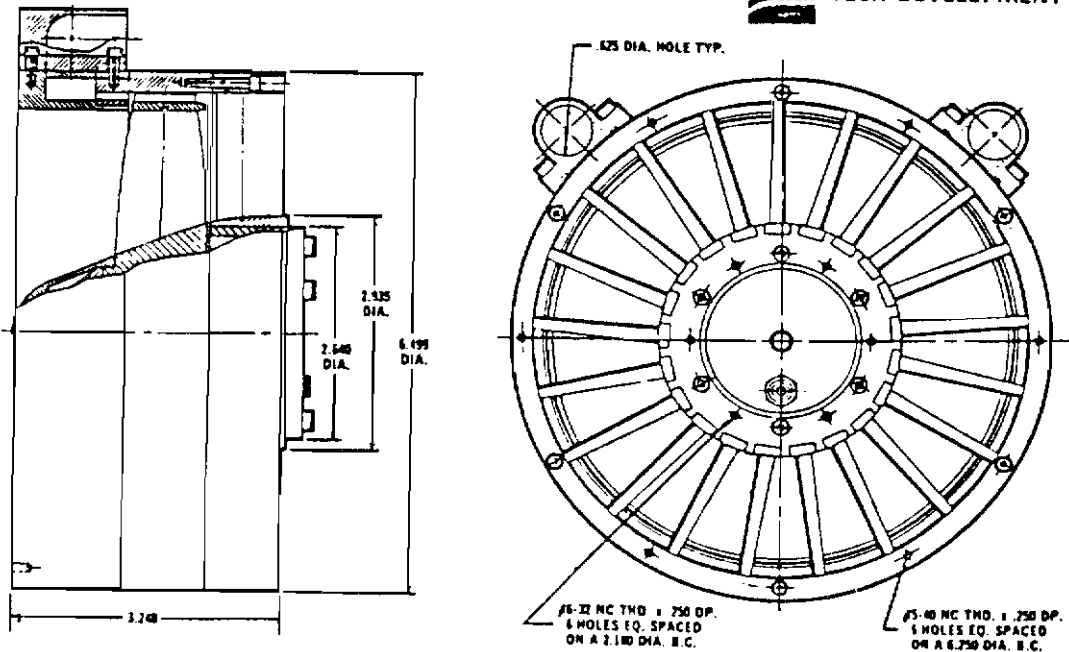


Figure 32 Model TD-457 Tip Turbine Fan

(REFERENCE 8)

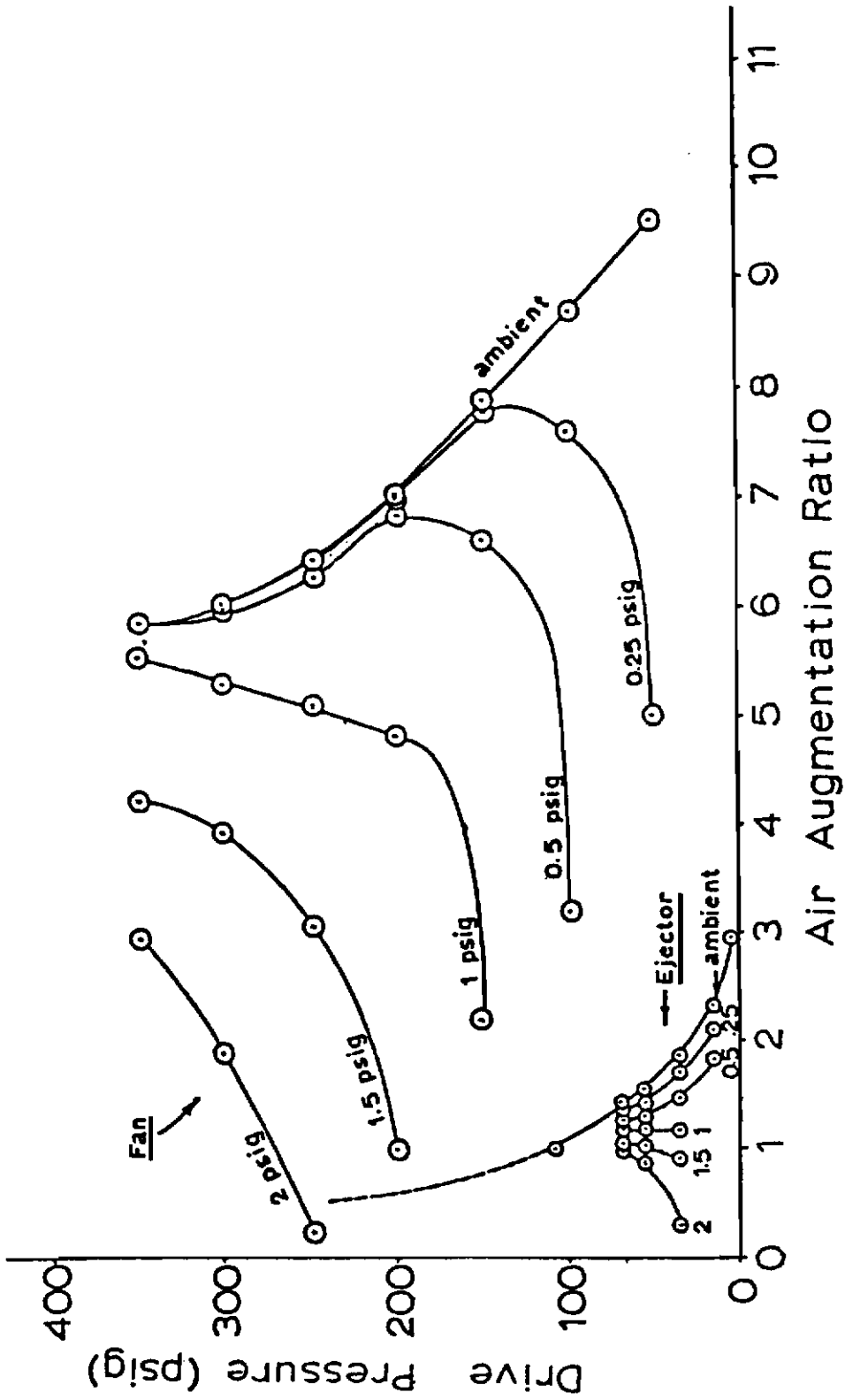


Figure 33 Air Augmentation Ratio as a Function of Drive Pressure for Fan and Ejector with Various Back Pressures

(REFERENCE 7)

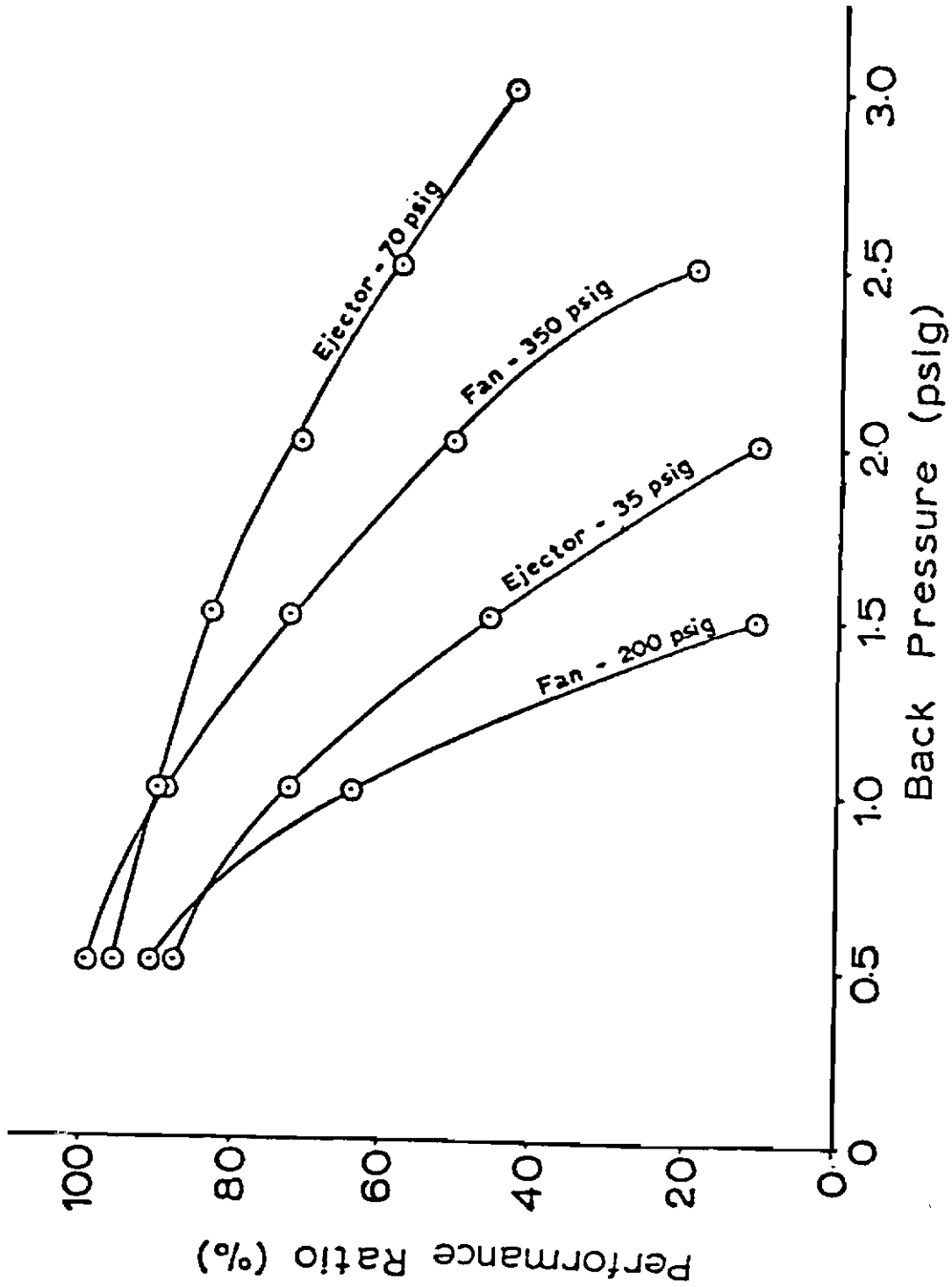
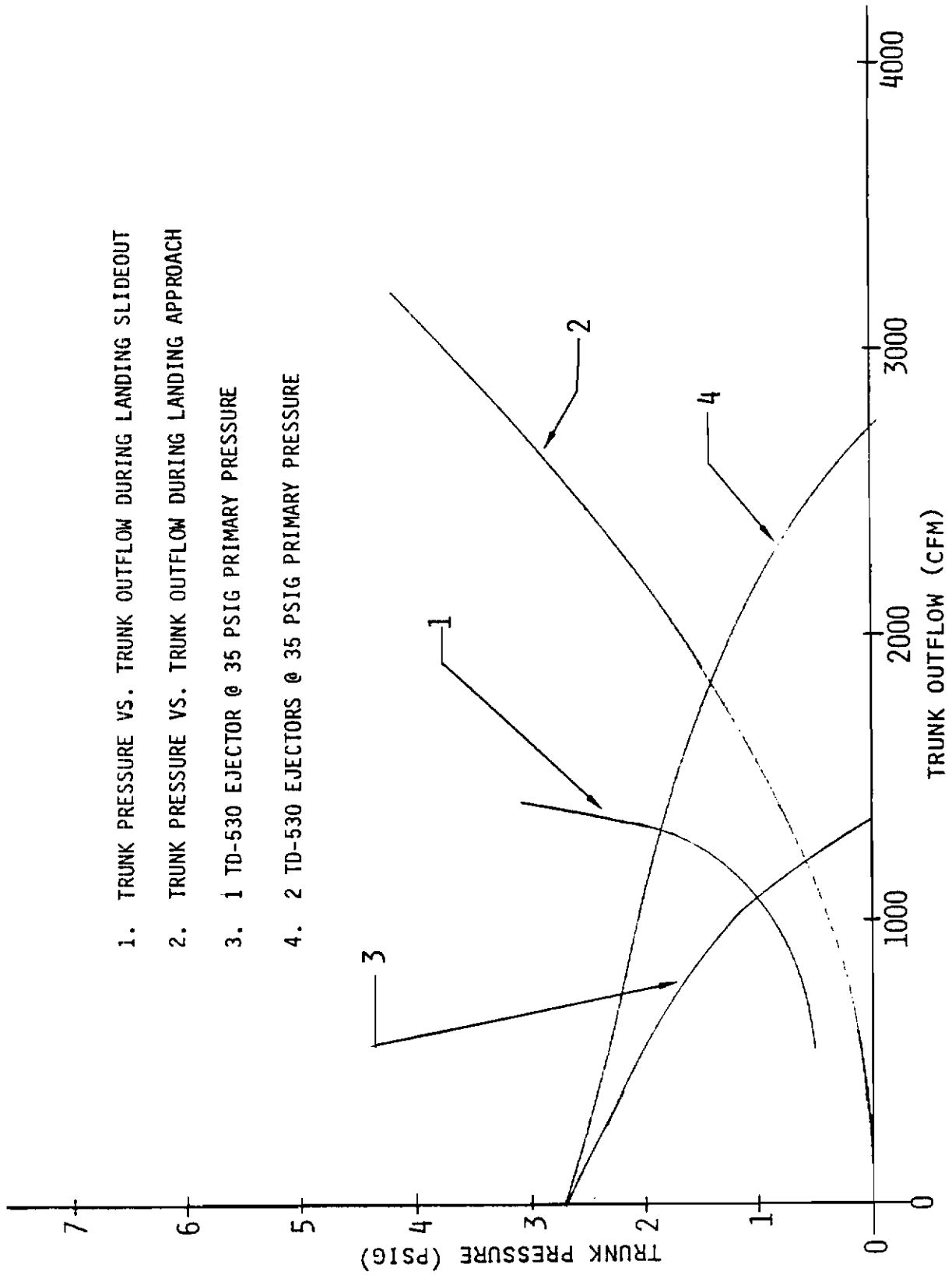


Figure 34 Performance Ratio as a Function of Back Pressure for Fan and Ejector at Various Drive Pressures

(REFERENCE 7)



- 1. TRUNK PRESSURE VS. TRUNK OUTFLOW DURING LANDING SLIDEOUT
- 2. TRUNK PRESSURE VS. TRUNK OUTFLOW DURING LANDING APPROACH
- 3. 1 TD-530 EJECTOR @ 35 PSIG PRIMARY PRESSURE
- 4. 2 TD-530 EJECTORS @ 35 PSIG PRIMARY PRESSURE

Figure 35 Pressure-Flow Characteristics for Boeing ARPV with ACRS

The number of ejectors, their size, and their primary pressures determine the trunk inflow. Figure 36 shows pressure-flow characteristics for the TD-530 ejector. The number of these ejectors and their primary pressures were varied during the simulations. The maximum possible primary pressure will be determined by the primary flow source. If bleed air is used, and a 15% line loss is assumed, then 59.5 psia (44.8 psig) primary ejector pressure is available with the engine at idle speed. This is a suitable pressure, but the maximum bleed air mass flow rate imposes a tighter constraint. The limit is 0.70 pounds mass per second, and Figure 37 shows that if two TD-530 ejectors are used, each supplied with 0.35 pounds mass per second, the maximum ejector drive pressure is approximately 18 psig.

An additional ejector is required if suction braking is used with the ACRS. Suction braking pressure-flow requirements were analyzed during the landing simulations and results are discussed in Paragraph 2.a.(5).

(b) Rockwell ARPV

The Rockwell ARPV uses the General Electric J85-GE-4 engine. Figure 38 shows the general layout of this engine. Table 10 lists engine performance data and Table 11 lists characteristics of the engine accessory drive pads. Four pads are available and pads P-2 and P-3 are identical. The baseline Rockwell ARPV uses pad P-4 to drive a small air compressor, pad P-3 to mount the integrated air turbine starter-electric generator unit, and pad P-1 is the conventional tachometer drive pad. Pad P-2 is not designated for any specific use and would be available to power an ACLS air supply system. The maximum continuous power rating for this pad is shown in Figure 39. It does have overload capability of 84 hp for five minutes in any given four hour period and it may be possible to expand these constraints for unmanned applications like the Rockwell ARPV.

Airbleed is also available from this engine. The maximum bleed rate for the J85 engine has been set at 3% of total compressor inlet flow. Figure 40 shows these maximum bleed rates for the man-rated J85 engine. If the

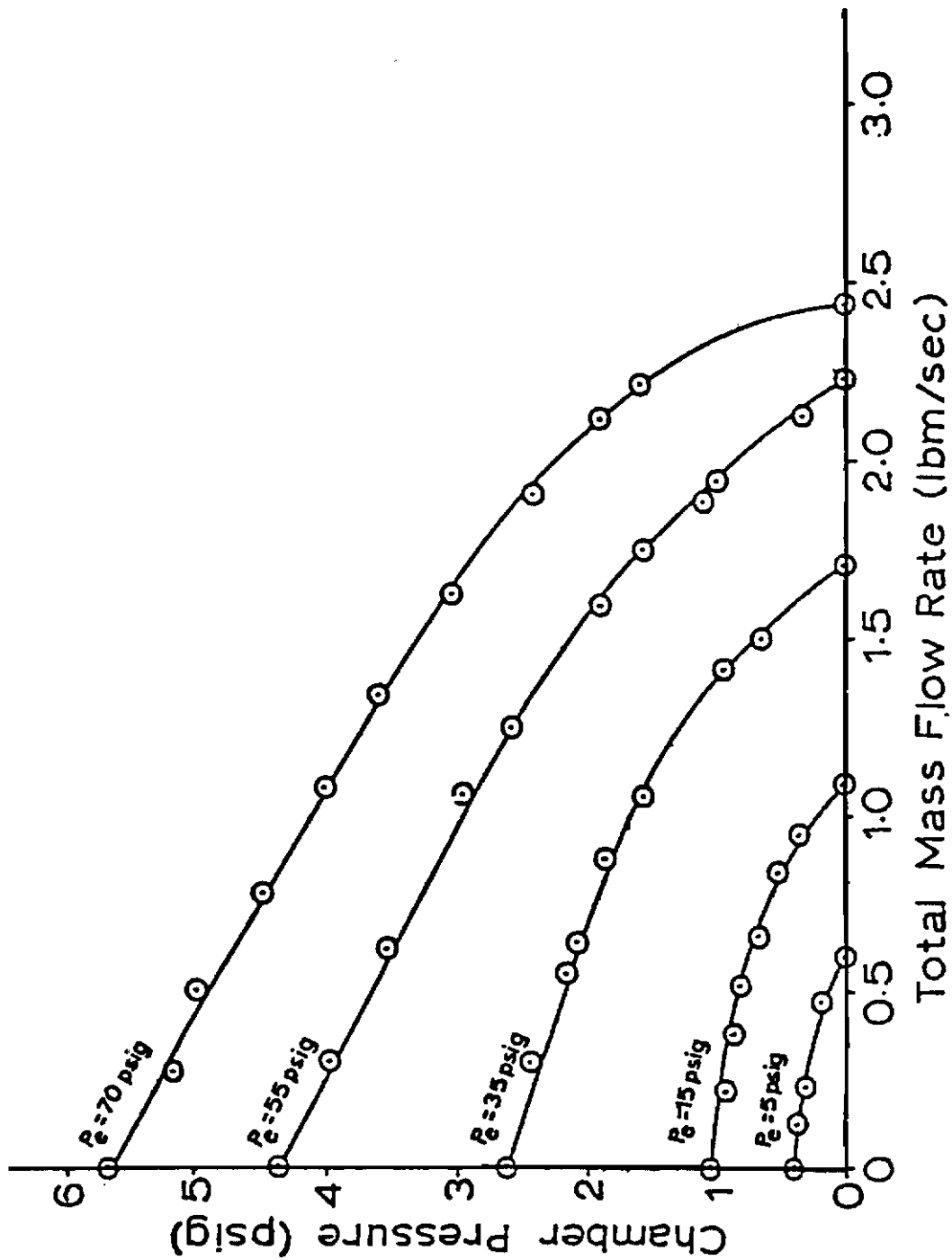
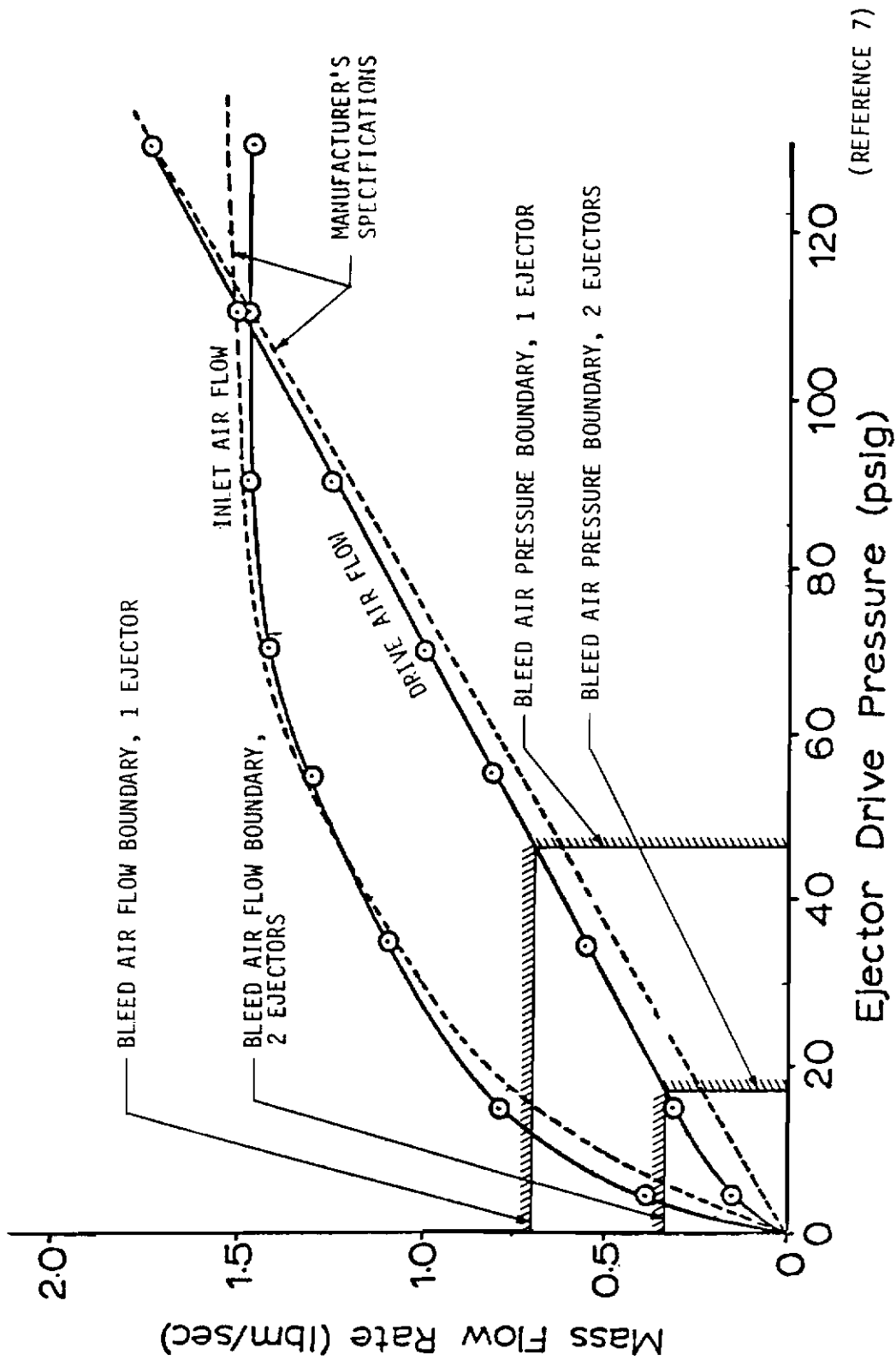


Figure 36 Total Air Mass Flow Rate Into Plenum Chamber as a Function of Back Pressure for Various Ejector Drive Pressures

(REFERENCE 7)



(REFERENCE 7)

Figure 37 Inlet and Drive Air Flow Rates as a Function of Ejector Drive Pressure with Ambient Back Pressure

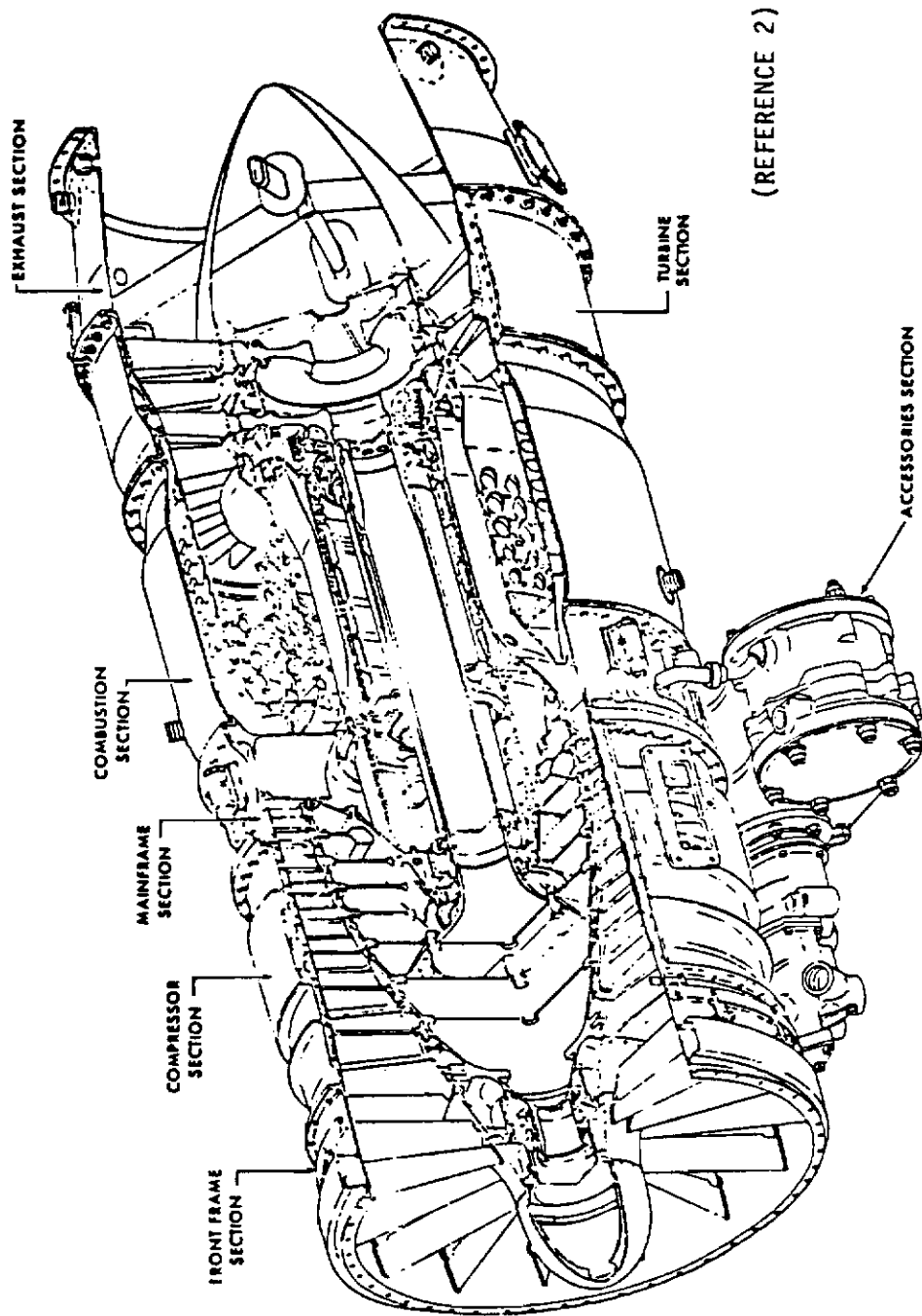


Figure 38 Basic Engine Assembly for Rockwell ARPV

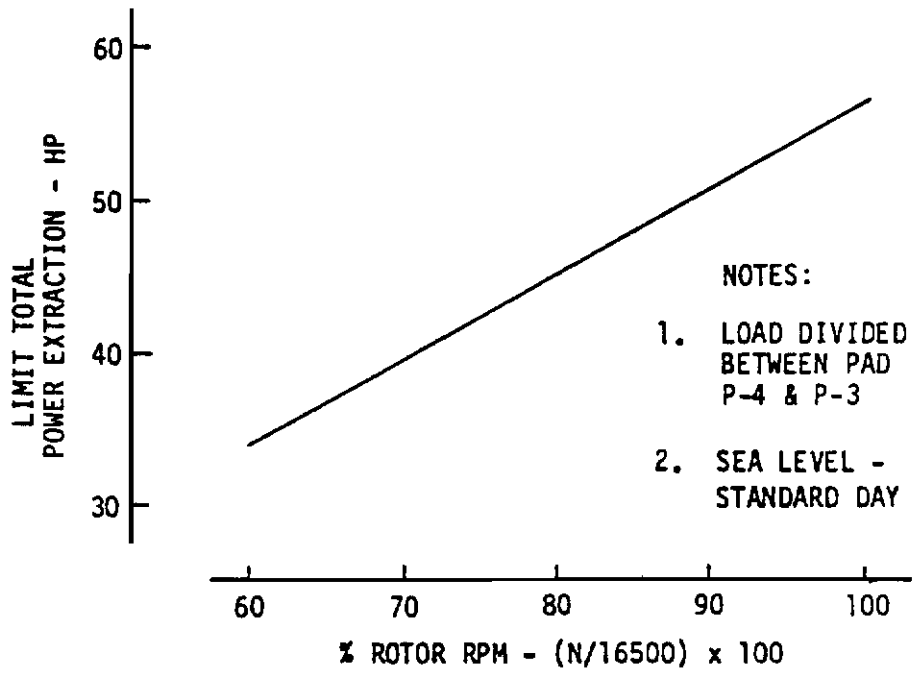


Figure 39 Maximum Power Extraction for J85-GE-4 Engine

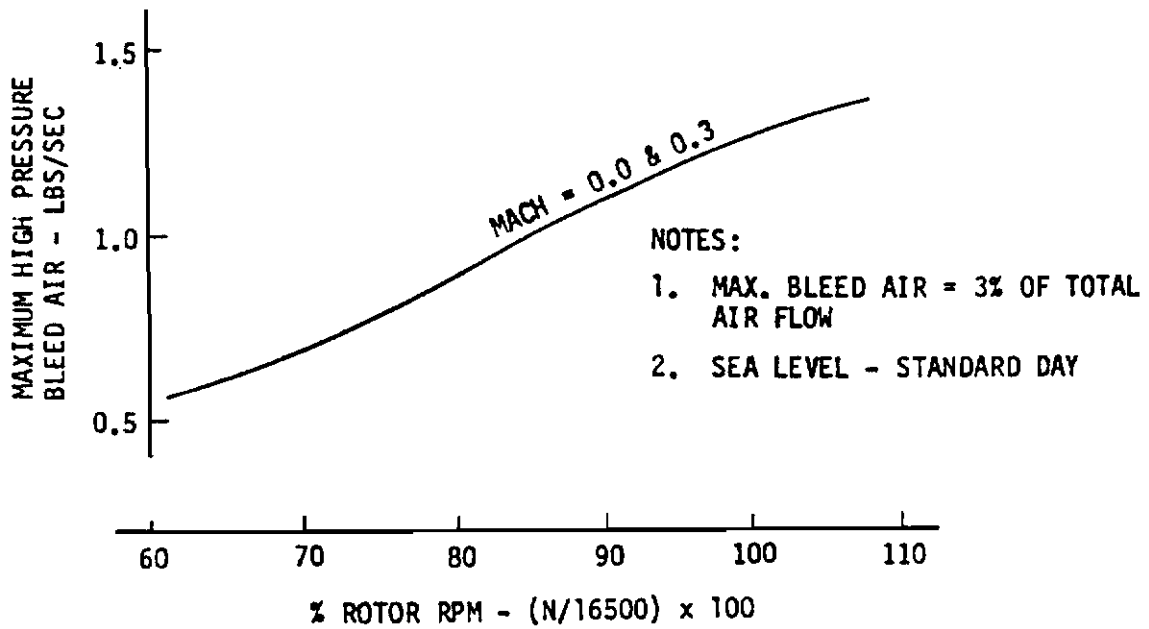


Figure 40 Maximum Bleed Air for J85-GE-4 Engine

Contrails

TABLE 10
J85-GE-4A ENGINE PERFORMANCE

ALTITUDE FT	MACH NUMBER	PERCENT RPM	NET THRUST LBS	SFC LB/HR/LB	AIRFLOW LB/SEC	
S.L.	0	100	2,950	.932	43.6	
		97	2,350	.936	41.0	
		91	1,590	.943	36.8	
		80	880	1.185	29.6	
	0.5	98.5	2,640	1.172	49.2	
		97	2,420	1.158	47.6	
		91	1,500	1.220	42.6	
		80	490	2.040	34.6	
	0.8	95	2,700	1.278	57.4	
		-	-	-	-	
		91	1,790	1.359	53.0	
		80	340	3.090	43.0	
15,000	0.5	104	1,760	1.137	30.6	
		100	1,550	1.098	29.8	
		97	1,320	1.100	28.2	
		91	780	1.191	25.2	
		80	270	2.078	20.4	
	0.8	101	1,930	1.222	37.2	
		97	1,630	1.190	35.0	
		91	950	1.285	31.4	
		80	180	3.220	25.4	
		-	-	-	-	
	25,000	0.6	106.5	1,300	1.153	22.4
			100	1,070	1.085	21.5
97			890	1.090	20.5	
91			520	1.231	18.2	
-			-	-	-	
0.8		104.5	1,420	1.198	25.8	
		100	1,235	1.150	25.2	
		97	1,030	1.145	23.9	
		91	590	1.289	21.3	
		-	-	-	-	
36,089		0.6	107.4	800	1.125	14.2
			100	640	1.062	13.5
	97		530	1.085	12.8	
	91		310	1.290	11.4	
	-		-	-	-	
	0.8	107.4	920	1.185	16.5	
		100	740	1.109	15.8	
		97	610	1.131	15.0	
		91	350	1.315	13.35	
		-	-	-	-	
	45,000	0.8	107.4	610	1.231	10.7
			100	482	1.161	10.15
97			397	1.198	9.6	
91			224	1.457	8.5	
-			-	-	-	

(REFERENCE 2)

TABLE 11
ACCESSORY DRIVE PAD CHARACTERISTICS FOR J85-GE-4 ENGINE

Pad	Nominal Use	AND Standard Type	Pad(a) Speed (rpm)	Speed Ratio	Rotation (Facing Pad)	Torque Ratings (c)		HP(b)	Max. Accessory Weight (lb)	Max. Overhung Moment (lb-in.)
						Continuous	Overloads (lb-in.)			
P-2	Starter Generator Alternator	20002 XII-D	7088	0.430:1	CCW	500	750	2200	65	500
P-3	Starter Generator Alternator	20002 XII-D	7088	0.430:1	CW	500	750	2200	65	500
P-4	Hydraulic Pump	20001 XI-B	7811	0.473:1	CW	250	375	1650	25	125
P-1	Tachometer	20005	4190	0.254:1	CCW	7	---	50	2.7	---

Notes

- (a) Pad speed values are given for 100% (rotor speed equals 16500 rpm).
- (b) Customer pad power-extraction limits are presented in Fig. A5. Total extraction in any combination of Pads P-2, P-3 and P-4 shall not exceed 65 hp (at 100% engine rotor speed = 16,500 rpm). Total combined extraction from Pads P-2 and P-3 shall not exceed 56 hp (at 100% engine rotor speed = 16,500 rpm).
- (c) Pad drives are capable of taking overload torque for 5 min in any given 4-hr period.

J85 current bleed system was modified by installing a larger bleed port, the maximum bleed could be increased to 2.0 pounds mass per second at maximum power. At idle power this maximum bleed would decrease to approximately 1.25 pounds mass per second. Figure 41 shows the engine thrust and bleed air properties for a bleed rate of 0.70 pounds mass per second. The bleed air temperature exceeds the ACLS trunk material temperature limit of 200 deg F so it must be mixed with cooler ambient air.

The tip turbine fan and ejector components were investigated for use with the bleed air source. Evaluations similar to those discussed in the previous section for the Boeing ARPV were performed and results were similar.

Shaft driven fans were also investigated for this air vehicle. Several fan drive train configurations are possible, such as:

- o electric motor driven fans powered by an electric generator mounted at pad P-2
- o hydraulic motor driven fans powered by a variable displacement hydraulic pump mounted at pad P-2
- o shaft driven fans driven by high speed drive train through a clutch at pad P-2

Two basic types of air supply systems were included in the program EASY math models of the Rockwell ARPV configurations - an ejector system and a shaft driven fan system.

The ejector system was selected as a practical air supply system for the lower flow requirements of the ACRS and ABSS. It was selected because of its insensitivity to back pressure variations, low complexity and reliability. Only the ejector component was included in the air supply system math model since the dynamics of valves and ducting will have minor effects on the system performance. As with the Boeing ARPV, the TD-530 ejector described by Figures 31 and 36 was modeled.

Contrails

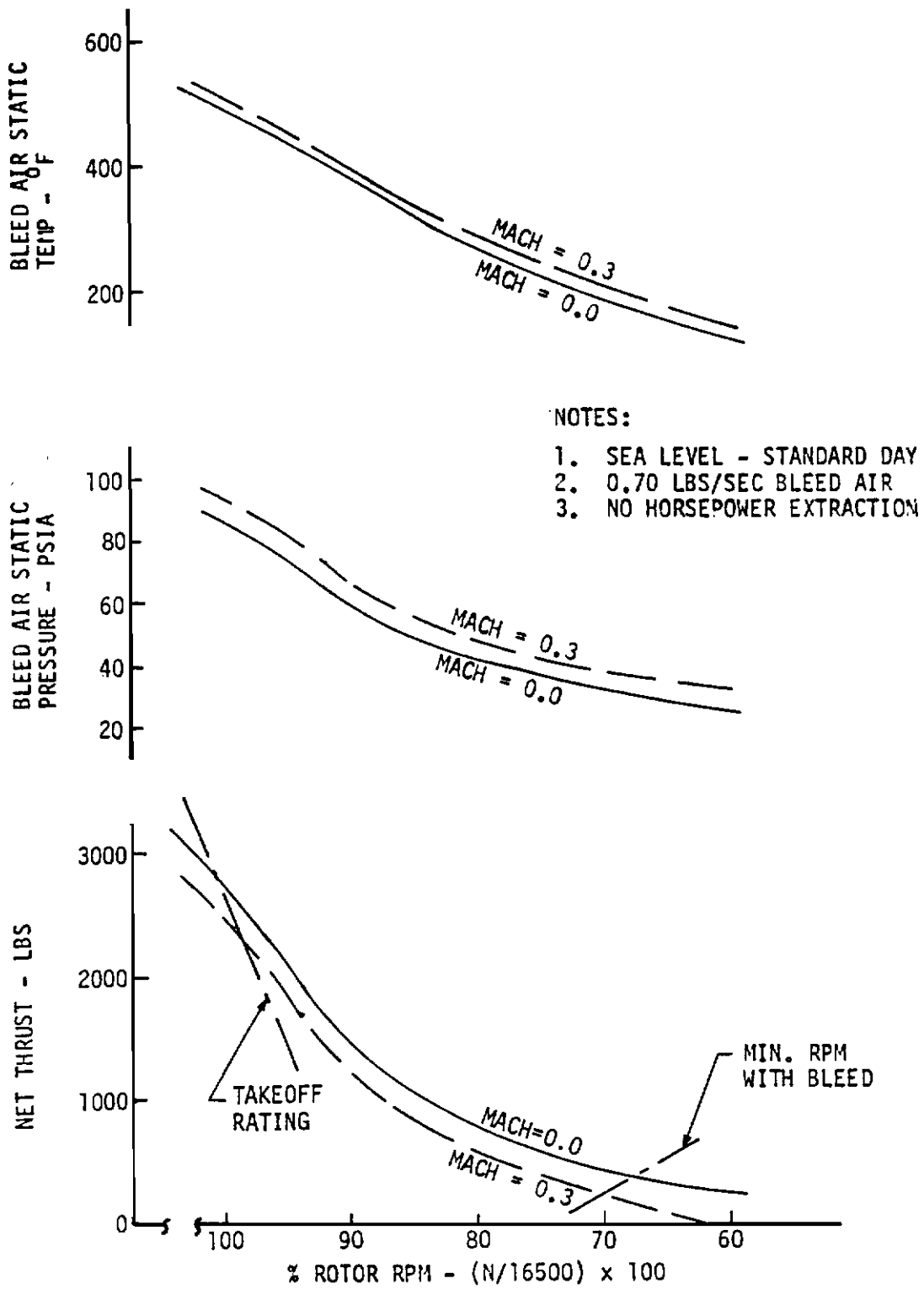


Figure 41 J85-GE-4 Performance with Bleed Air

A shaft driven fan system was included in the math model of air cushion systems for takeoff and recovery. This system is most capable of providing the large takeoff flow requirements. Only the fan component was included in the EASY math model since its dynamics will dominate the response of the air supply system. Performance data was not available for an actual two-stage axial fan with the necessary pressure-flow characteristics. Therefore, a theoretical rather than empirical fan map was used to represent the fan performance. This fan map was developed to satisfy takeoff and recovery pressure-flow requirements and is shown in Figure 42.

As with the Boeing ARPV, space for the air supply system installation is very limited. Practical installation considerations were not investigated in detail prior to the dynamic simulations. The approach followed consisted of 1) making preliminary estimates of the component sizes needed, 2) including these in system math models, 3) performing dynamic simulations and adjusting component sizes during the simulations to achieve satisfactory performance, 4) specifying component requirements and estimating their size, 5) preliminary design of the system installation and determination of its feasibility.

(5) Suction Braking

Suction braking requires the installation of a dedicated flow source for the air cushion. Previous results and preliminary analysis indicated that low suction braking flow rates will produce effective cushion suction. Analysis indicated that the TD-530 ejector would satisfy these flow requirements, so an attempt was made to model the ejector with the EASY ejector (EJ) component to produce suction braking. However, due to incompatible input/output requirements, problems were encountered when attempting to connect the EASY ejector component and air cushion trunk (TK) component to produce flow out of the cushion. Therefore, suction braking was modeled by connecting an inlet-outlet (IO) component to the cushion, with less than ambient pressure at the outlet of the IO component to produce a flow out of the cushion. This flow could be correlated into ejector performance requirements.

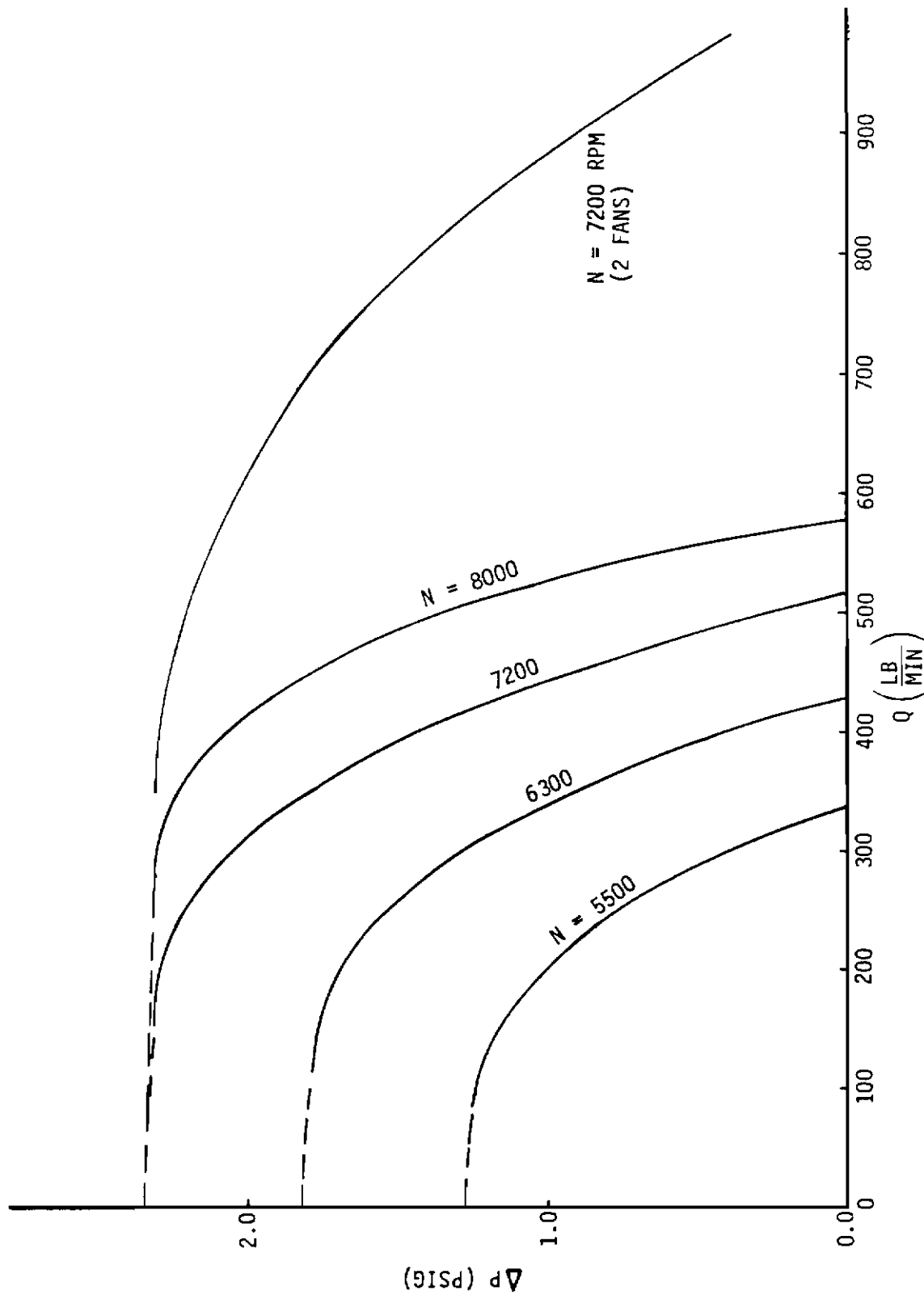


Figure 42 Fan Pressure-Flow Characteristics

(6) Arrestment Systems

Some of the dynamic simulations included landing arrestment of the air vehicles. The program EASY model of the All American Engineering Company "Water Twister" arresting system was used in these simulations. The general layout of a typical system is shown in Figures 43 and 44.

The principal design constraints for the arrestment systems were the structural load limits for the two air vehicles and air vehicle-to-ground clearances when arrestment loads are applied. These limits are 3g longitudinal for the Rockwell ARPV and 4g longitudinal for the Boeing ARPV.

The major design variables for the arrestment system are the air vehicle tail hook length and location, the water twister damping coefficient, and the tape drum diameter. Several other arrestment system design parameters having minor or negligible effects on dynamic performance were included as fixed parameters. Design variations were investigated during the program EASY dynamic simulations while attempting to achieve satisfactory performance. Table 12 lists the values of the baseline design parameters for the Boeing and Rockwell ARPV arrestment systems.

(7) Other Characteristics of the Landing Math Models

The program EASY landing math models basically consisted of standard components defining the air vehicle aerodynamic forces (OL, DL, VA), the air cushion trunk (TK or TS) or air bag skid (AB) forces, the air supply system (EJ, FR, IO), the arrestment system (AS), the air vehicle equations of motion (DS, SG, TT, or TL), and various other table definition, summation, and multiplication components (TA, TB, S3, S4, MA) used to combine air vehicle forces or control surface position commands.

Special coding was added to the air vehicle models to generate specific analysis information. Component TR which performs a coordinate system transformation is called from inside a loop in subroutine EQMO of program EASY and is used to calculate critical air vehicle-to-ground clearances.

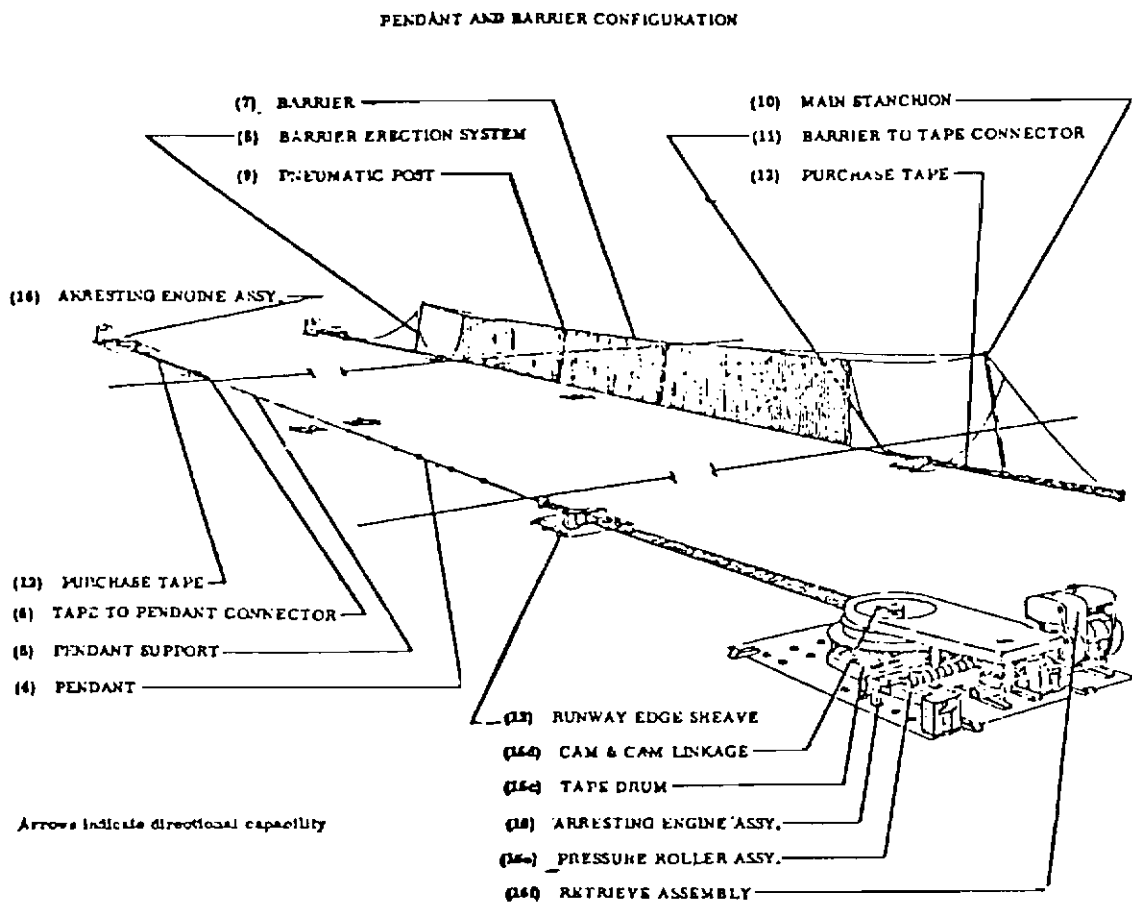


Figure 43 Schematic Arrangement - Rotary Hydraulic Arresting System

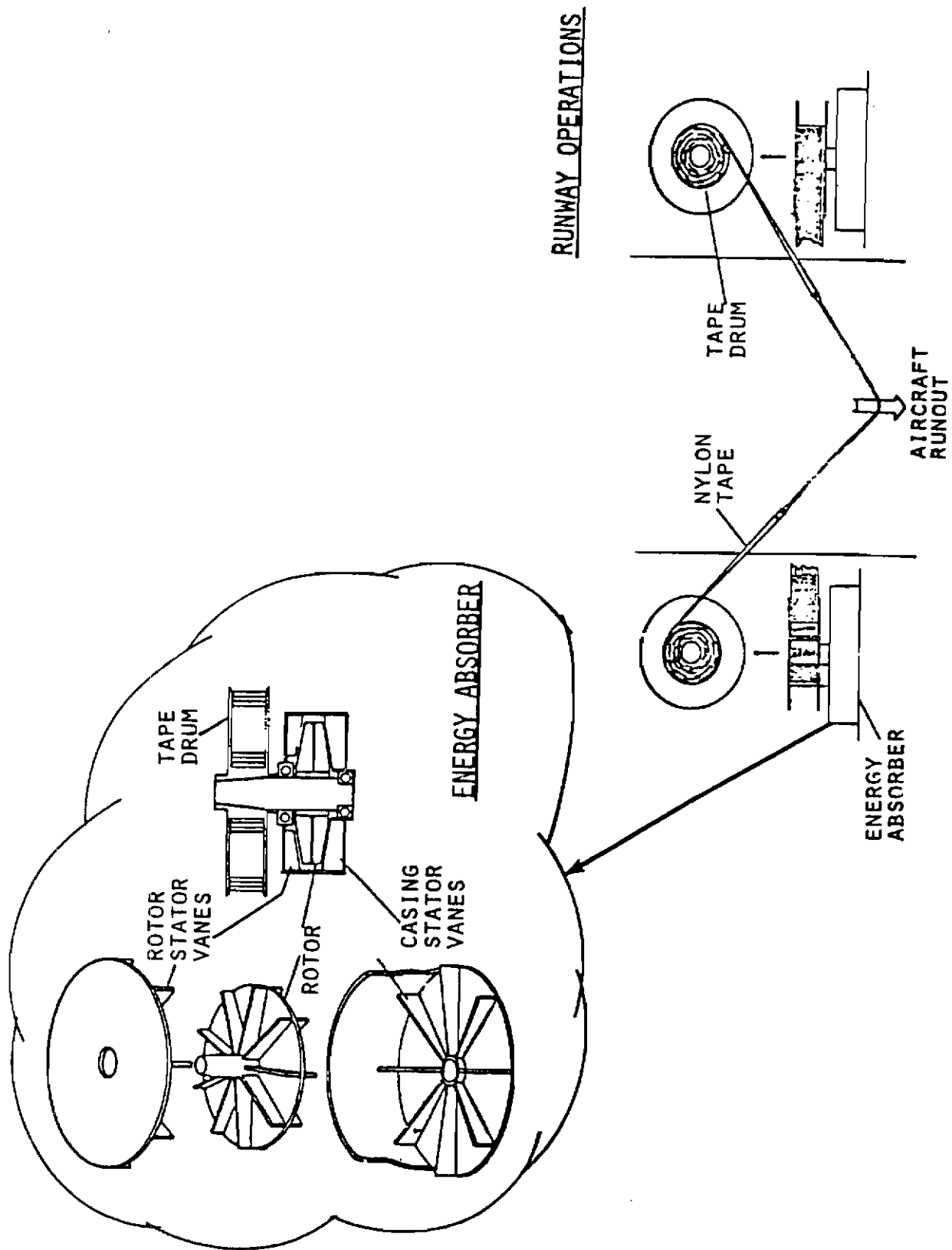


Figure 44 Water Twister Arresting System

TABLE 12
ARRESTMENT SYSTEM PARAMETERS

Runway span between sheaves (ft.)	100
Tape drum to sheave distance (ft.)	10
Initial cable height above runway (ft.)	0.5
Cable weight density (lb/in ³)	0.25
Cable cross sectional area (in ²)	0.2 (1/2" dia.)
Cable initial stress (psi.)	2500
Tape weight density (lb/in ³)	.03
Tape thickness (in.)	.15
Tape width (in.)	5
Tape drum inertia (lbm-in ²)	30000
Cable modulus of elasticity (psi.)	1.2 (10 ⁷)

Table 13 lists the clearances of particular interest for each air vehicle. Component FU was added to calculate the relief valve area; this variable is not a normal output of components TK or AB. Other coding was added so that tabular input information for components TK and TS could be used for parameter variations in root locus or steady state analyses.

b. Landing Simulation Results

The major objectives of the landing simulations were:

- o to identify the recovery system parameter values which achieve satisfactory performance or which provide the best achievable performance.

- o to develop parametric design information which relates recovery system performance to variations in design parameters.

- o to identify constraints on the air vehicle attitude and sink rate at touchdown.

- o to identify any modifications to the baseline airframe due to the ACLS installation.

Specific requirements which must be satisfied for acceptable performance under normal touchdown conditions are:

- o maximum landing impact loads must be less than the structural load limits for the airframe.

- o the unprotected fuselage and wing tips must not hit the ground.

- o the air vehicle must have directional stability during landing slideout.

Landing impact loads and ground-airframe clearances were first investigated using a three degree-of-freedom (DOF) longitudinal model instead of six DOF to reduce computation cost. The three DOF simulations could not be used to investigate directional stability, lateral

TABLE 13

AIR VEHICLE TO GROUND CLEARANCES CALCULATED BY PROGRAM EASY
DURING THE LANDING SIMULATIONS

Clearances (= height above ground of the following points on the airplane)	Program EASY Notation
--	--------------------------

Rockwell ARPV

- | | | |
|---|--------------------------------|------------------|
| o Most forward, bottom point on wing tip mounted AN/ALE-38 chaff dispensers | Left Wing
Right Wing | GAPLWF
GAPRWF |
| o Most aft, bottom point on wing tip mounted AN/ALE-38 chaff dispensers | Left Wing
Right Wing | GAPLWR
GAPRWR |
| o Bottom point on JTIDS antenna mounted on bottom of fuselage | Forward Antenna
Aft Antenna | GAPFF
GAPFR |
| o Distance between airplane c.g. and ground | | GAPCG |

Boeing ARPV

- | | | |
|---|-----------------------------|----------------|
| o Most outboard, aft point on the canard | Left Canard
Right Canard | GAPCL
GAPCR |
| o Most outboard, forward point on the wing | Left Wing
Right Wing | GAPWL
GAPWR |
| o Bottom point on fuselage at STA 131.5 | | GAPFF |
| o Bottom point on fuselage at STA 318 | | GAPFR |
| o Distance between airplane c.g. and ground | | GAPCG |

clearances, and arrestment system effects on the air vehicle but approximate impact loads were established. The six DOF simulations were made after a data base had been created by performing several three DOF simulations.

Since a multitude of parameters are involved in dynamic simulation of a vehicle recovery system, parametric investigation of all of them is not reasonable. Therefore, the key to proper analysis is to select as variables, only those data that have a major impact on system performance. The rigidity of this data varies from item to item; some of the input data are fixed for all cases (for instance, the air vehicle mass properties and aerodynamics), other input data can be changed to some extent, but modifications usually require a major effort and have a large impact on the air vehicle (for instance, the trunk shape and fan or ejector performance maps), and still other input data are simple to modify and in many cases are easily adjustable after the equipment is installed on the air vehicle (such as the relief valve cracking pressure, the ejector primary pressure or fan speed, and the arrestment system damping coefficient).

(1) Boeing ARPV Landing Simulations

(a) Boeing ARPV with ABSS

The baseline ARPV, Figure 26, uses an ABSS with an arrestment system for landing, so this design served as the starting point for these simulations. Figure 45 shows the layout of the two air bags. Each bag was modeled in the EASY program as six individual elements, free to move laterally and vertically relative to each other. Each bag is 120 inches long, 15 inches in diameter, and attached to the flat fuselage underbody along a 13 inch chord line. Figure 46 shows a sectional view of a general air bag installation and the dimensional terms used to define it. Program EASY requires input data defining the free bag shape, it then calculates the shape of the bag under various loading conditions and the loaded bag shape data are then tabulated by the program. These data have been plotted and are shown in Figures 47 through 49 for the baseline air bag. These relationships will change as

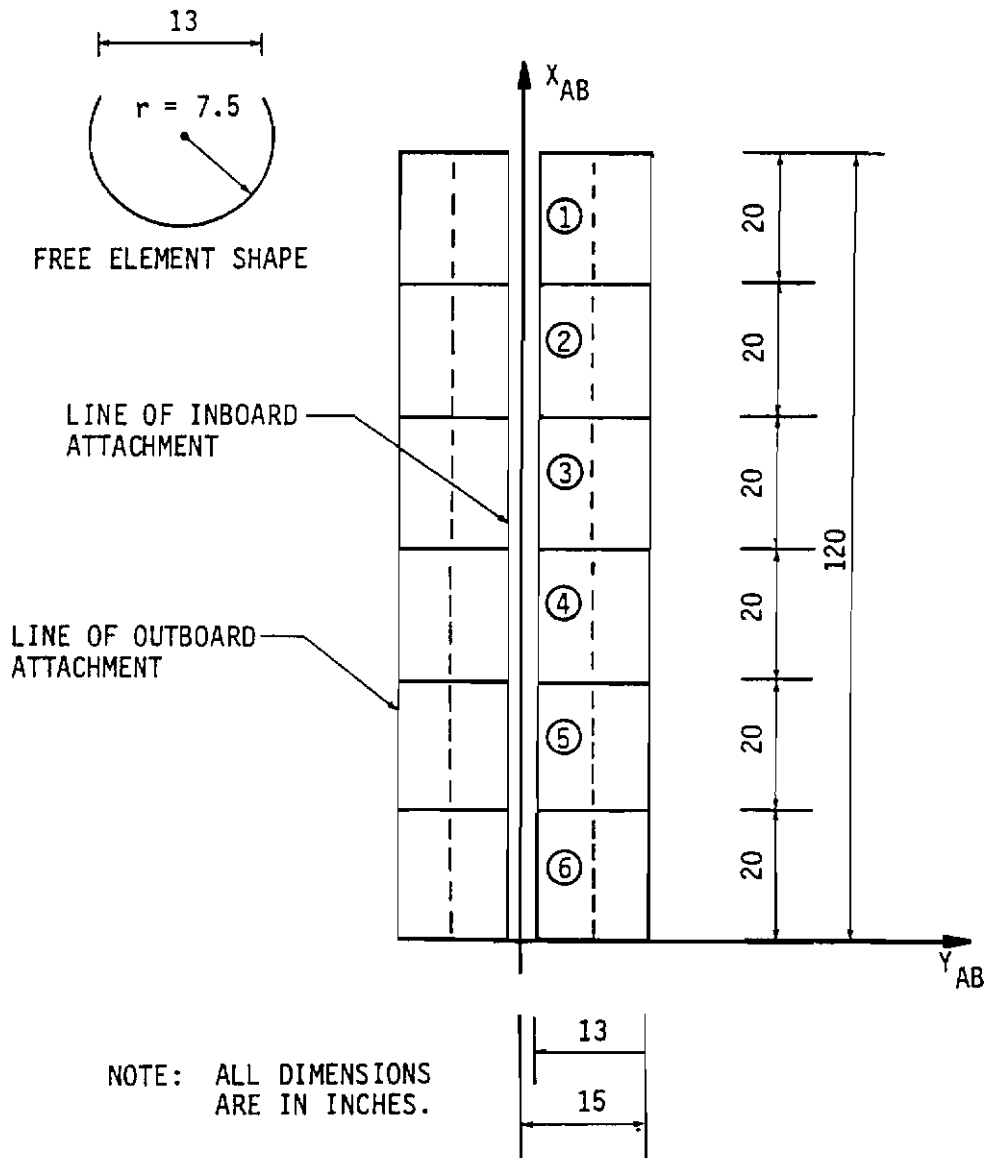


Figure 45 Baseline Air Bag Model for Boeing ARPV

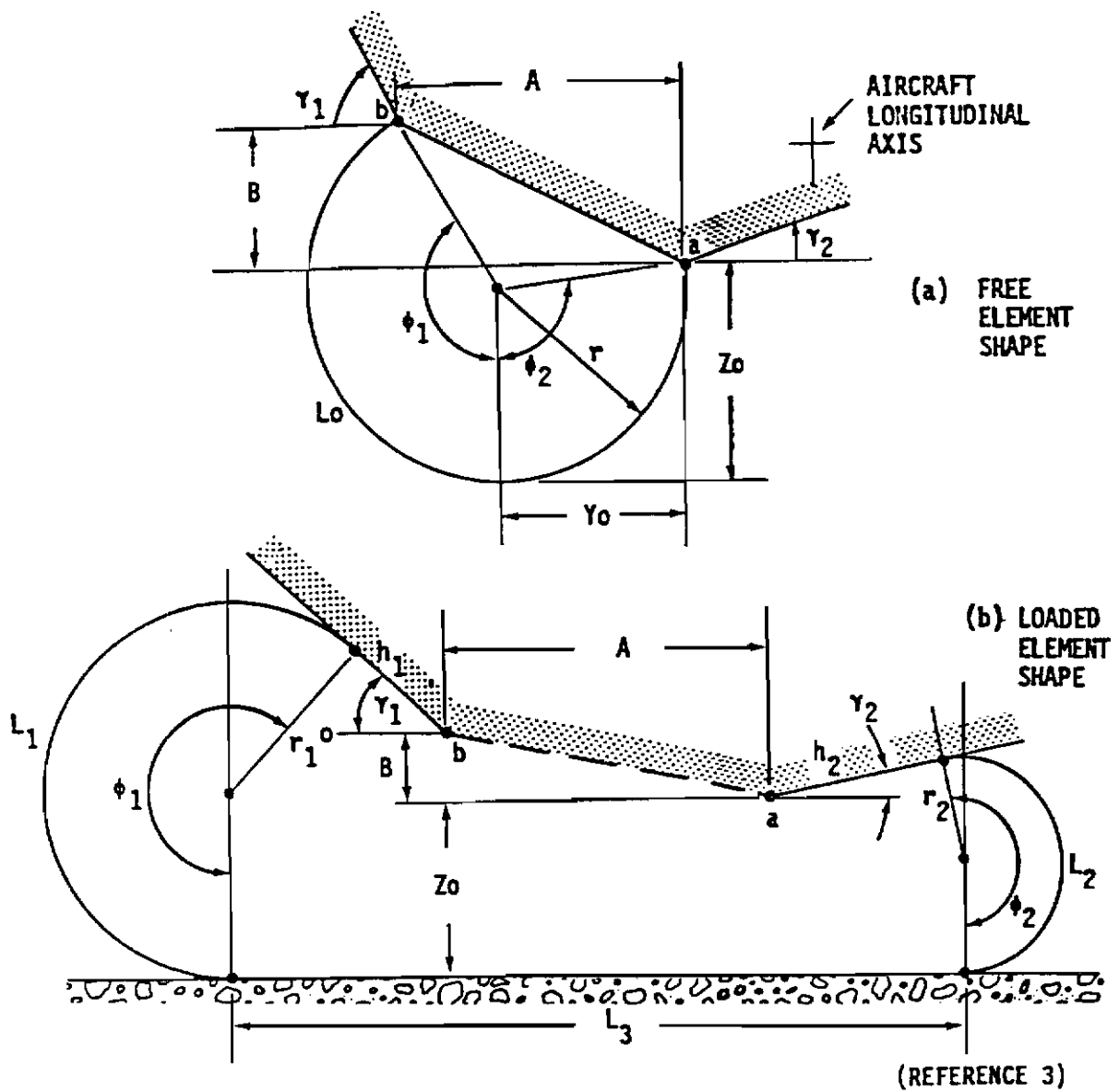


Figure 46 Air Bag Geometry

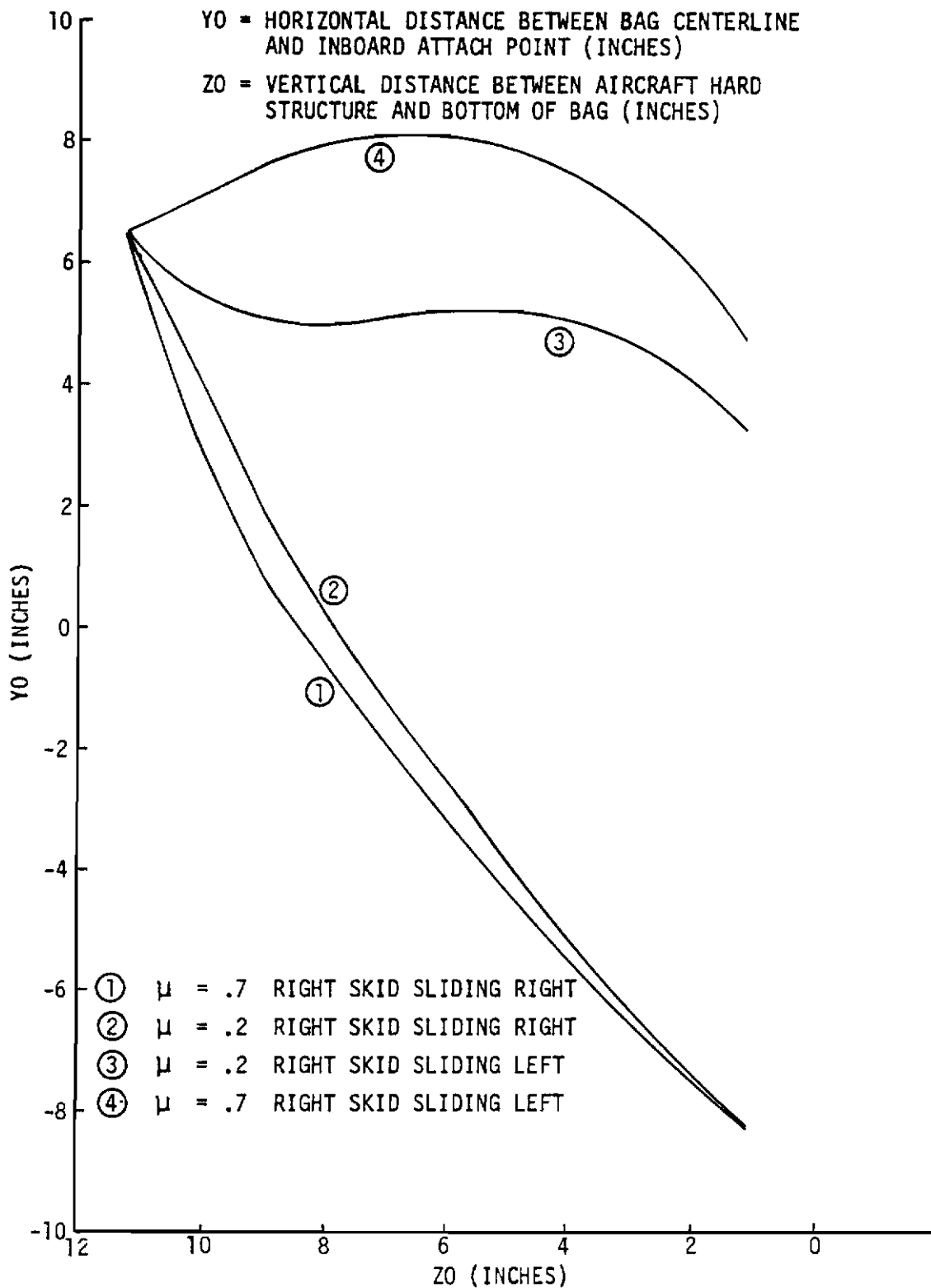


Figure 47 Air Bag Geometry for Boeing ARPV with Baseline ABSS, Y_0 vs. Z_0

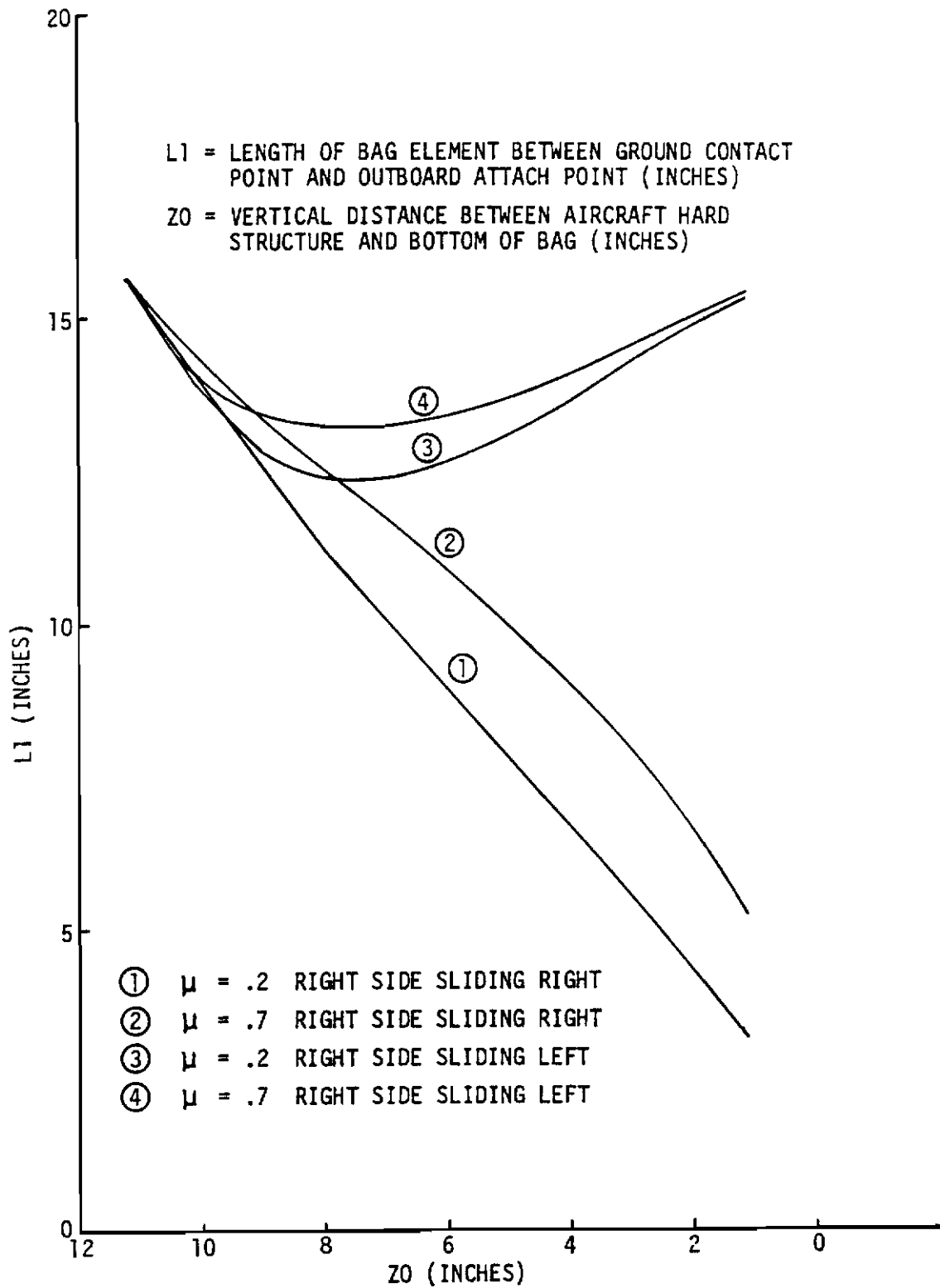


Figure 48 Air Bag Geometry for Boeing ARPV with Baseline ABSS, L1 vs. Z0

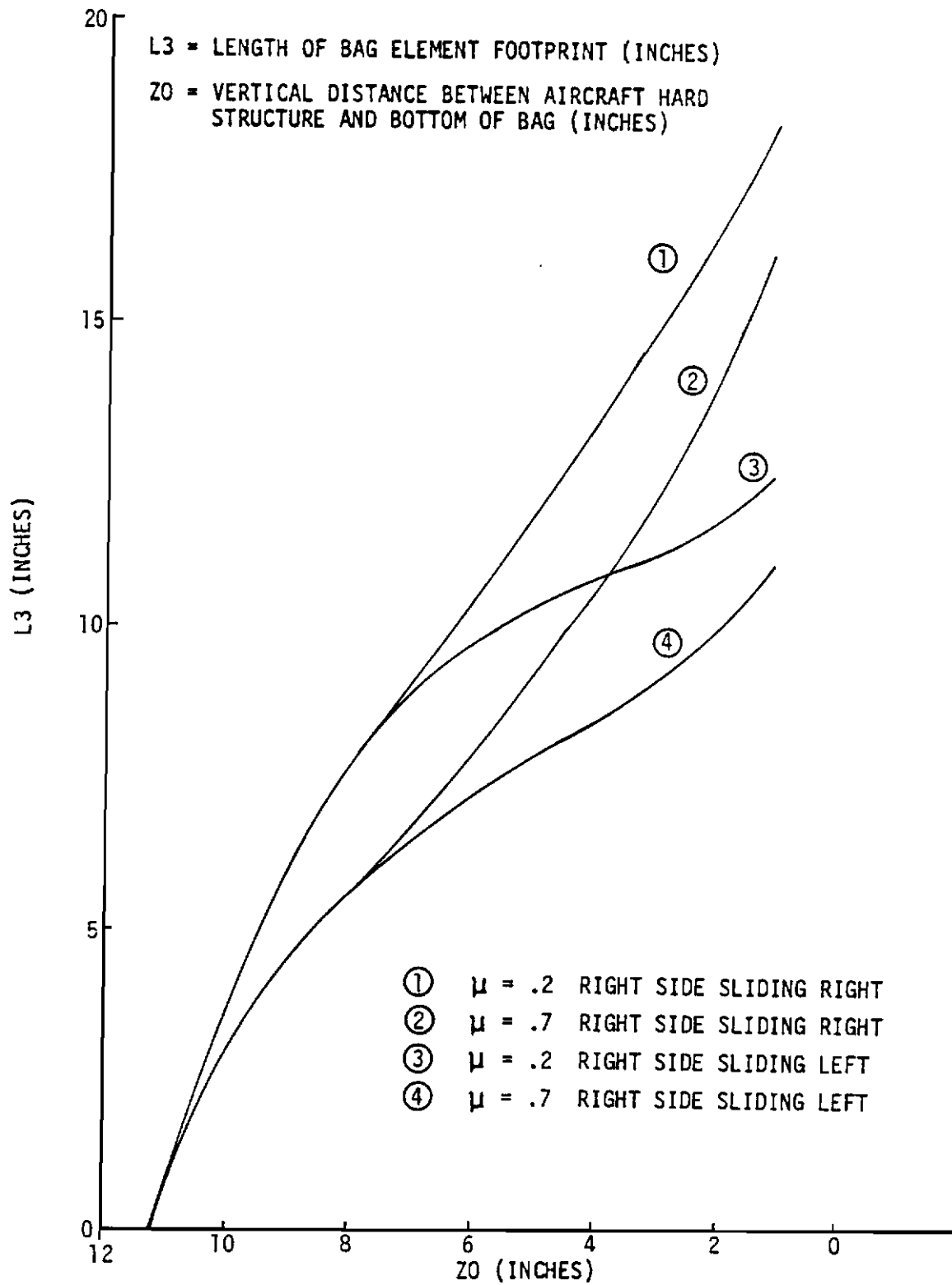


Figure 49 Air Bag Geometry for Boeing APRV with Baseline ABSS, L3 vs. Z0

the bag cross sectional dimensions are changed. Six different bag sizes were investigated during these simulations; their free shape dimensions are listed in Table 14.

Table 14

ALTERNATIVE AIR BAG SKID DIMENSIONS FOR THE BOEING ARPV

<u>Air Bag Model</u>	<u>Diameter (in.)</u>	<u>Length (in.)</u>
B-ABSS-1 (baseline)	15	120
B-ABSS-2	15	180
B-ABSS-3	30	160
B-ABSS-4	15	160
B-ABSS-5	15	140
B-ABSS-6	15	150

The TD-530 ejector, which was discussed in Paragraph 2.a(4), was modeled in program EASY for this simulation. One ejector model was used for each of the two bags.

The initial simulations were one second duration, three DOF longitudinal landings without arrestment. The purpose of these simulations was to investigate the landing impact performance of various air bag system designs to determine a minimum size bag which would satisfy both load limit constraints and longitudinal clearance constraints. These simulations used initial conditions which placed the air vehicle a few inches off the ground at an attitude and speed based upon the previously defined landing approach trim conditions. Touchdown initial conditions included perturbations from the mean trim conditions. Worst case landing impact conditions were defined by using the statistical approach outlined in MIL-A-8863A (Reference 5).

Contrails

The first several simulations were used to identify a bag length and diameter which would achieve satisfactory performance. Results are shown in Figures 50 and 51. As the bag length and diameter are increased, the minimum front and rear fuselage-to-ground clearances increase and the peak landing impact loads on the air vehicle increase. The large diameter bag requires a more complex installation since hinged panels are required for the more outboard attachment of the bag to the fuselage and the bag interferes with air flow over the wing. Also, increasing the bag diameter did not result in reduced loads to the vehicle. Therefore, this design was rejected. An air bag design which is 150 inches long and 15 inches in diameter gave satisfactory results in these simulations, so it was used in the succeeding simulations which investigated air supply system design variations.

During the next series of simulations, the effects of air vehicle sink rate at touchdown, the relief valve cracking pressure, and the initial bag pressure at landing impact were investigated. Results are shown in Figures 52 and 53. Fuselage-to-ground clearances and vehicle maximum acceleration are shown. The vehicle acceleration in the landing simulations of this document is the total resultant acceleration, that is, the product of the acceleration in each of the three axial directions. Fuselage-to-ground clearances appear to be satisfactory during these simulations, but the load limit of 6g for the Boeing ARPV is consistently exceeded when landing at the landing approach sink rate of 10 ft/sec, even at the lowest practical bag pressures and relief valve cracking pressures. The problem of exceeding the incremental load limit at touchdown arises partially from the circular cross section shape of the bags. Increasing the bag diameter to get more stroke also increases the contact area thus raising the peak load. An elliptical cross section which would allow an increase in bag height without an increase in width would alleviate this problem. This approach would increase the complexity of the bag.

Touchdown load limits for an air vehicle are usually established by the structural limitations of the landing gear and the reverse load

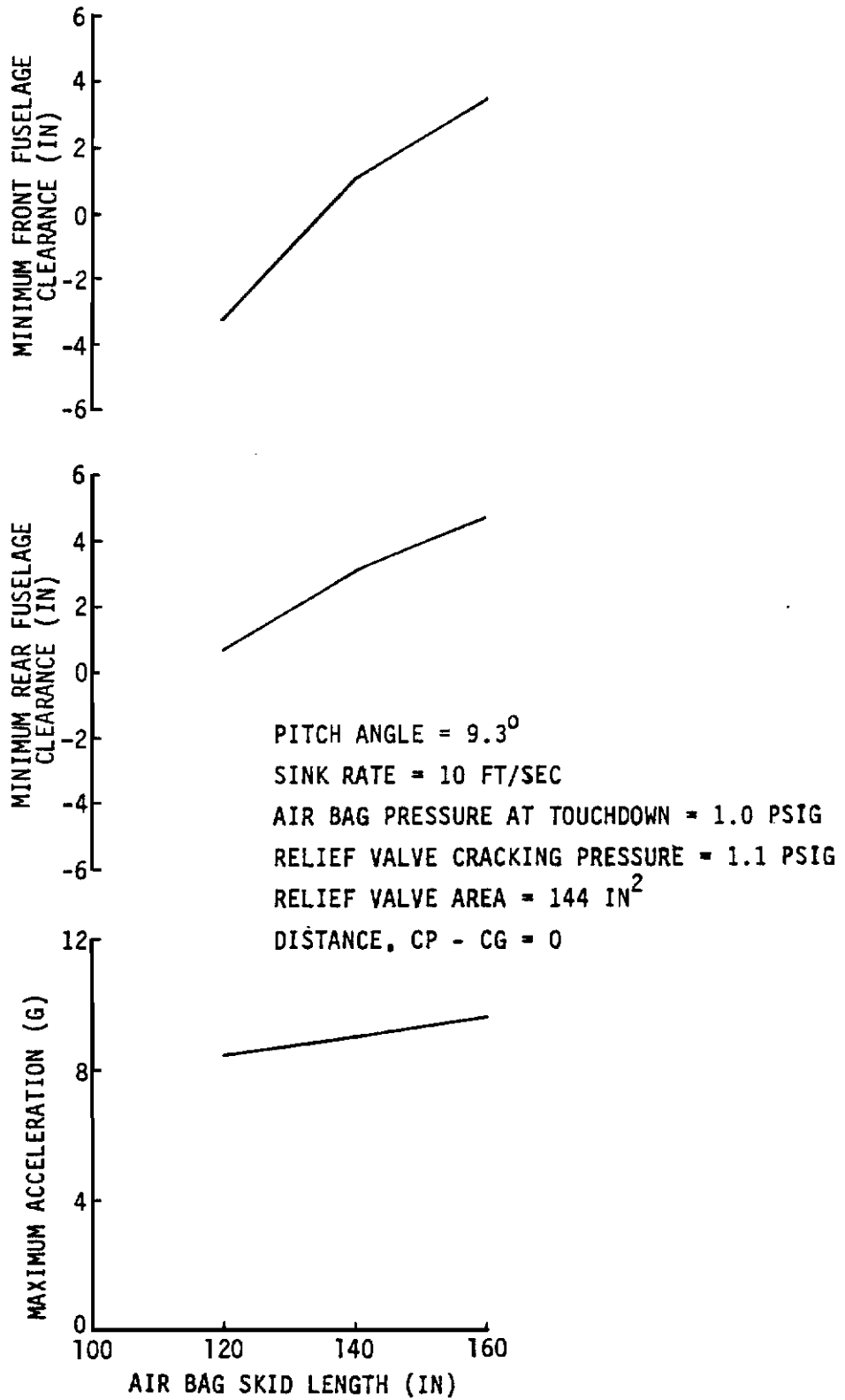


Figure 50 Boeing ARPV with ABSS, 3 DOF Landing Simulations, Air Bag Length vs. Acceleration and Clearances

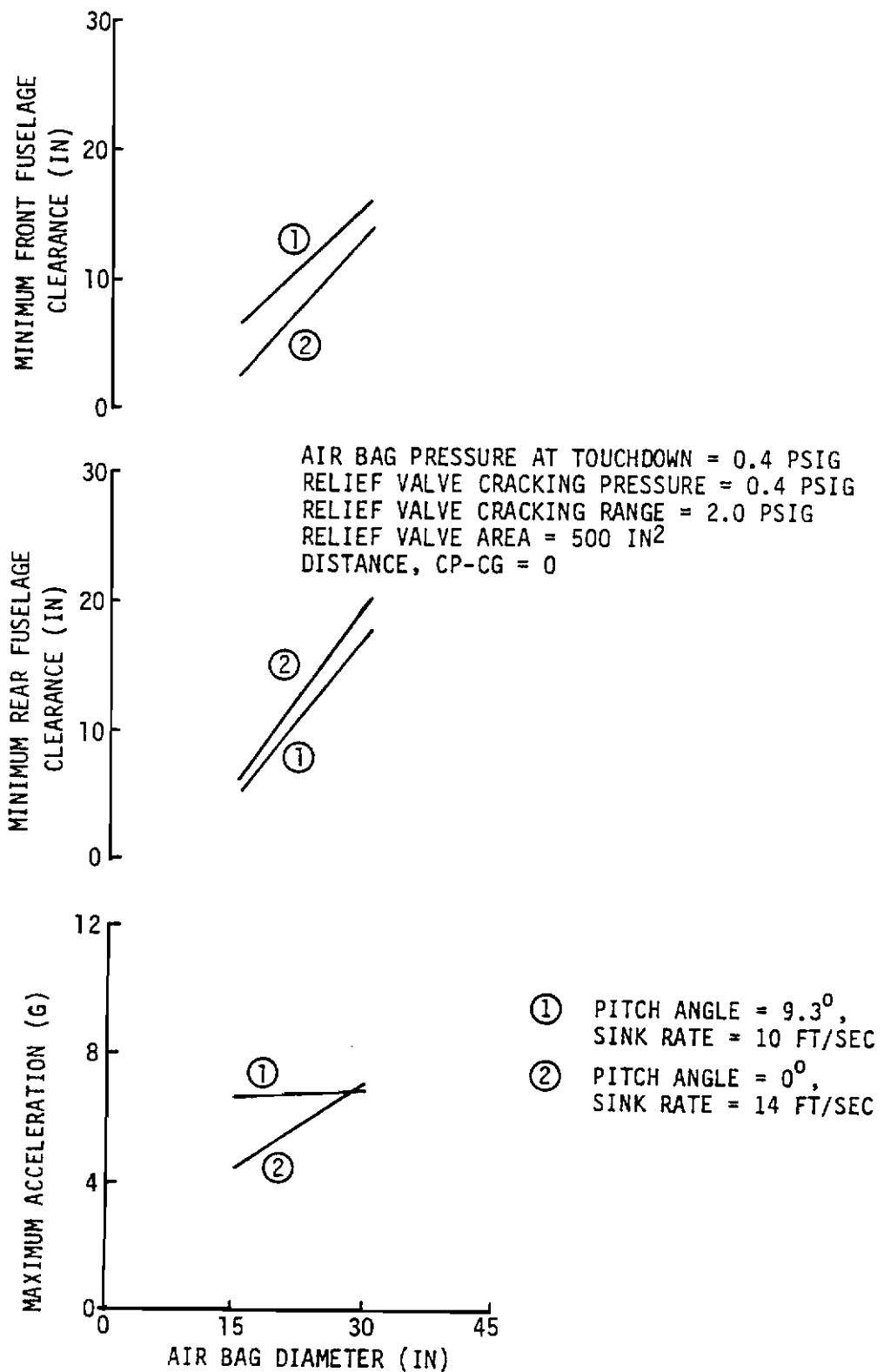


Figure 51 Boeing ARPV with ABSS, 3 DOF Landing Simulations, Air Bag Diameter vs. Acceleration and Clearances

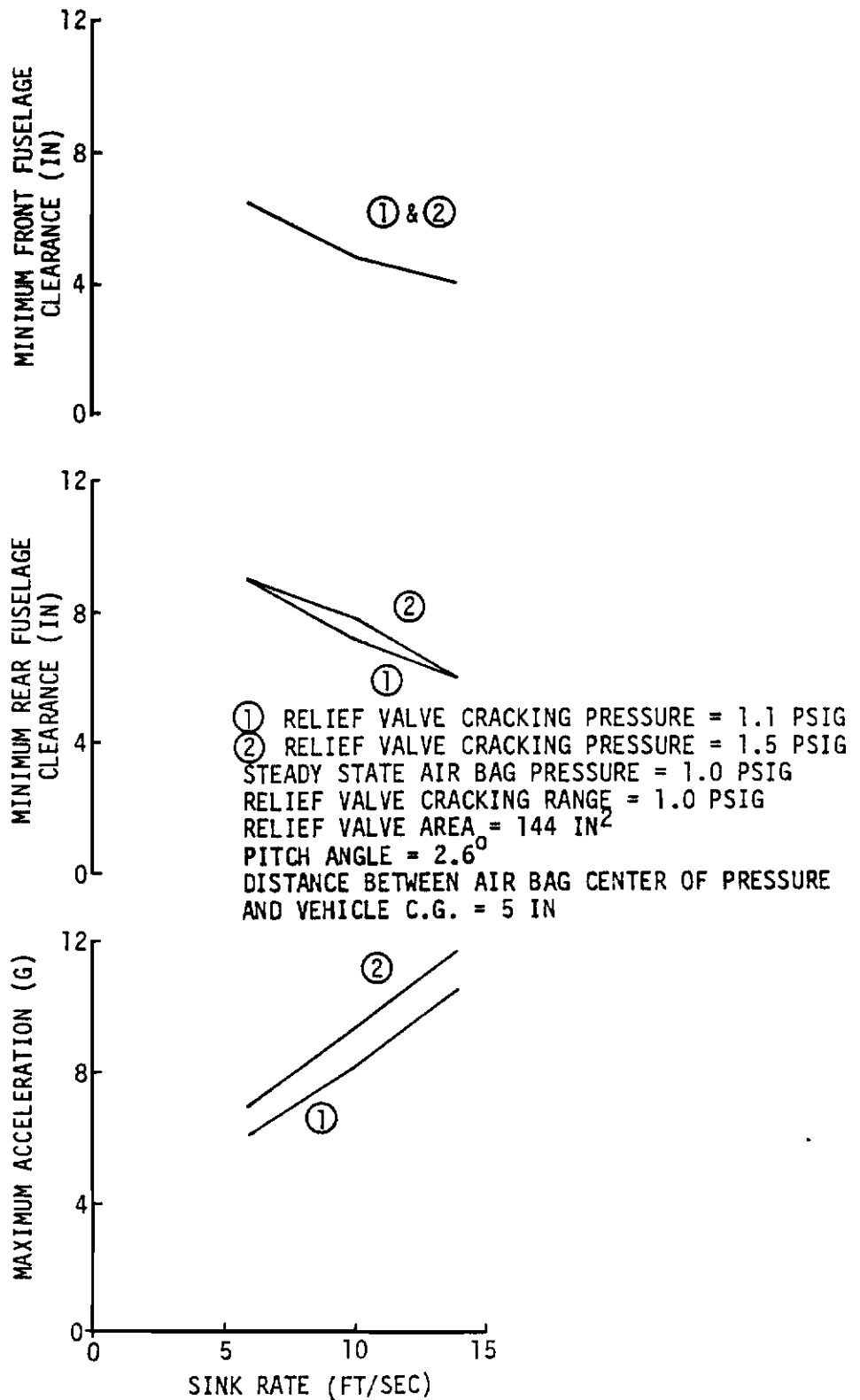


Figure 52 Boeing ARPV with ABSS, 3 DOF Landing Simulations, Relief Valve Cracking Pressure vs. Sink Rate

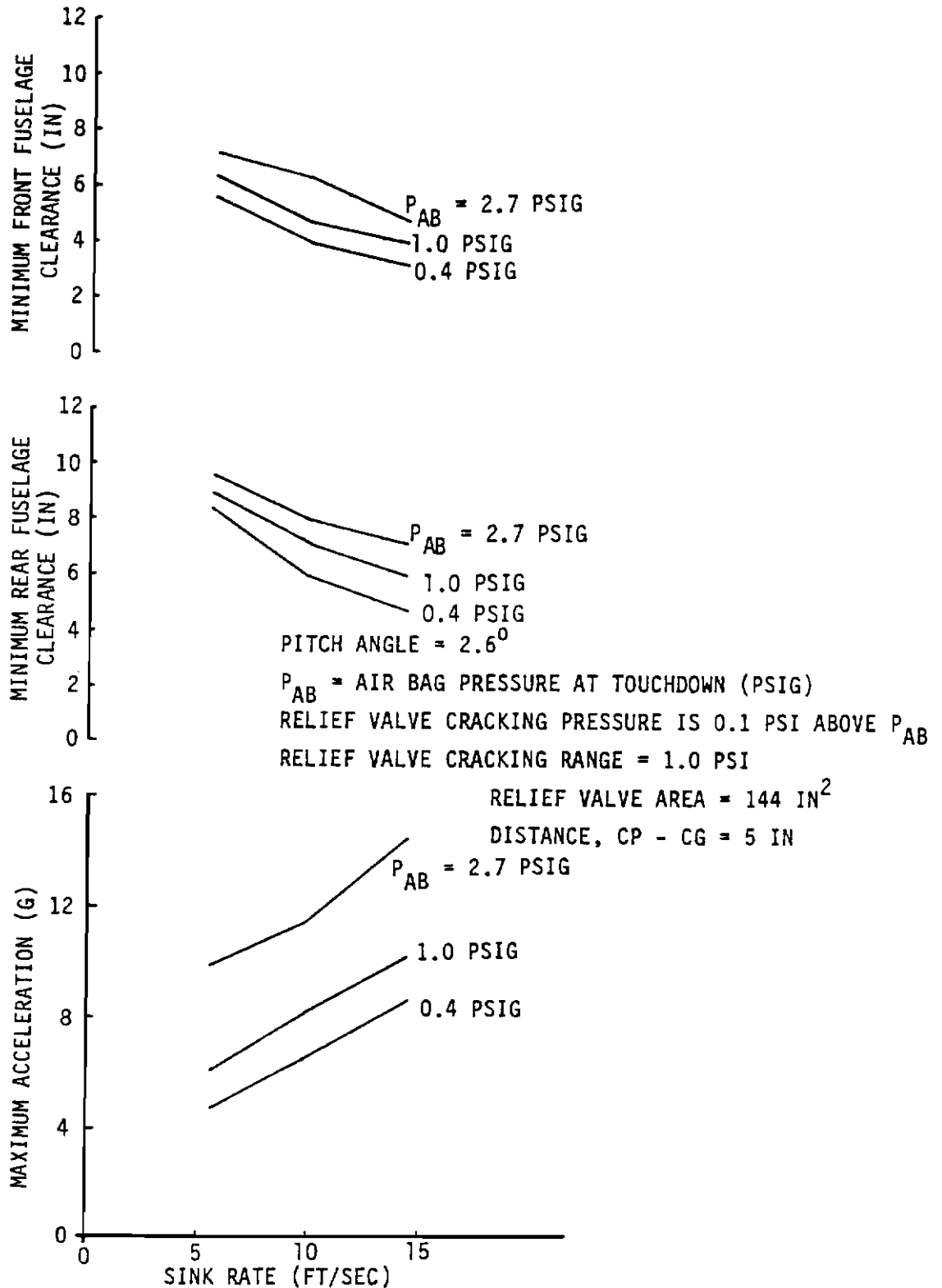


Figure 53 Boeing ARPV with ABSS, 3 DOF Landing Simulations, Air Bag Pressure vs. Sink Rate

Contrails

limitation of the wing structure. With an air cushion or air bag skid system the landing system loads are distributed along the fuselage so the wings become the limiting structure. For a vehicle such as the Boeing ARPV, with a short, small wing and no stores carried on the wing, the load factor can be increased to 8 or 10g with little effect on the structure weight.

The lower limit on the steady state bag pressure prior to touchdown is determined by the dynamic pressure acting on the bag at landing approach speeds. This dynamic pressure is approximately 0.5 psig at 130 knots, therefore a minimum bag pressure of about 1.0 psig will give the bags sufficient rigidity to prevent flutter and retain their cylindrical shape during minor maneuvers and wind gusts. A relief valve cracking pressure of 0.1 psi above the bag steady state pressure is a minimum from a practical design standpoint.

Another series of simulations were performed which investigated the effects of pitch angle and sink rate on peak landing impact loads. The relief valve cracking pressure was fixed at 1.1 psig and the initial bag pressure set at 1.0 psig for this series. Results are shown in Figures 54 and 55. The points where the constant pitch angle lines in Figure 54 cross the structural load limit lines have been plotted in Figure 55 to form a load limit constraint envelope for 6g, 8g and 10g. The shape of this curve with a minimum sink rate point at a pitch attitude of 4 degrees results from the manner in which the air bag skid forces and moments acting on the vehicle are affected by pitch angle. As pitch angle increases, initial bag-ground contact area is reduced so the effective bag spring rate is lower, resulting in lower force. However, as pitch angle increases the bag-ground force moment arm relative to the vehicle center of gravity increases and the moment acts for a longer period of time resulting in higher vehicle pitch-over rates. For this particular vehicle configuration, these counter trends reach a minimum at a pitch angle of about 4 degrees. Combinations of landing impact pitch angle and sink rate to the left of those envelopes will result in peak air vehicle loads below the load limit. A line defining the mean landing approach trim conditions has also been plotted in Figure 55. These mean

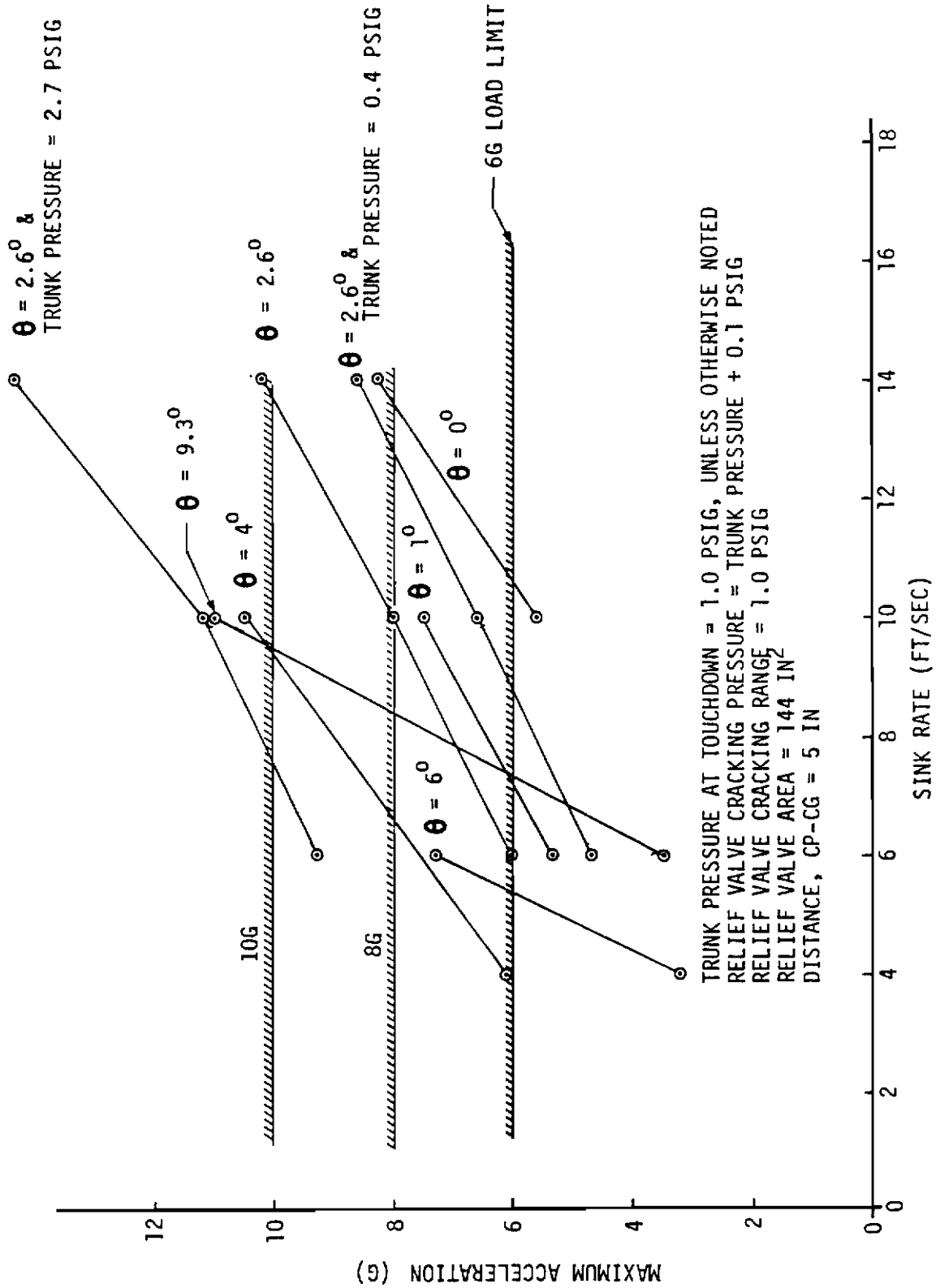


Figure 54 Boeing ARPV with ABSS, 3 DOF Landing Simulations, Maximum Acceleration vs. Sink Rate

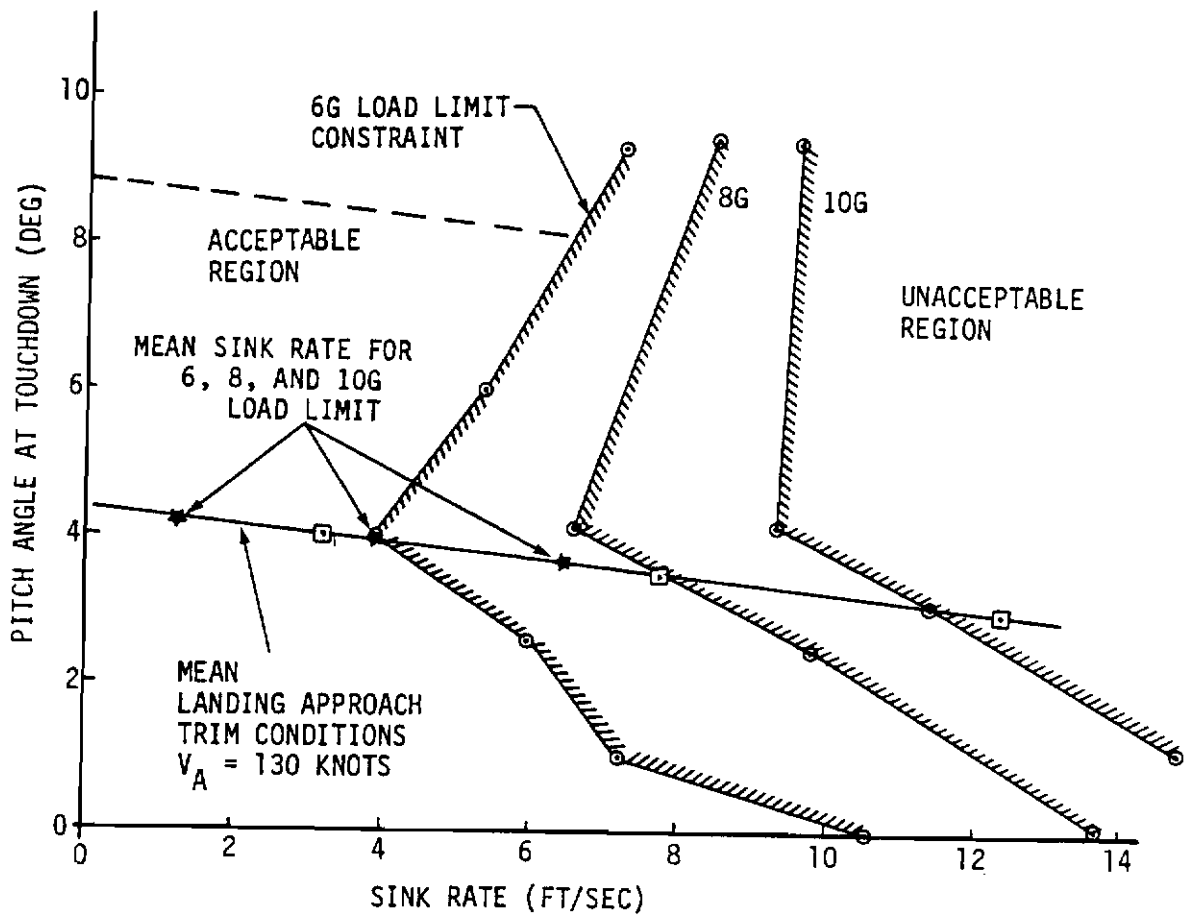


Figure 55 Boeing ARPV with ABSS, Landing Trim Conditions and Touchdown Constraints

Contrails

trim conditions were taken from Figure 14 shown in Paragraph 1.b. Air turbulence and wind gusts will cause the actual touchdown attitude of the air vehicle to be perturbed from these mean conditions. This can be described as a wide band centered on the mean conditions. According to MIL-A-8863A (Reference 5), the standard deviations for touchdown pitch and sink rate are 2.25 degrees and 1.33 ft/sec, respectively. If 2σ conditions are used to define the design conditions, the air vehicle sink rate must be less than 1.24, 4, and 6.5 ft/sec at touchdown for satisfactory performance with load limits of 6, 8 and 10g, respectively. Ground effects which tend to slow the vehicle rate of descent at touchdown, will permit a greater sink rate during approach but the magnitude of this effect was not known. Therefore, it was not considered in this estimate of the trimmed sink rate limit. From Figure 14, sink rates of 1.24, 4, and 6.5 ft/sec are achieved when the glide slope angles are 0.3, 1.0 and 1.7 degrees, respectively.

In general, these mean touchdown trim conditions of pitch angle = 4.25 degrees, sink rate = 1.24 ft/sec and glide slope angle = 0.3 degrees for the 6g limit condition are very restrictive. Therefore, an effort was made to modify the air bag system design so the 6g load limit line on Figure 55 would move to the right, but little success was achieved since the most influential design variables were already at their limits.

A design change that may improve system performance would be to change the bag shape from circular to elliptical to achieve greater stroke with reduced contact area. The EASY Air Bag Skid model was developed for analysis of circular cross sections only so elliptical shapes were not investigated. Restricting the bag width to achieve greater stroke without increasing foot print area is a technique used in design of impact attenuation bags such as those used on the B-1 bomber crew escape capsule.

After an air bag size had been established based upon the three DOF longitudinal simulations, six DOF simulations were performed to verify the lateral stability of the recovery system during landing. These simulations were made with and without the arrestment system and included

approximately the first three seconds after landing impact. Figures 56 through 58 show that the air vehicle is directionally unstable when it lands without arrestment. Roll and yaw angles begin diverging less than one second after touchdown, and air vehicle loads rapidly increase because of this unstable motion. Results of an identical landing simulation with arrestment are shown in Figures 59 and 60. These results show that the arrestment system gives the air vehicle directional stability, but the peak loads on the air vehicle are well over its 6g load limit. Landing impact loads combined with arrestment loads result in a peak load of approximately 20g on the air vehicle. Based upon these results, the arrestment system design variables were modified to reduce the peak arrestment loads. Water twister damping coefficient, tape drum radius, and tail hook length and location were the principal design variables to be adjusted. However, if the peak arrestor loads occur simultaneously with the landing impact loads, the results were still unacceptable. Each of these events must occur far enough apart so that the loads due to each do not occur simultaneously.

The previous results for the unarrested landing indicate that the air vehicle can be expected to remain directionally stable during the first second after impact. Also, these simulations were carried out with the air vehicle control surfaces fixed in their landing approach trim positions. In reality, the control surfaces would be active during the first few seconds after landing impact, and because of the high air speed, they will be capable of controlling the air vehicle direction and heading until its speed has reduced by about 50%. Therefore, the recovery operations can be planned such that touchdown occurs prior to cable engagement. Arrestor system parameters are listed in Table 12.

(b) Boeing ARPV with ACRS

The baseline ARPV with the ACRS installation is shown in Figure 23. This figure shows a cool gas generator supplying primary flow to the trunk ejector. However, the math model used in the simulations only included the ejector component since it is the dominant component of the air supply system. The dynamic characteristics of primary flow ducting, valves and the cool gas generator are not

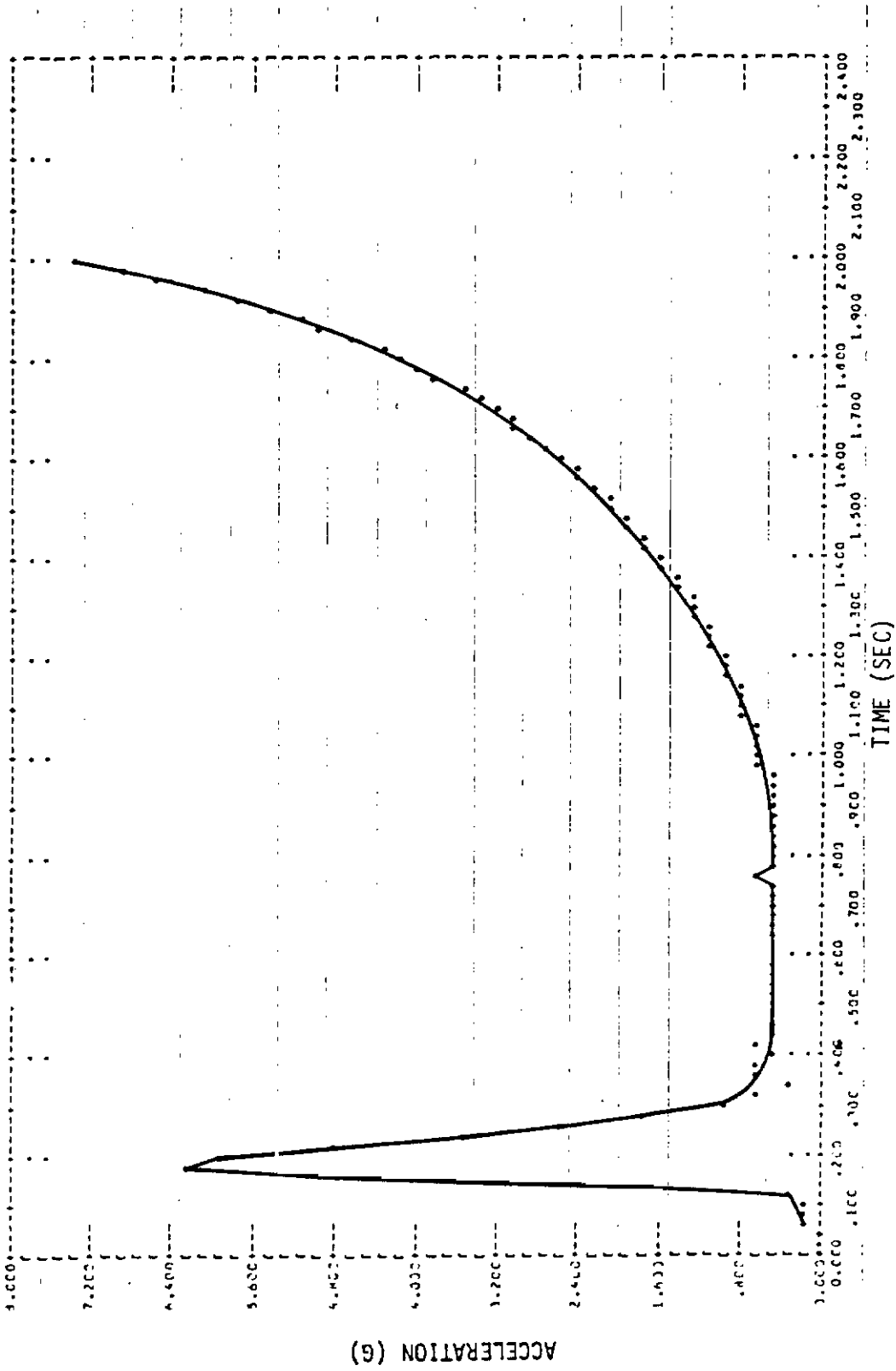


Figure 56 Boeing ARPV with ABSS, 6 DOF Landing Simulation without Arrestment, Acceleration vs. Time

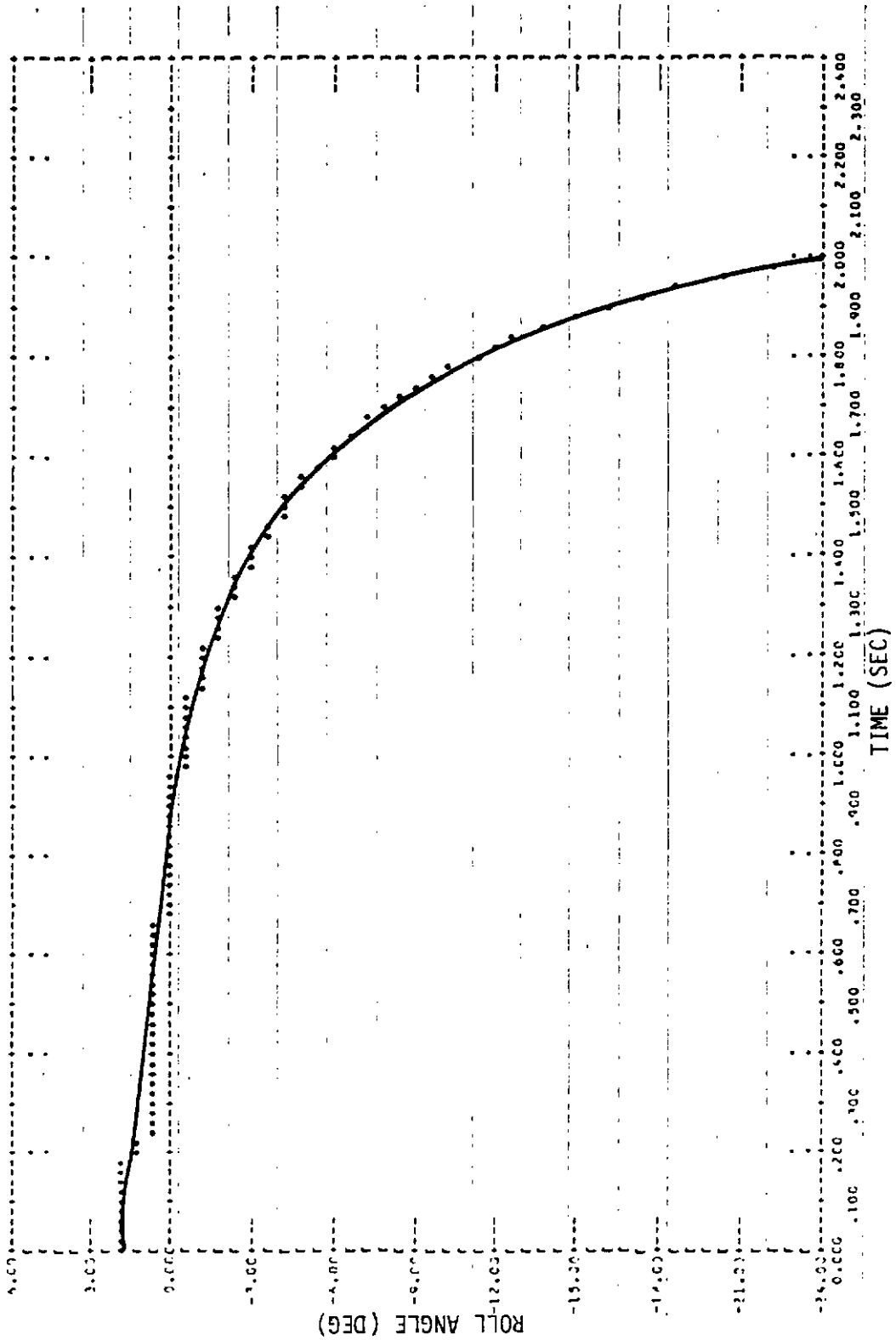


Figure 57 Boeing ARPV with ABSS, 6 DOF Landing Simulation without Arrestment, Roll Angle vs. Time

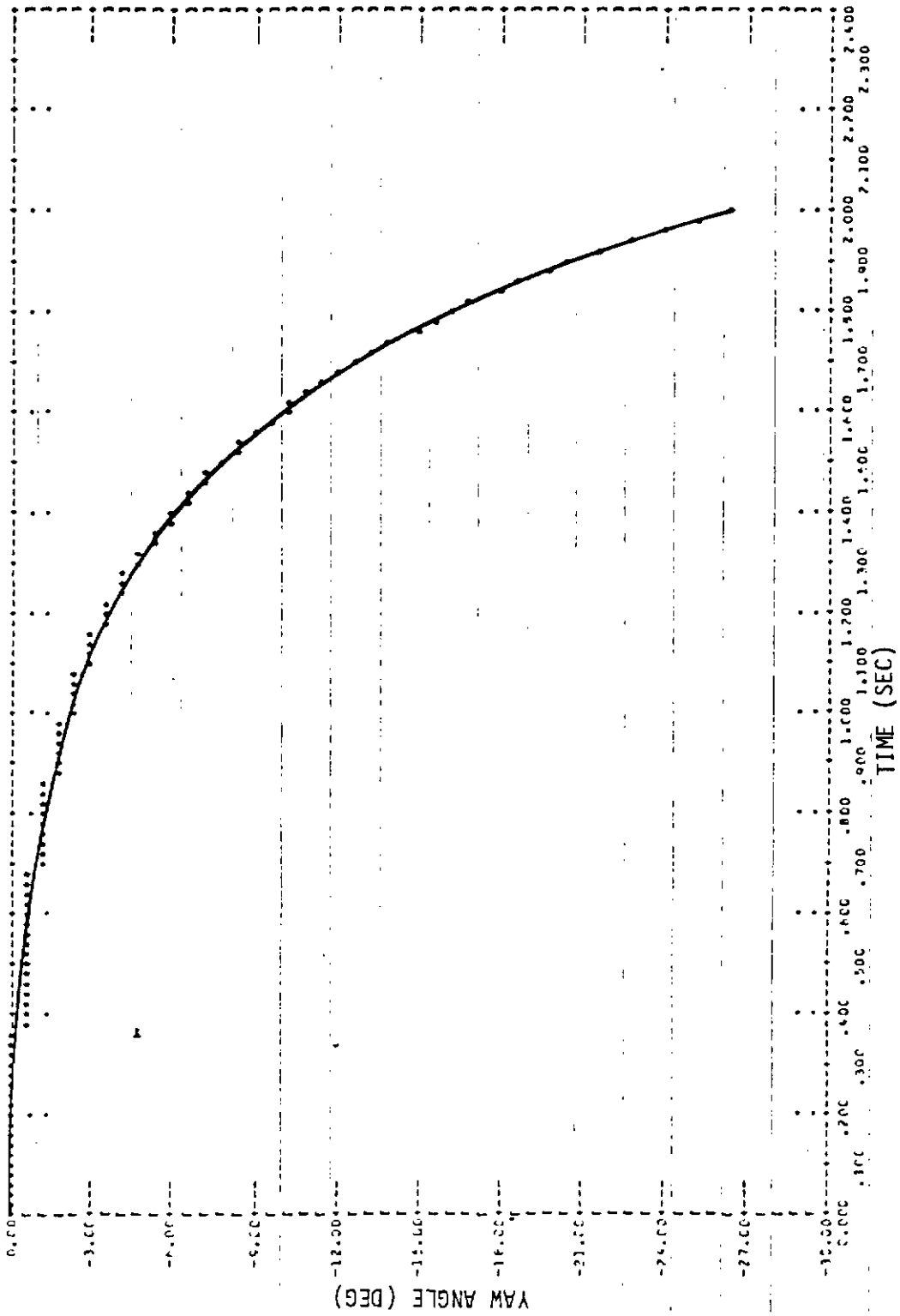


Figure 58 Boeing ARPV with ABSS, 6 DOF Landing Simulation without Arrestment, Yaw Angle vs. Time

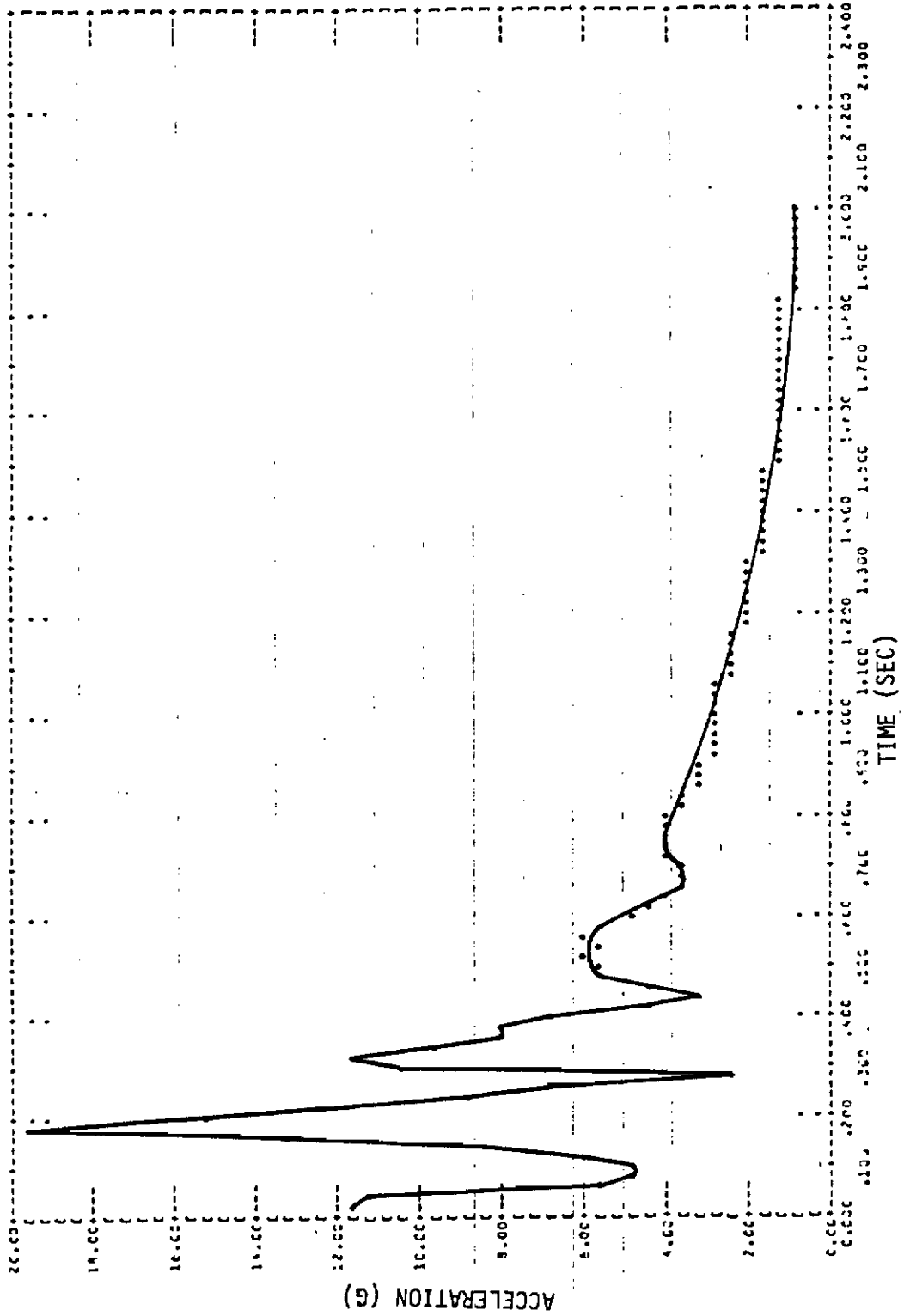


Figure 59 Boeing ARPV with ABSS, 6 DOF Landing Simulation with Arrestment, Acceleration vs. Time

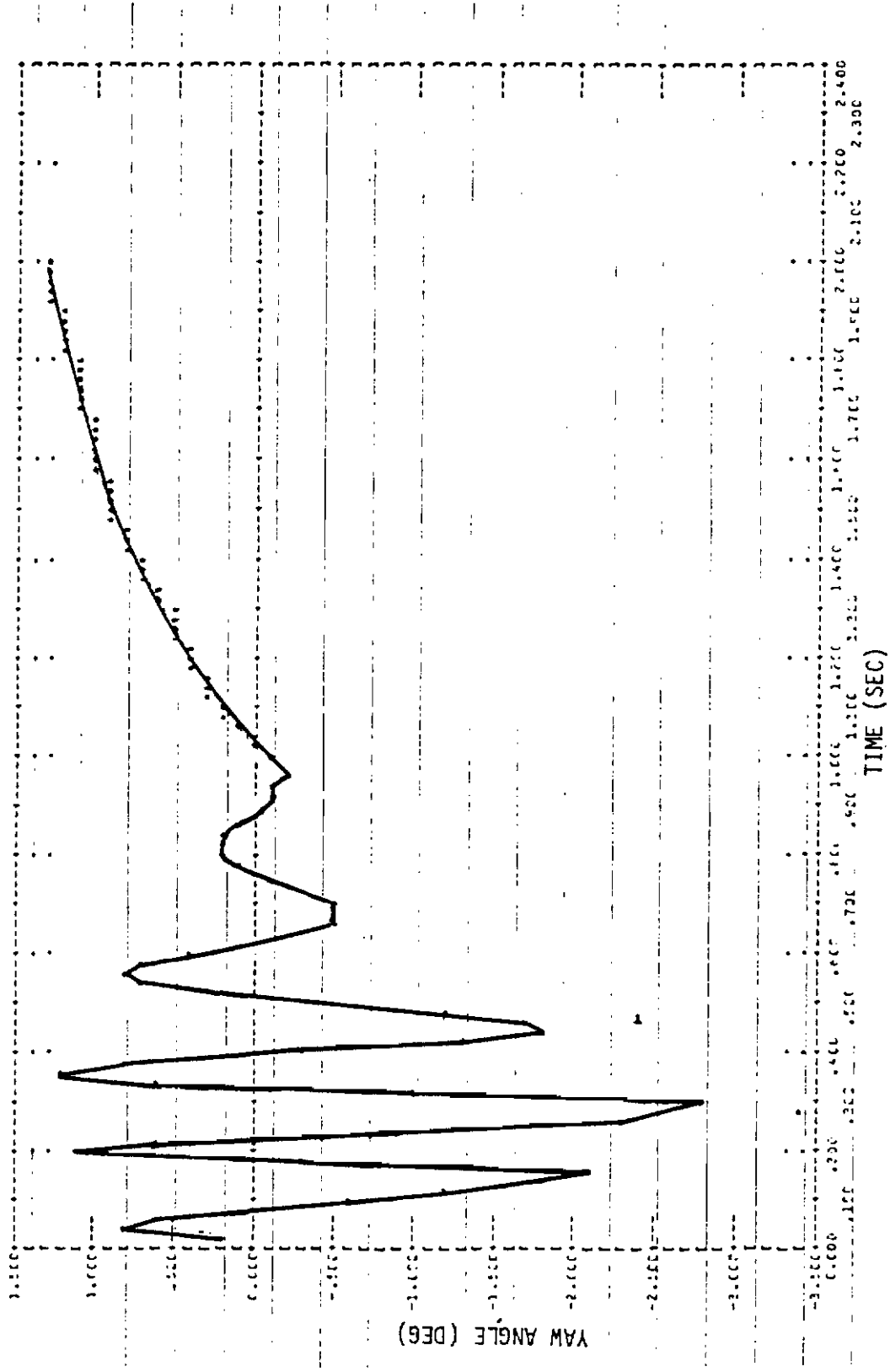


Figure 60 Boeing ARPV with ABSS, 6 DOF Landing Simulation with Arrestment, Yaw Angle vs. Time

Contrails

significant in these landing simulations because ejector back pressure does not effect primary flow.

The original air cushion trunk used in the simulations was 120 inches long and 30 inches wide. The trunk length being defined as the longitudinal distance between the most forward attachment point and the most aft attachment point. The trunk width being defined as the lateral distance between outboard attachment points. Figure 61 shows the principal dimensions of this trunk installed on the air vehicle. The sectional shape of the trunk varies as trunk pressure, cushion pressure, and air vehicle height change. These geometric relationships are determined by program EASY and are shown in Figures 62 through 65.

As with the air bag skid system, the touchdown initial conditions for these simulations were based upon MIL-A-8863A (Reference 5) and the air vehicle mean landing approach trim conditions, as shown in Table 6 and Figures 12 and 13. The stability derivatives for the air cushion trunk shape are slightly different than those for the air bag skid shape, therefore the attitude of the air vehicle when trimmed for a given glide path and sink rate is also slightly different. These are discussed in Paragraph 1.b, Boeing ARPV Inflight Simulation. All control surfaces were fixed at their trim positions during these landing simulations, unless otherwise noted.

Analysis approach was the same as for the air bag skid system. One second duration, three DOF landing simulations were made to determine peak impact loads and minimum clearances for alternative trunk designs during realistic landing conditions. From results of these studies, a trunk design giving satisfactory performance was selected.

Various trunk sizes and air supply system designs were investigated. Trunk length was varied between 120 and 160 inches. Because the air bag skid simulations showed that an increased trunk width was not necessary, such design variations were not investigated for the Boeing vehicle with ACRS.

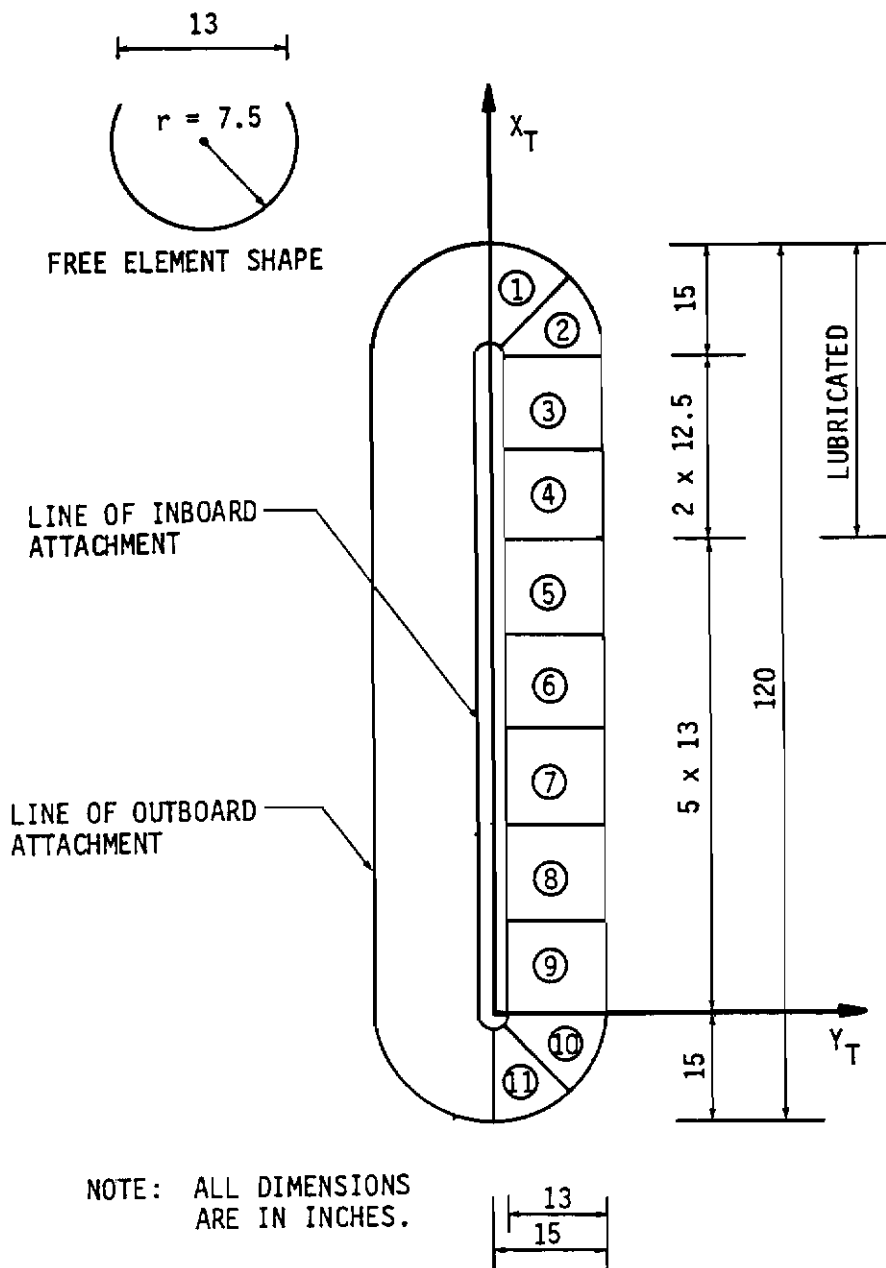


Figure 61 Baseline Air Cushion Model for Boeing ARPV

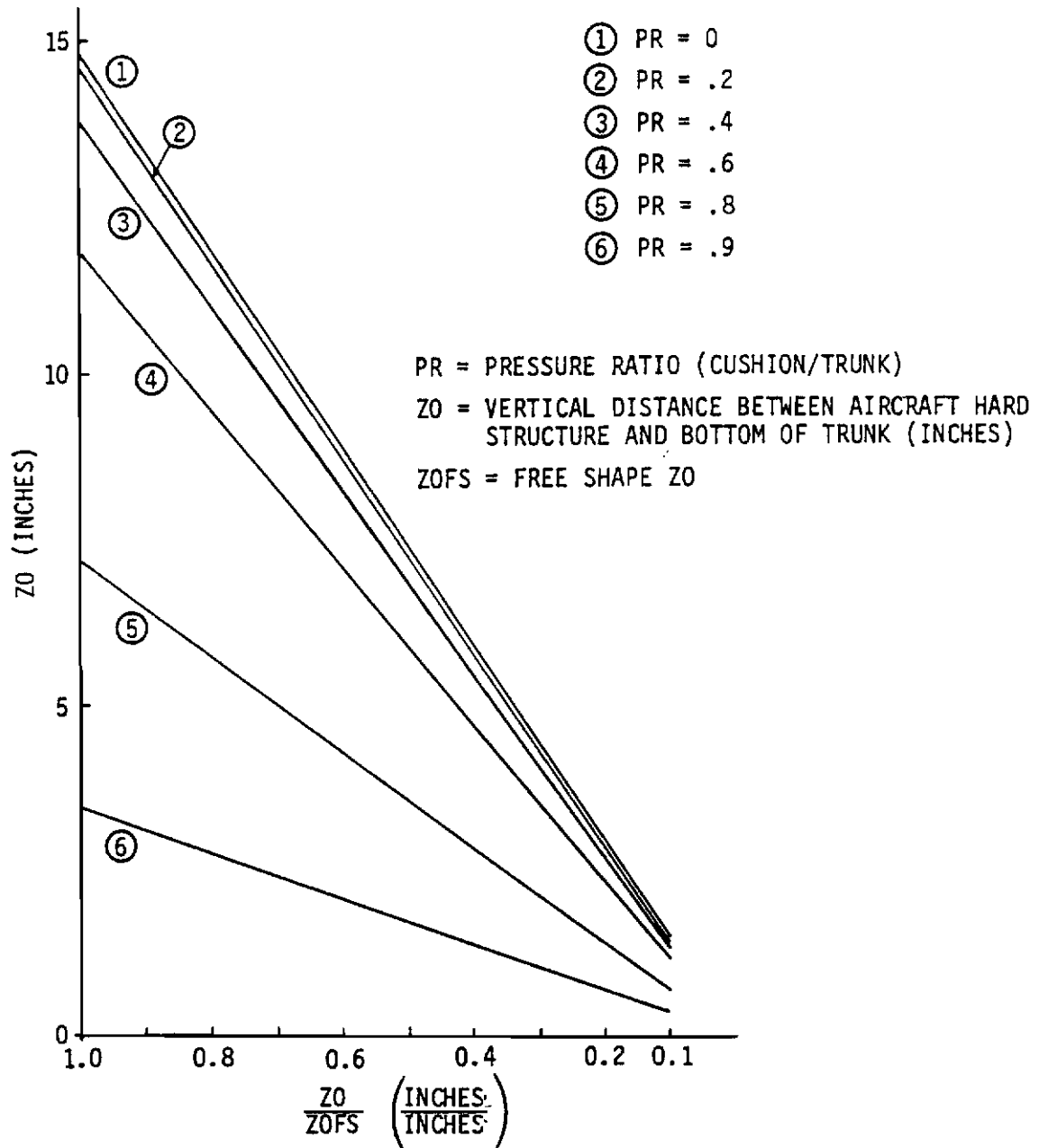


Figure 62 Trunk Geometry for Boeing ARPV with Baseline ACRS, Z0 vs. Z0/ZOFS

Contrails

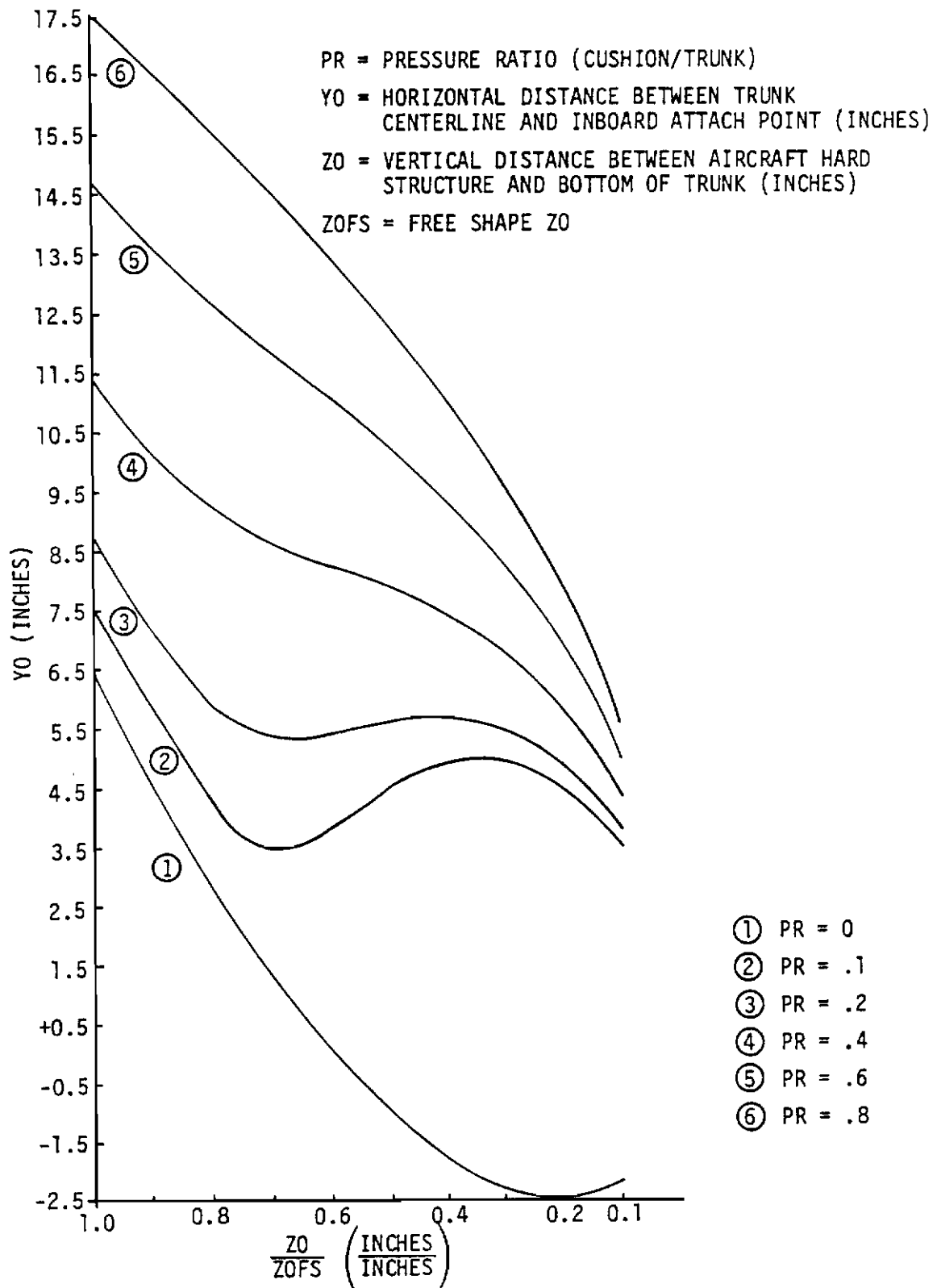


Figure 63 Trunk Geometry for Boeing ARPV with Baseline ACRS, YO vs. ZO/ZOFS

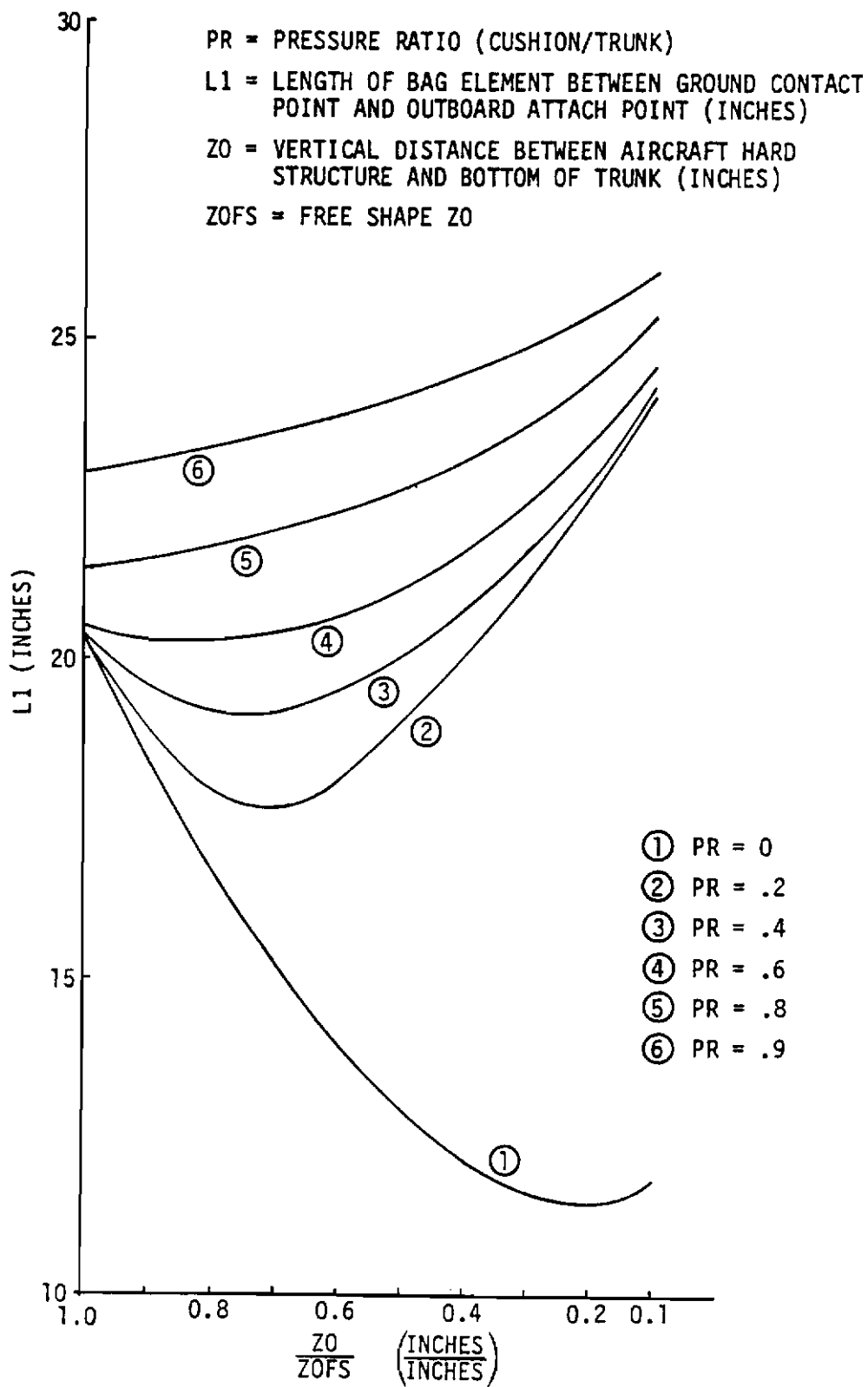


Figure 64 Trunk Geometry for Boeing ARPV with Baseline ACRS, L1 vs. ZO/ZOFS

Contrails

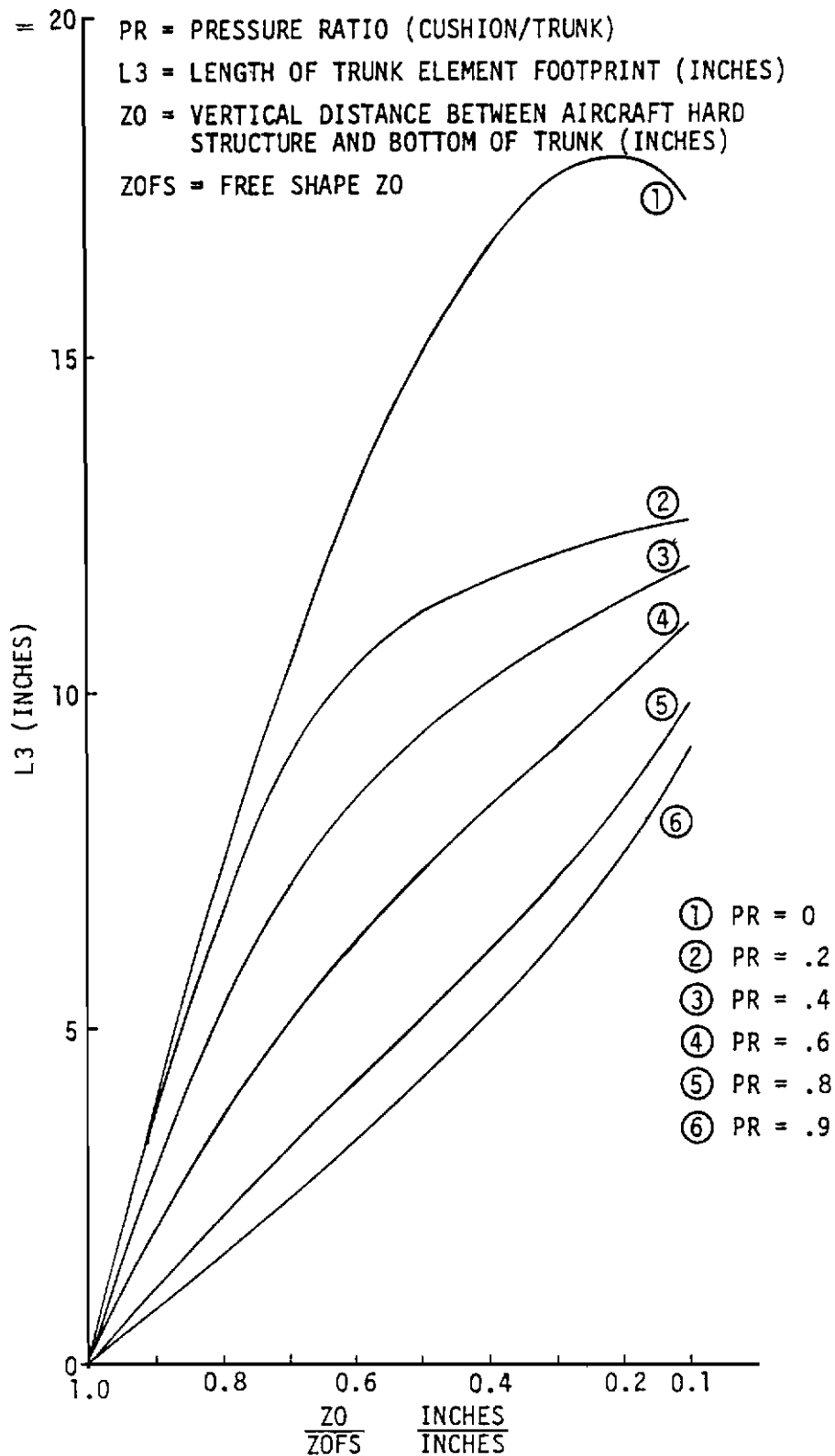


Figure 65 Trunk Geometry for Boeing ARPV with Baseline ACRS, L3 vs. Z0/ZOFS

Contrails

The design variables investigated during these simulations to improve ACRS landing performance included trunk flow requirements, relief valve cracking pressure, initial trunk pressure at touchdown, distance between the trunk center of pressure and the air vehicle center of gravity, addition of a cushion vent to reduce cushion pressures, use of the elevons to reduce pitch rates and maximum pitch angles at landing impact, and control of the ejector primary pressure and flow.

The flow requirements for this air cushion trunk are more complex than those for the air bag skid system because the forward one-third of this trunk is lubricated. Analysis determined that different steady state pressures and flows are required before and after landing impact. This implies that control of the primary ejector pressure and flow are needed. Different trunk flow requirements would also exist if the trunk leakage had increased due to damage sustained during a mission. The controller would sense trunk pressure to control primary ejector pressure.

Results from these simulations indicated that a trunk length of 138" gives satisfactory performance. Results from several simulations which varied the sink rate and pitch angle of the air vehicle at touchdown are shown in Figure 66. Points on these curves where the 6, 8, and 10g load limit lines are crossed were again plotted and results are shown in Figure 67. Figure 67 defines a 6, 8, and 10g load limit constraint envelope for the air vehicle pitch angle and sink rate at touchdown. These curves follow the same trends as that shown for the Boeing vehicle with an ABSS which was discussed earlier.

A line defining the mean trim conditions for the Boeing ARPV with its ACRS deployed is also shown. All combinations of touchdown sink rate and pitch angle to the left of the envelopes will result in satisfactory landings. When the statistical characteristics of touchdown conditions are considered, a design touchdown condition can be specified. This condition is shown as point * on Figure 67 for each of the three load limits specified. A clearance constraint envelope is also shown in Figure 67, but it is not an active constraint for the shown trim conditions. Figure 68 shows more clearly that longitudinal clearances are not a problem for this trunk design.

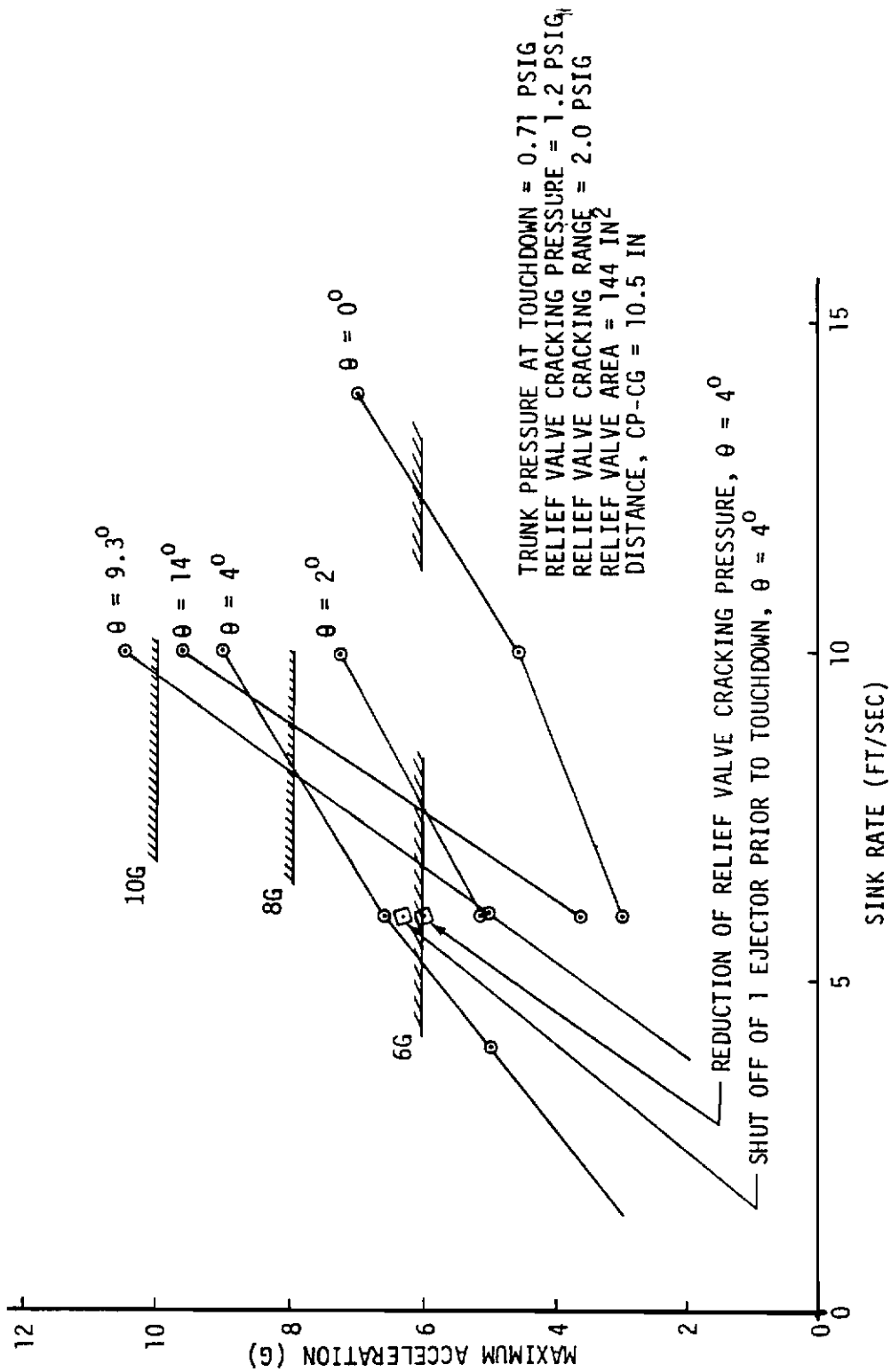


Figure 66 Boeing ARPV with ACRS, 3 DOF Landing Simulations, Maximum Acceleration vs. Sink Rate

Contrails

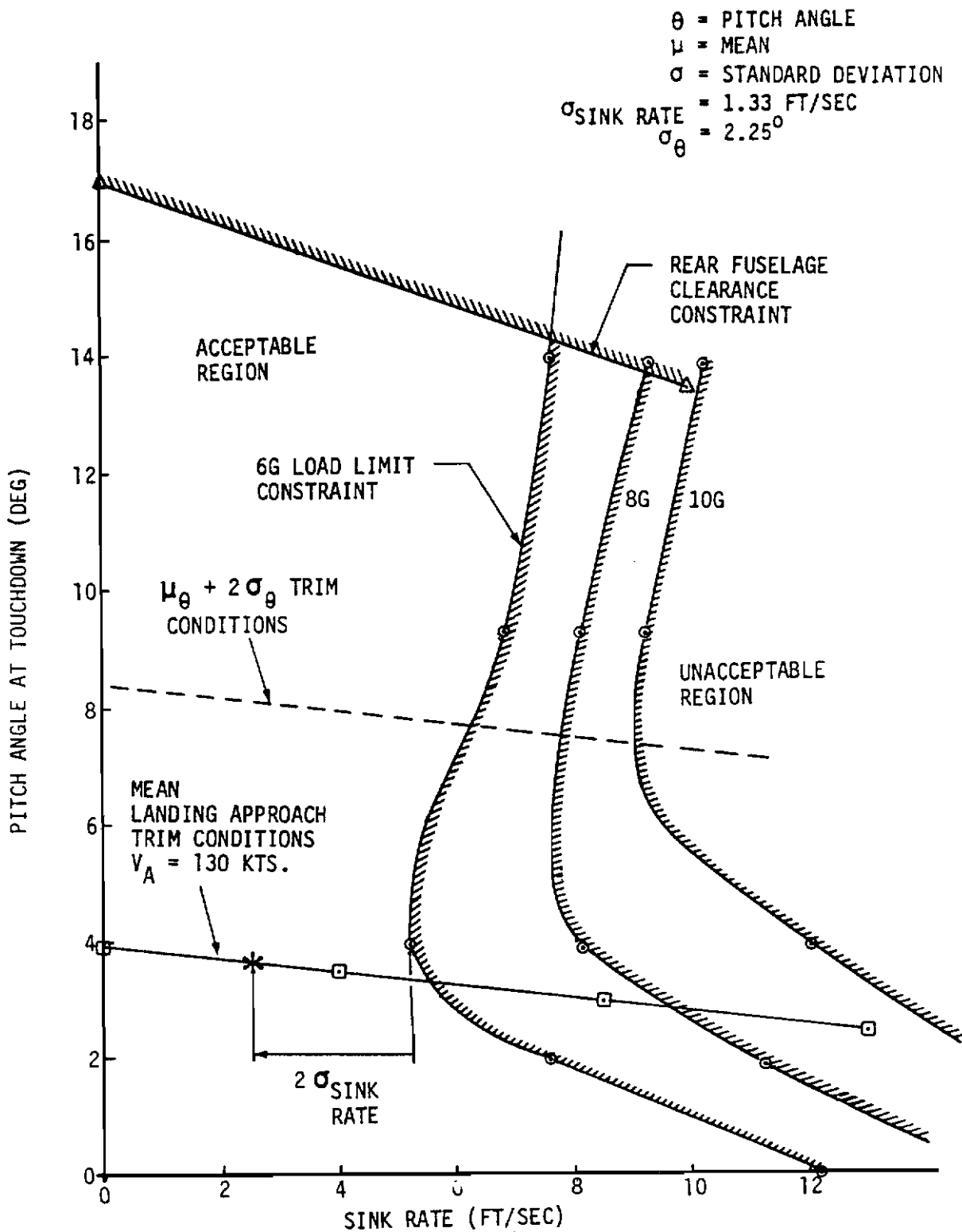


Figure 67 Boeing ARPV with ACRS, Landing Trim Conditions and Touchdown Constraints

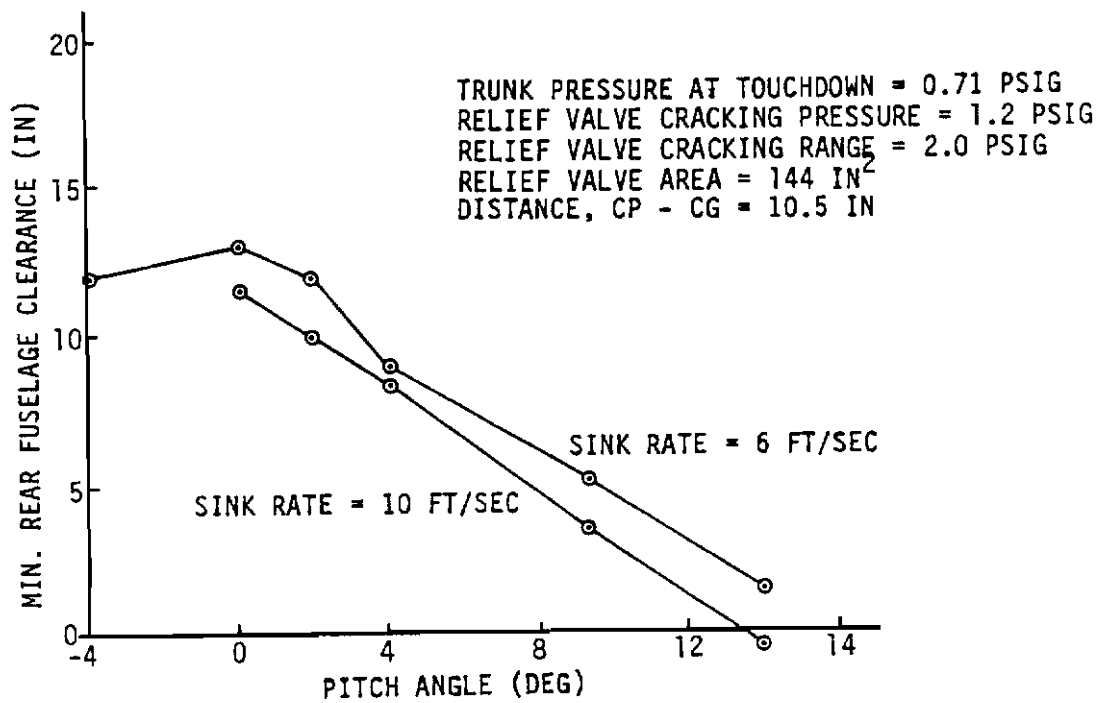
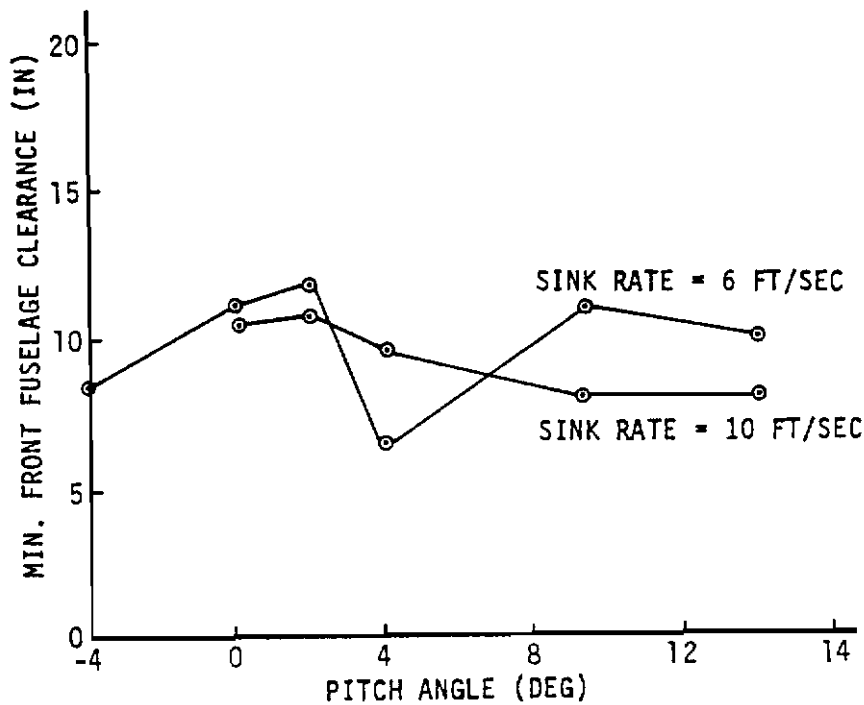


Figure 68 Boeing ARPV with ACRS, 3 DOF Landing Simulations, Clearances vs. Pitch Angle

Contrails

Simulations were also made to determine the feasibility of using the air vehicle control surfaces to reduce landing impact loads. Peak impact loads occur in the direction of the air vehicle Z body axis.

Accelerations along this axis are caused by a combination of forces acting along the Z axis and two cross products, $\bar{U}\bar{X}\bar{Q}$ and $\bar{V}\bar{X}\bar{P}$, where:

\bar{U} = Vehicle x axis velocity

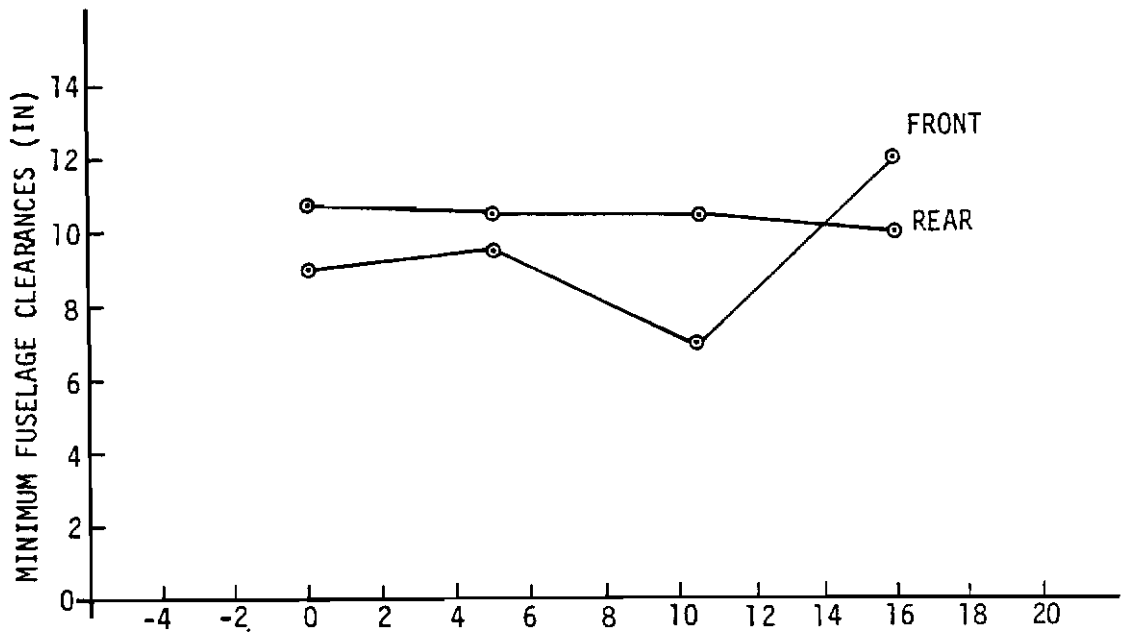
\bar{Q} = Vehicle pitch rate

\bar{V} = Vehicle y axis velocity

\bar{P} = Vehicle roll rate

The \bar{V} and \bar{P} rates are essentially zero for all touchdown conditions. Forces along the Z axis are primarily the aerodynamic lift, trunk loads, and the air vehicle weight. For this air vehicle, the $\bar{U}\bar{X}\bar{Q}$ cross product is a major contribution to peak impact loads. This air vehicle lands at a rather high speed of 130 knots, and because it normally lands in a nose-up attitude, negative pitching moments occur when the aft end of the trunk contacts the ground. These pitching moments combined with the rather low pitching moment of inertia result in high pitch accelerations and rates during landing impact. The elevon control surface can be used to increase pitch damping to reduce these pitch rates and the corresponding impact loads. Simulations were performed which used the elevon as a pitch damper and results indicated that this can be effective in reducing the peak landing impact loads. The effectiveness of this method is limited by the maximum available elevon rate. The distance between the trunk center of pressure and the air vehicle center of gravity was also varied during these simulations to determine its effect on landing performance. Figure 69 shows that the minimum fuselage to ground clearances are not affected significantly by variations in this distance, but the peak landing impact load has a definite tendency to decrease as the trunk is moved further forward on the fuselage. This reduction in peak landing loads is due to the decreased pitching moment arm between the aft end of the trunk and the air vehicle c.g. A reduced moment arm reduces the negative pitch moment at impact, which reduces pitch rate, \bar{Q} . The cross product $\bar{U}\bar{X}\bar{Q}$, a principal component of the peak landing impact load, is therefore reduced.

Contrails



PITCH ANGLE = 4°
 SINK RATE = 6 FT/SEC
 TRUNK PRESSURE AT TOUCHDOWN = 0.71 PSIG
 RELIEF VALVE CRACKING PRESSURE = 1.2 PSIG
 RELIEF VALVE CRACKING RANGE = 2.0 PSIG
 RELIEF VALVE AREA = 144 IN²

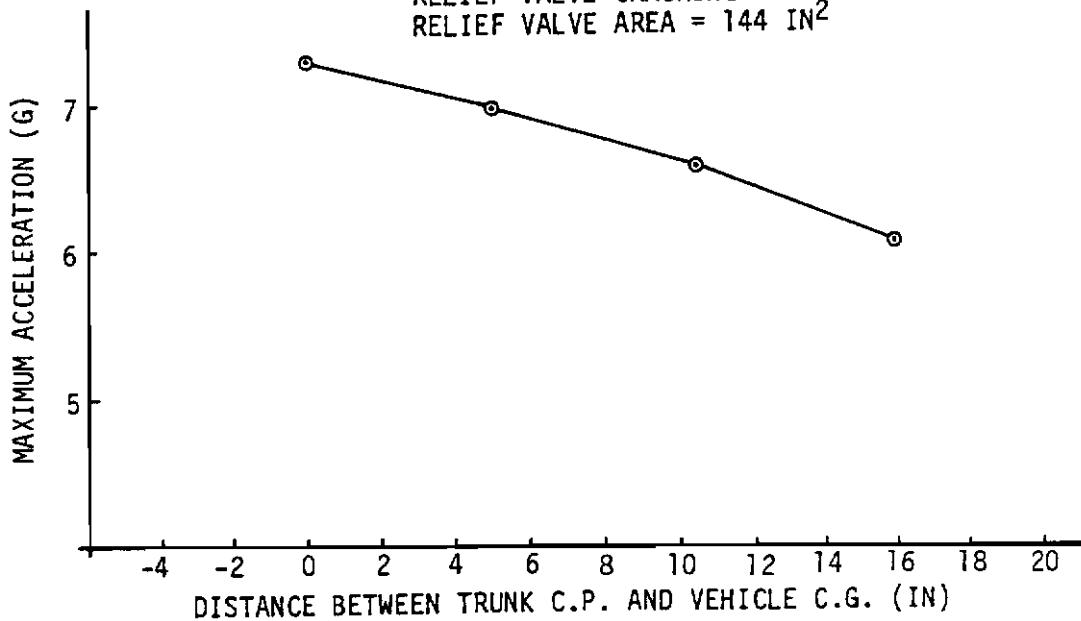


Figure 69 Boeing ARPV with ACRS, 3 DOF Landing Simulations,
 Distance Between Trunk C.P. and Vehicle C.G.
 vs. Acceleration and Clearances

After the most significant results from the three DOF simulations were obtained, six DOF simulations were performed to check the lateral motion and directional stability of the recommended trunk design. Suction braking was also simulated.

The effectiveness of suction braking was analyzed for the Boeing ARPV with the ACRS installation for both wet and dry runway conditions. Results are shown in Figure 70. This analysis included the effect of aerodynamic lift and drag forces and engine idle thrust. The Boeing ARPV stopping distance is approximately 2000 feet with its engine operating at idle thrust, when the runway is dry and no suction braking is used. With a wet runway, the engine idle thrust of 300 pounds force is greater than the retarding friction force for the air vehicle so the stopping distance becomes indefinite. The effect of reducing the idle thrust is shown in the figure. Even with the engine shut off, the air vehicle takes 4000 ft to come to a complete stop on a wet runway with no suction braking. This analysis indicates that suction braking is necessary to stop the unarrested air vehicle within a satisfactory runout distance. Also, the steepness of the curves in Figure 70 indicates that just a small amount of suction braking makes very significant reductions in runout distance. A cushion pressure less than -0.75 psig will give satisfactory performance. This results in a wet runway stopping distance of less than 3000 feet.

(2) Rockwell ARPV (Inelastic) Landing Simulations (a) Rockwell ARPV with ABSS

This configuration uses two air bag skids and an arrestor hook for recovery of the air vehicle. Figure 27 shows the initial installation. The bags are mounted on deployable doors which increase the vehicle ground clearance and give the system a wide stance. An alternate arrangement, bags stowed under doors was studied for the Rockwell vehicle with ABSS as well as with ACRS. However, early analysis of this arrangement showed that the excessive trunk volume resulted in unacceptably low spring rate and damping characteristics. Therefore, it

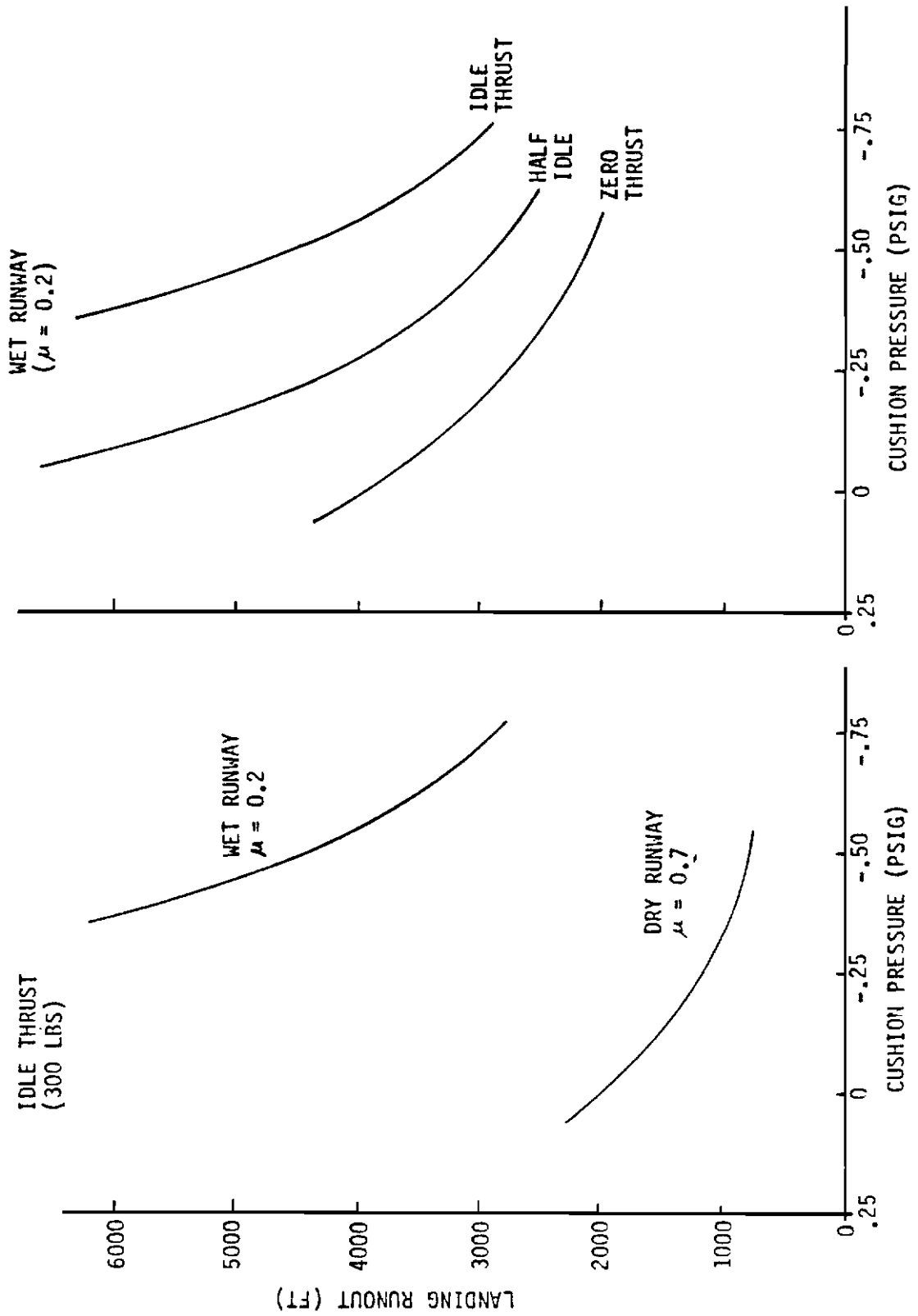


Figure 70 Landing Runout Distance for Boeing ARPV with ACRS

Contrails

was dropped from further consideration. The initial bag design to be evaluated was 120 inches long. Figure 71 shows the program EASY model of the bags. This math model divides each bag into six elements whose motion is independent of the adjacent elements. The bags are 26 inches in diameter when out of ground effect and connect to the supporting doors along a chord line.

Each bag uses an ejector nozzle for inflation. The bags do not use air lubrication since an arrestment system is used for stopping which also gives the vehicle directional stability. Therefore, the principal flow demands occur during inflation and just after landing impact when the air vehicle rebounds and air lost through the relief valve must be replaced. Engine bleed air is used as the primary gas source for the ejector nozzles. The TD-530 ejector nozzle was modeled and used in the simulations. Relationships between bag dimensions, air vehicle height, and trunk-to-ground coefficient of friction are shown in Figures 72 through 74.

The first series of three DOF simulations were carried out to determine a satisfactory bag length. Results in Figure 75 show that for bag lengths less than 150 inches, the forward end of the fuselage hit the ground. Aft fuselage clearance was satisfactory for all bag lengths from 120 to 160 inches. A bag length of 160 inches was selected as a suitable length and was used in the remaining simulations.

The second series of three DOF simulations were used to investigate those design parameters which affect the peak landing impact loads. Initial bag pressure, relief valve design, bag center of pressure relative to air vehicle center of gravity, and the air vehicle attitude at touchdown were investigated. Previous results indicated that the peak impact loads are not significantly affected by changing the bag length, as shown in Figure 75. Figure 76 shows how peak impact loads and minimum clearances vary with sink rate and initial bag pressures. The minimum practical bag pressure is approximately 1.0 psig. If the bag pressure is less than this during landing approach, the bag may deform or flutter due to aerodynamic loads acting upon it.

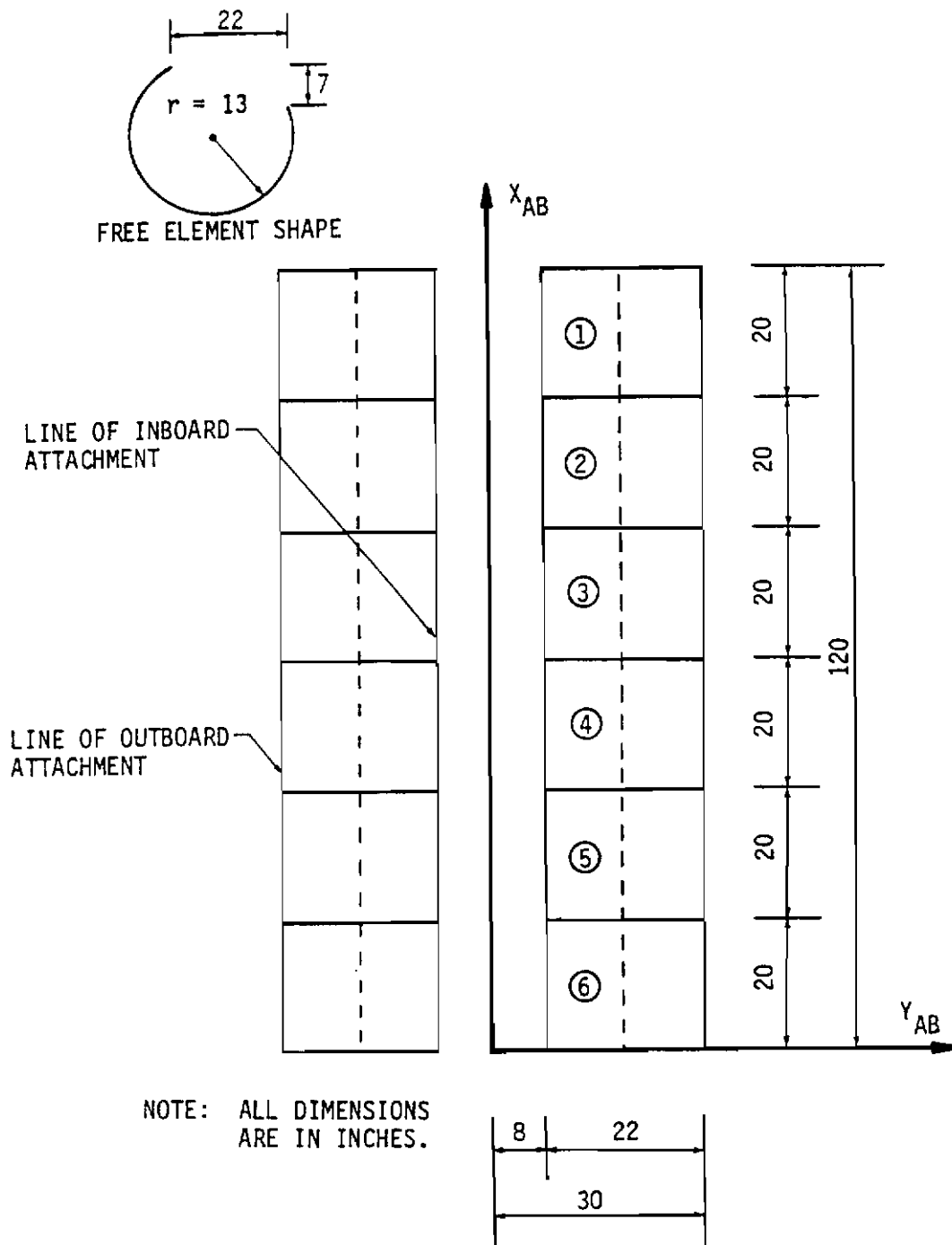


Figure 71 Baseline Air Bag Model for Rockwell ARPV

Contrails

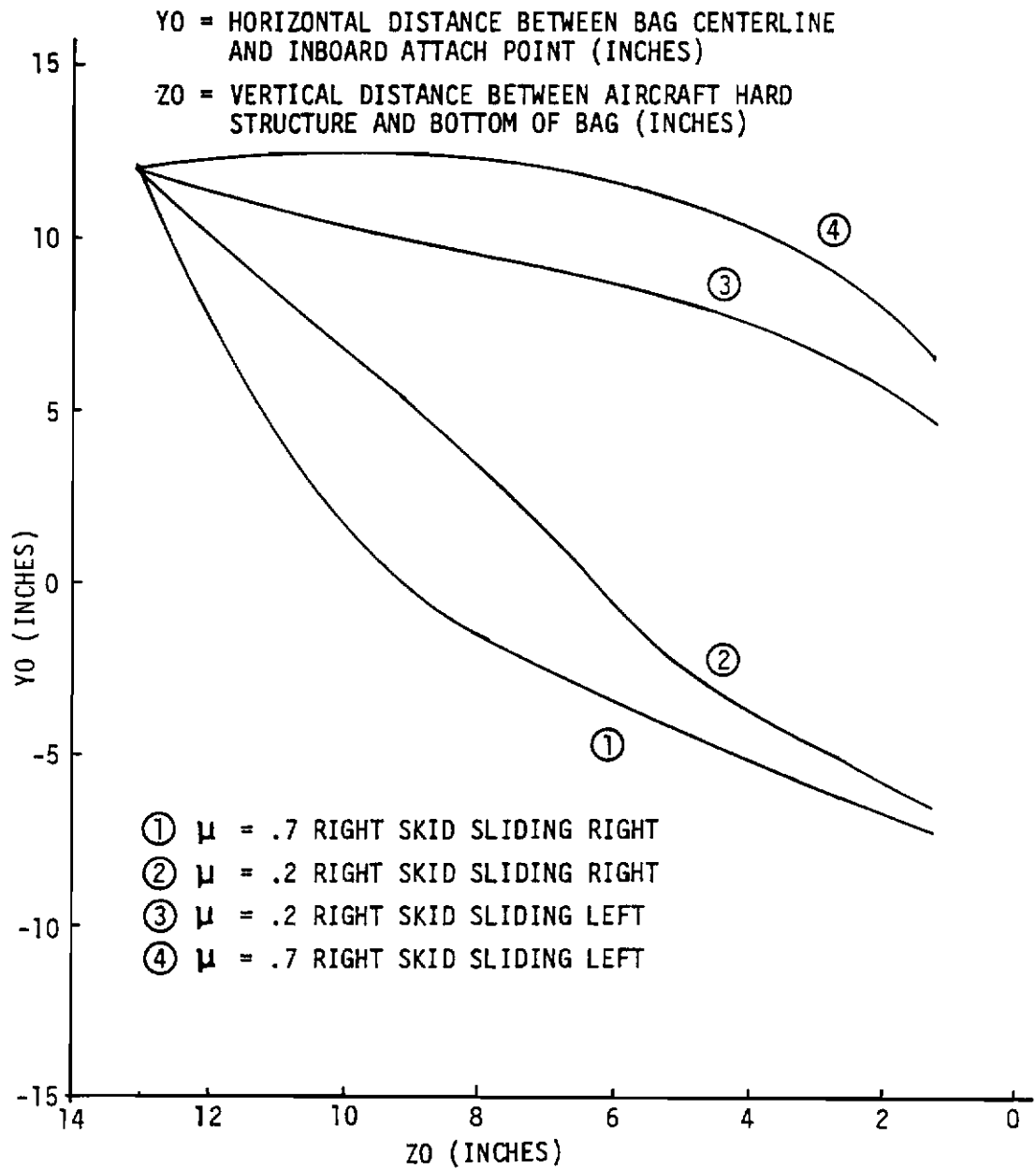


Figure 72 Air Bag Geometry for Rockwell ARPV with Baseline ABSS,
YO vs. ZO

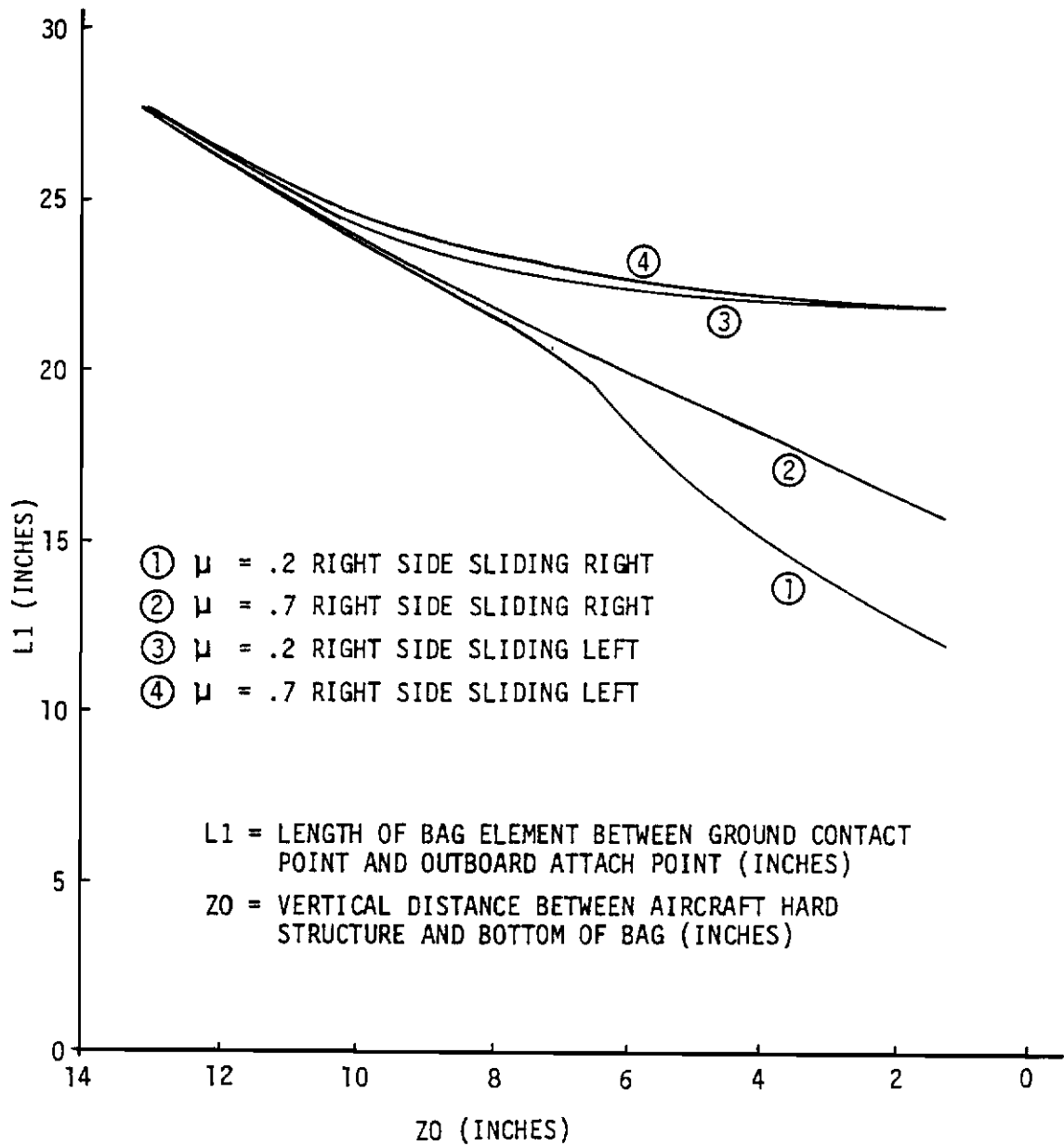


Figure 73 Air Bag Geometry for Rockwell ARPV with Baseline ABSS, L1 vs. Z0

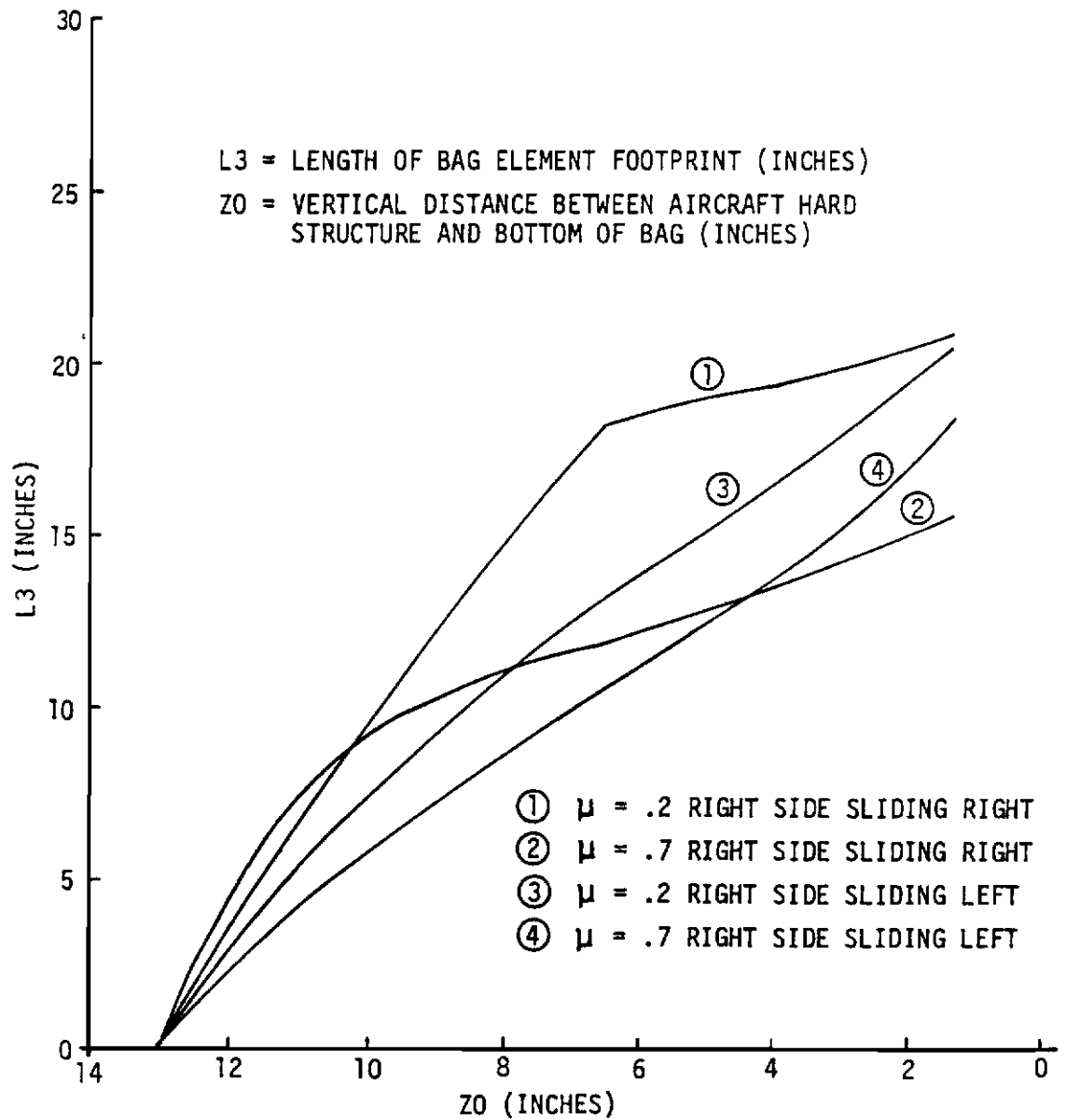
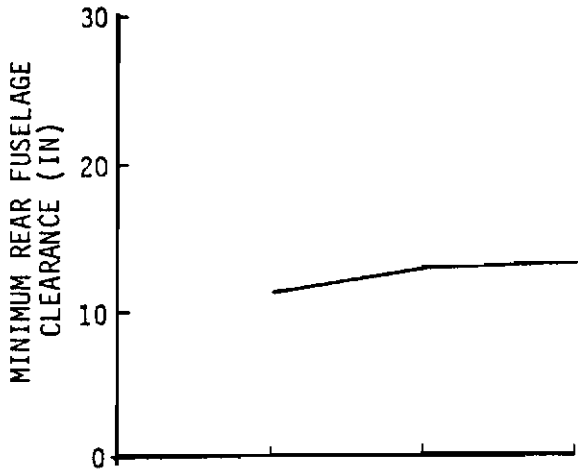
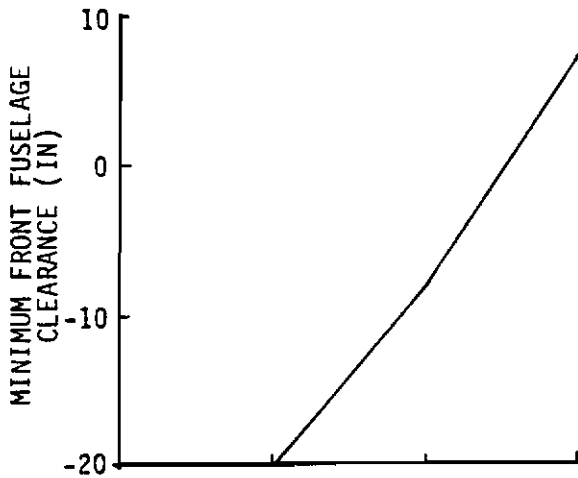


Figure 74 Air Bag Geometry for Rockwell ARPV with Baseline ABSS, L3 vs. Z0



PITCH ANGLE = 9.75°
 SINK RATE = 7 FT/SEC
 AIR BAG PRESSURE AT TOUCHDOWN = 2.7 PSIG
 RELIEF VALVE CRACKING PRESSURE = 2.8 PSIG
 RELIEF VALVE CRACKING RANGE = 0.25 PSIG
 RELIEF VALVE AREA = 144 IN^2
 DISTANCE, CP - CG = 2 IN FOR AIR BAG LENGTH = 120 & 140 IN
 DISTANCE, CP - CG = 12 IN FOR AIR BAG LENGTH = 160 IN

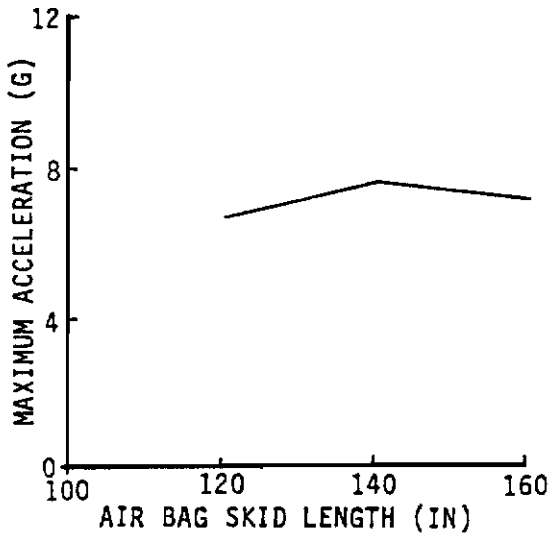


Figure 75 Rockwell ARPV with ABSS, 3 DOF Landing Simulations, Air Bag Length vs. Acceleration and Clearances

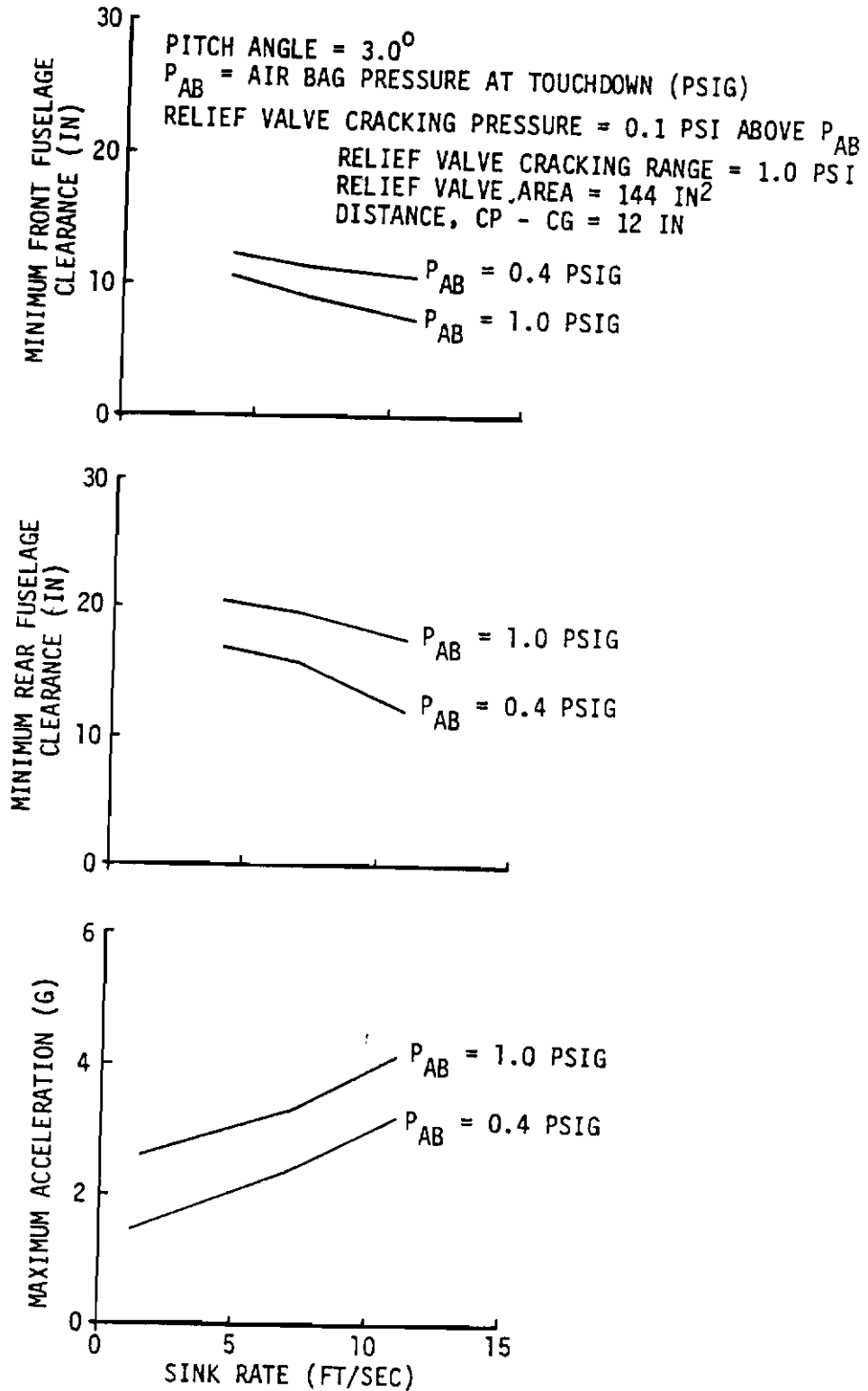


Figure 76 Rockwell ARPV with ABSS, 3 DOF Landing Simulations, Air Bag Pressure vs. Sink Rate

With an initial bag pressure of 1.0 psig and a relief valve cracking pressure of 1.1 psig, another series of simulations were performed which varied the air vehicle attitude and sink rate at landing impact. Minimum clearances and peak acceleration results from these simulations are shown in Figures 77 and 78. Forward and aft fuselage clearances were satisfactory for all of the cases investigated. Figure 78 shows that the 4g load limit was exceeded for some of the large pitch angles and sink rate cases. Points on Figure 78 where the 4g load limit line is crossed were plotted again in Figure 79 and show a 4g load limit constraint envelope for pitch angle and sink rate combinations. This curve does not have the same characteristic shape as that for the Boeing vehicle with ABSS, rather the allowable rate of sink continues to decrease with increasing pitch angle. Landing impact conditions which lie to the left of the envelope will result in acceptable landings, those to the right of the envelope will violate the load limit constraint. Figure 79 also shows the mean trim conditions for the air vehicle when approaching the runway at 100 knots and during its flare maneuver which reduces its airspeed to 80 knots just before landing impact. These are mean trim conditions which will be perturbed by wind gusts and air turbulence. The results show that with a flare maneuver, assuming a 2σ condition, the maximum sink rate is 2 ft/sec. If no flare maneuver is used, the allowable sink rate is about 6 ft/sec.

(b) Rockwell ARPV with ACRS

The initial air cushion recovery system installation for the Rockwell ARPV is shown in Figure 24. As with the ABSS installation for the Rockwell vehicle, deployable doors are used to support the trunk. The trunk is 108 inches long and 60 inches wide. Figure 80 shows how the trunk was divided into 16 different elements for modeling with program EASY. The forward one-third of the trunk is lubricated to reduce its coefficient of friction and increase its directional stability during slideout when suction braking is used for stopping. Figures 81 through 84 show program EASY results describing the relationship between trunk dimensions, air vehicle height, and trunk and cushion pressures.

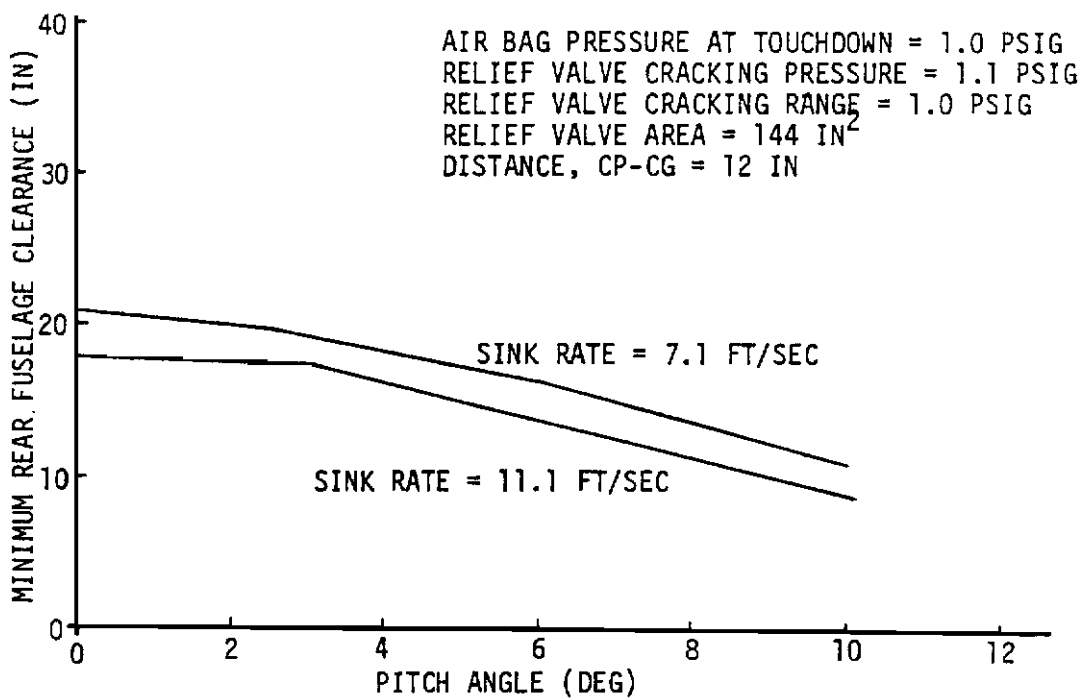
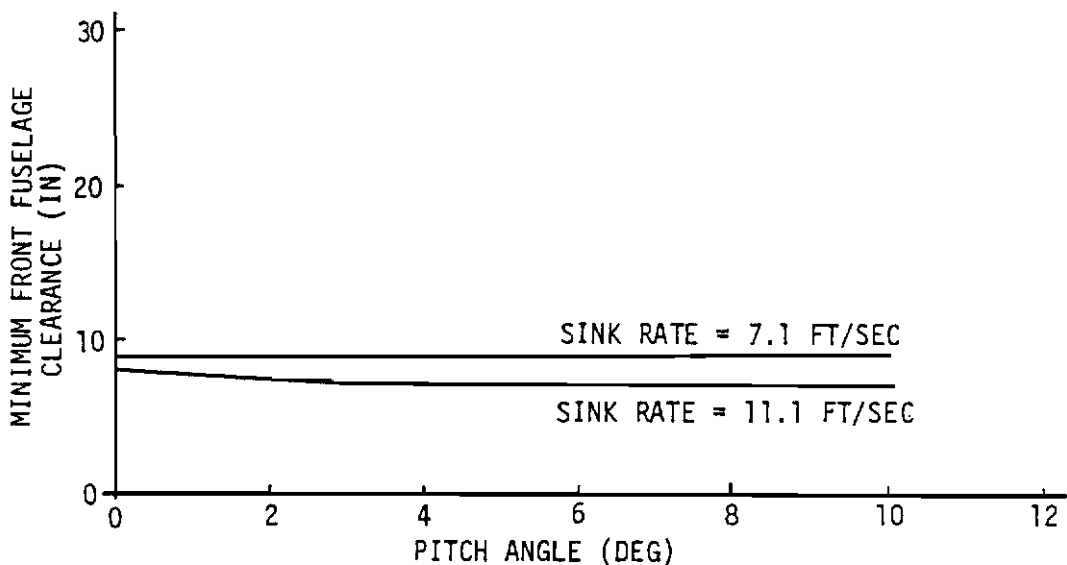


Figure 77 Rockwell ARPV with ABSS, 3 DOF Landing Simulations, Clearances vs. Pitch Angle

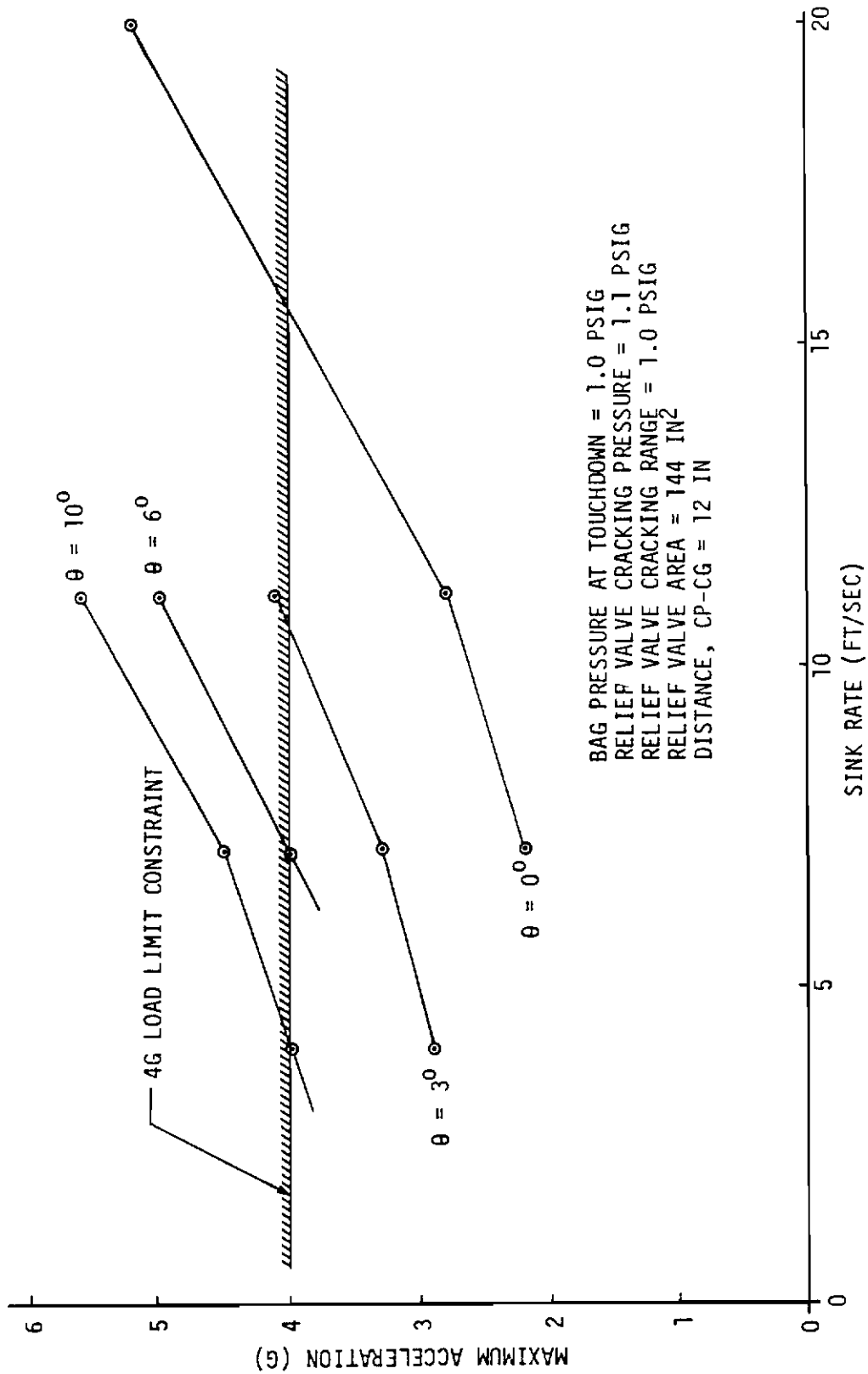


Figure 78 Rockwell ARPV with ABSS, 3 DOF Landing Simulations, Maximum Acceleration vs. Sink Rate

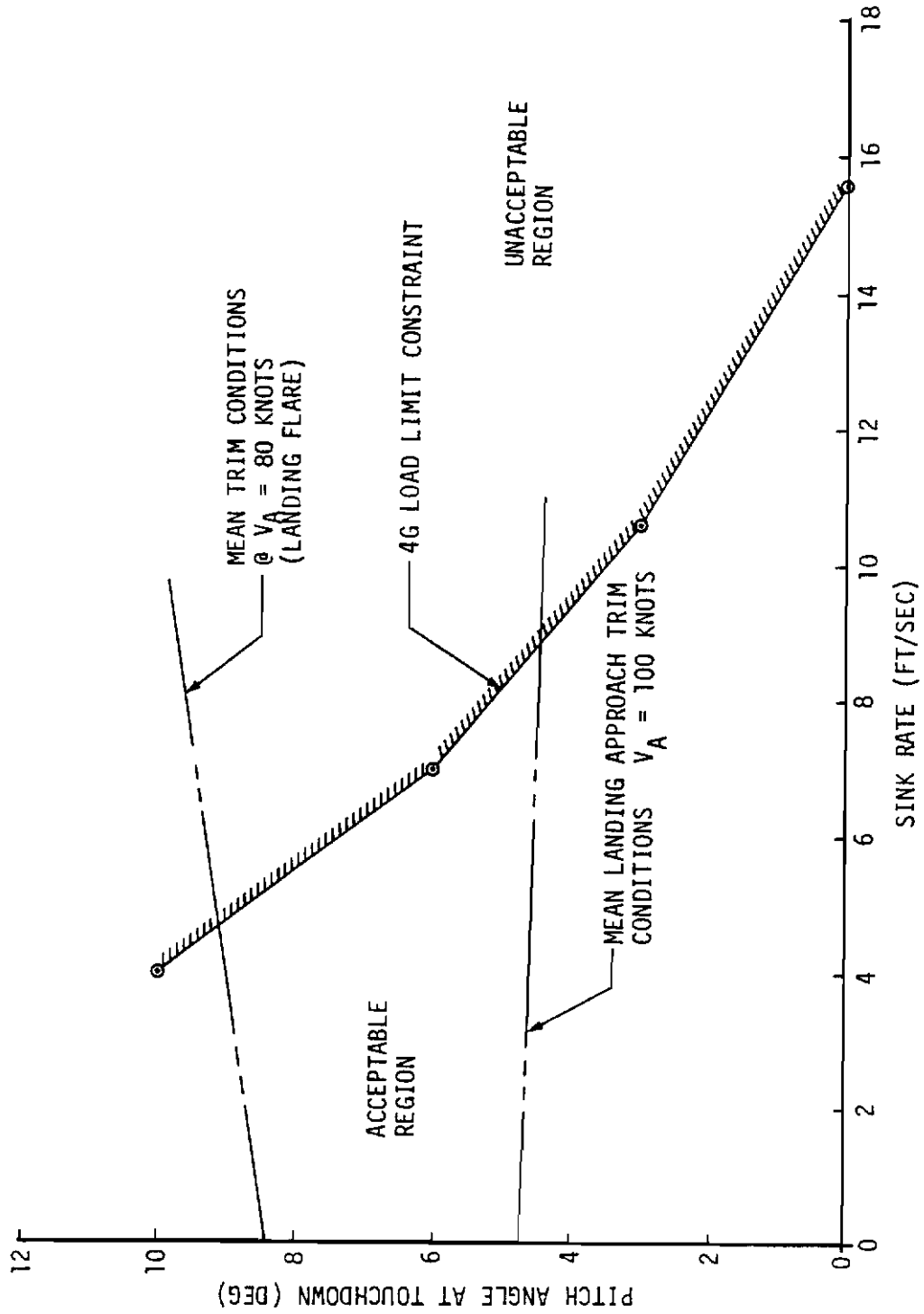


Figure 79 Rockwell ARPV with ABSS, Landing Trim Conditions and Touchdown Constraints

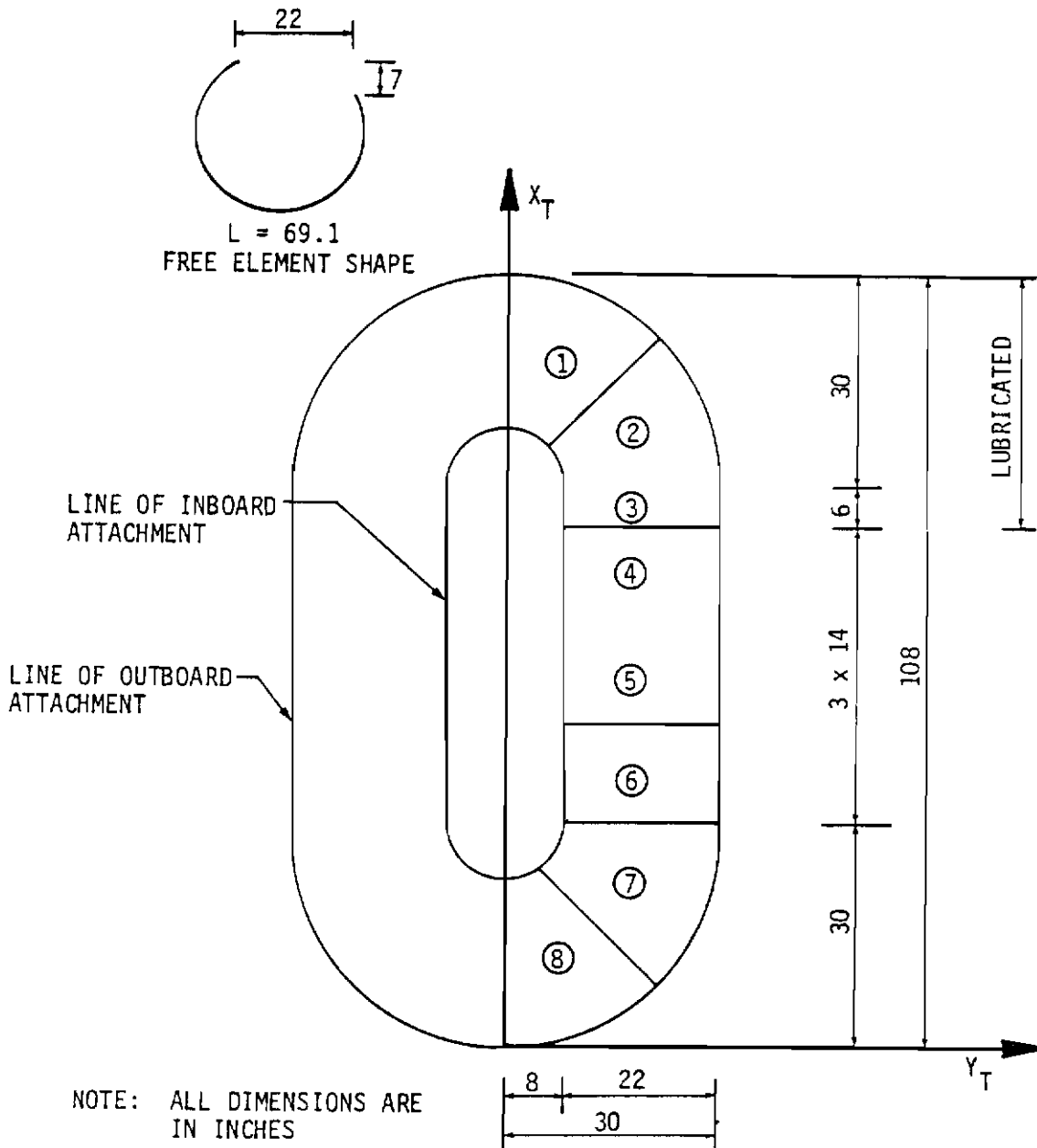


Figure 80 Baseline Air Cushion Model for Rockwell ARPV

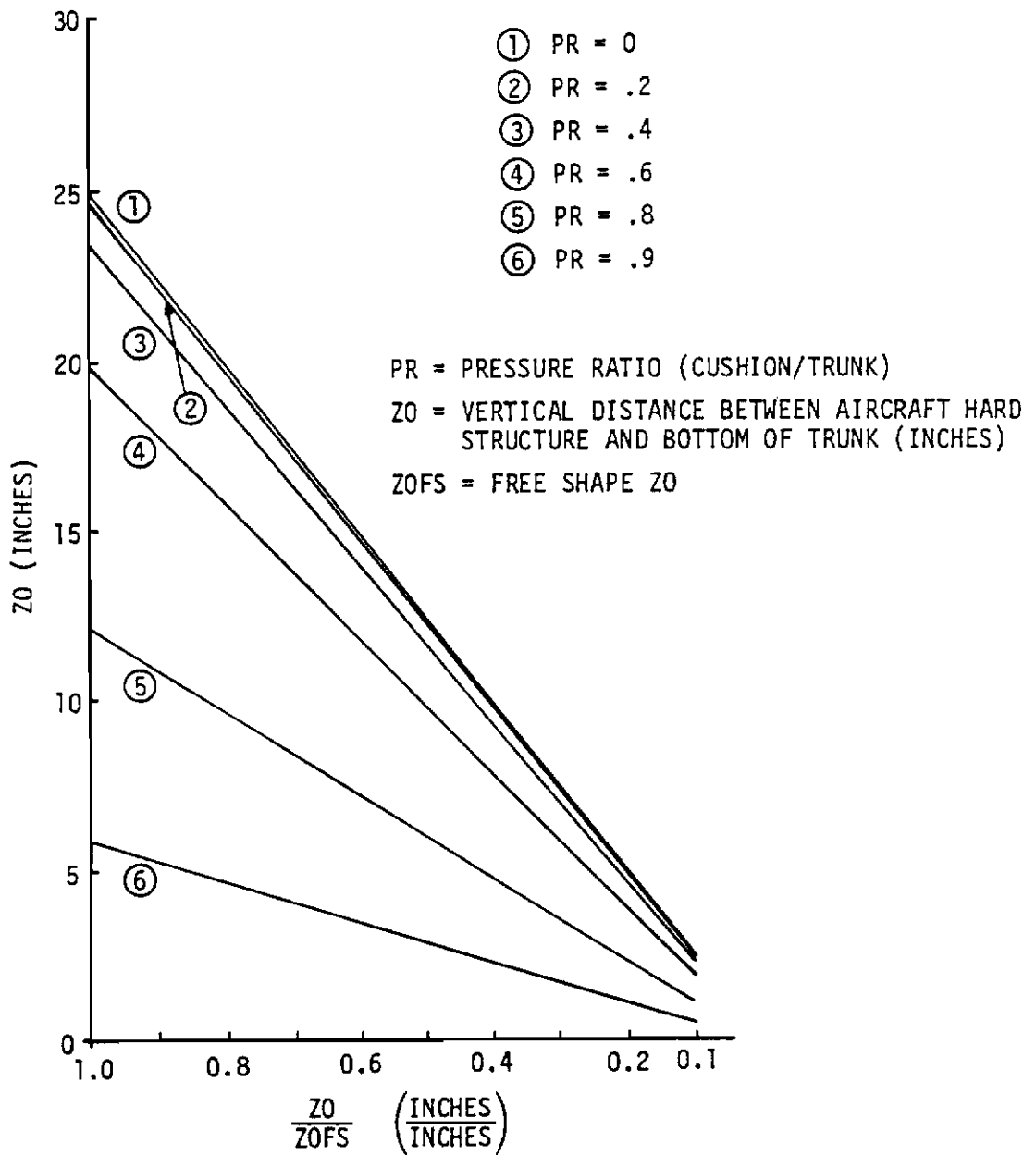


Figure 81 Trunk Geometry for Rockwell ARPV with Baseline ACRS,
Z0 vs. Z0/ZOFS

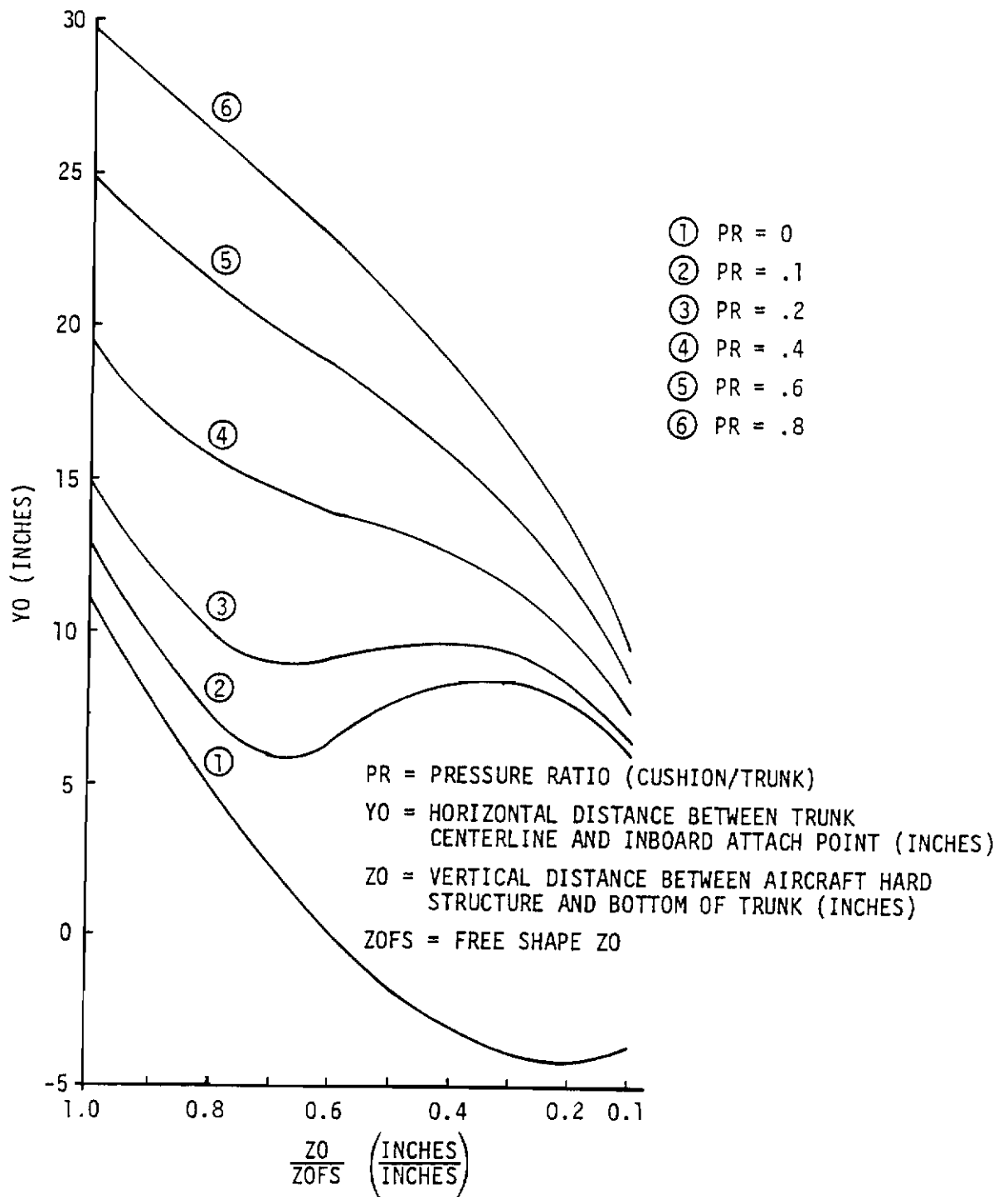


Figure 82 Trunk Geometry for Rockwell ARPV with Baseline ACRS, YO vs. ZO/ZOFS

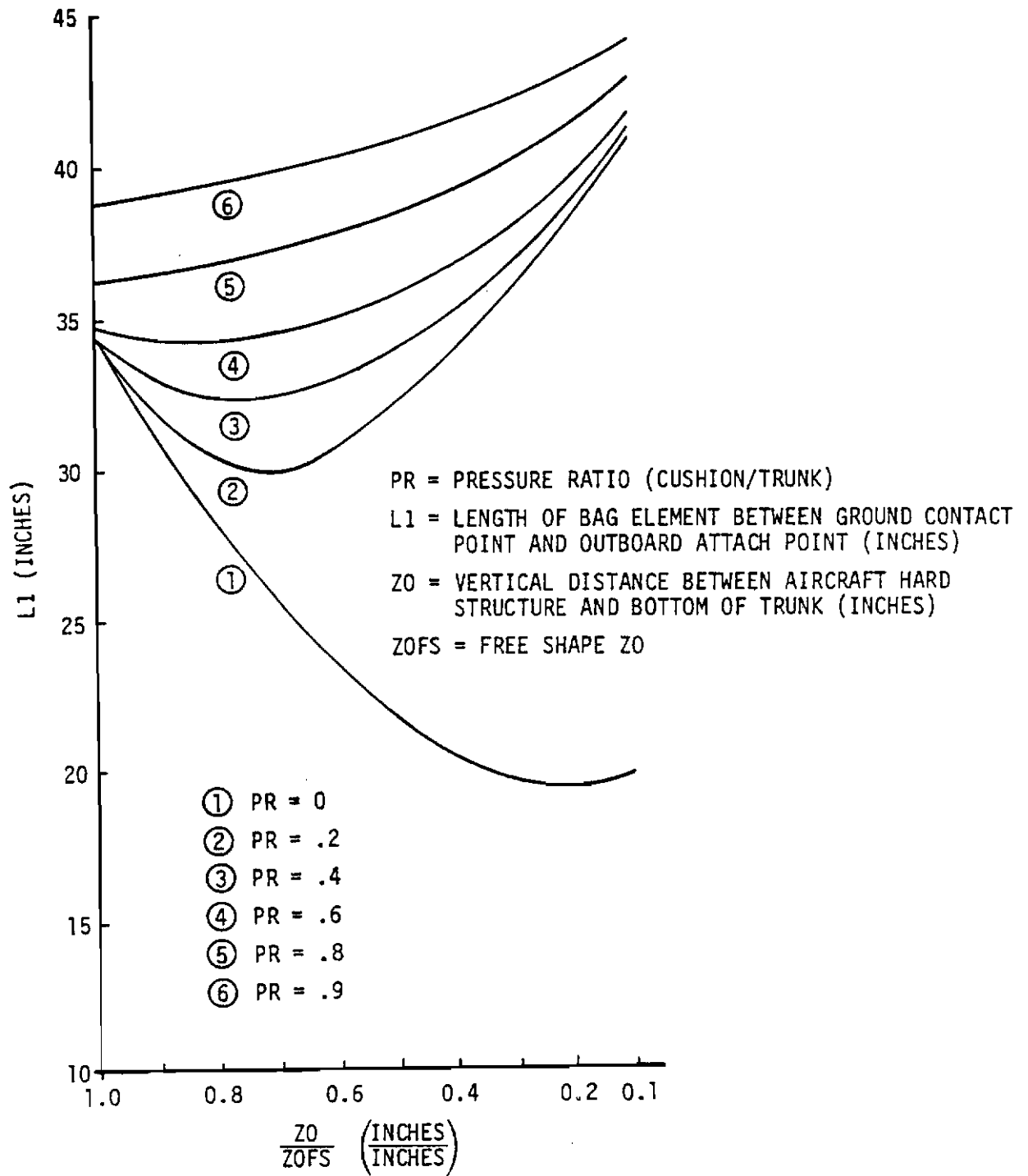


Figure 83 Trunk Geometry for Rockwell ARPV with Baseline ACRS, L1 vs. ZO/ZOFS

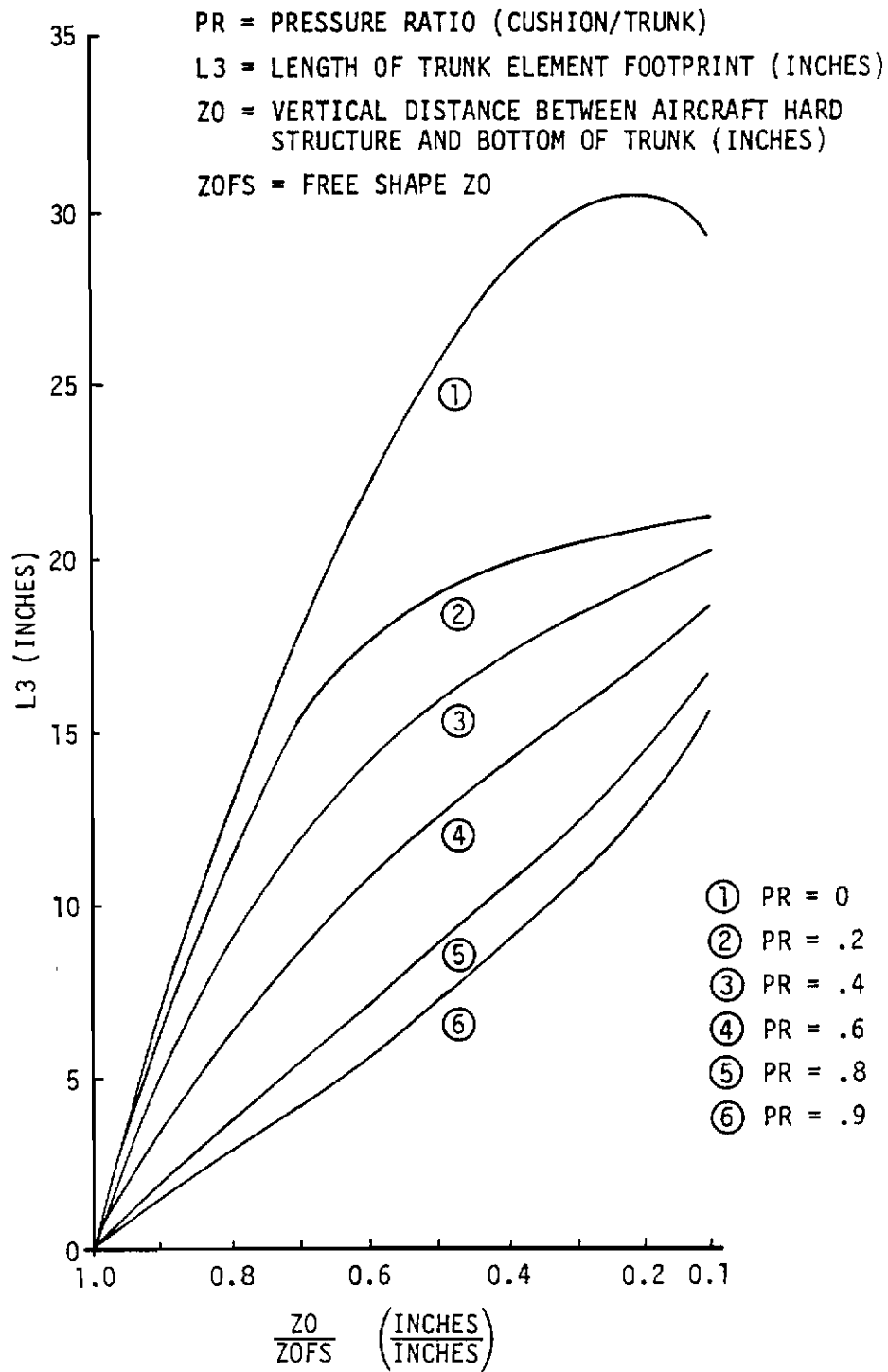


Figure 84 Trunk Geometry for Rockwell ARPV with Baseline ACRS, L3 vs. ZO/ZOFS

Contrails

Possible air sources for this trunk include ejector nozzles and shaft driven fans; both were considered in the simulations. Since the ACRS uses lubrication flow, the peak air flow rate requirements for this system are greater than those for the ABSS installation.

Initial three DOF simulations were made to investigate effects of variations in trunk dimensions. Results from the first simulations using the baseline trunk shown in Figure 24 indicated that the trunk was too stiff. The trunk steady state pressure at landing impact was approximately 1.0 psig and the relief valve cracking pressure was slightly greater than this, but the peak impact loads were approximately 4.4g which is greater than the air vehicle 4g load limit. To reduce these peak loads, the trunk meridian dimensions were changed to reduce its footprint area, and thus its stiffness, during landing impact. Figure 85 shows the dimensions for ACRS trunk no. 2. A landing simulation under the same conditions using this trunk resulted in a peak impact load of 3.8g. The minimum air vehicle to ground clearances were reduced by two to four inches, but were still adequate.

The next series of three DOF simulations investigated how variations in the air vehicle attitude and sink rate at touchdown affect the peak impact loads and minimum air vehicle-to-ground clearances. Results for these simulations are shown in Figures 86 and 87. Points in Figure 87 where the 4g load limit was crossed are plotted in Figure 88 to define a 4g load limit constraint envelope. This curve has the same characteristic shape as that for the Rockwell ARPV with ABSS. Combinations of pitch angle and sink rate to the right of this envelope at landing impact will result in unacceptable landings. Mean trim conditions for this air vehicle with the trunk deployed are also shown in Figure 88. In this case the allowable sink rate is 5 ft/sec for the 2σ mean trim condition with flare.

Suction braking was also investigated for the Rockwell ACRS. Figure 89 shows the results for various cushion pressures and runway conditions. These results show that a small amount of cushion suction is very effective in reducing the landing runout distance on a wet runway. The

TRUNK	A(IN.)	B(IN.)	L(IN.)
ACRS#1 (BASELINE)	22	7	69.1
ACRS#2	18	3	56.58

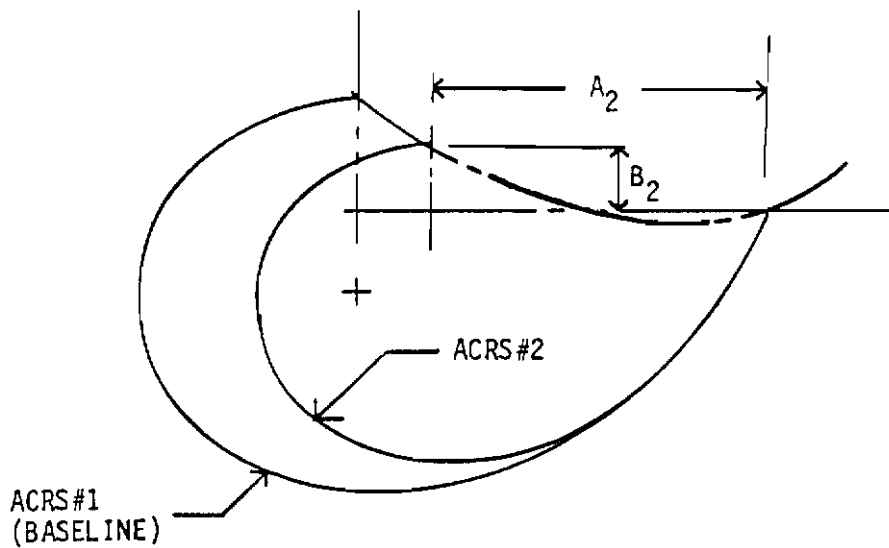


Figure 85 Trunk Meridian Dimensions for Rockwell ARPV with ACRS

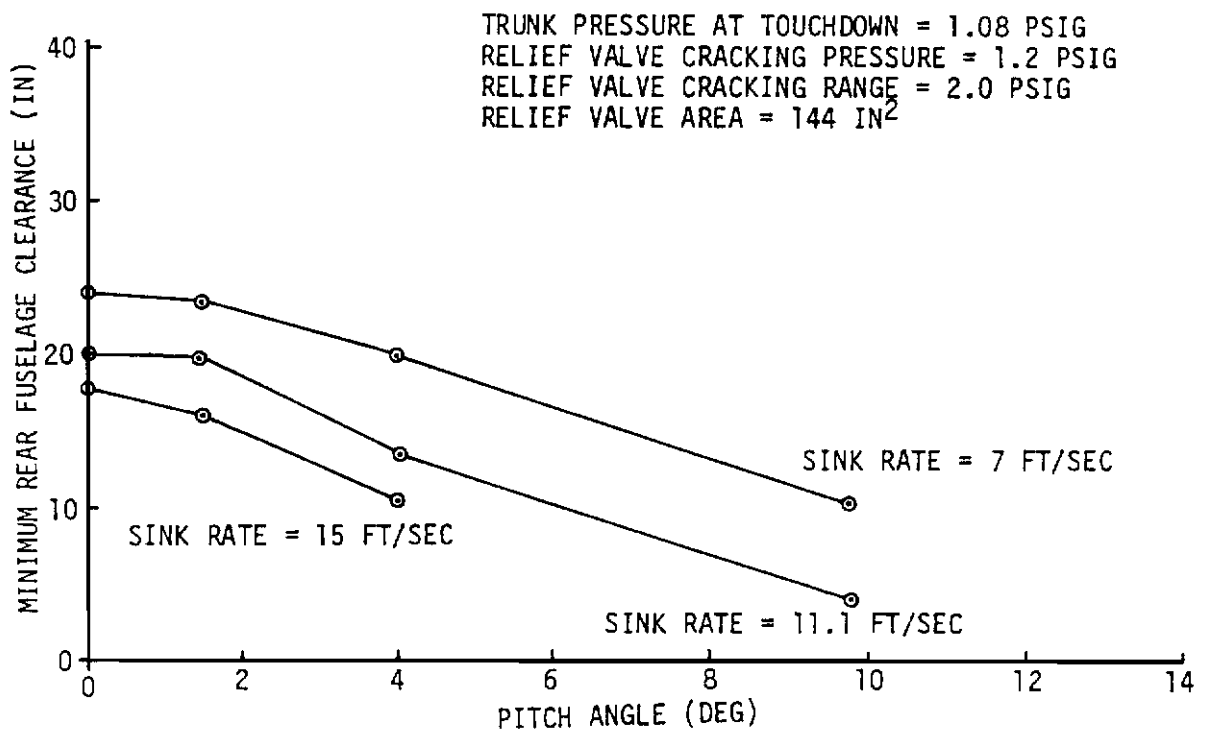
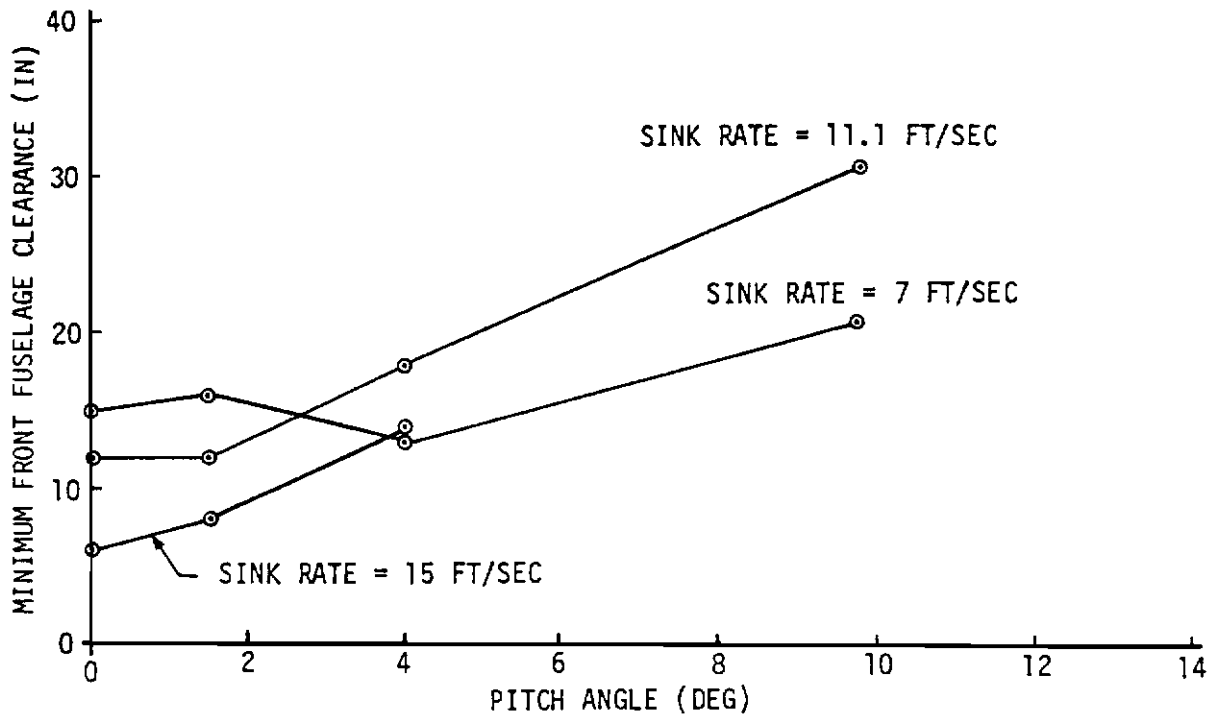


Figure 86 Rockwell ARPV with ACRS, 3 DOF Landing Simulations, Clearances vs. Pitch Angle

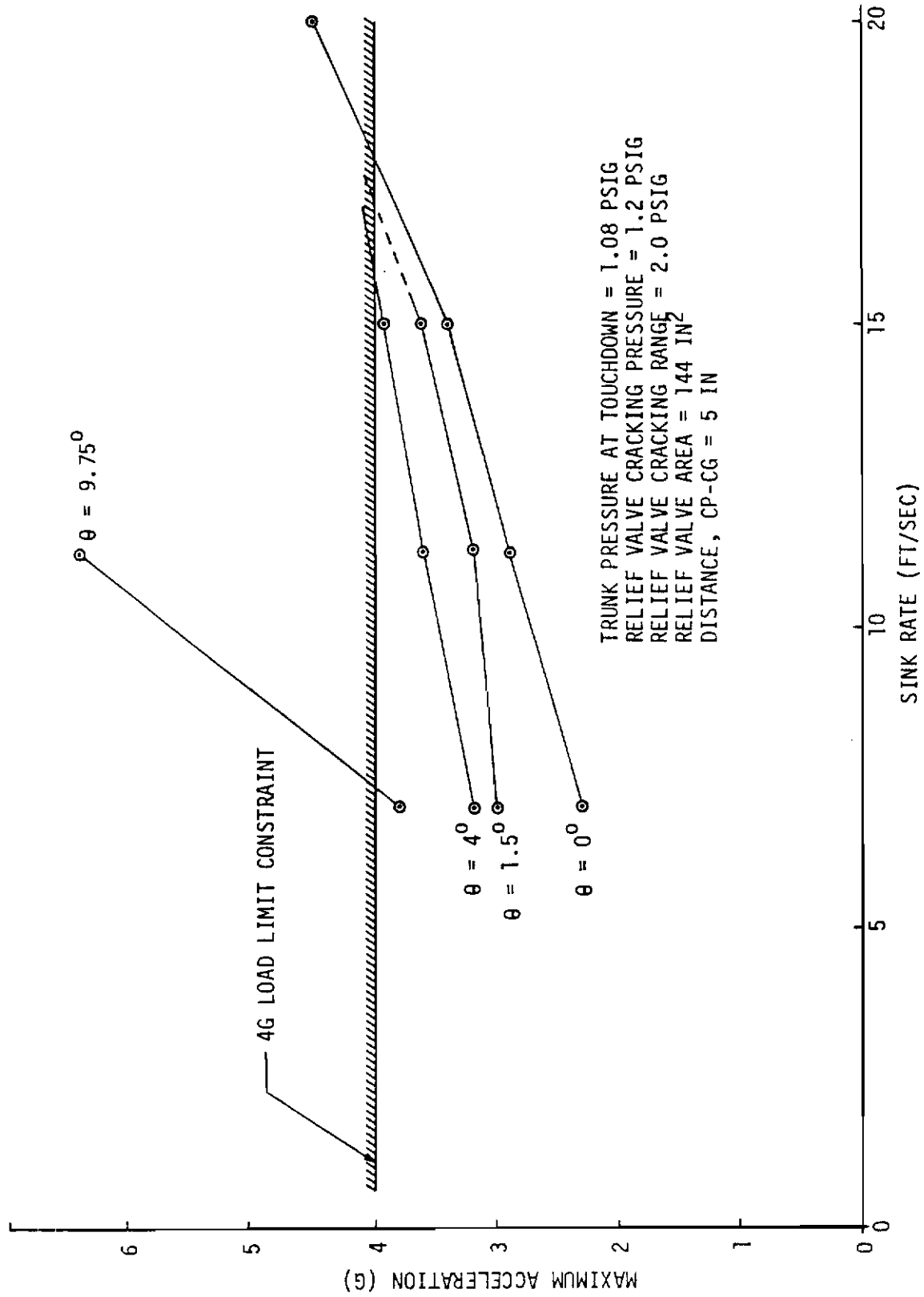


Figure 87 Rockwell ARPV with ACRS, 3 DOF Landing Simulations, Maximum Acceleration vs. Sink Rate

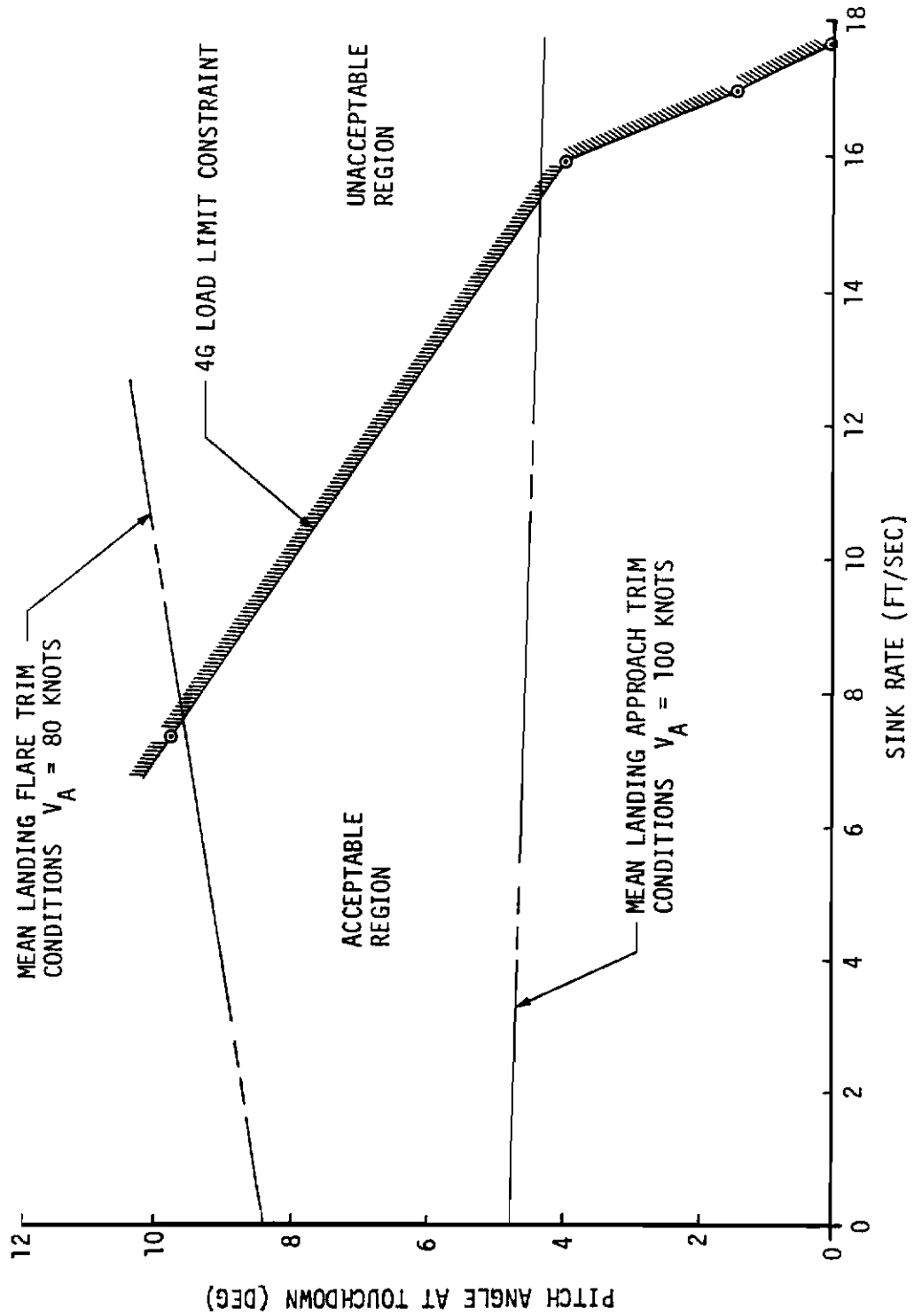


Figure 88 Rockwell ARPV with ACRS, Landing Trim Conditions and Touchdown Constraints

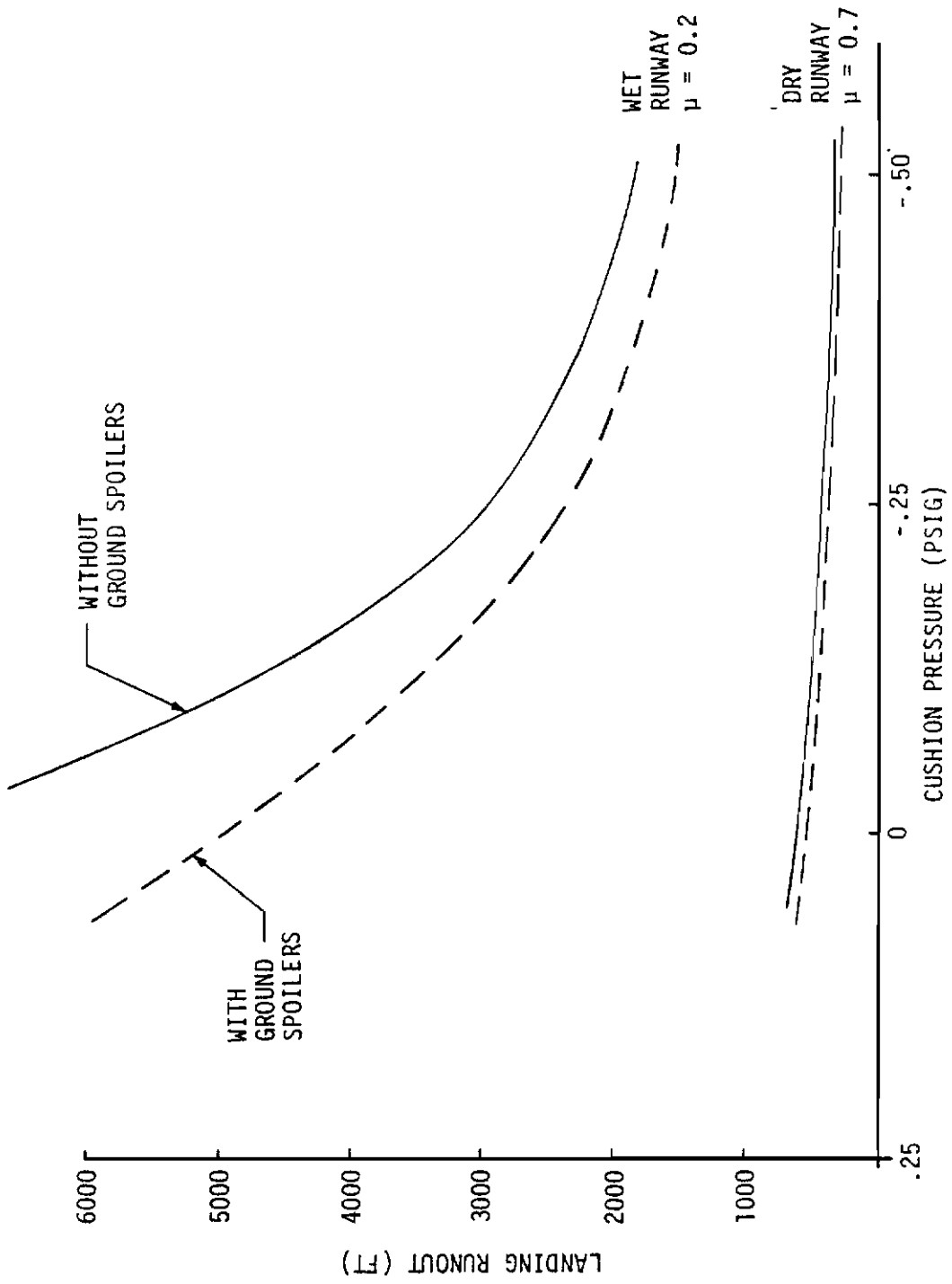


Figure 89 Landing Runout Distance for Rockwell ARPV with ACRS

change is not as apparent for a dry runway. Also, ground spoilers will reduce the wet runway runout distance by several hundred feet. These results show that a cushion pressure of -0.50 psig will reduce the stopping distance to 1500 feet when ground spoilers are used and to 1800 feet without ground spoilers.

(3) Rockwell ARPV (Elastic) Landing Simulations

The IACS configuration uses an elastic trunk that is sized for the takeoff gross weight of the air vehicle. The elastic trunk is mounted on deployable doors as was the ACRS trunk to gain the required ground clearance for the vehicle. The relaxed size of the trunk is such that it fits tightly against the external surface of the doors when they are stowed against the fuselage. When inflated, the trunk expands to the size required for satisfactory air cushion performance through proper selection of the stress-strain relationship for each element of the trunk.

In this case, the entire trunk footprint area is lubricated by nozzles around the periphery of the trunk to minimize ground friction for takeoff. Because of this lubrication provision, the IACS requires a high air flow rate to the trunk, the trunk drag does not have a stabilizing effect on the vehicle, and the stopping distance becomes excessive.

To overcome these problems, friction pads must be added to the trunk along with provisions in the air supply system for reducing the cushion pressure to enable friction pad contact. An alternate approach is to use an arrestment system. The air supply system in this case was assumed to be a shaft driven fan with power supplied by the engine accessory drive. Further discussion of this IACS is presented in Section II.3, Takeoff Simulation and Analysis.

Initial simulations using the inelastic trunk model (program EASY Component TK) investigated several variations in trunk dimensions. However, the elastic trunk model (EASY Component TS) is much more complex than the inelastic model, and the user cannot directly input the trunk size. It is an analysis tool rather than a preliminary design tool in that trunk characteristics must be previously defined for effective use

Contrails

of the component model. As a result, investigation of a desired trunk size requires a trial-and-error process of inputting trunk material load/deflection curves until the output trunk dimensions match the trunk dimensions desired.

Due to the time involved in obtaining the desired trunk dimensions only one elastic trunk size was investigated. This elastic trunk IACS was evaluated at various landing and takeoff conditions but the trunk and cushion parameters, except for relief valve cracking pressure, were held constant to avoid changing the trunk size.

Figure 90 shows the trunk size investigated. The overall trunk length is 160 inches, the width is 60 inches and the pressurized meridian length is 59 inches. The trunk was divided into 16 different elements and modeled with program EASY. Figure 91 shows the trunk material load/deflection curves which produced the trunk size for a steady state trunk pressure of 16.2 psia.

The same approach was used as in the analysis of the other landing simulations. First, a series of three DOF simulations were made to determine the effects of variations in the air vehicle attitude and sink rate at touchdown. No arrestment or braking was included in these simulations. Figure 92 shows the ground-to-structure clearance as a function of pitch angle at a sink rate of 11.1 ft/sec. The results indicate the ground-to-structure clearance is not limiting even at the worst sink rate condition at touchdown having a maximum probability of 3σ . This is due to the fact that the trunk is sized for the takeoff condition so it is more than adequate for landing.

Figure 93 shows the peak impact loads as a function of sink rate and pitch angle. Points in Figure 93 where the 4g load limit was crossed are plotted in Figure 94 to define a 4g load limit constraint envelope. Combinations of pitch angle and sink rate to the right of the envelope at landing impact will result in unacceptable landings.

The acceptable region of Figure 94 is much smaller than the acceptable regions of the Rockwell vehicle with the ACRS. This is in part due to

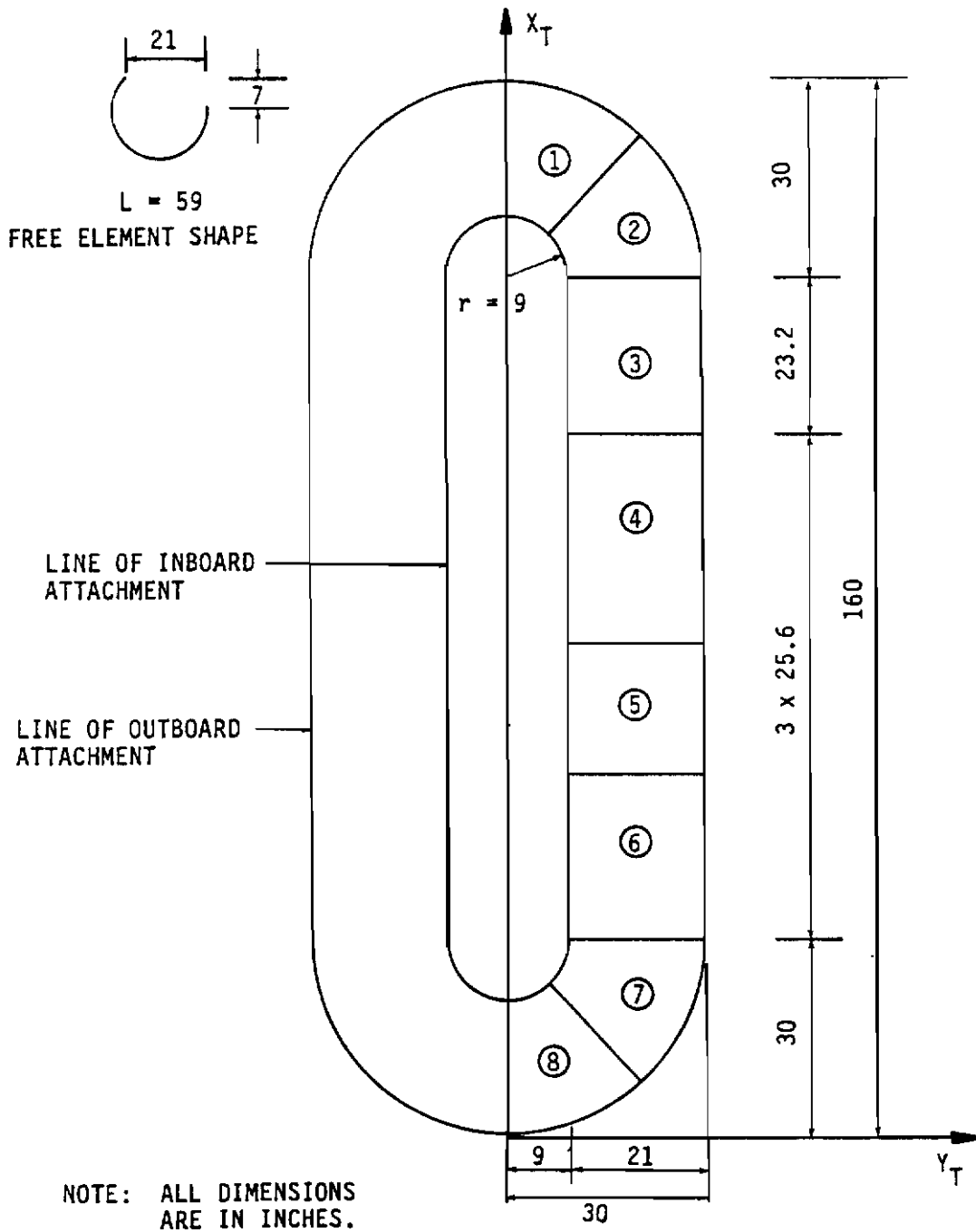
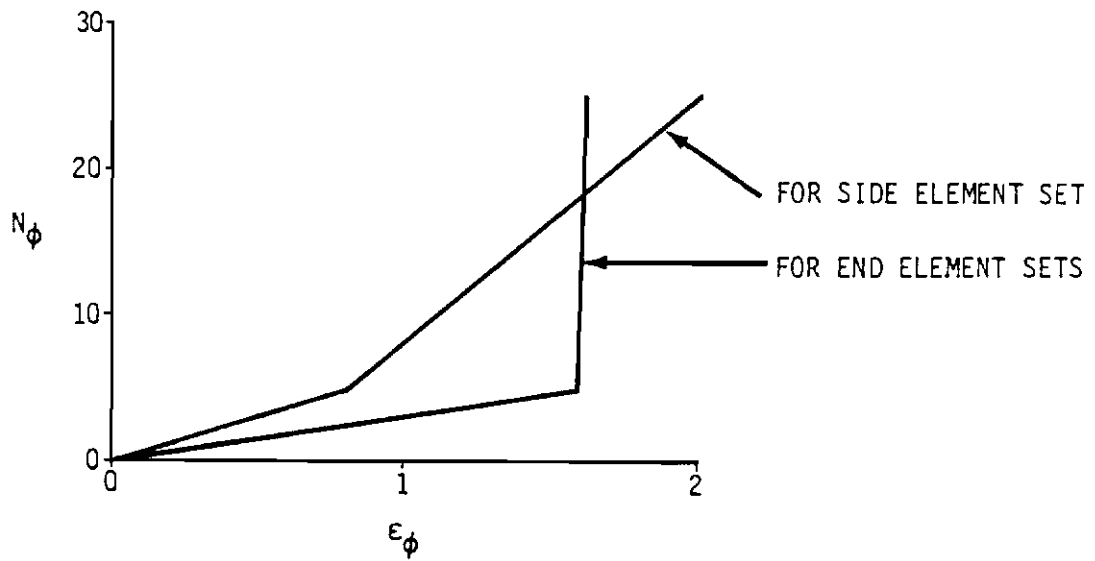
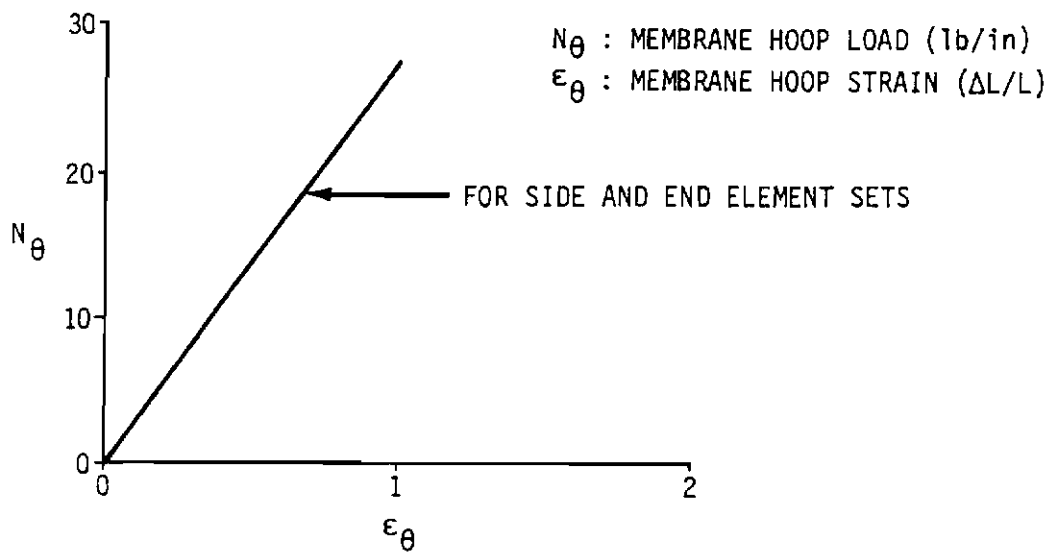


Figure 90 Elastic IACS Model for Rockwell ARPV

Contrails



N_ϕ : MEMBRANE MERIDIAN LOAD (lb/in)
 ϵ_ϕ : MEMBRANE MERIDIAN STRAIN ($\Delta L/L$)



N_θ : MEMBRANE HOOP LOAD (lb/in)
 ϵ_θ : MEMBRANE HOOP STRAIN ($\Delta L/L$)

Figure 91 Elastic Trunk Load/Deflection Curves Used in Dynamic Analysis

Contrails

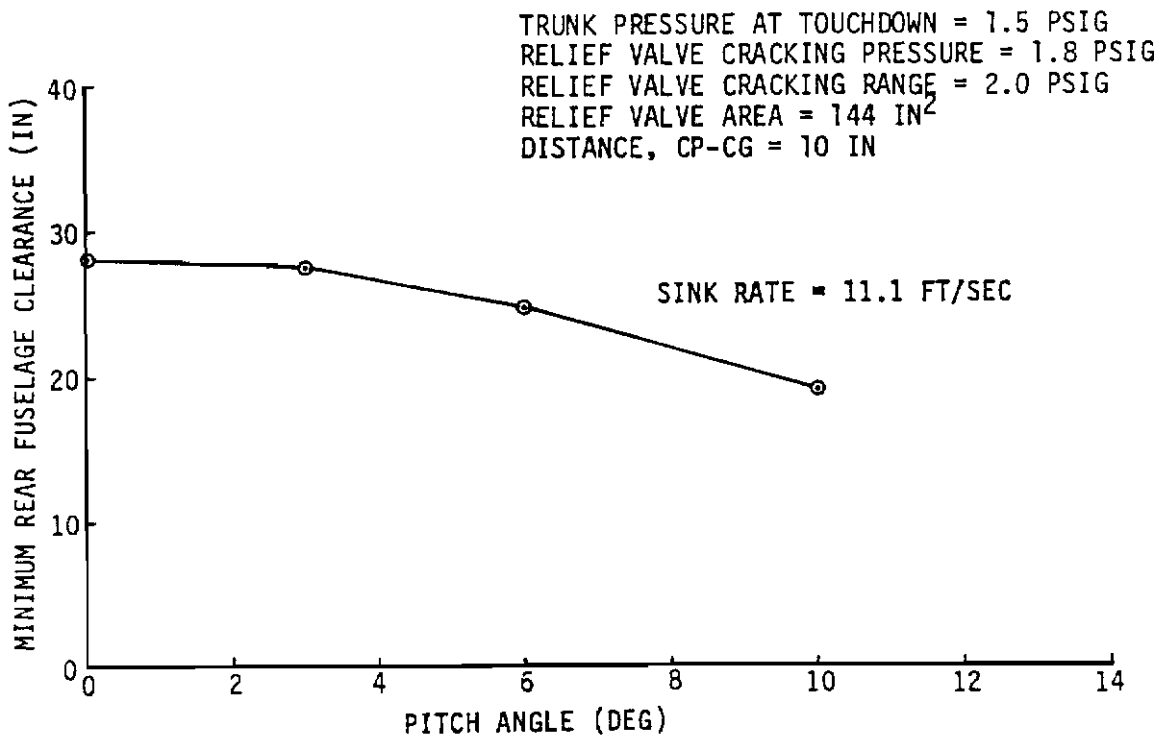
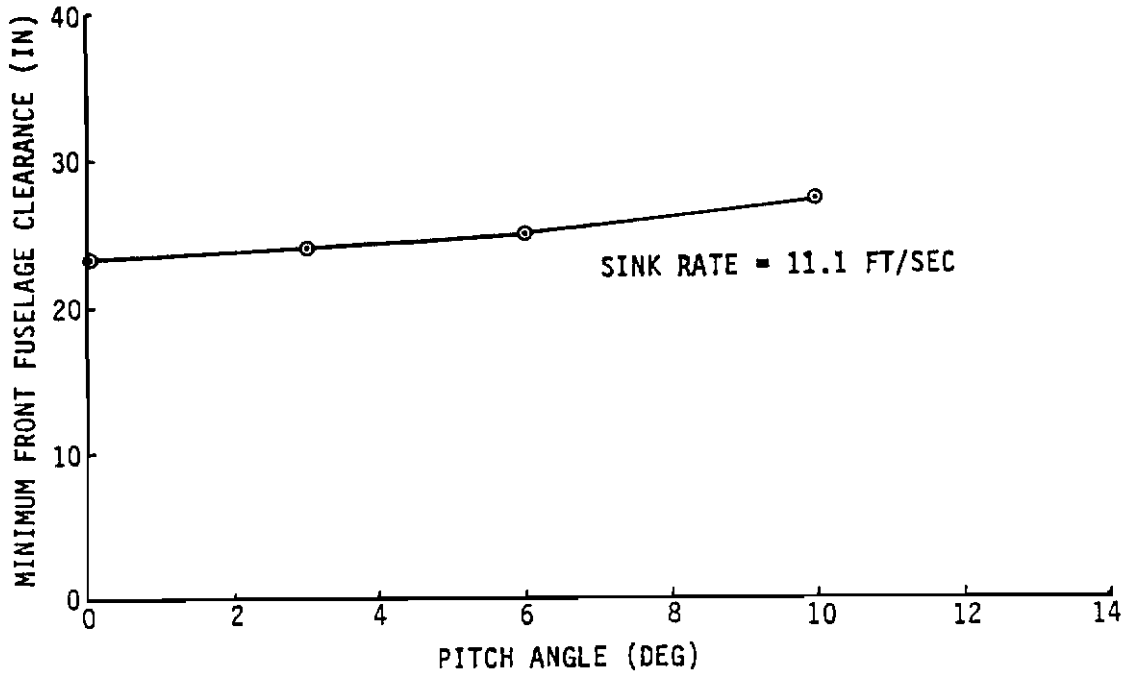


Figure 92 Rockwell ARPV with IACS (Elastic), 3 DOF Landing Simulations, Clearances vs. Pitch Angle

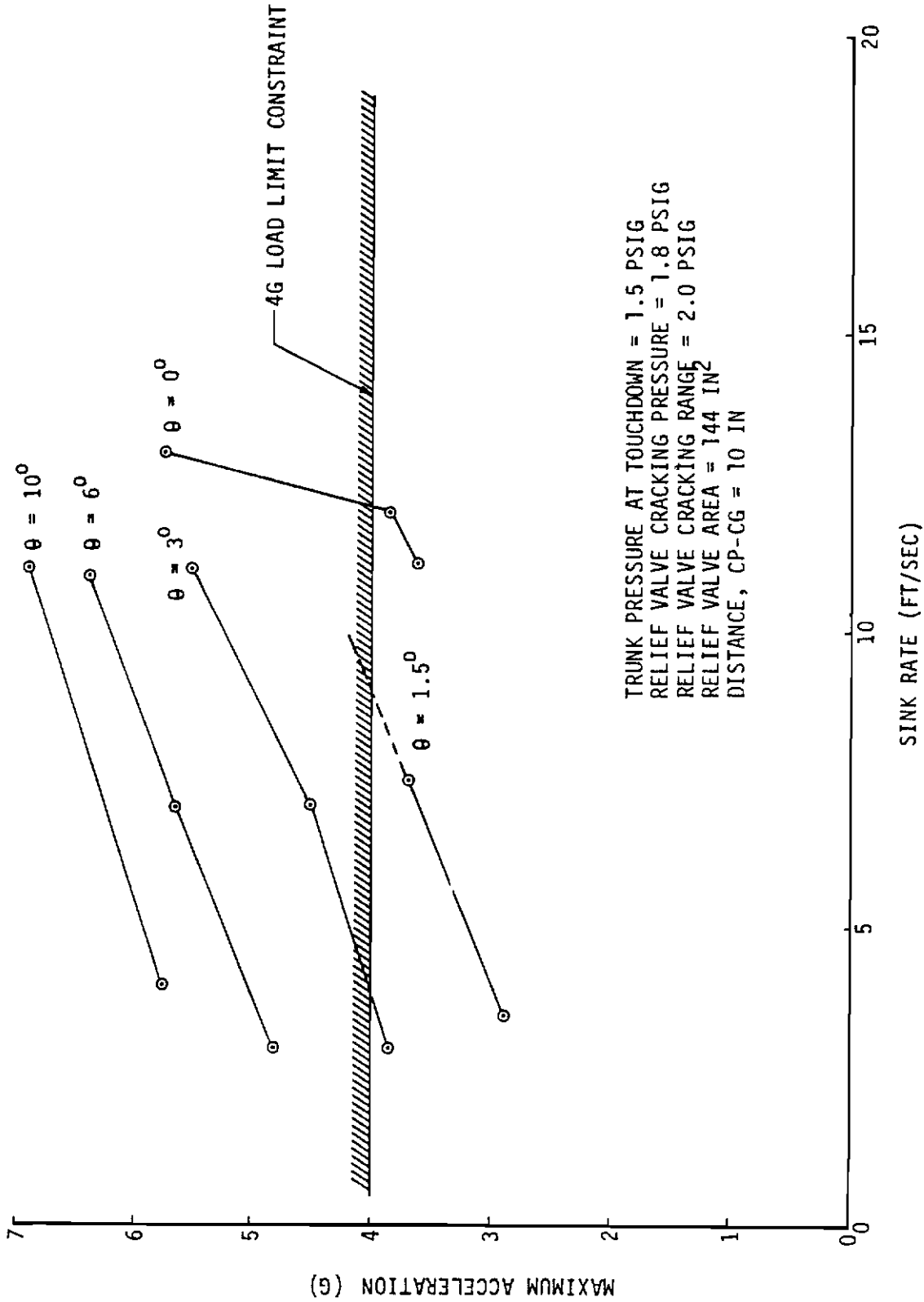


Figure 93 Rockwell ARPV with IACS (Elastic), 3 DOF Landing Simulations, Maximum Acceleration vs. Sink Rate

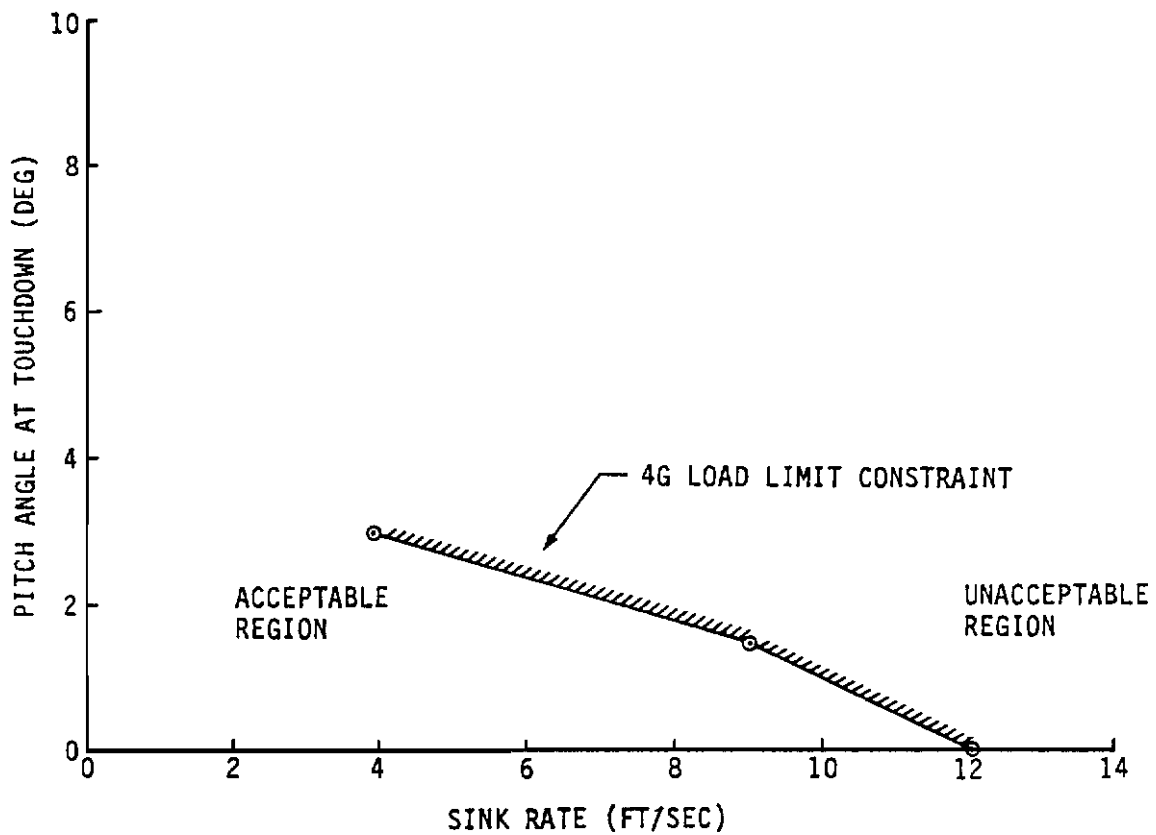


Figure 94 Rockwell ARPV with Elastic IACS, Touchdown Constraints

the fact that the trunk size was not optimized but, to a larger extent, to the fact that the trunk was sized for the takeoff gross weight of the aircraft.

Simulations with six DOF were performed in which the relief valve cracking pressure was varied. The air vehicle was simulated while landing without arrestment at mean touchdown conditions. Figure 95 shows the impact of relief valve cracking pressure on ground-to-structure clearance and peak impact loads. The results show that minimizing the relief valve cracking pressure is important to achieve acceptable loads. The trunk size and pressure are overriding factors. Changes in trunk pressure could not be investigated because of the nature of the elastic trunk model.

A series of six DOF simulations were performed in which the air vehicle was arrested. A comparison between arrested and unarrested landings at the mean touchdown conditions was performed. The results in Figures 96 and 97 show landing with and without arrestment, respectively. These results indicate that the peak load is higher with arrestment (5.5g with arrestment compared to 4.7g without) but the difference is not as dramatic as was indicated in simulation of the Boeing vehicle with ABSS (Figure 59).

Stopping distance for the Rockwell vehicle with the elastic trunk IACS with brake pags was estimated to be the same as that of the Rockwell vehicle with ACRS and no suction braking. This estimate is based on the assumption that the brake pads are located in the aft two-thirds of the trunk, the forward one-third remains lubricated for directional stability, and the air cushion is vented. The stopping distance, from Figure 89, is approximately 700 feet on a dry runway and about 5000 feet on a wet runway assuming the engine at idle thrust, ground spoilers deployed and a brake-pad-to-runway friction coefficient of 0.2.

c. Landing Simulation Conclusions

Throughout these analyses and simulations of the different landing systems, the most restrictive constraint to achieving

Contrails

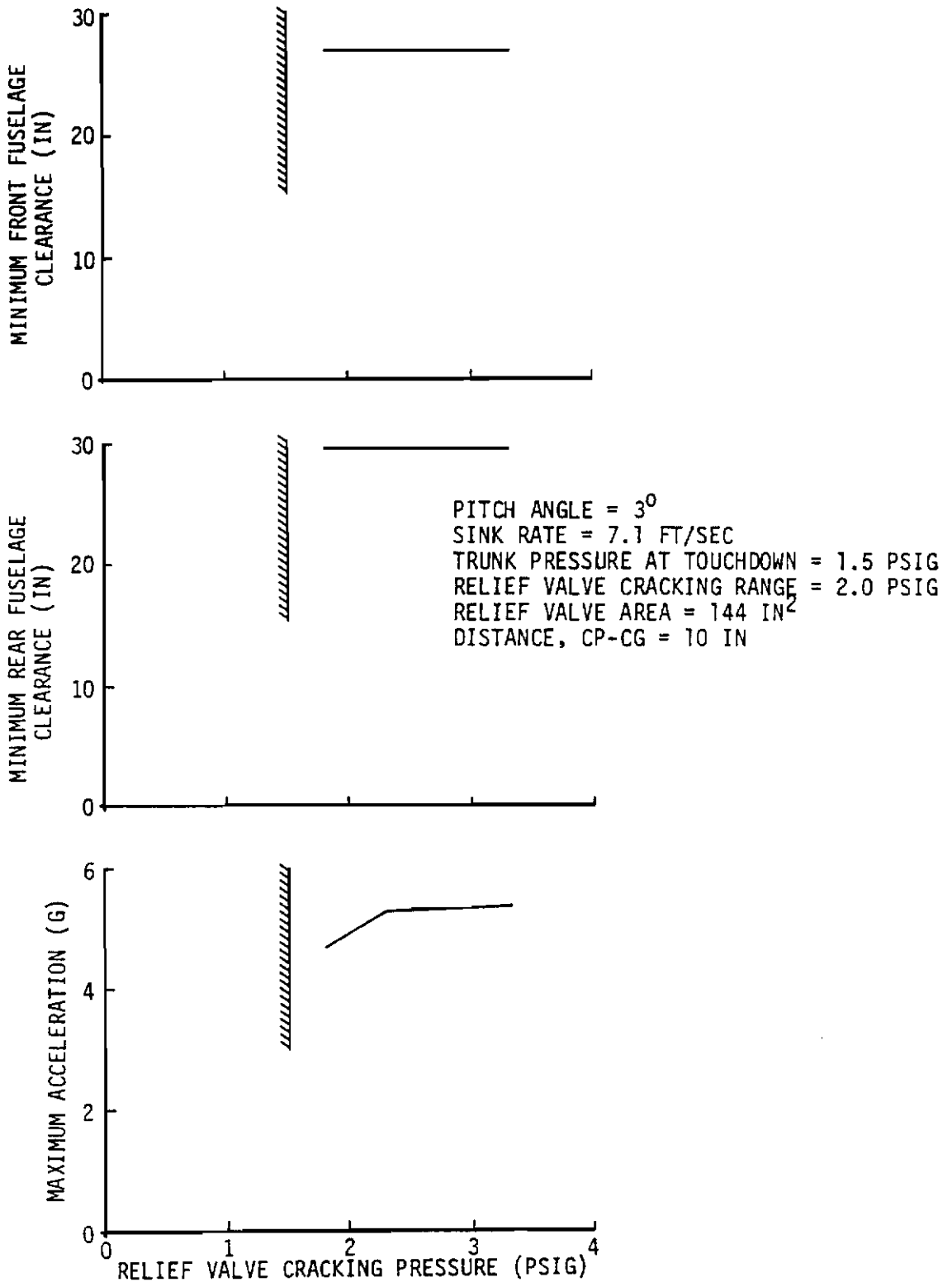


Figure 95 Rockwell ARPV with IACS (Elastic), 6 DOF Landing Simulations, Relief Valve Cracking Pressure vs. Acceleration and Clearances

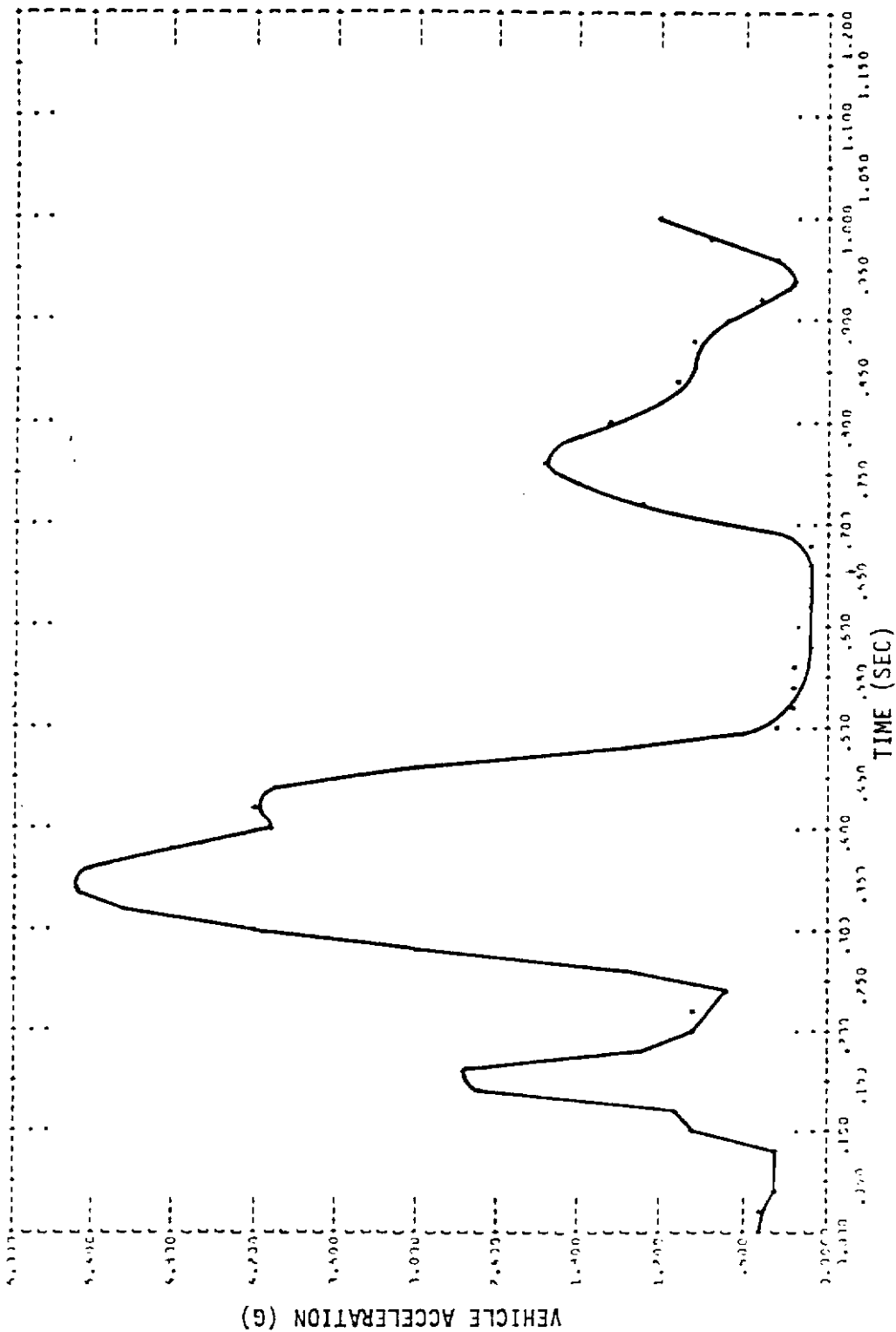


Figure 96 Rockwell ARPV with IACS (Elastic), 6 DOF Landing Simulation with Arrestment, Vehicle Acceleration vs. Time

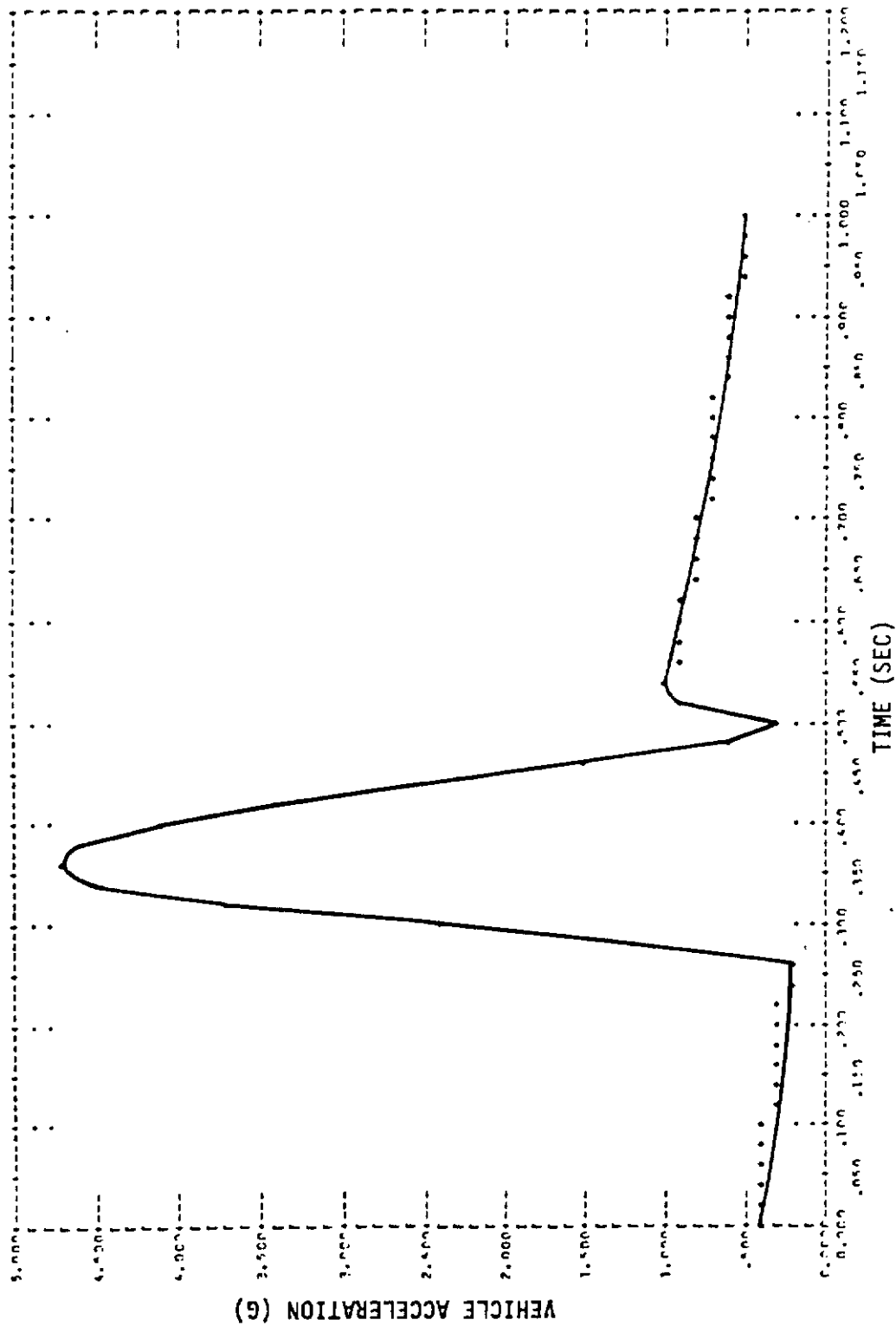


Figure 97 Rockwell ARPV with IACS (Elastic), 6 DOF Landing Simulation without Arrestment, Vehicle Acceleration vs. Time

Contrails

satisfactory performance was the design landing load limit based on wing strength load factor.

The depth of the original ARPV studies did not extend to structural sizing so only a structural weight allowance is involved. The predicted 8g landing for the Boeing ARPV should not affect the structural weight. The wings are quite small and have little inertia loading. The fuselage is loaded by the skids which are producing the load factor so the actual internal loads should not increase and the weight should not change.

The Rockwell ARPV carries its payload on the wings and is therefore susceptible to landing load factor limitations. The landing impact analysis indicates a peak load factor of 4.0. Assuming the wing strength to be adequate for the 5g maneuver condition with a 1.25 safety factor, the wing will sustain a 4.1g landing impact without exceeding the factor of safety of 1.5 applicable to launch and recovery. The fuselage of the Rockwell ARPV should be strong enough to sustain the 4.0g since the loads are distributed along the fuselage rather than at discrete gear attachments as in the proposed ARPV.

One of the principal components in the equation defining landing impact loads is the $\bar{U}\bar{X}\bar{Q}$ cross product. This is basically a cross product of air vehicle forward speed and pitch rate which results in an acceleration along the air vehicle Z body axis. When looking at the trunk and air bag skid installations on the Boeing ARPV and the Rockwell ARPV, three items which influence this cross product stand out.

First of all, an air cushion trunk (or air bag skid) extends quite a distance aft of the air vehicle center of gravity. This most aft end of the trunk is the first part to contact the ground during a normal nose up landing. This imparts a negative pitching moment to the vehicle which results in rather large negative \bar{Q} values during landing impact. A conventional landing gear has the main gear located very close to the air vehicle center of gravity, therefore large negative pitch rates do not tend to develop when landing.

Contrails

Secondly, two air vehicles have previously flown and landed successfully with an air cushion trunk installation, the LA-4 and the CC-115. The LA-4 touchdown speed was about 50 knots, and the CC-115 has landed at about 80 knots. The Boeing ARPV lands at 130 knots and the Rockwell ARPV lands at 80 knots. Therefore, the touchdown speeds and kinetic energy of the ARPVs is as great or greater than the vehicles which have successfully landed with air cushion trunks.

Thirdly, these small RPVs have a low pitching moment of inertia. Therefore, this high speed combined with the trunk geometry and low inertia tend to produce high pitch rates resulting in high impact loads at touchdown.

These high impact loads resulted in severe restrictions on the vehicle approach conditions to the point that in some cases it would not be practical to operate with the landing load factor limits established for the two vehicles that were analyzed.

The Boeing and Rockwell ARPVs with circular cross section air bag skirts are limited to a sink rate of 4 ft/sec with normal vehicle pitch angles at touchdown. Results of the study indicate that this limit could be improved by changing the bag shape to reduce the foot print area. However, analysis of other than circular cross section bags was beyond the capability of the simulation model.

Cable arrestment during touchdown cause the landing impact load limits to be exceeded under all practical landing conditions so that touchdown must occur prior to cable-hook engagement. However, arrestment is necessary to stabilize the vehicle after touchdown.

The rate of sink limit for the Boeing ARPV with ACRS is about 5 ft/sec and that for the Rockwell ARPV is 7.5 ft/sec at normal vehicle touchdown pitch attitudes. The rate of sink limitations on the Rockwell vehicle with an elastic trunk IACS were unacceptable under touchdown pitch attitudes above 4 degrees. However, these results were inconclusive because adequate trade study of the IACS design parameters was not made. The study was limited by the complexity of the simulation model. Both

the Boeing and the Rockwell vehicles were stable during slide out with the ACRS when the forward one-third of the trunk is lubricated.

Suction braking is required to achieve reasonable stopping distances with the ACRS on wet runways. The Boeing vehicle with ACRS on a wet runway will not stop because the engine idle thrust exceeds the braking force. Suction braking reduces the wet runway distance to about 3000 feet.

The Rockwell vehicle wet runway stopping distance with ACRS without suction braking is about 5000 feet if ground spoilers are deployed. Suction braking reduces the distance to about 1500 feet. Stopping distance with an integrated air cushion system is equivalent to that of the ACRS without suction braking, that is, about 5000 feet on a wet runway.

Achieving adequate ground clearance with the ABSS or ACRS on a vehicle such as the Rockwell ARPV that was designed for conventional landing gear required extra complication of the system. In this case, doors were added to provide flat surfaces upon which to mount the trunks. These added extra weight and complexity that would not be required if the vehicle had been originally designed for ACRS.

3. TAKEOFF SIMULATIONS AND ANALYSIS

The objective of this part of the study was to evaluate the performance of several different takeoff or launch systems by using program EASY. Air cushion takeoff systems were investigated for the Rockwell ARPV. The design variables of each takeoff system configuration were investigated to determine their effects on takeoff performance, to identify conditions under which satisfactory performance is achieved, and to arrive at an optimum configuration.

The simulations were to include takeoff roll, air vehicle rotation, platform or trunk release, and climbout for each configuration.

The configurations analyzed included two integrated air cushion systems (IACS) concepts and an air cushion launch platform. One of the IACS

concepts was an inelastic trunk system where the trunk could be retractable to stow it in flight and extend it for landing or it could be jettisonable and used for the takeoff only. The second IACS concept was an elastic trunk system in which the trunk is stowed during flight by deflating it and allowing it to collapse against the air vehicle fuselage. The general approach followed in this analysis was similar to that used for the landing simulations. Math models of the takeoff or launch system components were constructed for use in program EASY by first developing preliminary configuration of the systems including the air cushion trunks and air supply systems. These math models were then used in several three and six degree-of-freedom simulations which showed the variations to the touchdown initial conditions and the system design variables.

a. Development of Math Models

The air cushion takeoff systems consist of several interacting components. The principal components which dominate the dynamic behavior of the systems were included in the system math models. Standard program EASY subroutines were available for all of these components but input parameters describing each particular piece of hardware had to be defined. The development of the air vehicle models was described in Paragraph 1. This section described how air supply components were defined for inclusion in program EASY.

(1) Air Supply Systems

Air supply systems investigated for both takeoff and recovery air cushion systems were discussed in Paragraph 2.a (4). The required air flow rate for takeoff is much higher than for recovery because the takeoff trunk is larger, a higher cushion pressure is required, and the entire trunk footprint area must be lubricated to reduce sliding friction. The shaft driven fan system with fan characteristics is shown in Figure 42 was chosen for the Rockwell vehicle with the IACS. This system is capable of providing the large takeoff flow and is compatible with the engine accessory drive if the drive pad is operated under overload conditions. The overload capacity of the engine accessories drive pad P-2 is 84 hp which is near the required power for the IACS fan. The Rockwell vehicle engine does not have

sufficient bleed air capacity to power a turbo fan. Also, a turbo fan is sensitive to back pressure which can induce oscillatory modes in the air cushion system. Therefore, a turbo fan was not used in this study.

(2) Air Cushion Takeoff Trunk

(a) Inelastic Trunk IACS

A preliminary study was made to investigate the parameters which affect the dynamic characteristics of an air cushion takeoff trunk constructed of inelastic materials. The trunk was sized for the takeoff gross weight of the ARPV. Design relationships were developed and those input parameters required by program EASY were specified. Air vehicle constraints outlined in Paragraph 1.a were considered in configuring the trunk. Lubrication area, porosity, air flow rate and friction force relationships were derived. The trunk parameters are listed in Table 15. This trunk could be used as a one trunk (retractable) or a two trunk (jettisonable) configuration. Trunk attachment and stowage details were not considered during the dynamic simulation.

(b) Elastic Trunk IACS

Another IACS concept that was simulated was the elastic trunk system.

Only one elastic trunk size was investigated, as stated in Paragraph 2.b(3), due to the time involved in obtaining the desired trunk dimensions. The takeoff conditions dictated the trunk size and air flow arrangement. The trunk size is shown in Figure 90 and parameters are listed in Table 15.

The preliminary configuration of the elastic trunk was developed as follows. Using the stress/strain characteristics for the CC-115 ACLS Trunk Composite material it was determined that the design elongation for the trunk should be approximately 300%. Figure 85 is a front view drawing of the Rockwell vehicle with the inelastic trunk installed. The trunk cross section perimeter is approximately three times the distance between the trunk attachment points on the fairing. Therefore, an

TABLE 15
BASELINE ROCKWELL IACS DIMENSIONS AND PARAMETERS

<u>Parameters</u>	<u>Rockwell IACS (Inelastic and Elastic)</u>
Trunk Coefficients of Friction (Lubricated around entire periphery)	0.2
Trunk Porosity	.0282
Area of Trunk Lubrication	
Width of Perforated Area (inches)	10.0
Periphery length (inches)	366
Flow Discharge Coefficients	
CDGAP (gap between trunk and ground)	0.9
CD1 (free portion of trunk)	0.6
CD2 (flattened portion of trunk)	0.2
CDA (relief value)	0.9
Trunk Damping Coefficient (lbf-sec/in ³)	0.02
Trunk Dimensions	
A (horiz. distance between fuselage attach points, inches)	22
B (vert. distance between fuselage attach points, inches)	7
LO (trunk meridian length, inches)	69.1
Number of trunk elements per side	11
Distance between trunk center of pressure and vehicle C. G.(inches)	10
Overall length (inches)	160

elastic trunk mounted in the same manner would have approximately the same shape as the inelastic trunk.

The fairings on which the trunk is mounted are required for an elastic or an inelastic trunk for this particular vehicle geometry to achieve the required wing tip pod ground clearance. These fairings were added as a means of installing an air cushion system on this vehicle without redesign of the basic air vehicle, which was beyond the scope of this study.

The air supply systems and trunk lubrication arrangement was assumed to be the same as that for the inelastic trunk.

(3) Launch Platform

The launch platform concept that was simulated is shown in Figure 98. This concept was applied to the Rockwell ARPV. The recovery mode for the air vehicle was assumed to be the ACRS. Preliminary configuration analysis included consideration of platforms with and without thrust engines and platforms with multiple vehicle capability. Air cushion trunk variations such as multiple trunks and compartmentalization were evaluated. Platform arrestment methods considered included suction braking and an external cable or net system. The configuration shown in Figure 98 was selected for its simplicity, and low overall cost. These trades are discussed further in Section III.

This launch platform concept consists of a flat, honeycomb core platform to which the trunk, air supply equipment and air vehicle supports are attached. The trunk is sized to provide good vehicle pitch and roll stability during the takeoff run. The air vehicle is supported by a forward support link and two aft support links that engage the vehicle just aft of the center of gravity. The air vehicle rotates about the aft support link attachment point at platform-air vehicle separation.

The air cushion air supply system includes a shaft driven fan powered by an APU. The fan characteristics shown in Figure 42 were used in this simulation. The air cushion trunk parameters are listed in Table 16.

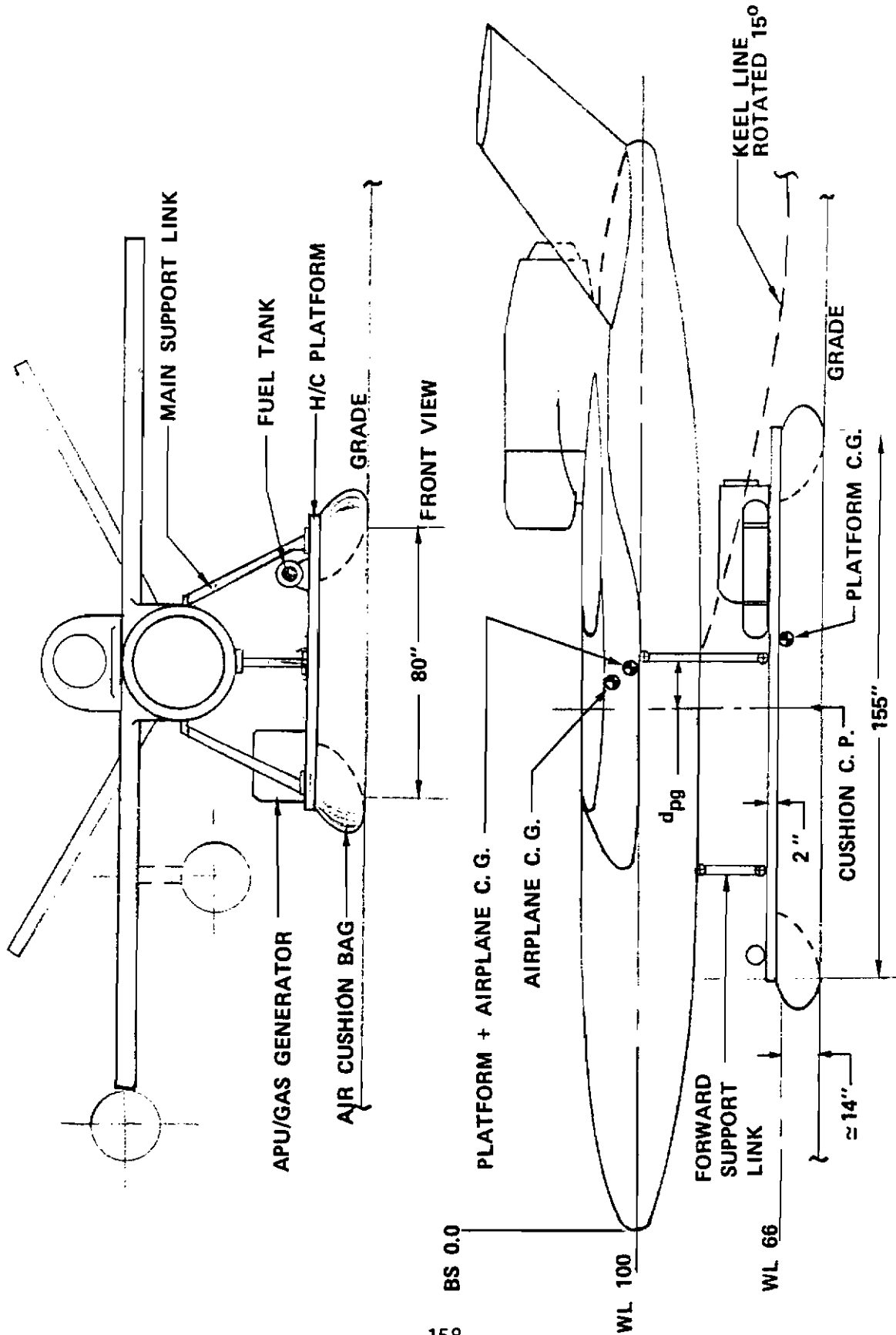


Figure 98 Rockwell Air Cushion Launch Platform

TABLE 16
BASELINE ROCKWELL ACLP DIMENSIONS AND PARAMETERS

<u>Parameters</u>	<u>ALCP</u>
Trunk Coefficients of Friction (Lubricated around entire periphery)	0.2
Trunk Porosity	.0186
Area of Trunk Lubrication	
Width of Perforated Area (inches)	20.0
Periphery length (inches)	401
Flow Discharge Coefficients	
CDGAP (gap between trunk and ground)	0.9
CD1 (free portion of trunk)	0.6
CD2 (flattened portion of trunk)	0.2
Trunk Damping Coefficient (lbf-sec/in ³)	0.02
Trunk Dimensions	
A (horiz. distance between platform attach points, inches)	14
B (vert. distance between platform attach points, inches)	0
LO (trunk meridian length, inches)	44
Number of trunk elements per side	13
Distance between trunk center of pressure and vehicle C. G.(inches)	0
Overall length (inches)	155

b. Takeoff Simulation Results

(1) Rockwell ARPV with Air Cushion Launch Platform

The baseline launch platform that was initially simulated is shown in Figure 98. The trunk footprint length is 155 inches and the width is 80 inches. The program EASY model of the trunk consisted of 13 elements per side as shown in Figure 99. Trunk inboard and outboard attachments are 14 inches apart, trunk height is 11.9 inches out of ground effect. Lubrication and other parameters used in the simulation are listed in Table 16. The simulated air supply system consisted of a shaft driven fan, with characteristics as shown in Figure 42, ducting from the fan to the trunk, and the trunk and cushion.

Initial simulations of the vehicle in ground roll were three DOF. The intent was to evaluate vehicle stability throughout takeoff roll. However, as the vehicle reached a speed of approximately 100 ft/sec it became unstable. Figures 100, 101 and 102 show the launch platform simulated in three DOF for ground roll with forward velocity from 100 ft/sec to 125 ft/sec. Figures 101 and 102 show the plots of pitch angle and altitude diverging shortly after the simulation is initiated.

Similar results were experienced during a previous simulation of the Jindivik drone with an inelastic air cushion trunk during takeoff (Reference 9), and results of that analysis are shown in Figure 103. It was not determined if this behavior is realistic or is due to some deficiency in the math model.

Because of the instability, the simulation of the launch platform was not continued beyond this point.

(2) Rockwell ARPV with Inelastic IACS

The baseline inelastic trunk, shown in Figure 104, was divided into 16 individual elements and modeled with program EASY. This trunk has a length of 160 inches and a width of 60 inches. Geometrical shape of the trunk, which varies with trunk pressure, cushion pressure and height were determined by program EASY and are similar to those shown for the ACRS in Figures 81 through 84.

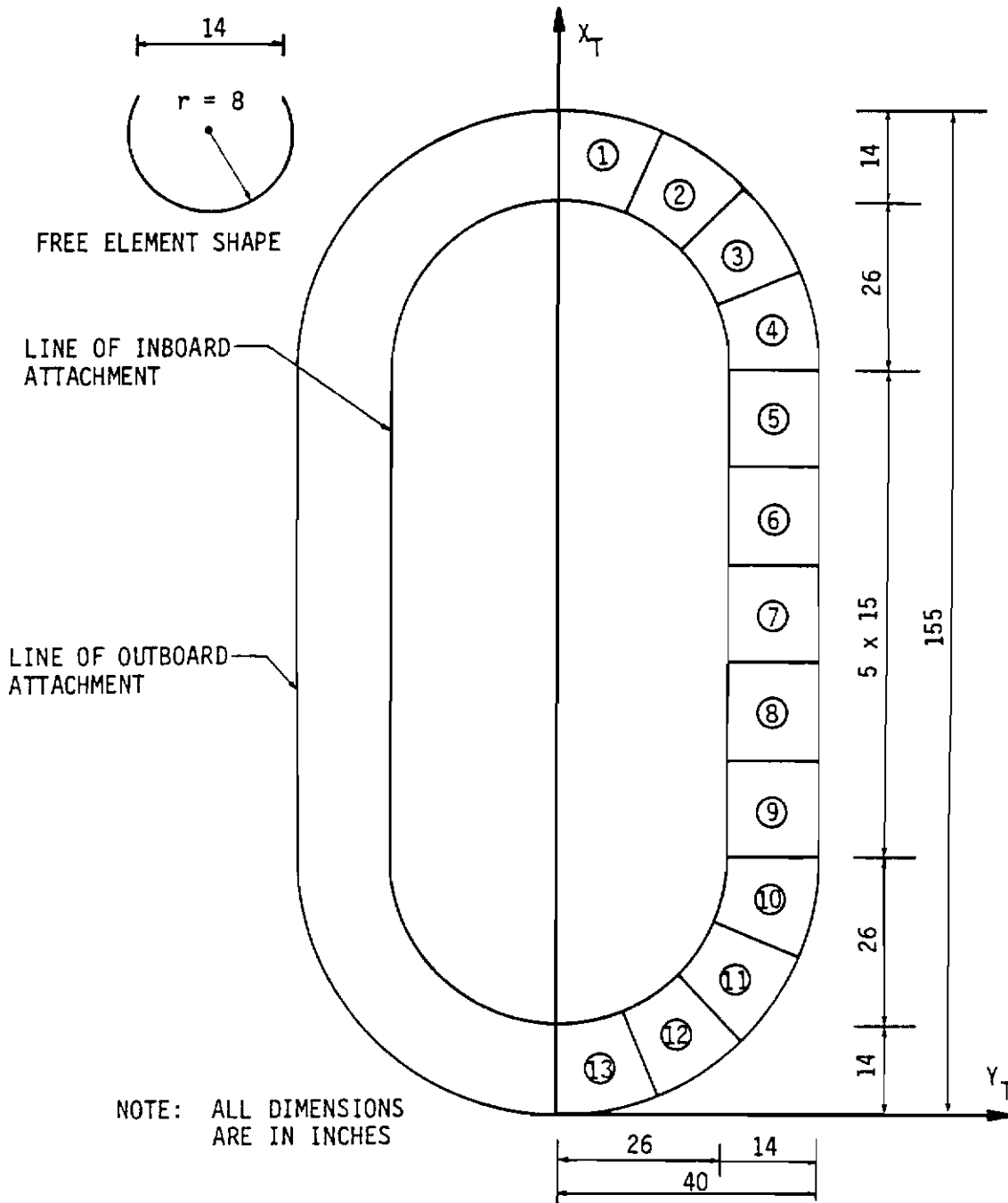


Figure 99 Launch Platform Trunk Model for Rockwell ARPV

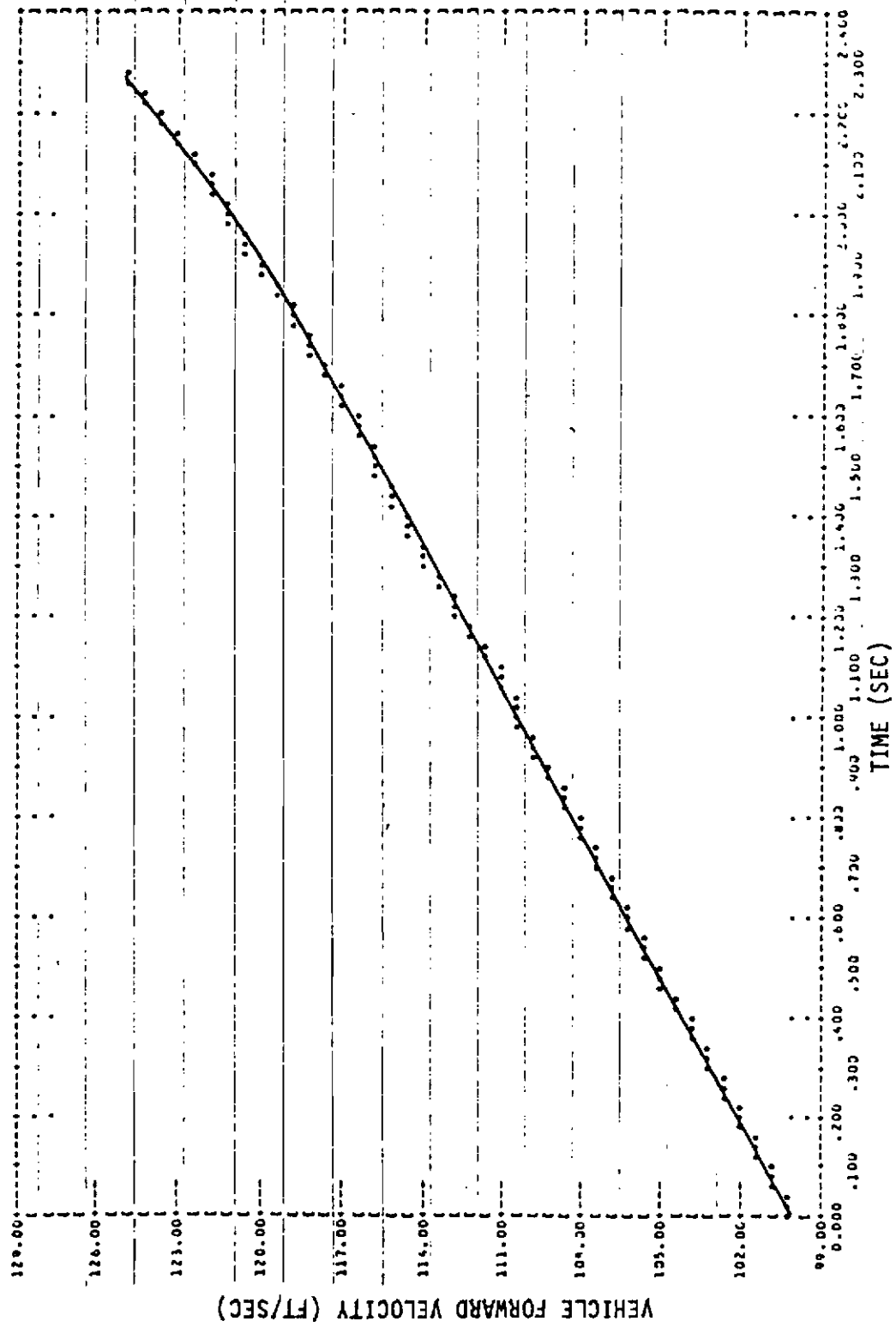


Figure 100 Rockwell ARPV with ACLP (Inelastic), 3 DOF Takeoff Simulation, Vehicle Forward Velocity vs. Time

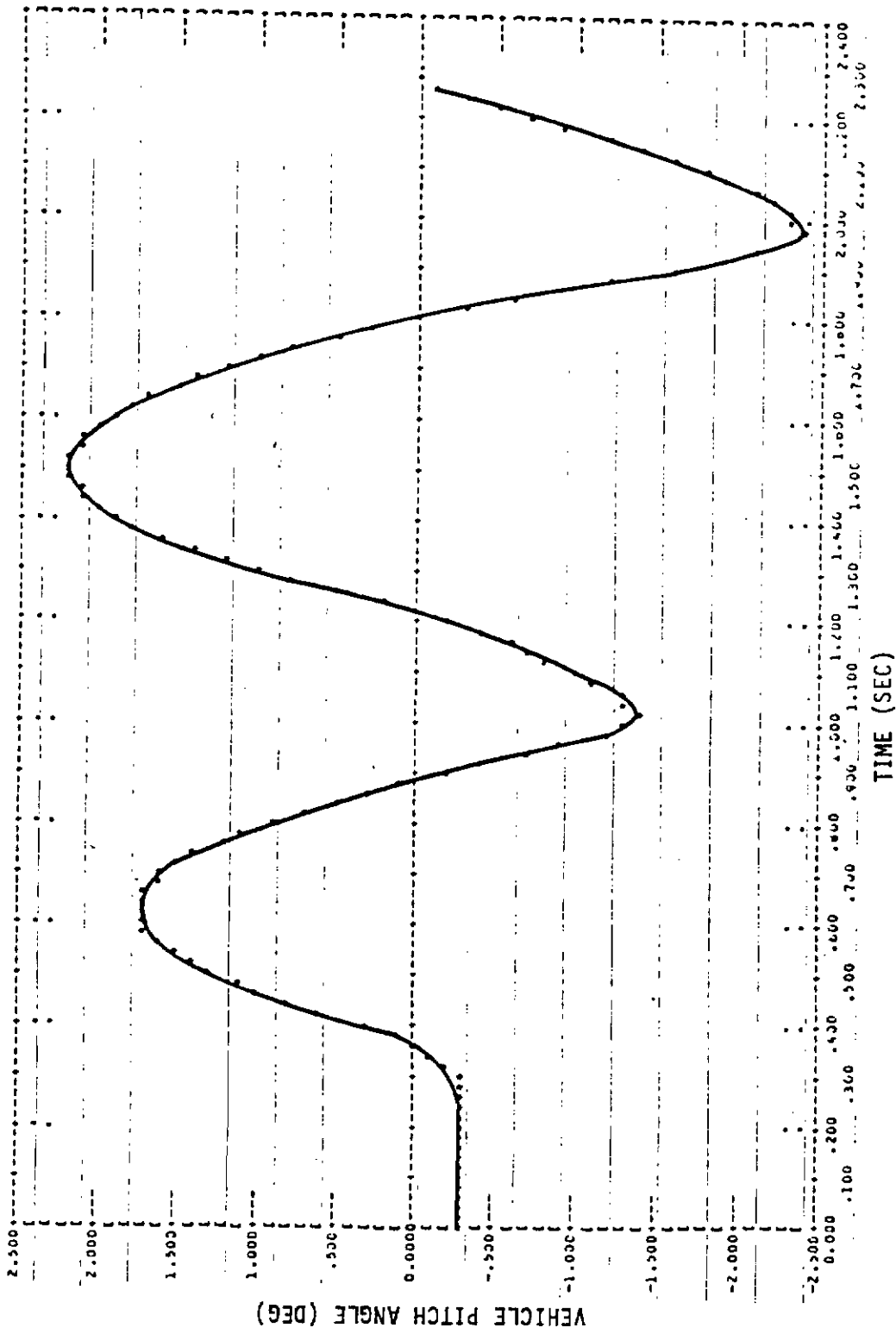


Figure 101 Rockwell ARPV with ACLP (Inelastic), 3 DOF Takeoff Simulation, Vehicle Pitch Angle vs. Time

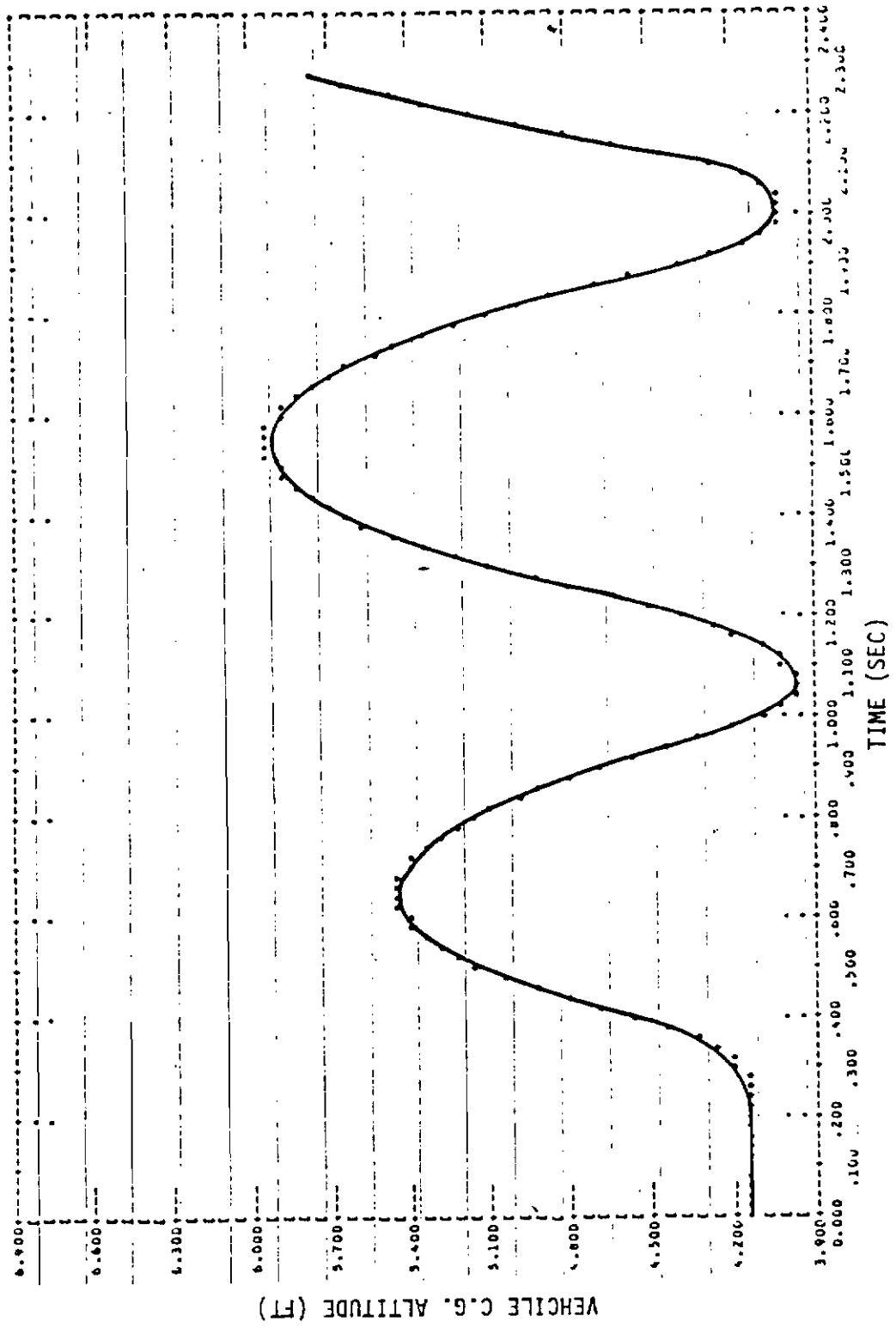
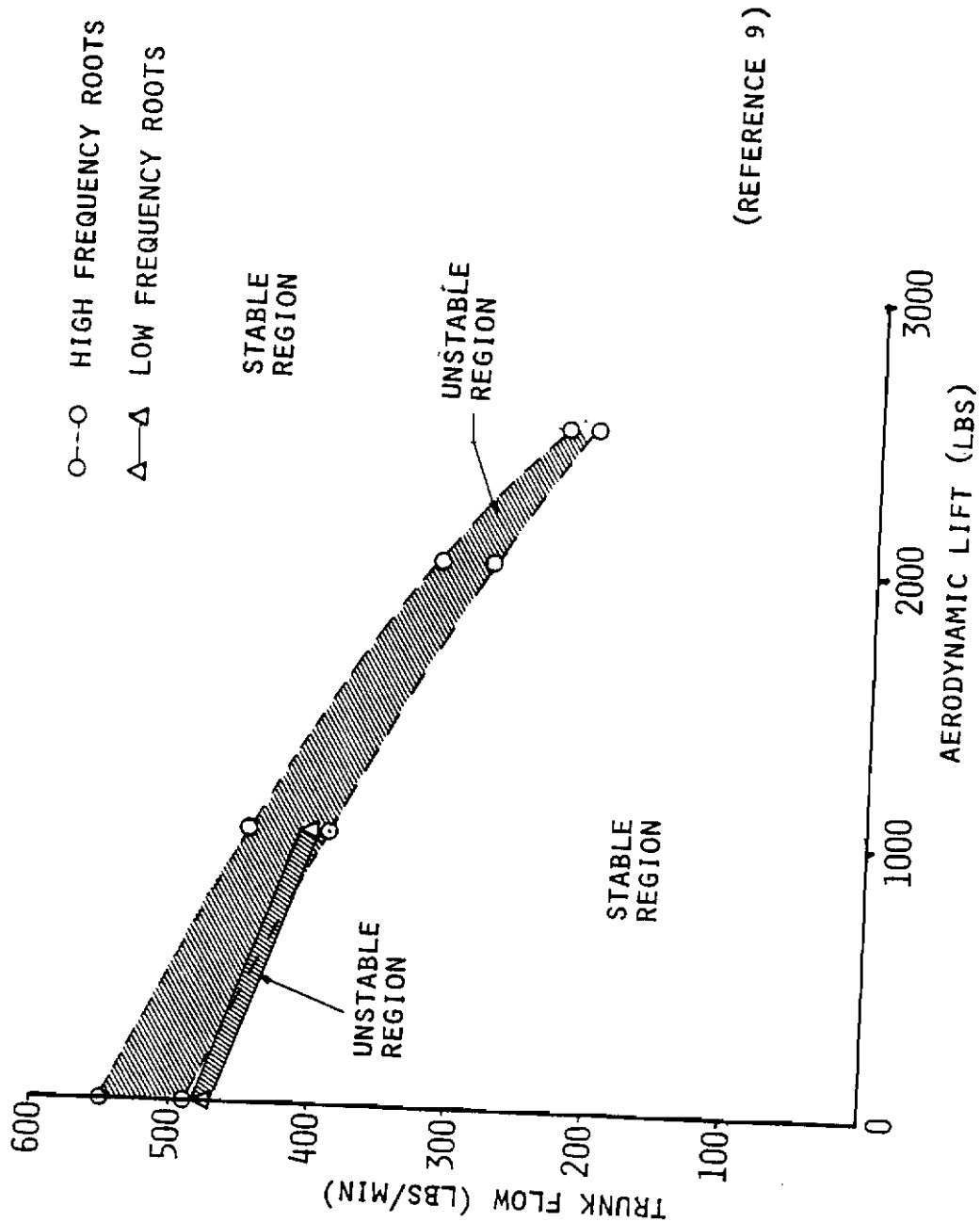


Figure 102 Rockwell ARPV with ACLP (Inelastic), 3 DOF Takeoff Simulation, Vehicle C.G. Altitude vs. Time



(REFERENCE 9)

Figure 103 Stability Analysis Results for EASY Model of Jindivik with Inelastic Trunk

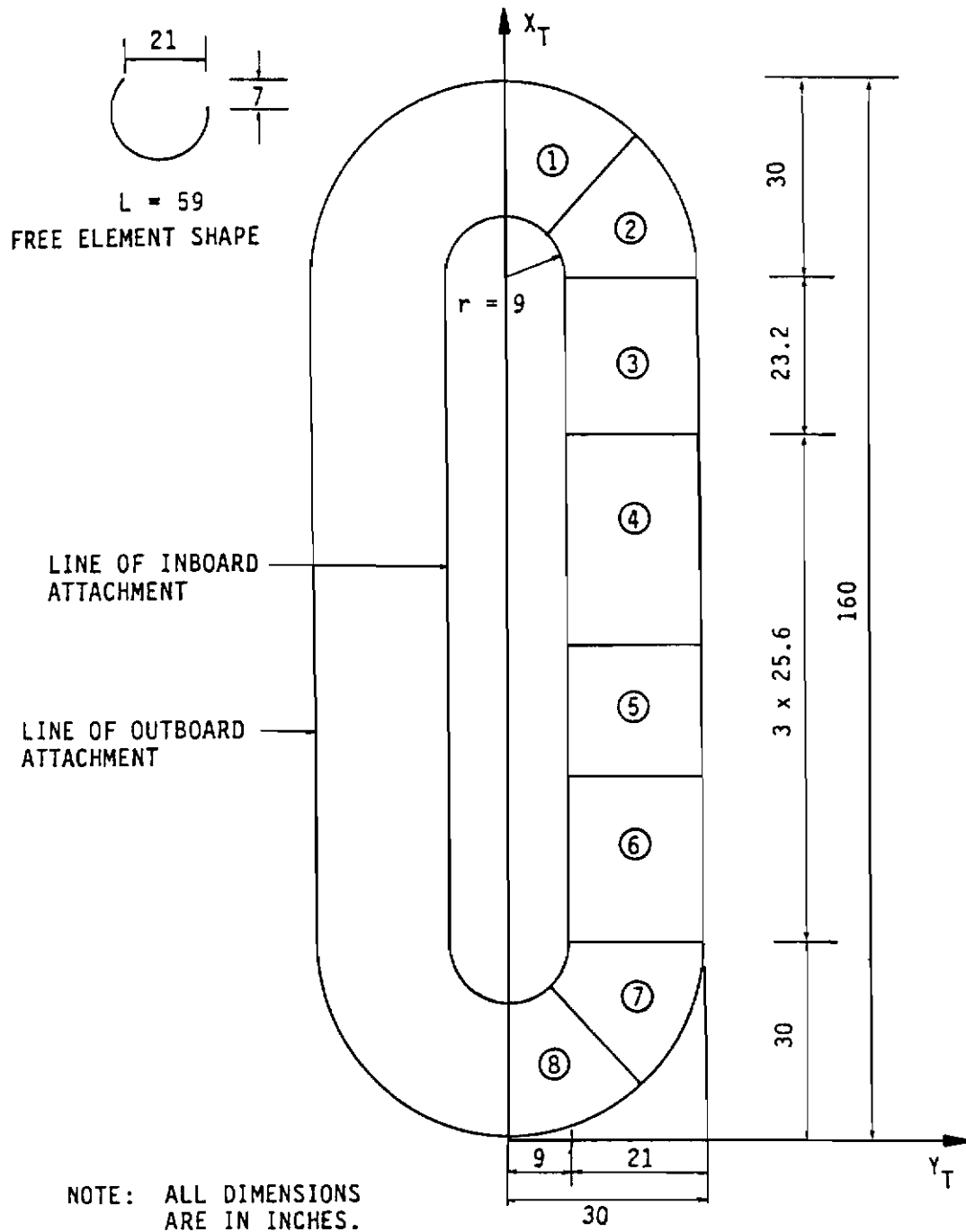


Figure 104 Inelastic IACS Model for Rockwell ARPV

The same air supply system as was modeled for the ACLP was used here.

As in the ACLP study, the Rockwell vehicle with the inelastic trunk IACS was simulated in takeoff roll using a three DOF simulation. The vehicle again went unstable at about 100 ft/sec forward speed. The results were similar to those shown for the ACLP in Figures 100, 101 and 102.

(3) Rockwell ARPV with Elastic IACS

The elastic trunk that was simulated is shown in Figure 90. The trunk was divided into 16 different elements for modeling in program EASY. Figure 91 shows the trunk material load/deflection curves which produced the proper trunk size. Lubrication and other parameters used in this simulation are listed in Table 15. The air supply was the same as that used with the inelastic trunk IACS.

The vehicle was simulated during the following takeoff conditions:

- o ground roll
- o rotation
- o trunk stowage
- o initial climbout

Unlike the takeoff simulations with the inelastic trunk, the vehicle remained stable through the ground roll. Therefore, the entire takeoff sequence could be simulated. Results of a six DOF simulation run are shown in Figures 105 through 110. In this case the ground roll was simulated from a forward velocity of 50 ft/sec to rotation speed at about 230 ft/sec (Figure 105). Figures 106 and 107 show that the vehicle pitch and altitude are stable throughout this region.

Trunk and cushion characteristics are shown in Figures 108 through 110. Parameters shown are trunk pressure, trunk volume, and cushion pressure, respectively. Trunk pressure and volume changes can be seen at vehicle rotation and at air supply cut off. The cushion pressure changes as aerodynamic lift increases and finally goes to atmospheric pressure at liftoff.

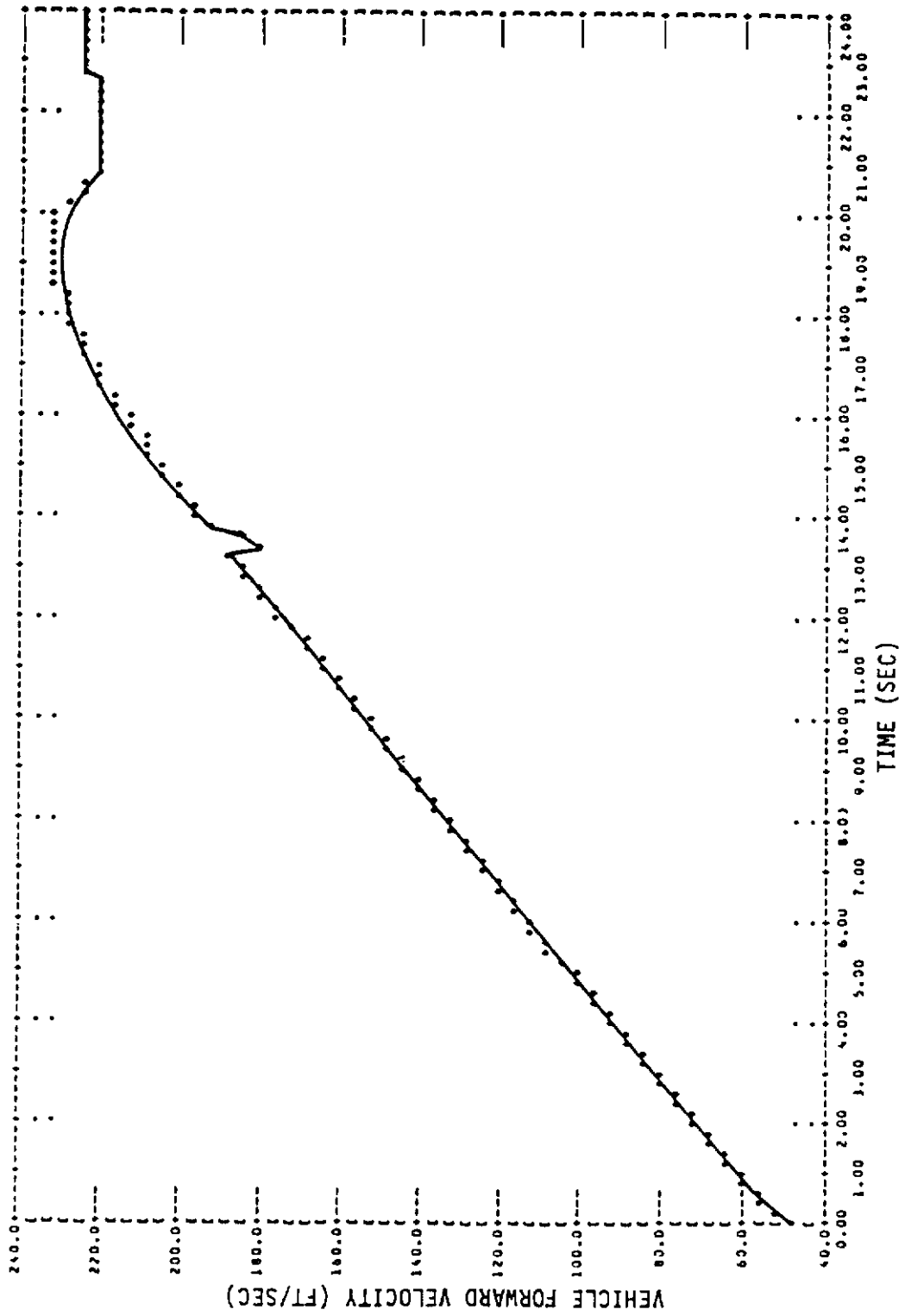


Figure 105 Rockwell ARPV with IACS (Elastic), 6 DOF Takeoff Simulation, Vehicle Forward Velocity vs. Time

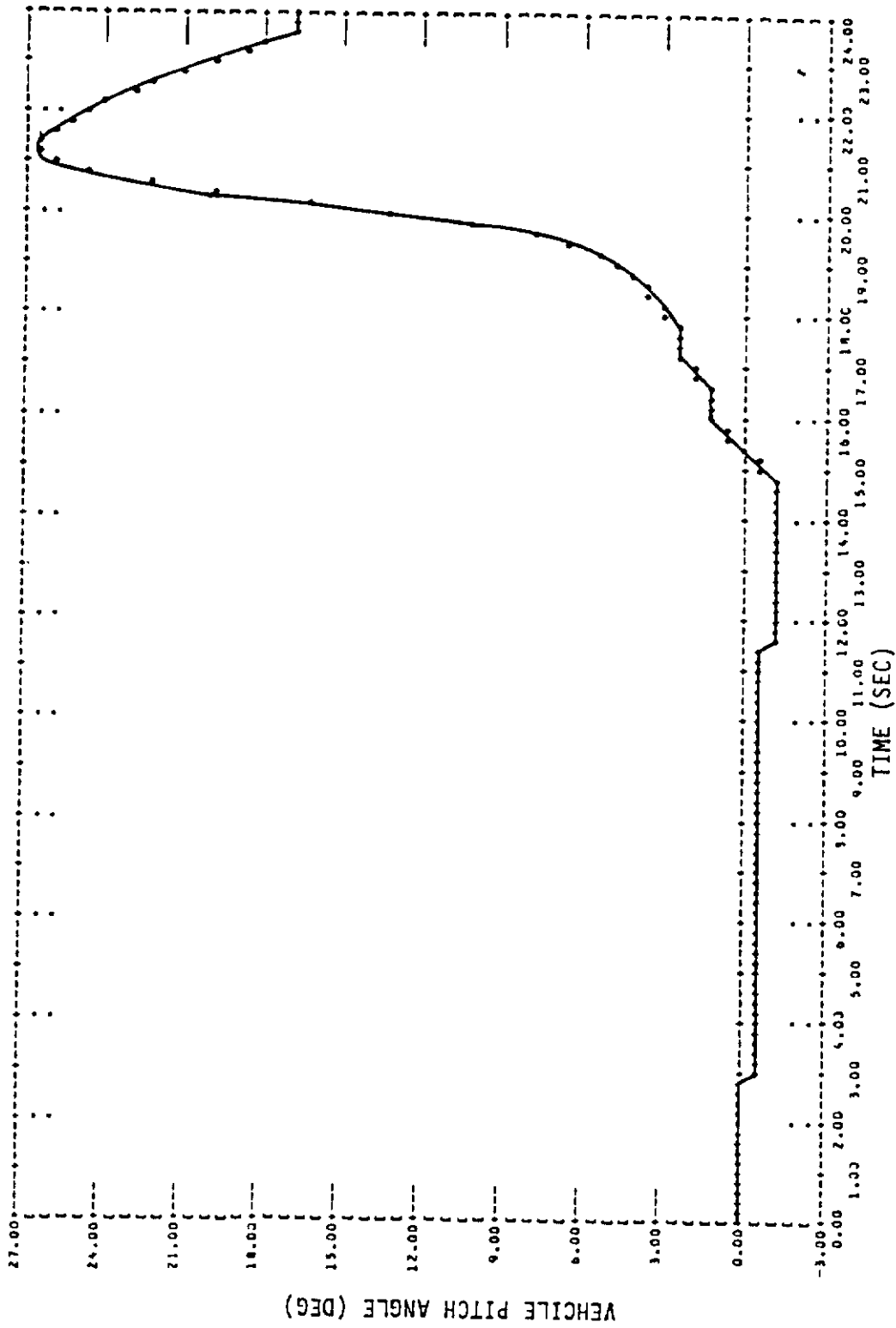


Figure 106 Rockwell ARPV with JACS (Elastic), 6 DOF Takeoff Simulation, Vehicle Pitch Angle vs. Time

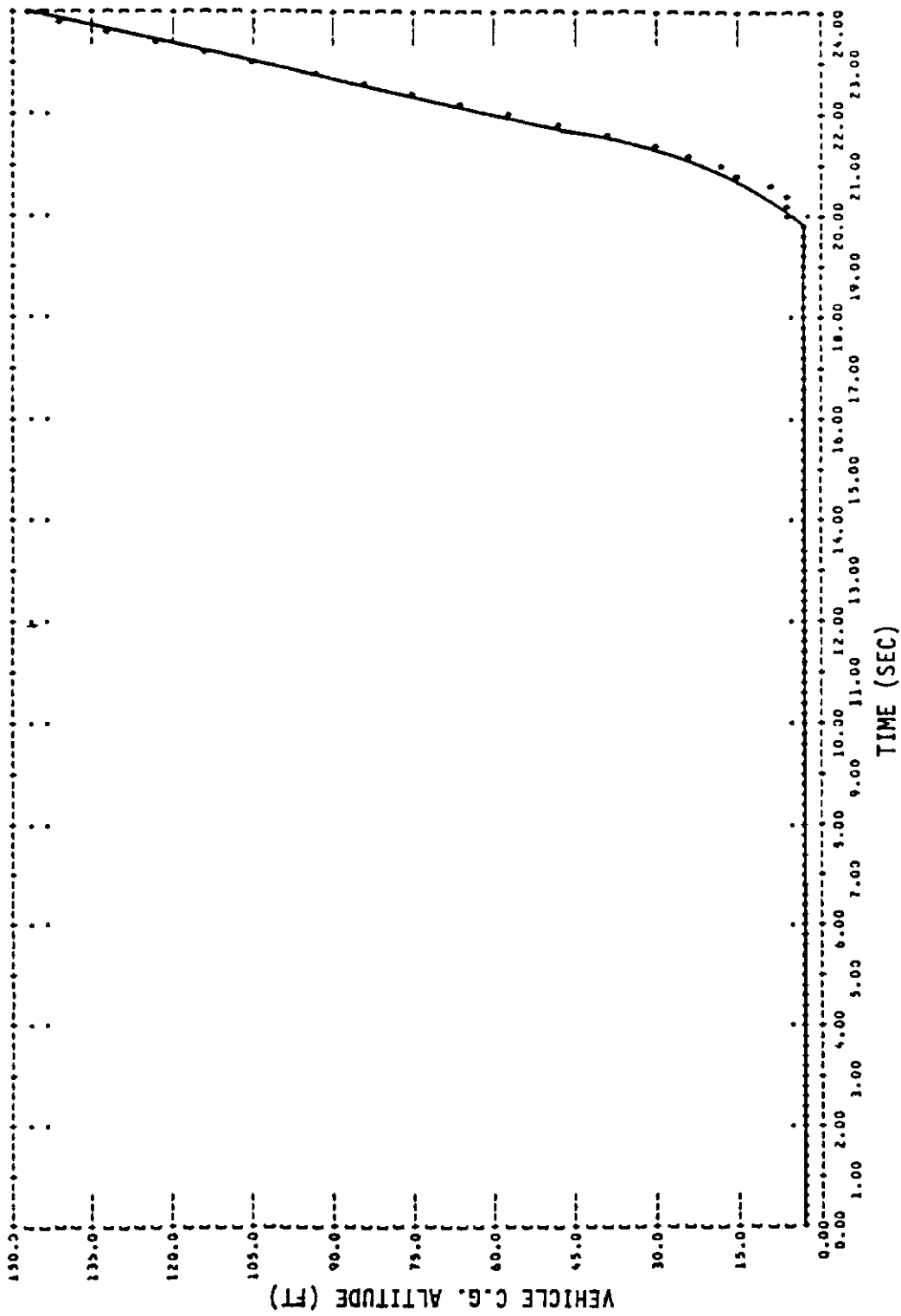


Figure 107 Rockwell ARPV with IACS (Elastic), 6 DOF Takeoff Simulation, Vehicle C.G. Altitude vs. Time

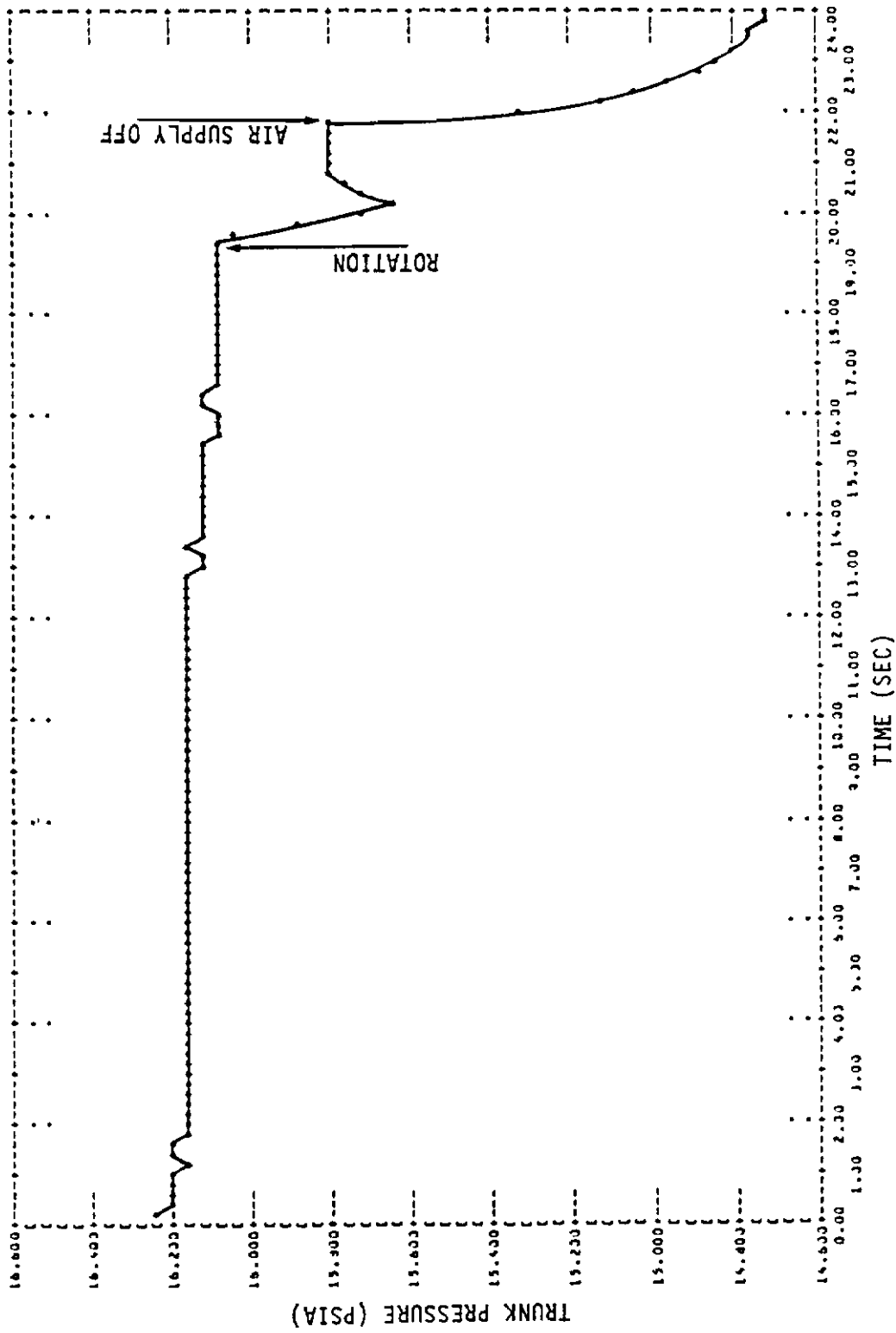


Figure 108 Rockwell ARPV with IACS (Elastic), 6 DOF Takeoff Simulation, Trunk Pressure vs. Time

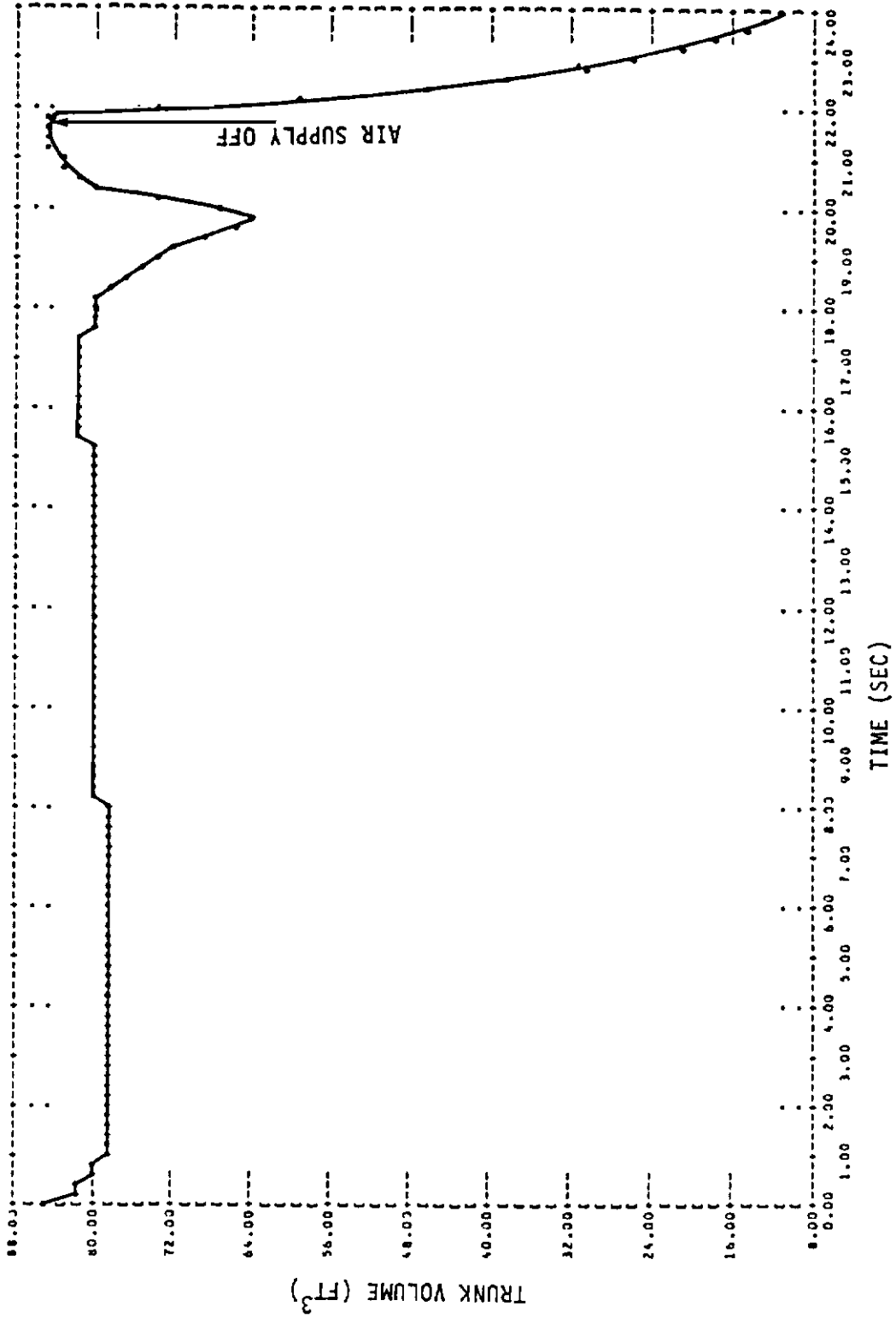


Figure 109 Rockwell ARPV with IACS (Elastic), 6 DOF Takeoff Simulation, Trunk Volume vs. Time

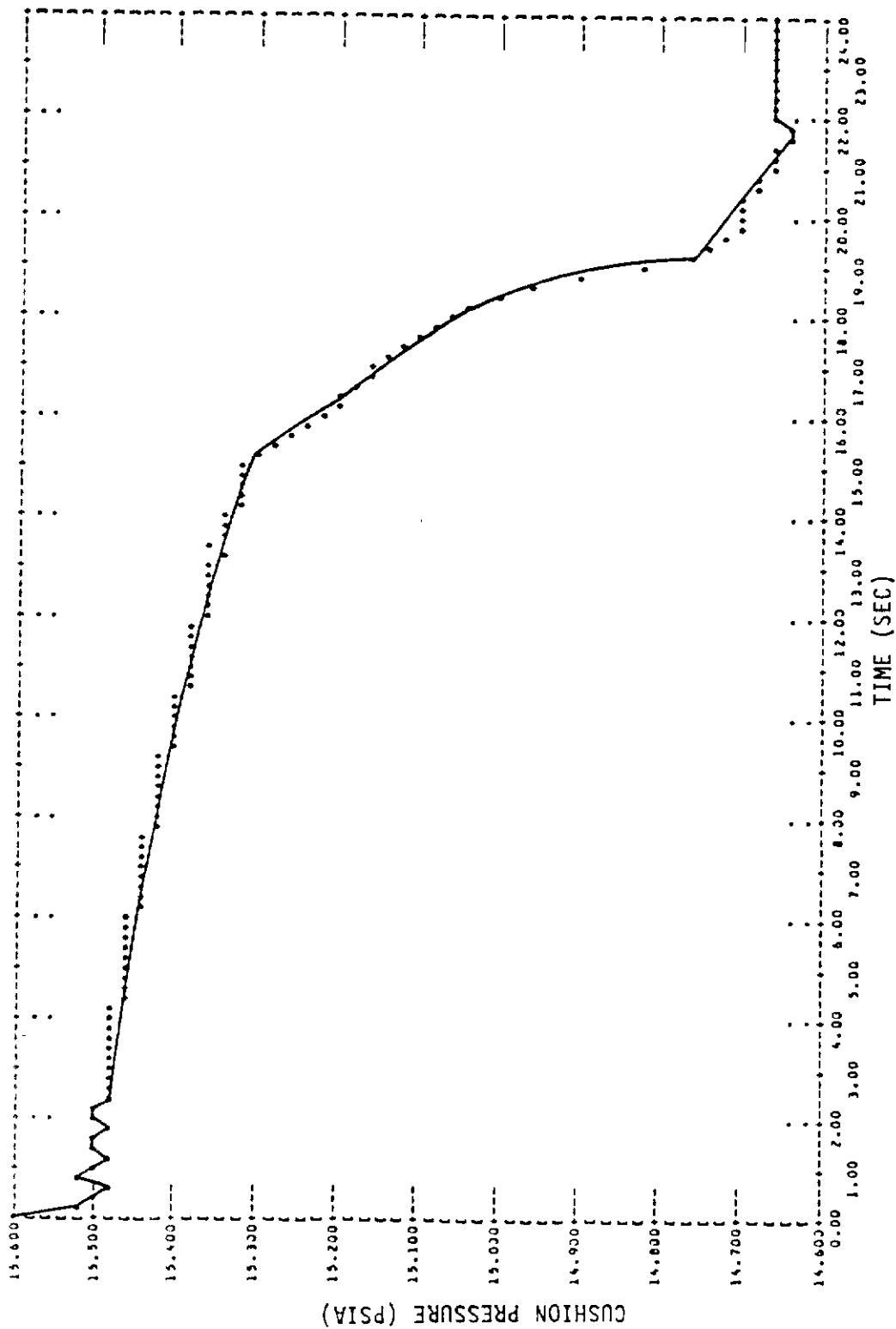


Figure 110 Rockwell ARPV with IACS (Elastic), 6 DOF Takeoff Simulation, Cushion Pressure vs. Time

c. Takeoff Simulation Conclusions

The following conclusions were drawn from results of the takeoff simulations:

- o Air supply power requirements are near the short duration overload limits for the accessory drive pad on the Rockwell vehicle for the IACS configuration.
- o Sufficient bleed air was not available to power the IACS for takeoff.
- o The vehicle remains stable throughout takeoff roll, rotation, trunk stowage and initial climbout with an elastic trunk IACS.
- o Takeoff simulations using an inelastic trunk for the IACS and ACLP were unsuccessful because of inelastic trunk model instabilities.
- o The elastic trunk EASY model requires modification to be used as a preliminary design tool.

SECTION III PRELIMINARY DESIGN

This task consists of applying the dynamic analysis results to the design of those configurations recommended for further study after the simulation analysis. The basic airframe designs for the Boeing and Rockwell vehicles were used with appropriate modifications to incorporate the results of the dynamic analysis and the requirements of the various launch/recovery systems.

The configurations that were recommended for preliminary design and cost/performance studies were selected on the basis of results of the dynamic analysis. Also, an attempt was made to get a complete cross section of the types of systems that were studied. Including all combinations of the launch or takeoff and recovery systems that were simulated was not practical nor were all of them satisfactory. The following configurations were included in this phase of the program:

- o Boeing ARPV with ABSS and arrestor
- o Boeing ARPV with ACRS and suction braking
- o Rockwell ARPV with ACRS and suction braking
- o Rockwell ARPV with IACS (elastic trunk) and arrestor
- o Rockwell ARPV with ACLP

The launch system concept for the Boeing configurations is unchanged from the baseline, a takeoff (RATO) from a zero length launcher.

1. BOEING ARPV RECOVERY SYSTEM CONCEPTS

a. Boeing ABSS Configuration

Both engine bleed air and a cool gas generator have been considered as primary ejector nozzle flow sources for the Boeing ARPV with the air bag skid system. System design parameters are shown in Table 17.

Drawing LO-DJ86-225 (Figure 111) shows the ABSS installation with a cool gas generator and ejector inflation source. A cool gas generator size of

TABLE 17
LAUNCH AND RECOVERY SYSTEM DESIGN PARAMETERS

	Boeing ARPV with ABSS and Arrestor	Boeing ARPV with ACRS and Suction Braking	Rockwell ARPV with IACS (Elastic Trunk) and Arrestor	Rockwell ARPV with ACRS and Suction Braking	Rockwell ARPV with ALCP ACLP Arrestor
Cool Gas Generator					
Size	5" Dia. x 12"				
Total Flow Rate (lbm/sec)	0.70				
Temperature (°F)	340				
Pressure (psia)	60				
Number of Ejectors	2				
Bleed Air					
Total Flow Rate (lbm/sec)	0.70	0.70		1.25	
Temperature (°F)	475	475		200	
Pressure (psia)	59.5	59.5		35	
Number of Ejectors	2	2		2	
Fan					
Number				1	1
Diameter (in)				18	18
Shaft Power (hp)				71.1	78.4
Flow Rate (lbm/sec)				11.5	12.2
Air Bag Skid					
Length (in)	150				
Diameter (in)	15				
Air Cushion Trunk					
Length (in)	138	138		140	155
Diameter (in)	15	15		26	16

Contrails

5 inches in diameter by 12 inches long provides sufficient flow for air bag inflation, replacement of air lost through relief valves at landing impact, and provision for leakage loss for battle damage to the air bag. A seven square inch hole was assumed for leakage loss rate calculations.

Drawing LO-DJ86-226 (Figure 112) shows the Boeing ARPV with an ABSS and an engine bleed air inflation source. Bleed air at 59.5 psia and 475 deg F is used as the primary gas source for the ejector nozzle.

The optimum air bag size was determined from landing simulations using program EASY to be 15 inches in diameter and 150 inches long. The air bags are attached to the air vehicle in prepacked stowage modules. Figure 113 shows an assembly buildup view of an ABSS module. The use of folded inelastic air bags or trunks is appropriate for applications where retraction is not required in flight. The dacron/polyurethane material provides an inexpensive air bag or trunk for the low pressures anticipated. It showed acceptable handling qualities during drop tests of the Navy test specimen when the hard structure was permitted to settle on top of the collapsed trunk. Polyurethane treads have not been tested with forward velocity but there is no known objection to them at this time.

The trunk material in the ABSS concept with a bleed air primary gas source must be protected locally against the initial blast of 475 deg F bleed air through the ejector. This can best be accomplished by a silicone pad attached to the trunk. The trunk is then folded such that the silicone pad interfaces with the ejector outlet. An alternate method to consider is using thick polyurethane as a heat sink at the air inlet port.

In order to inflate the skids the primary flow source, whether from engine bleed or cool gas generator, requires augmentation by an ejector nozzle. A flapper valve on the ejector nozzle prevents backflow, so air bag pressure increases until the folded air bag breaks through the frangible styrene cover holding it in place. The depth of a scribed line along the center of the cover determines the necessary breaking

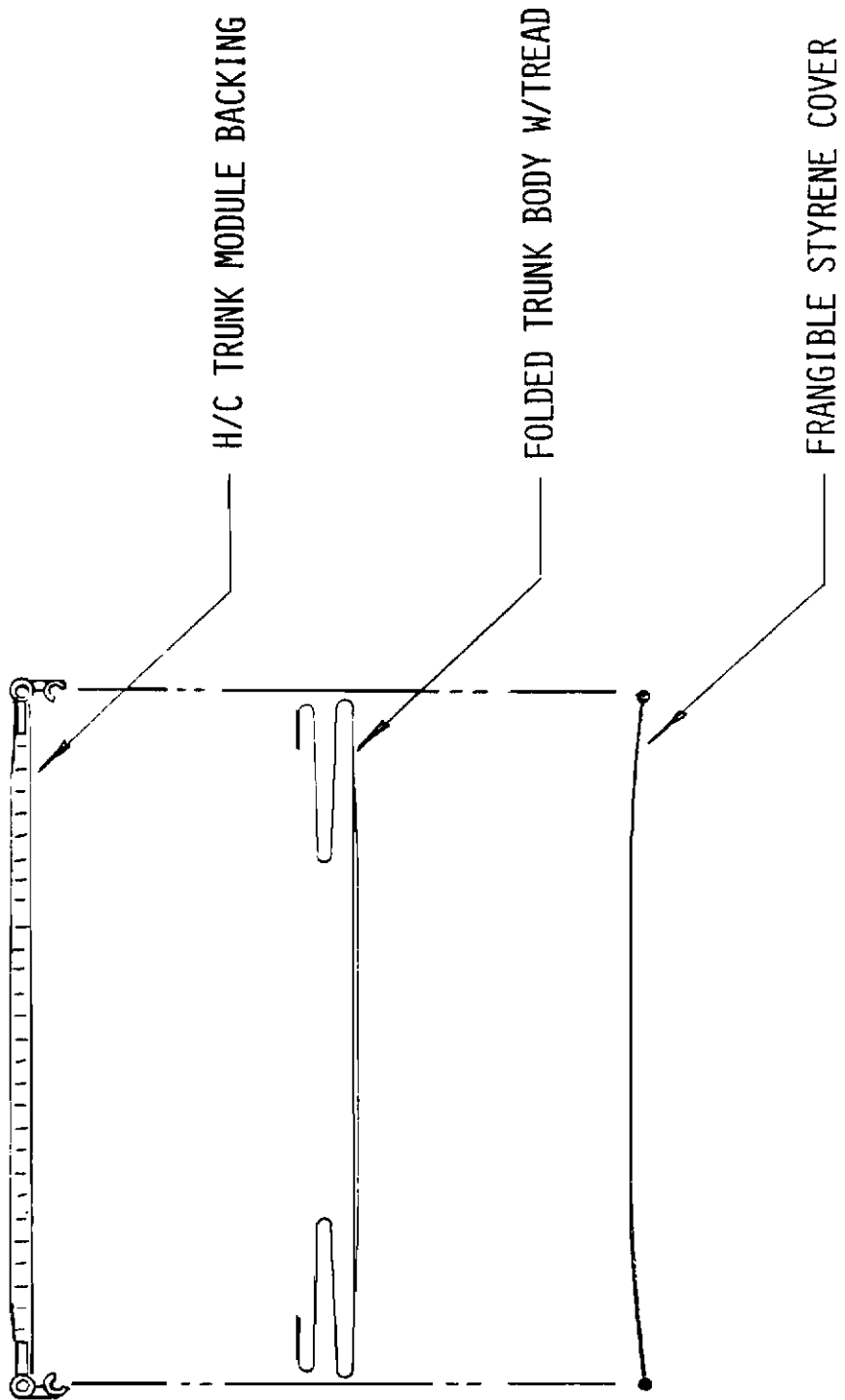


Figure 113 Boeing ABSS Assembly Build-up

pressure. The prepacked air bag modules are attached to the bottom of the fuselage with a piano hinge (cres pin). When the vehicle comes to a stop after arrestment and the engine is turned off, it will settle onto the partially filled air bags. Dolly wheels with pneumatic jacking actuators are then attached to hard points on the vehicle. The vehicle is lifted off the ground and a jeep is used to tow it off the recovery field to a maintenance area where it is readied for takeoff. The used air bag skid modules are removed and replaced with new air bag skid modules. For Boeing ABSS with cool gas generator, the generator unit will be removed and replaced.

Table 18 shows the aircraft installed equipment list for ABSS with a cool gas generator, which details the changes made to the Boeing baseline. The vehicle weight increased by 41 pounds due to these changes.

Table 19 shows the aircraft installed equipment list for ABSS with bleed air. The weight increase for this configuration was 32 pounds.

The runway dimensions required for the recovery of the Boeing ABSS vehicles with arrestment are 300 feet long by 100 feet wide.

b. Boeing ACRS Configuration

Drawing LO-DJ86-227 (Figure 114) shows the Boeing ACRS installation. Engine bleed air at 59.5 psia and 475 deg F is used as the primary gas source for the ejector nozzle. Design parameters are shown in Table 17.

The optimum trunk size, determined from landing simulations, is 138 inches long and 30 inches wide. The trunk module is attached to the vehicle in prepacked stowage modules.

As with the Boeing ABSS bleed air concept, the trunk material must be protected locally against the initial blast of 475 deg F bleed air through the ejector. This is accomplished with a silicone pad attached to the trunk, and facing the ejector nozzle outlet.

TABLE 18

AIRCRAFT INSTALLED EQUIPMENT FOR BOEING ARPV WITH ABSS WITH COOL GAS GENERATOR

<u>Component Description</u>	<u>Quantity</u>	<u>Material</u>	<u>Incremental Impact</u>
Air Bag Skids (larger than baseline)	2	Polyurethane/ Dacron	+
Cool Gas Generator (larger than baseline)	1		+
Air Bag Storage Module and Attachment Fittings (larger than baseline)	2	Al/Styrene	+

Total Impact of Installation is Weight Increase of 41 pounds.

TABLE 19

AIRCRAFT INSTALLED EQUIPMENT FOR BOEING ARPV WITH ABSS WITH BLEED AIR

<u>Component Description</u>	<u>Quantity</u>	<u>Material</u>	<u>Incremental Impact</u>
Air Bag Skids (larger than baseline)	2	Polyurethane/ Dacron	+
Engine Modifications			
Engine Bleed Port	1	Steel	+
Bleed Valve	1		
Air Bag Storage Module and Attachment Fittings (larger than baseline)	2	Al/Styrene	+
Removal of Cool Gas Generator	1		-

Total Impact of
Installation is
Weight Increase
of 32 pounds.

Contrails

The engine bleed air, augmented with the ejector nozzle is used to inflate the trunk. A flapper valve on the ejector nozzle prevents backflow, so trunk pressure increases until the folded trunk breaks through the frangible styrene covers holding it in place. The depth of a scribed line along the center of the covers determines the necessary breaking pressure. The stowed trunk is contained in a prepacked trunk stowage module which is attached to the doors and fuselage with a piano hinge along the sides and quick-release fasteners around the ends. Braking is provided by trunk to ground friction along the rear two-thirds of the trunk. The forward one-third of the trunk is lubricated to improve directional stability during landing slideout.

Suction braking is used to reduce the landing slideout distance. Cushion suction is provided by a second ejector nozzle, also powered by bleed air.

When the air vehicle comes to a stop after landing and the engine is turned off, the trunk will collapse and the air vehicle will settle onto the ground. Cantilevered dolly wheels with pneumatic jacking actuators are then attached to the air vehicle forward and aft of the trunk doors. The air vehicle is lifted off the ground and a jeep is used to tow it off the recovery field to an adjacent site where it is prepared for takeoff. The used recovery trunk module is removed and replaced with a new trunk module.

Table 20 shows the aircraft installed equipment list, which details the modifications made to the Boeing baseline to obtain the ACRS configuration. The results of the weight analysis for the changes shows the ACRS to weigh 16 pounds more than the baseline.

The runway dimensions required for the Boeing ACRS configuration are 4500 feet long and 200 feet wide. During the first part of slideout the flight control surfaces and engine thrust provide directional guidance. However, at lower speed the control surfaces are ineffective and the vehicle may drift off-course. Therefore, greater runway width is required. These dimensions account for suction braking stopping distances on wet ground with crosswind. The dry ground recovery distance

TABLE 20
AIRCRAFT INSTALLED EQUIPMENT FOR BOEING ARPV WITH ACRS

<u>Component Description</u>	<u>Quantity</u>	<u>Material</u>	<u>Incremental Impact</u>
Air Cushion Trunk	1	Polyurethane/ Dacron	+
Trunk Ejector Nozzle with Backflow Check Valve	1	Al	-
Relief Valve	1	Al	-
Air Cushion Trunk Storage Module and Attachment Fittings	1	Al/Styrene	+
Suction Braking Ejector Nozzle	1	Al	+
Engine Modifications Engine Bleed Port Bleed Valve	1 1	Steel	+
Removal of Arresting Hook	1	Steel	-
Removal of Cool Gas Generator	1		-

Total Impact of
Installation is
Weight Increase
of 16 pounds.

is 800 feet. Field length and width requirements for each of the configurations are listed in Section IV.1.

2. ROCKWELL ARPV LAUNCH AND RECOVERY SYSTEM CONCEPTS

The configurations of the Rockwell ARPV recommended for further study were the air cushion recovery system (ACRS) with suction braking, the air cushion launch platform (ACLP), and the integrated air cushion system (IACS) with an elastic trunk. The basic Rockwell airframe design with landing gear provisions removed, was used with appropriate modifications to incorporate the results of the dynamic analysis and the requirements of the launch/recovery systems.

a. Rockwell ACLP (Launch) and ACRS (Recovery)

This configuration uses an air cushion launch platform (ACLP) for takeoff, and an air cushion recovery system (ACRS) with suction braking for landing.

The Rockwell ACRS installation is shown in Drawing LO-DJ86-228 (Figure 115). The ACRS trunk shape was determined after several landing simulations using program EASY. The deployed trunk is supported by doors which extend and provide a wide surface for the trunk. The use of structural doors to spread the trunk was proposed in previous air cushion system application studies for both the A-4 and AMST installations. In these cases the doors were also for trunk protection while on the Rockwell ARPV they only serve to spread the trunk. The doors deploy when pneumatic locks are actuated and the extension cells are inflated. Further detail of the trunk door lock mechanism is shown in Figure 116. The actuators and extension cells use compressed air from the 2000 psia pneumatic accumulator which is used for engine starting and was designated for landing gear retraction on the baseline vehicle. A pressure of approximately 15 psig is needed in the extension cells.

After the doors extend, the recovery trunk is deployed. Engine bleed air at 35 psia and 200 deg F is the primary gas source for an ejector nozzle used for trunk inflation. A flapper valve on the ejector nozzle prevents

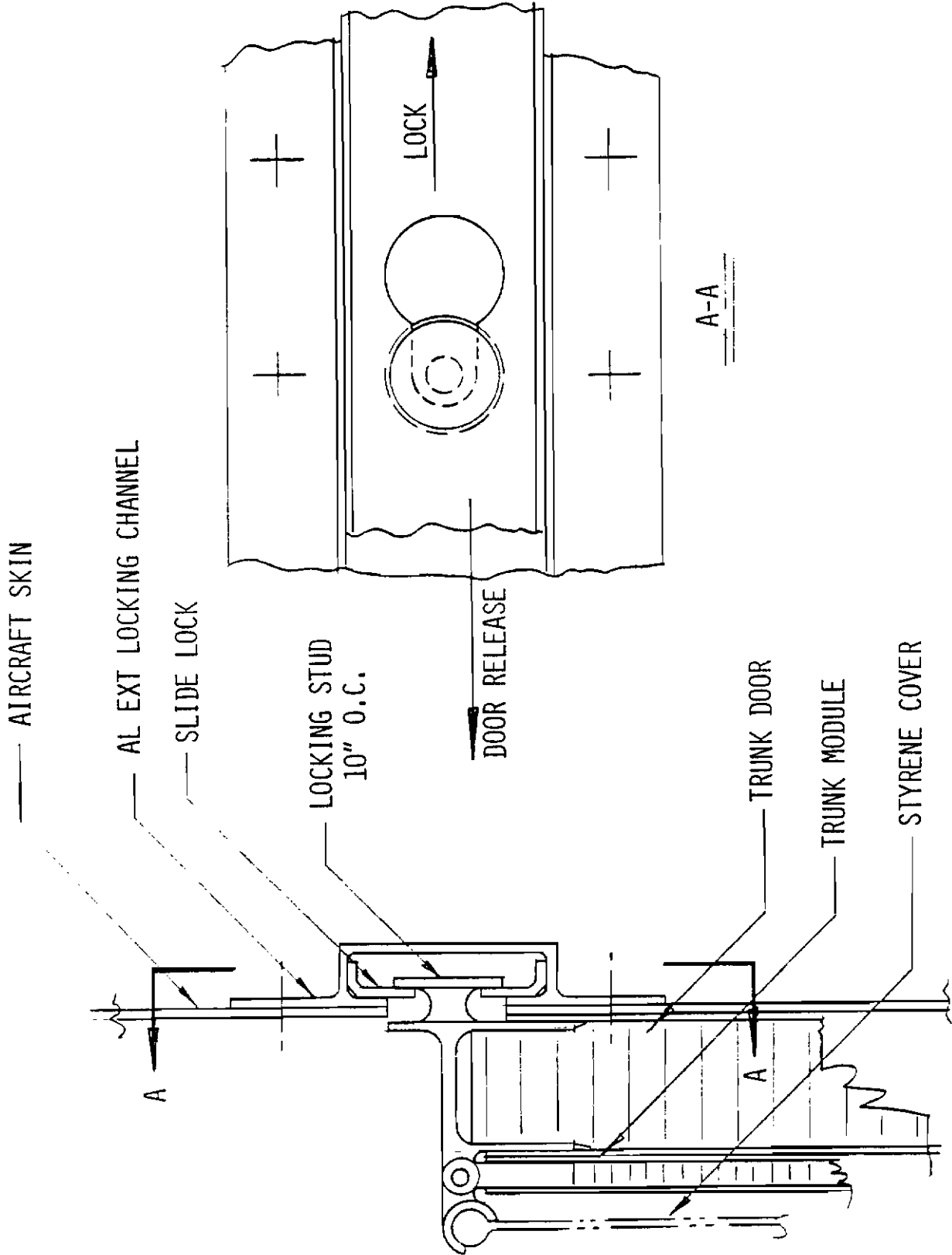


Figure 116 Rockwell ACRS Door Locking Mechanism Detail

Contrails

backflow, so trunk pressure increases until the folded trunk breaks through the frangible styrene covers holding it in place. The depth of a scribed line along the center of the covers determines the necessary breaking pressure. The stowed trunk is contained in a prepacked trunk stowage module which is attached to the doors and fuselage with a piano hinge along the sides and quick release fasteners around the ends. Figure 117 shows an assembly buildup view of the ACRS module. Braking is provided by trunk-to-ground friction along the rear two-thirds of the trunk. The forward one-third of the trunk is lubricated to improve directional stability during landing slideout.

During the first part of landing slideout, the flight control surfaces and residual engine thrust provide directional guidance. However, when the ARPV speed is slowed to less than 50 knots, the flight control surfaces are not effective. Sufficient runway width must be provided to account for crosswinds, which may force the ARPV off-course during its final slideout phase.

Suction braking is used to reduce the landing slideout distance. Cushion suction is provided by a second ejector nozzle, also powered by bleed air.

The baseline vehicle camera installations are moved forward into the former nose wheel well. This relocation provides more room for the ejector nozzle installations and helps to keep the air vehicle correctly balanced after the original landing gear and fairings are removed.

Two ports exist in the fuselage, which are covered by the doors when they are up and locked. One port is used to provide clearance for the door mounted relief valve when the door is closed and is also used as an air inlet for the trunk ejector nozzle. The second port is the outlet for the suction braking ejector. The suction braking ejector installation displaces some fuel but there will be an overall fuel savings due to the reduced weight and drag of this system relative to the original landing gear system.

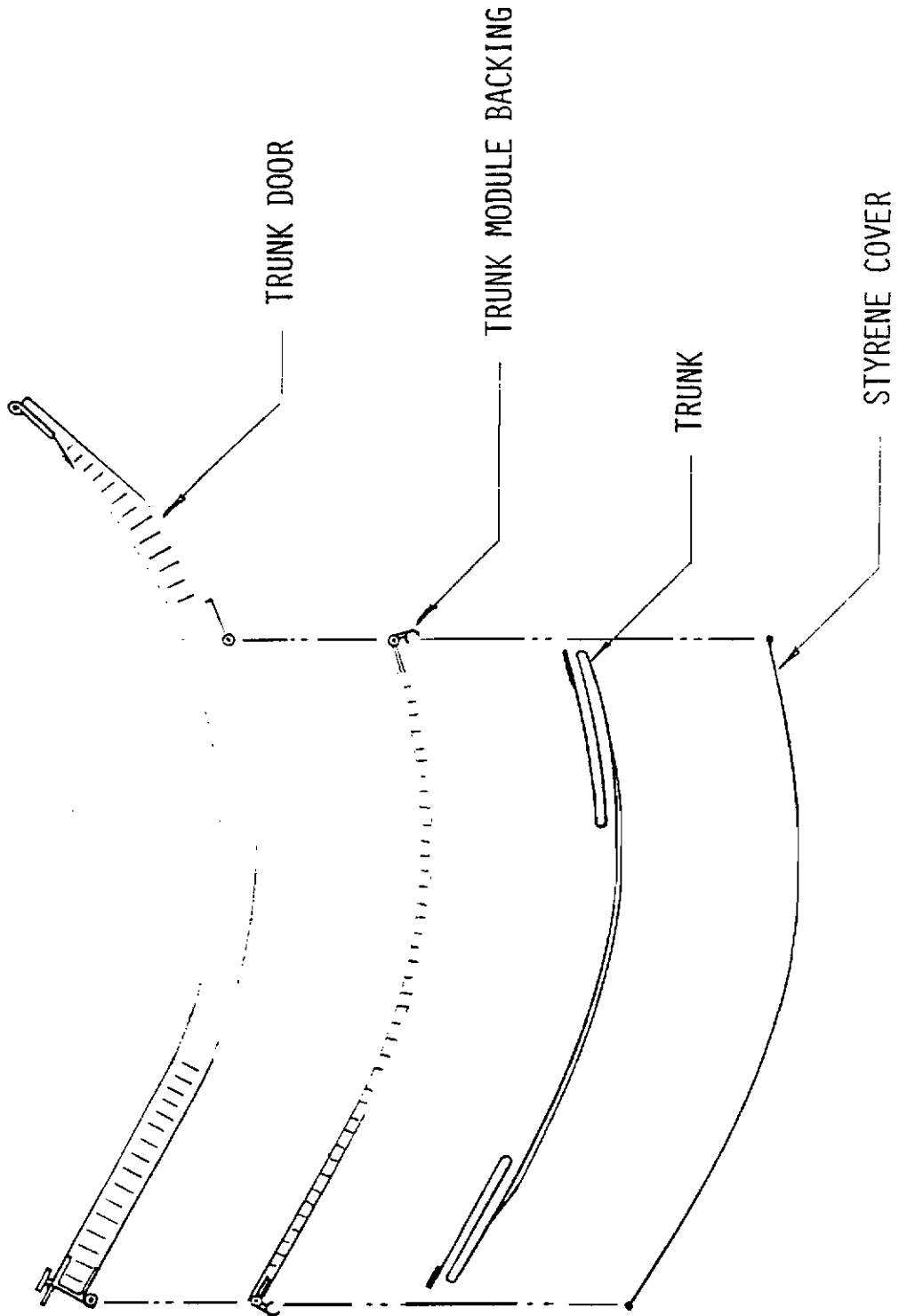


Figure 117 Rockwell ACRS Assembly Build-up

Contrails

Table 21 shows the aircraft installed equipment list, which details the modifications made to the Rockwell baseline to obtain the ACRS configuration. Table 22 shows the results of the weight analysis for the changes. Total vehicle weight is 31 pounds less than the baseline. Note that the ACRS configuration did not realize the true weight savings of ACLS because the Rockwell vehicle was adapted to use ACLS. The adaptation required trunk doors and extension cells which are not necessary for a vehicle designed for ACLS.

The removal of the landing gear and its fairings reduced the wetted area of the vehicle by 5.9 square feet. The baseline vehicle has a wetted area of 528.8 square feet, and because the drag is proportional to the wetted area, the drag was reduced by $5.9/528.8 = 1.1\%$.

The runway dimensions required for the Rockwell ACRS configuration are 1600 feet long and 150 feet wide at one end and 350 feet wide at the other. These dimensions account for suction braking stopping distances on wet ground. The dry ground recovery distance is 300 feet.

When the air vehicle comes to a stop after landing and the engine is turned off, the trunk will collapse and the air vehicle will settle onto the deployed doors. Dolly wheels with pneumatic jacking actuators are then attached to hard points on the vehicle forward and aft of the trunk doors. Figure 118 shows details of the dolly wheels. The air vehicle is lifted off the ground and a jeep is used to tow it off the recovery field to an adjacent site where it is prepared for takeoff. The used recovery trunk module is removed and replaced with a new trunk module. The used module is inspected, repaired as required, and repackaged for use on another vehicle.

For takeoff the air vehicle is towed to the takeoff field on the dolly wheels where it will be mounted on the launch platform carriage, Drawing LO-DJ86-229 (Figure 119). The launch platform engine is turned off so its trunk is collapsed under the platform on the ground. Tracks on the platform allow the air vehicle to be rolled over the platform so it is positioned above the air vehicle carriage. The air vehicle is lowered

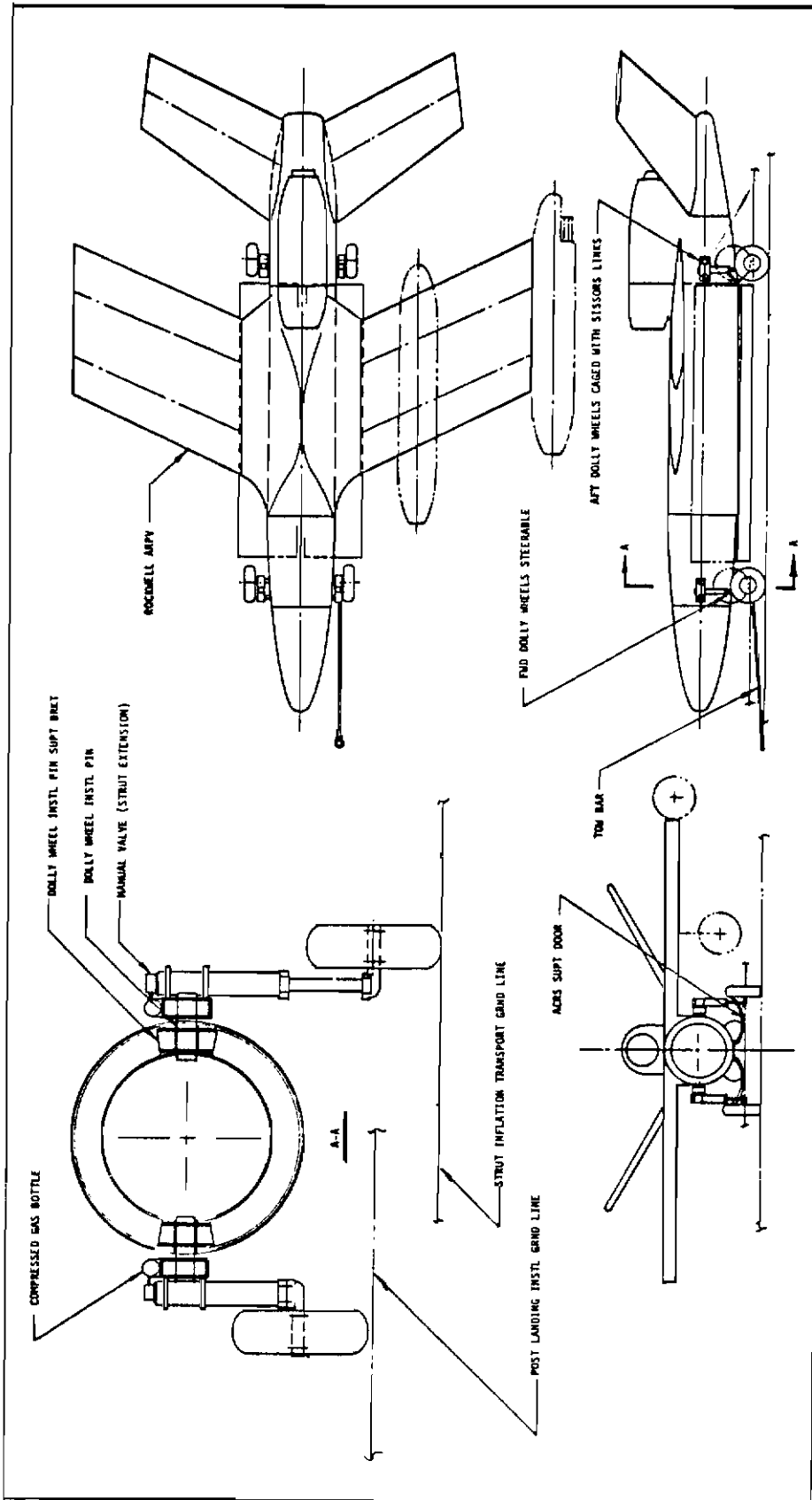


Figure 118 Rockwell ACRS Dolly Wheel Installation

TABLE 21

AIRCRAFT INSTALLED EQUIPMENT FOR ROCKWELL ARPV WITH ACRS

<u>Component Description</u>	<u>Quantity</u>	<u>Material</u>	<u>Incremental Impact</u>
Air Cushion Trunk	1	Polyurethane/ Dacron	+
Landing Gear and Fairings			-
Trunk Ejector Nozzle with Backflow Check Valve	1	Al	+
Cushion Ejector Nozzle	1	Al	+
Cushion Ejector Exhaust Chute	1	Al	+
Relief Valve	1	Al	+
High Pressure Ducting with Fittings	2	Steel	+
High Pressure Flow Control System with Valves	1		+
Hinged Trunk Doors and Attachment Fittings	2	Al	+
Air Cushion Trunk Storage Module with Cover and Fasteners	1	Al/Styrene	+
Removal of Arresting Hook	1	Steel	-
Low Pressure Ducting with Fittings	2	Al	+
Trunk Door Extension Cells	2	Rubber	+

TABLE 22
ROCKWELL ACRS WEIGHT ANALYSIS

<u>Component</u>	<u>Δ Weight (lbs)</u>
Removal of:	
Conventional Landing Gear	-186
Landing Gear Fairings	- 20
Landing Gear Hard Structure	- 42
Arresting Hook	- 25
Addition of:	
Air Cushion Trunk	+116
Trunk Doors & Fasteners + Inflation System	+126
Overall Δ Weight	- 31

Contrails

onto the carriage by releasing air from the dolly wheel jacks, and then the dolly wheels are detached.

The launch platform is constructed of aluminum honeycomb. An inelastic heavy duty air cushion trunk is mounted under it. Air to the trunk is provided by an aluminum block, 80 hp, two-cycle, gasoline engine and a two-stage axial fan. The engine also drives a small air compressor which charges a pneumatic accumulator. This high pressure source is used by pneumatic actuators for releasing the air vehicle carriage at takeoff rotation.

Platform braking after takeoff, or platform plus vehicle braking during an aborted takeoff, is provided by a water twister arrestor, as shown in Drawing LO-DJ86-229 (Figure 119). The purchase tape passes through a sheave and is then connected to a steel cable which extends down the centerline of the runway. The other end of the cable hooks onto a ground stake so the cable can be pulled tight prior to takeoff. Cable guides are mounted to the forward and aft ends of the launch platform. During the first 300 feet of takeoff acceleration while the air vehicle speed is below 50 knots, the vehicle rudder does not provide effective directional control. During these first few seconds, the cable and guides control the vehicle and launch platform direction. After the vehicle control surfaces become effective, the forward guide is released and raised from the cable. When the platform attains the proper speed, the vehicle rotates and is released. The rear guide continues sliding along the cable until reaching its end. A fitting at the end of the cable catches the slide and the purchase tape begins unwinding from the water twister tape drum. Approximately 2800 feet of one-half inch diameter steel cable would be required. A shock absorber built into the rear cable guide would reduce the impact load when it reaches the end of the cable. The runway dimensions required for launch with ACLP are 2800 feet in length and 50 feet wide. Table 23 shows the results of the launch platform weight analysis. The total platform weight is 1100 pounds.

The air cushion launch platform described above was selected after a preliminary trade study was performed. The advantages and disadvantages

TABLE 23
ROCKWELL ACLP WEIGHT ANALYSIS

<u>Component</u>	<u>Weight (lbs)</u>
80 hp 2 Cycle Piston Engine	180
Fuel Tank & Plumbing	20
2-stage Fan	25
Platform Structure	736
Main Supports	62
Air Cushion Trunk	77
Total Weight	1100

of the different approaches to implementing the various launch platform functions were weighed as shown in Table 24. Complexity, maintenance and reliability were factors in selecting the concept.

b. Rockwell IACS

The other system concept recommended for the Rockwell ARPV uses an integrated air cushion system for launch and recovery. The elastic trunk is totally lubricated in order to reduce friction for takeoff ground roll. For recovery, an arrestment system is used to stop the vehicle. The use of friction brake pads with cushion venting were considered. However, this concept was discarded because its effectiveness is limited with a totally lubricated trunk. The stopping distance for this configuration on a wet runway was estimated to be 5000 feet.

The Rockwell IACS installation is shown in Drawing LO-DJ86-232 (Figure 120). Like the Rockwell ACRS configuration, the deployed trunk is supported by doors which extend and provide a wide surface for the trunk. The doors deploy when pneumatic locks are actuated, the extension cells are inflated, and the cables on the electric powered, motor/reel assemblies unwind. The actuators and extension cells use compressed air from the 2000 psia pneumatic accumulator. A pressure of approximately 15 psig is needed in the extension cells. After the doors extend, the elastic trunk is deployed.

When deflated, the elastic trunk clings tightly to its prepacked stowage module. The module is attached to the doors and fuselage with a piano hinge along the sides and quick-release fasteners around the ends.

A shaft-driven two-stage axial fan is used for trunk inflation. The fan is powered from the accessory drive pad via a clutch plus high speed drive train shafting.

The camera installations are moved forward into the former nose wheel well. This relocation provides space for the fan installation and helps to keep the vehicle correctly balanced after the original landing gear and fairings are removed.

TABLE 24
AIR CUSHION LAUNCH PLATFORM TRADE STUDY RESULTS

Function	Method of Implementation	Advantages	Disadvantages	Influence Factor
				+ -
Takeoff Acceleration	o Air vehicle thrust	o Simple, lowest cost	o Longer takeoff roll o Requires tow vehicle	✓
	o Auxiliary thrust engine	o Shorter takeoff roll o Power for air supply o Power for direction control o Power for remote taxi	o Complex, high cost o High maintenance o Lower reliability o Fire hazard in accident o High weight	✓
Deceleration of Platform After Launch	Suction Braking	o No additional ground equipment required o Can be used with remote taxi with thrust engines	o Longer field length (in addition to takeoff roll) o Direction control system required o Not effective because of trunk lubrication	✓
	Arrestor cable and water twister absorber	o Short stop distance o Cable can be used to guide platform during takeoff roll o Tow vehicle may not be required	o Additional ground equipment and support personnel required o Limited flexibility on launch direction	✓

TABLE 24
AIR CUSHION LAUNCH PLATFORM TRADE STUDY RESULTS (cont'd.)

Function	Method of Implementation	Influence Factor		
		+	-	
Direction Control	Thrustor system	<ul style="list-style-type: none"> o Can be used with remote taxi o No additional ground equipment 	<ul style="list-style-type: none"> o Complex o Reduced reliability o High maintenance 	✓
	Yawed thrust engine	<ul style="list-style-type: none"> o Remote taxi capability o No additional ground equipment 	<ul style="list-style-type: none"> o Complex o High weight o High maintenance o Fire hazard o High cost 	✓
Trunk	Cable	<ul style="list-style-type: none"> o Simple o Used with arrester 	<ul style="list-style-type: none"> o Additional ground equipment o Limited flexibility on launch direction 	✓
	Single	<ul style="list-style-type: none"> o Simple o Adequate 		✓
	Multiple		<ul style="list-style-type: none"> o Higher maintenance o More complex 	✓
	Compartmentalized		<ul style="list-style-type: none"> o Not required for stability 	✓

TABLE 24
AIR CUSHION LAUNCH PLATFORM TRADE STUDY RESULTS (cont'd.)

Function	Method of Implementation	Advantages	Disadvantages	Influence Factor
				+ -
Taxi	Tow vehicle	<ul style="list-style-type: none"> o Simplest platform o No thrust engine required o No control system required if used with cable arrest. o Most reliable 	<ul style="list-style-type: none"> o Additional ground equipment 	✓
	Remote control	<ul style="list-style-type: none"> o Less ground equipment 	<ul style="list-style-type: none"> o Complex o Reduced reliability o Increased maintenance o Increased hazard o Heavy, complex platform o Requires thrust engine o Requires complex control system 	✓
Air Supply	Turbo-fan	<ul style="list-style-type: none"> o Slightly lower wt. 	<ul style="list-style-type: none"> o Higher maintenance 	✓
	Shaft fan/internal combustion engine	<ul style="list-style-type: none"> o Simple operation o High reliability o Low maintenance 	<ul style="list-style-type: none"> o Slightly higher wt. 	✓
Platform Sizing	Single vehicle	<ul style="list-style-type: none"> o Simple o Lightweight o Low cost o Simple launch sequence 	<ul style="list-style-type: none"> o Larger number of platforms required 	✓

TABLE 24
 AIR CUSHION LAUNCH PLATFORM TRADE STUDY RESULTS (cont'd.)

Function	Method of Implementation	Advantages	Disadvantages	Influence Factor
				+ -
	Multiple vehicle	<ul style="list-style-type: none"> o Fewer number of platforms required 	<ul style="list-style-type: none"> o Complex o Heavy o Complex launch sequence o High risk to vehicles o Thrust engine required o Control system required 	✓

Contrails

Two ports exist in the fuselage, which are covered by the doors when they are up and locked. One port is used to provide clearance for the door mounted relief valve when the door is closed. The second larger port is the air inlet for the trunk fan.

When the air vehicle comes to a stop after landing and the engine is turned off, the trunk will collapse and the air vehicle will settle onto the deployed doors. Dolly wheels with pneumatic jacking actuators are then attached to hard points on the vehicle forward and aft of the trunk doors. Figure 118 shows details of the dolly wheels. The air vehicle is lifted off the ground and a jeep is used to tow it off the recovery field to an adjacent site where it is prepared for takeoff.

For takeoff the air vehicle is towed to the takeoff field on the dolly wheels. The ARPV engine is started, the trunk is inflated, and the dolly wheels are removed. For directional control during ground roll, the vehicle uses a vector thrust control system until it reaches a speed of 50 knots. Figure 121 show details of a vector thrust control system from Reference 10. At speeds greater than 50 knots the flight control surfaces can effectively guide the vehicle.

After rotation and initial climb, the fan is shut off and the trunk deflates to its original position, clinging tightly to the trunk doors. The extension cells deflate and the motor/reel assembly winds in the cables attached to the trunk door until the door lock mechanism is latched.

A large fan is required to satisfy the large air flow requirements for lubrication during takeoff ground roll. The power available to drive the fan is marginal. The fan size is indicated on Figure 120. However, a component of this size would have great impact on the structure in the area of its installation. Note the structure has not been resized to accommodate the fan.

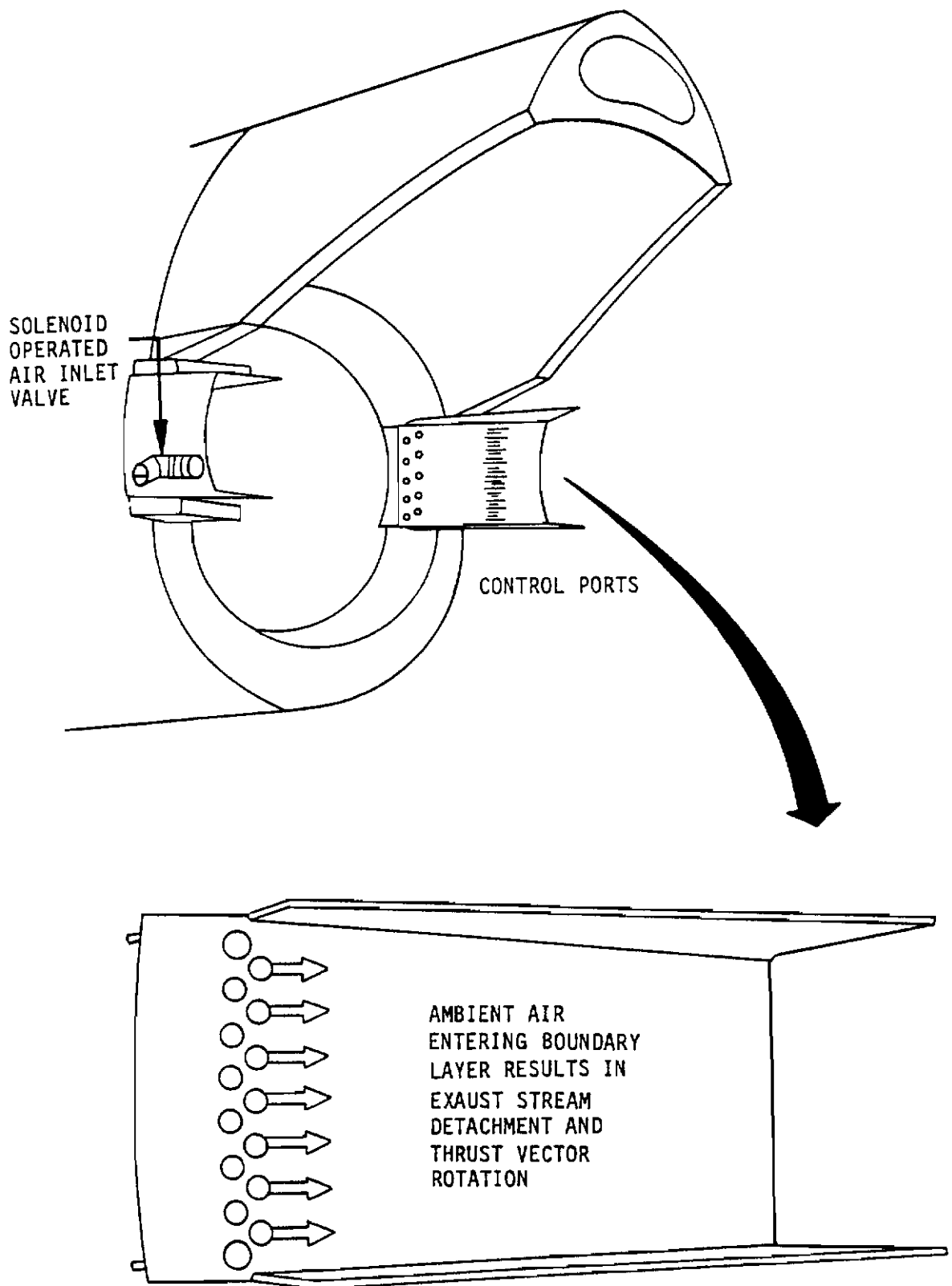


Figure 121 Thrust Vector Control System Concept

Contrails

Table 25 shows the aircraft installed equipment list, which details the modifications made to the Rockwell baseline to obtain the IACS configuration. Table 26 shows the results of the weight analysis for the modifications. This IACS configuration weighs 115 pounds more than the baseline.

As with the ACRS configuration, the removal of the landing gear and its fairings reduced the drag by 1.1%. The runway dimensions required for the recovery of the Rockwell IACS air vehicle are 200 feet by 100 feet. The dimensions required for launch are 2200 feet by 150 feet.

TABLE 25

AIRCRAFT INSTALLED EQUIPMENT FOR ROCKWELL ARPV WITH IACS

<u>Component Description</u>	<u>Quantity</u>	<u>Material</u>	<u>Incremental Impact</u>
Air Cushion Trunk	1	Polyurethane/ Dacron	+
Landing Gear and Fairings			-
Shaft-Driven Fan + High Speed Drive Train Shafting + Clutch	1	Steel	+
Relief Valve	1	A1	+
Hinged Trunk Doors and Attachment Fittings	2	A1	+
Air Cushion Trunk Storage Module with Fasteners	1	A1	+
Trunk Door Retraction System with Cables, Electric Motors and Reels	2		+
Low Pressure Ducting with Fittings	2	A1	+
Trunk Door Extension Cells	2	Rubber	+
Engine Modification Valving for Vector Thrust Control System			+

TABLE 26
ROCKWELL IACS WEIGHT ANALYSIS

<u>Component</u>	<u>Δ Weight (lbs)</u>
Removal of:	
Conventional Landing Gear	-186
Landing Gear Fairings	- 20
Landing Gear Hard Structure	- 42
Addition of:	
Air Cushion Trunk	+131
Trunk Doors & Fasteners + Inflation System	+232
Overall Δ Weight	+115

SECTION IV PERFORMANCE/COST ANALYSIS

A performance and cost analysis was made for each of the preliminary design configurations using results of the dynamic analysis and design studies as well as other advantages and disadvantages identified for each configuration. The cost and performance factors were evaluated with respect to the baseline Rockwell ARPV. A review of the baseline system was included so that the delta cost and performance factors were based on common assumption.

The following factors were included in this study but only to the extent that they effect or are affected by the launch/recovery systems.

- o Complexity
- o Fuel requirements
- o Adverse weather capability
- o Ground equipment and facilities
- o Survivability/vulnerability levels
- o Reliability and maintainability
- o System acquisition and life cycle costs

1. ANALYSIS

a. Complexity

The approach followed in evaluating the complexity of each launch/recovery system was to develop increments from the Rockwell baseline system. The baseline system with landing gear was assigned a complexity factor of 1.0.

The following factors were evaluated with respect to each launch/recovery system:

- o aircraft installed equipment
- o ground site equipment
- o extent-of-development effort
- o recovery control system, e.g., autoland system

The overall system complexity factor is the product of the four factors. The basis of the aircraft installed equipment complexity factor is the

number of installed components (line replaceable units, LRU) for the launch/recovery system.

The other three complexity factors developed are more subjective. The ground site equipment complexity factor is based on the number and types of ground equipment required. The extent of development complexity factor is a function of the magnitude of potential problems foreseen in implementing the system. The number of unproven techniques and components to be used in the system affects this factor. The recovery control system complexity factor is based on the sophistication of autoland system required. This is largely a function of whether the vehicle is stopped by an arrestment system or suction braking. The autoland guidance system must be more precise for launch/recovery systems using arrestment in order to ensure hook engagement.

Table 27 shows the results of the complexity analysis. The Boeing ACRS configuration was determined to be the least complex launch/recovery system.

The landing gear of the Rockwell baseline system was examined and found to have 13 LRU. This value was assigned an aircraft installed equipment complexity factor of 1.0, and the five ACLS configurations were compared to it. The air cushion landing systems for the Rockwell configurations (Rockwell ACRS and Rockwell IACS) were found to have 15 and 17 LRU, respectively.

The air cushion landing systems for the Boeing configurations (Boeing ABSS with cool gas generator, Boeing ABSS with bleed air, and Boeing ACRS) were found to have 11, 11, and 9 LRU, respectively. Aircraft installed equipment complexity factors were assigned on the basis of number of LRU and are shown in Table 27.

The ground site equipment for launch/recovery of the Rockwell baseline vehicle was found to consist of tow vehicles for transportation to the launch site and from the recovery area, a nosewheel trough for launch, and arresting gear for recovery. This system was given a ground site equipment complexity factor of 1.0.

TABLE 27
RESULTS OF COMPLEXITY ANALYSIS

	Rockwell Baseline	R-ACRS + R-ACLP	R-IACS	B-ABSS with cool gas gen.	B-ABSS with bleed air	B-ACRS
Number of Aircraft Installed Components (LRU)	13	15	17	11	11	9
Aircraft Installed Equipment Complexity Factor	1.0	1.05	1.1	0.95	0.95	0.90
Ground Site Equipment Complexity Factor	1.0	1.3	1.0	1.05	1.05	0.95
Extent of Development Complexity Factor	1.0	1.5	1.3	1.1	1.1	1.15
Recovery Control System Complexity Factor	1.0	0.90	1.0	1.0	1.0	0.90
Overall System Complexity Factor	1.0	1.84	1.43	1.10	1.10	0.88

Contrails

The Rockwell ACRS launch/recovery system requires tow vehicles and dolly wheels for transportation to the launch site and from the recovery site, and an air cushion launch platform (ACLP) for takeoff. The ACLP includes a water twister and cable arrangement to stop the platform. A ground site equipment complexity factor of 1.3 was assigned to this system, largely due to the unproven ACLP. The Rockwell IACS launch/recovery system is similar to the Rockwell baseline. It requires tow vehicles and dolly wheels for transportation to the launch site and from the recovery area, and arresting gear for recovery. This system was awarded a ground site equipment complexity factor of 1.0, because of its similarity to the baseline.

The ground site equipment requirements for launch/recovery of the Boeing ABSS with cool gas generator and Boeing ABSS with bleed air configurations are identical. A tow vehicle is required to transport the ARPV to the launch site, and a tow vehicle plus dolly wheels are needed to move the vehicle from the recovery area. Additionally, a RATO and launcher are required for launch, and arresting gear is needed for recovery. This system was assigned a ground site equipment complexity factor of 1.05, the incremental increase due to the RATO and launcher. The Boeing ACRS launch/recovery system requires a tow vehicle to transport the ARPV to the launch site and a tow vehicle plus dolly wheels is needed to transport the vehicle from the recovery area. A RATO and launcher are used for launch. This system was assigned a complexity factor of 0.95. Its basic difference from the baseline is the addition of a RATO and launcher and the deletion of nosewheel trough and arresting gear.

The Rockwell baseline vehicle has an extent of development complexity factor of 1.0. The landing gear on the Rockwell ARPV consists of standard gear components, like wheels, tires, and struts, whose design and production are well-known. The development complexity factor for the ACLS configurations will be higher in each case, due to structural design and production details to be resolved.

The Rockwell ACRS configuration requires the development of an ACLP, and a satisfactory trunk door/extension cell arrangement. The extent of development complexity factor assigned is 1.5. The Rockwell IACS configuration requires the development of a trunk door/extension cell/motor-reel retraction scheme to both retract and open the trunk doors. The complexity factor for this development is 1.3.

The Boeing ABSS with cool gas generator and Boeing ABSS with bleed air configurations are similar. The development problems associated with these configurations are determining the optimum air bag module attachment schemes. The complexity factor for the development of these systems is 1.1. The major Boeing ACRS configuration development problems are in determining the optimum trunk module, but because the trunk module has more complex attachment requirements than the Boeing ABSS configurations the assigned complexity factor is 1.15.

The recovery control system of the Rockwell baseline ARPV must be sufficiently precise to ensure arrestor hook engagement. The autoland guidance system for this precision was assigned a complexity factor of 1.0. The recovery control systems of the Rockwell IACS, Boeing ABSS with cool gas generator, and Boeing ABSS with bleed air configurations also use an arrestment system for recovery. So the recovery control system complexity factor for these configurations is the same as the Rockwell baseline, i.e., 1.0. The Rockwell ACRS and Boeing ACRS configurations use suction braking and sliding friction to stop the vehicle. The autoland guidance system need not be as precise as the baseline because the ARPV is not required to touchdown at a particular location. The recovery control system complexity factor for these configurations is 0.9.

b. Fuel Requirements

The system descriptions developed in preliminary design yielded incremental fuel requirements for each launch/recovery system. The incremental fuel requirements were based on the fuel required for air cushion power and delta vehicle weight and volume (drag). The Breguet equation (shown below) was used to convert the incremental fuel requirements to delta mission range.

Contrails

Breguet Equation:
$$\text{Range} = \frac{V}{\text{SFC}} \left\{ \frac{L}{D} \right\} \ln_e \left\{ \frac{W_{\text{initial}}}{W_{\text{final}}} \right\}$$

V: Velocity

SFC: Specific Fuel Consumption

L: Lift

D: Drag

W: Weight

The Rockwell and Boeing ARPVs were designed for different missions, so the output of the analysis (delta mission range) for the Rockwell configurations must be related to the Rockwell baseline, and the Boeing configurations must be compared to the Boeing baseline vehicle.

The results of the fuel requirements analysis found the fuel for air cushion power to have negligible impact on the delta mission range. This is largely because the air cushion system is used for only a small portion of the total mission time. The factors which did impact the mission range were the delta vehicle weight and volume. The Breguet equation (shown above) was used to measure the impact. The results of the analysis are shown in Table 28.

The vehicle volumes of the Rockwell configurations (Rockwell ACRS and Rockwell IACS) are reduced from the baseline. The landing gear fairings were removed and the wetted area of the vehicle was reduced by 5.9 square feet. This modification reduced the vehicle drag and therefore increased the range. The wetted area of the baseline vehicle is 528.8 square feet. The Rockwell configurations also had a change of weight from the baseline. The Rockwell ACRS design weighs 31 pounds less than the baseline. The delta weight is due to the deletion of the tricycle landing gear and fairings, but is somewhat offset by the addition of trunk doors, trunk module, ejectors, ducting, and valves. The overall impact of the reduced weight and volume (i.e., drag) on delta range is an increase in mission range of 1.72%. The Rockwell IACS configuration weighs 115 pounds more than the baseline. The additional weight in the Rockwell IACS design over the Rockwell ACRS is due to the slightly larger trunk and trunk doors, the addition of an arresting hook, and, to a large

Table 28
RESULTS OF FUEL REQUIREMENTS ANALYSIS

<u>Configuration</u>	<u>Weight (lbs)</u>	<u>Drag (ft of wetted area)</u>	<u>Range (%)</u>
Rockwell Baseline	-	-	-
R-ACRS	- 31	-5.9	+1.72
R-IACS	+115	-5.9	-0.94
Boeing Baseline	-	-	-
B-ABSS with cool gas generator	+41	-	-1.84
B-ABSS with bleed air	+32	-	-1.34
B-ACRS	+16	-	-0.67

extent, to the huge shaft-driven fan needed to provide air flow requirements for takeoff. The overall impact of an increase in weight and decrease in drag on delta mission range is a decrease in range of 0.94%.

The Boeing configurations (Boeing ABSS with cool gas generator, Boeing ABSS with bleed air, and Boeing ACRS) did not have a change in vehicle volume from the Boeing baseline, so there was no impact on range due to drag. The significant change from the baseline was in vehicle weight. The Boeing ABSS with cool gas generator weighs 41 pounds more than the Boeing baseline. The impact of the increased weight is a decrease in range of 1.84%. The Boeing ABSS configuration with bleed air weighs 32 pounds more than the baseline. The impact of the increased weight is a reduction in mission range of 1.34%. The Boeing ACRS design weights 16 pounds more than the baseline. The increased weight results in a decrease in mission range of 0.67%. The additional weight for the Boeing configurations is due to larger air bag/trunk modules, ejectors for flow augmentation, ducting, and valving.

c. Adverse Weather Capability

The two major considerations in evaluating the adverse weather capability of the Rockwell baseline ARPV equipped with conventional tricycle landing gear, against the capability of the ACLS configuration are runway surface strength requirements and crosswind performance.

The Rockwell baseline vehicle is limited by surface conditions for both launch and recovery. For launch, the ARPV requires a ground roll distance of 2200 feet. Sufficient quantities of snow, mud, or water on the runway can foul the nose gear guide trough and prevent launch. For recovery, the ARPV is arrested in a distance of 200 feet. For this case also, excessive moisture can restrict the use of the runway surface.

Perhaps the most significant advantage of air cushion landing systems over conventional landing gear is their performance on low strength, unimproved surfaces. ACLS have demonstrated the capability for operation on snow, mud, and water so that runway surface conditions are not a limiting factor. Therefore, the ACLS configurations are superior to the baseline system.

The baseline vehicle is not disturbed appreciably by crosswinds while on the ground. During launch, a nosewheel trough provides directional stability until the vehicle reaches a speed of 50 knots and then the flight control surfaces can provide directional guidance. During landing impact and slideout, the arresting gear provide control. However, crosswinds do affect the baseline ARPV during landing approach. A crosswind approach may require the vehicle with conventional landing gear to perform a decrabbing maneuver at touchdown.

The ACLS configurations are more susceptible to the effects of crosswinds while on the ground than the baseline, because the air cushion will not produce a side force like that of a rolling tire. However, this is beneficial when landing in crosswinds at high crab angles. A discussion of the effect of wind on the various ACLS configurations follows.

Contrails

The Rockwell ACRS configuration uses an air cushion launch platform (ACLP) for launch. The ACLP developed uses a cable for directional guidance and also to arrest the platform. The cable provides excellent control in crosswinds. For recovery, the vehicle uses suction braking and ground slideout to stop. The vehicle speed at touchdown is 80 knots. During slideout at speeds greater than 50 knots, the flight control surfaces can maintain directional control. This coupled with residual engine thrust counteracts the effects of crosswind. The forward one-third of the trunk is lubricated to assist in this control scheme. However, when the ARPV slows to a speed of less than 50 knots, the flight control surfaces become ineffective and a crosswind may force it off course. Thus, a wider runway is required.

The Rockwell IACS configuration takes off in a conventional manner requiring a ground roll like the baseline vehicle. Instead of a nosewheel trough for low-speed guidance, the Rockwell IACS has a thrust vector control system to control its heading. The thrust vector system utilizes the Coanda effect. This type of system was proposed for use on the Jindivik ACLS aircraft, Reference 10. At ground roll speeds greater than 50 knots, the flight control surfaces are effective. For recovery, the ARPV uses an arrestment system which provides sufficient control in crosswind.

The Boeing ABSS launch/recovery systems (both with cool gas generator and with bleed air) have good performance in crosswind. For launch, a RATO and zero length launcher are used so crosswind has little effect on its performance. For recovery, the ARPV uses an arrestment system which provides sufficient control in crosswind.

The Boeing ACRS launch system also uses a RATO and launcher. The recovery system uses suction braking and ground slideout. During slideout the vehicle flight control surfaces and residual engine thrust can control its heading at higher speeds to counteract crosswind effects. The forward one-third of the trunk is lubricated for the purpose of assisting in directional control during slideout.

Vehicles with ACLS do not require a decrabbing maneuver at touchdown in a crosswind. Following touchdown, the vehicle remains in a crabbed attitude and the engine idle thrust provides a counteracting force to that of the crosswind.

d. Ground Equipment and Facility Requirements

The Rockwell baseline vehicle launch/recovery ground equipment and facility requirements were examined, along with these requirements of the five ACLS configurations. The requirements examined were launch/recovery site dimensions, and type of ground equipment for launch, recovery, transport, and maintenance.

The launch/recovery site dimensions for each configuration were determined in the dynamic analysis. They are shown in Table 29.

The types of ground equipment for launch, recovery, transport, and maintenance of ARPVs were determined. The steps required for the operations mentioned for each configuration are listed in Tables 30 through 35, for comparison.

e. Survivability/Vulnerability

Survivability/vulnerability factors were evaluated for each launch/recovery system. These factors included basic vehicle survival parameters (threat avoidance and vulnerability) plus related operational parameters (combat damage repairability and launch/recovery site vulnerability).

The threat avoidance capability of the aircraft is based primarily on two factors: detectability, and performance and maneuver.

For the Rockwell configurations, the modifications made do not affect the performance and maneuver factor determined for the baseline. However, the detectability of the Rockwell ACLS vehicles is incrementally reduced, because the landing gear and its fairings were removed, which will reduce both the presented area and the radar cross section area. Sufficient information was not available to calculate a specific delta. Presented area and radar cross section data were not presented in the Reference 2 report.

TABLE 29
LAUNCH AND RECOVERY SITE DIMENSIONS AND AREA

<u>Configuration</u>	<u>Site Dimensions (ft x ft)</u>		<u>Total Area (ft²)</u>
	<u>Launch</u>	<u>Recovery</u>	
Rockwell Baseline	2200 x 150	200 x 100	350,000
Rockwell ACRS	(Hard Surface) 2700 x 50	(Hard Surface) 1600 x 300	(Hard Surface) 615,000
Rockwell IACS	2200 x 150	200 x 100	350,000
Boeing ABSS with cool gas generator	Zero Length Launcher	300 x 100	30,000
Boeing ABSS with bleed air	Zero Length Launcher	300 x 100	30,000
Boeing ACRS	Zero Length Launcher	4500 x 200	900,000

TABLE 30

LAUNCH AND RECOVERY OPERATION SEQUENCE

Rockwell Baseline Vehicle

- Launch:
1. In maintenance area, tow bar is attached to ARPV.
 2. Tow vehicle tows ARPV to launch site, where nosewheel is placed in the launch trough.
 3. Tow bar and tow vehicle are disconnected from ARPV.
 4. ARPV taxis and takes off.
 5. Tow vehicle returns to maintenance area.
- Recovery:
1. On landing approach, the landing gear is deployed.
 2. Arresting hook is deployed.
 3. Arresting hook strikes arresting cable and ARPV rolls to a stop.
 4. Tow vehicle arrives at ARPV and disconnects arresting cable.
 5. Arresting cable rewinds itself.
 6. Tow bar is attached to ARPV.
 7. Tow vehicle tows ARPV to maintenance area.
- Maintenance:
1. Landing gear (tires, brakes, oleo) is inspected.
 2. Arresting hook is latched into position.

TABLE 31

LAUNCH AND RECOVERY OPERATION SEQUENCE

R-ACRS (Rockwell Air Cushion Recovery System)

- Launch:
1. In maintenance area, four pneumatic dolly wheels are attached to ARPV.
 2. Tow vehicle tows ARPV onto air cushion launch platform (ACLP).
 3. ARPV is attached and supported at three points on ACLP.
 4. Dolly wheels and tow vehicle are disconnected from ARPV.
 5. ACLP fan is started and inflates the air cushion trunk.
 6. ACLP cable guide is attached to cable.
 7. ARPV engine is started and propels the ACLP along the cable until takeoff velocity is achieved.
 8. ARPV is rotated and released from ACLP.
 9. ACLP reaches the end of the cable and water twister brings it to a stop.
 10. Tow vehicle arrives at ACLP and disconnects arresting cable.
 11. Arresting cable rewinds itself.
 12. Tow vehicle tows ACLP back to launch origin.
 13. ACLP fan is stopped and ACLP settles to the ground.
 14. Tow vehicle with dolly wheels returns to maintenance area.
- Recovery:
1. On landing approach, engine bleed air is turned on, and air supply system inflates and deploys air cushion trunk.
 2. Trunk strikes the ground and slides out, until it is stopped by friction and suction braking.
 3. Tow vehicle arrives at ARPV and attaches four pneumatic dolly wheels.
 4. Tow vehicle tows ARPV to maintenance area.
- Maintenance:
1. Air cushion trunk module is removed and replaced with a repacked module.
 2. Module removed is inspected and repacked.
 3. Compressed gas bottles on the eight dolly wheels are replaced.

TABLE 32

LAUNCH AND RECOVERY OPERATION SEQUENCE

R-IACS (Rockwell Integrated Air Cushion System)

- Launch:
1. In maintenance area, four pneumatic dolly wheels are attached to ARPV.
 2. Tow vehicle tows ARPV to launch site.
 3. Dolly wheels are disconnected from ARPV.
 4. ARPV ending is started and engine bleed air (via air supply system) inflates the elastic air cushion trunk.
 5. ARPV taxis and takes off.
 6. Tow vehicle with dolly wheels returns to maintenance area.
- Recovery:
1. On landing approach, engine bleed air is turned on and air supply system inflates and deploys elastic air cushion trunk.
 2. Arresting hook is deployed.
 3. Arresting hook strikes arresting cable and ARPV slides to a stop.
 4. Tow vehicle arrives at ARPV and disconnects arresting cable.
 5. Arresting cable rewinds itself.
 6. Four pneumatic dolly wheels are attached to ARPV.
 7. Tow vehicle tows ARPV to maintenance area.
- Maintenance:
1. Air cushion is inspected.
 2. Arresting hook is latched into position.
 3. Compressed gas bottles on the eight dolly wheels are replaced.

TABLE 33

LAUNCH AND RECOVERY OPERATION SEQUENCE

Boeing Air Bag Skid System With Cool Gas Generator

- Launch:
1. In maintenance area, dolly wheels are attached to ARPV.
 2. RATO is installed to ARPV.
 3. Tow bar is attached.
 4. Tow vehicle tows ARPV to launch site and onto launcher.
 5. Tow bar and dolly wheels are disconnected.
 6. ARPV is launched.
 7. Tow vehicle returns to maintenance area.
- Recovery:
1. On landing approach, cool gas generator is initiated, and air supply system inflates and deploys the air bag skids.
 2. Arresting hook is deployed.
 3. Arresting hook strikes arresting cable and ARPV slides to a stop.
 4. Tow vehicle arrives at ARPV and disconnects arresting cable.
 5. Arresting cable rewinds itself.
 6. Four pneumatic dolly wheels are attached to ARPV.
 7. Tow vehicle tows ARPV to maintenance area.
- Maintenance:
1. Air bag skid module is removed and replaced with a repacked module.
 2. Module removed is inspected and repacked.
 3. Cool gas generator is replaced.
 4. Arresting hook is latched into position.
 5. Compressed gas bottles on the four dolly wheels are replaced.

TABLE 34

LAUNCH AND RECOVERY OPERATION SEQUENCE

Boeing Air Bag Skid System With Bleed Air

- Launch:
1. In maintenance area, dolly wheels are attached to the vehicle to ARPV.
 2. RATO is installed to ARPV.
 3. Tow bar is attached.
 4. Tow vehicle tows ARPV to launch site and onto launcher.
 5. Tow bar and dolly wheels are disconnected.
 6. ARPV is launched.
 7. Tow vehicle returns to maintenance area.
- Recovery:
1. On landing approach, engine bleed air is initiated, and air supply system inflates and deploys the air bag skids.
 2. Arresting hook is deployed.
 3. Arresting hook strikes arresting cable and ARPV slides to a stop.
 4. Tow vehicle arrives at ARPV and disconnects arresting cable.
 5. Arresting cable rewinds itself.
 6. Four pneumatic dolly wheels are attached to ARPV.
 7. Tow vehicle tows ARPV to maintenance area.
- Maintenance:
1. Air bag skid module is removed and replaced with a repacked module.
 2. Module removed is inspected and repacked.
 3. Arresting hook is latched into position.
 4. Compressed gas bottles on the four dolly wheels are replaced.

TABLE 35

LAUNCH AND RECOVERY OPERATION SEQUENCE

B-ACRS (Boeing Air Cushion Recovery System)

- Launch:
1. In maintenance area, dolly wheels are attached to ARPV.
 2. RATO is attached to ARPV.
 3. Tow bar is attached to ARPV.
 4. Tow vehicle tows ARPV to launch site and onto launcher.
 5. Tow bar and tow vehicle are disconnected.
 6. ARPV is launched.
 7. Tow vehicle returns to maintenance area.
- Recovery:
1. On landing approach, engine bleed air is turned on, and air supply system inflates and deploys air cushion trunk.
 2. Trunk strikes the ground and slides out, until it is stopped by friction and suction braking.
 3. Tow vehicle arrives at ARPV and attached four pneumatic dolly wheels.
 4. Tow vehicle tows ARPV to maintenance area.
- Maintenance:
1. Air cushion trunk module is removed and replaced with a repacked module.
 2. Module removed is inspected and repacked.
 3. Compressed gas bottles on the four dolly wheels are replaced.

For the Boeing ACLS designs, the modifications made do not impact the threat avoidance factor, and so it is unchanged from the baseline.

The major vulnerability consideration was the investigation of the shielding provided by the air cushion landing system. Specifically, to investigate whether the air bag or trunk modules attached to the underside of the vehicle would provide protection from potential threats. Also to determine whether judicious location of components would provide shielding of critical air vehicle components. The results of the investigation revealed that the ACLS trunk module does not offer significant resistance against the 12.7 mm API (armor piercing incendiary) or 23 mm HEI (high explosive incendiary) projectiles. Functional requirements and the limited space available on the ARPVs created little choice for location of ACLS components. Therefore, the judicious location of components for shielding of critical components was not a significant factor.

The combat damage repairability operational parameter was assessed. The landing gear of the Rockwell baseline ARPV was determined to require more repair if damaged than the air cushion launch/recovery systems. The ACLS components are less complex and more readily replaceable than the components of a landing gear system.

The vulnerability of the ARPV launch/recovery site is directly proportional to the site area. The launch/recovery systems were evaluated using a comparison parameter of square feet of prepared real estate. These areas are shown in Table 29.

f. Reliability and Maintainability

The reliability and maintainability studies performed on the Rockwell and Boeing baseline systems in the original contract studies evaluated reliability in terms of mean cycles between failure (MCBF) and mean time between failure (MTBF), and maintainability in terms of maintenance manhours per flight hour (MMH/FH). The results of the R&M studies were used to determine the operating and support costs of the baseline systems.

A reliability and maintainability evaluation was performed for each launch/recovery system developed in the preliminary design work. The impact

of each configuration on the reliability, maintainability, and operating and support costs of the baseline systems was assessed. The results of the evaluations are shown in Table 36.

The Rockwell air cushion recovery system (Rockwell ACRS) which uses an air cushion launch platform (ACLP) for takeoff was examined. The deletion of the retractable landing gear and arresting hook, and replacing them with a bleed air inflated air cushion trunk for landing improves the reliability and maintainability of the ARPV. However, the addition of the air cushion launch platform (ACLP), ground cable and water twister will add maintenance and reduce total system reliability.

The deletion of the landing gear from the Rockwell ARPV with IACS has a positive impact on airframe MTBF which is somewhat offset by the addition of the air cushion trunk and the trunk inflation system. The addition of the dolly wheel system will have a slight negative impact on reliability. The maintainability will be degraded by the air cushion trunk and its extension cells which have to be refurbished after each flight and the replacement of dolly wheel gas bottles.

The reliability and maintainability of the Boeing air bag skid system with cool gas generator was assessed relative to the Boeing baseline vehicle. The larger air bag skids should provide greater stability and support of the ARPV during landing impact and slideout, resulting in a small increase in reliability and a corresponding decrease in maintenance requirements for airframe repair.

The deletion of the cool gas generator and the use of engine bleed air for air bag skid inflation combined with the use of the larger air bag skids produces an increase in reliability and a significant improvement effect on maintainability due to reduced airframe maintenance through use of the larger skids and elimination of the cool gas generators replacement task after each landing. The elimination of consumption of cool gas generators will reduce spares cost and maintenance time.

TABLE 36
RESULTS OF RELIABILITY AND MAINTAINABILITY ANALYSIS

Configuration	Δ R	Δ M	Δ O&S Cost
R-ACRS/R-ACLP	Replace Recovery/Arresting System MTBF of 200 Hr with an Air Cushion Trunk System with an MTBF of 490 Hour. Revise Propulsion System MTBF from 625 hr to 600 hr. Add ACLP System with MTBF of 50 hr. Add Dolly Wheel System with MTBF of 1800 hr.	Increase system MMH/FH by 20% to cover changes to ARPV plus addition of ACLP maintenance and turnaround.	+10%
R-IACS	Revise Landing Gear/Arresting System MTBF from 200 to 250 Hr. Add Air Cushion Trunk System with MTBF of 490 Hr. Add Dolly Wheel System with MTBF of 1800 hr.	Increase system MMH/FH by 10%. + 5%	+ 5%
B-ABSS (cool gas generator)	10% improvement in Pneumatic Skid System MCBF.	10% reduction in Airframe MMH/FH.	- 1%
B-ABSS (with bleed air)	30% improvement in Pneumatic Skid System MCBF.	10% reduction in Airframe MMH/FH.	- 4%
B-ACRS	10% reduction in Pneumatic Skid System MCBF. Delete Arresting System MCBF from calculations.	10% reduction in Airframe MMH/FH. 20% reduction in Postflight MMH/FH. Delete Arresting System MMH/FH.	- 8%

The reliability and maintainability of the Boeing air cushion recovery system (Boeing ACRS) was examined relative to the Boeing baseline vehicle. The incorporation of the air cushion trunk in lieu of air bag skids increases the surface exposed to damage during ground slideout and will increase trunk damage even with heavier treads. This was weighed against the savings associated with deleting the arresting system.

g. System Acquisition and Life Cycle Costs

The acquisition costs were determined from component sizes, weights, and numbers and ground equipment and facilities from the preliminary design work. Development costs were estimated using complexity factors.

Current life cycle cost (LCC) estimates for the baseline Rockwell and Boeing ARPVs were made to establish points of departure for calculating the LCC impact of trades made in this study. Each was separately estimated. Site preparation was included under support investment and site upkeep was included in operations and support.

The baseline LCC estimates reflect the particular design features and support requirements of the two baseline systems. Development, production, and support investment costs were estimated using standard techniques based on Boeing cost history, vendor quotes, and identification of analogous systems and their costs. Operations and support costs were estimated using the Air Force CACE Model from AFR 173-10. In the case of the Boeing ARPV the LCC consisted mainly of updating the prior LCC estimate. The primary objective in estimating the Rockwell ARPV LCC was to make the estimating criteria comparable to the Boeing ARPV LCC estimate.

The results of the LCC analysis is shown in Table 37. All costs are in FY 1977 dollars.

TABLE 37
SYSTEM ACQUISITION AND LIFE CYCLE COSTS

QUANTITY -A/C	ROCKWELL ARPV (1977 DOLLARS IN MILLIONS)		BASELINE AND DERIVATIVE BOEING ARPV (1977 DOLLARS IN MILLIONS)											
	900	900	900	ROCKWELL ACRS	900	BOEING BASELINE ARPV	900	BOEING ABSS COOL GAS GEN.	900	BOEING ABSS BLEED AIR	900	BOEING ACRS AIR CUSHION		
ORIGINAL BASELINE	900	NEW BASELINE	900	ROCKWELL ACRS	900	ROCKWELL TACS	900	BOEING BASELINE ARPV	900	BOEING ABSS COOL GAS GEN.	900	BOEING ABSS BLEED AIR	900	BOEING ACRS AIR CUSHION
	\$ 36.430	\$ 36.430	\$ 34.939	\$ 34.939	\$ 35.740		\$ 45.922	\$ 46.036	\$ 45.979	\$ 46.005		\$ 45.979	\$ 46.005	
AIRFRAME														
ENGINES	3.288	3.288	3.288	3.288	3.788		17.212	17.212	17.298	17.298		17.298	17.298	
AVIONICS	26.133	26.133	26.133	26.133	26.133		19.030	19.030	19.030	19.030		19.030	19.030	
OTHER	55.718	55.718	53.422	53.422	54.646		29.758	29.832	29.795	29.795		29.795	29.472	
SUB TOTAL	\$ 121.569	\$ 121.569	\$ 117.782	\$ 117.782	\$ 120.307		\$ 111.922	\$ 112.110	\$ 112.102	\$ 112.102		\$ 112.102	\$ 111.805	
PRODUCTION														
AIRFRAME	\$ 129.075	\$ 129.075	\$ 123.791	\$ 123.791	\$ 126.649		\$ 100.228	\$ 101.803	\$ 100.424	\$ 100.424		\$ 100.424	\$ 100.275	
ENGINES	61.985	61.985	61.985	61.985	62.525		17.073	17.073	17.298	17.298		17.298	17.298	
AVIONICS	157.073	157.073	157.073	157.073	157.073		92.460	92.460	92.460	92.460		92.460	92.460	
SUB TOTAL	\$ 348.133	\$ 348.133	\$ 342.849	\$ 342.849	\$ 346.247		\$ 209.761	\$ 211.336	\$ 210.182	\$ 210.182		\$ 210.182	\$ 210.033	
SUPPORT INVESTMENT														
INITIAL SPARES	\$ 40.101	\$ 40.101	\$ 39.492	\$ 39.492	\$ 39.888		\$ 46.397	\$ 46.764	\$ 44.950	\$ 44.883		\$ 44.950	\$ 44.883	
SUPPORT EQUIPMENT	88.674	88.674	69.941	69.941	70.634		42.799	42.799	42.722	41.077		42.722	41.077	
SITE PREPARATION	3.472	3.472	6.285	6.285	6.130		6.415	6.415	6.415	8.225		6.415	8.225	
SUB TOTAL	\$ 132.247	\$ 132.247	\$ 115.718	\$ 115.718	\$ 116.652		\$ 95.611	\$ 95.978	\$ 94.087	\$ 94.185		\$ 94.087	\$ 94.185	
OPERATING & SUPPORT	\$ 301.547	\$ 196.965	\$ 216.662	\$ 216.662	\$ 206.813		\$ 176.650	\$ 174.735	\$ 169.584	\$ 162.518		\$ 169.584	\$ 162.518	
ATTRITION/REPLACEMENT A/C COST	\$ 240.557	\$ 240.557	\$ 236.909	\$ 236.909	\$ 239.257		\$ 204.939	\$ 206.514	\$ 205.135	\$ 204.986		\$ 205.135	\$ 204.986	
TRANSPORTATION & DEPLOYMENT COST	\$ 2.112	\$ 2.112	\$ 4.113	\$ 4.113	\$ 4.113		\$ 4.839	\$ 4.839	\$ 4.839	\$ 4.839		\$ 4.839	\$ 4.839	
TOTAL LIFE CYCLE COSTS	\$ 1,146,165	\$ 1,041,583	\$ 1,034,033	\$ 1,034,033	\$ 1,033,389	5	\$ 803,722	\$ 805,512	\$ 795,929	\$ 788,366		\$ 795,929	\$ 788,366	
DELTA COST	0	0	\$ -7,550	\$ -7,550	\$ -7,194		0	\$ +1,790	\$ -7,793	\$ -15,356		\$ -7,793	\$ -15,356	

△ SOME OF THE SITE PREPARATION COSTS ARE INCLUDED IN SUPPORT EQUIPMENT

SECTION V CONCLUSIONS

1. Air bag skid or air cushion recovery systems can be adapted to multimission type remotely piloted vehicles such as the Boeing and Rockwell ARPV concepts. The vehicles remain stable in flight with deployment of the recovery system, although a stability augmentation system may be required.
2. Air bag skid and air cushion recovery systems on these vehicles induce high incremental loads at touchdown. These loads are due to the high approach speed and the high pitch rate induced by the recovery system trunk with touchdown at high angles of attack. These high loads impose severe wing structure weight penalty on aircraft such as the Rockwell ARPV where stores are carried on the wing. Conversely, vehicles such as the Boeing ARPV with short, small wings can tolerate landing load factors to 8 or 10g with little penalty to the structure so impact load is not a detrimental constraint.
3. The induced loads at touchdown appear to be higher with a one trunk integrated air cushion system than with an air cushion recovery system because the trunk for the former is sized for takeoff gross weight of the air vehicle. The extent of the difference could not be verified. Because of limitations of the EASY model, the integrated air cushion system was not optimized during the dynamic analysis.
4. An RPV with an air bag skid recovery system requires arrestment by hook and cable for stability during slideout. Arrestment tends to increase the peak touchdown loads. However, the vehicle remains stable in the first few seconds after touchdown so arrestor engagement can be delayed until after touchdown.
5. An air cushion recovery system with suction braking is the simplest and lowest cost recovery approach for these RPVs. The overall cost

Contrails

of the arrestor system required for the air bag skid system is greater than the additional cost of the more complex air cushion system plus the cost of the additional runway required for recovery. However, if available site space is a critical factor, the air bag skid system with arrestment is superior.

6. Stopping capability of an integrated air cushion system on a wet runway is poor. Resultant runway length requirements are excessive for vehicles with approach speeds above 100 knots. Therefore, arrestment is required with this system.
7. The power available from the RPV engine is marginal in meeting the air flow requirements for an integrated air cushion system. The requirements are met with the Rockwell vehicle by using the limited duration, overload power extraction capability of the engine accessory drive.
8. An air vehicle such as the Rockwell ARPV that was designed with conventional landing gear, does not lend itself well to adapting an air cushion system. A weight and volume penalty is incurred when fitting a trunk to a narrow, rounded fuselage.
9. RATO/launcher appears to be a least complex, low cost method of launch. However, results of the air cushion launch platform study were not conclusive so it too may be a favorable means of launch. A simple, lightweight platform appears to be the best approach.
10. Air cushion or air bag skid systems offered little change in air vehicle survivability/vulnerability from that of conventional landing gear. However, oversizing of the gas supply system to overcome some trunk leakage is required.
11. Difference in fuel requirements between the air vehicles with air cushion or air bag skid systems and the conventional landing gear configuration are reflected in the differences in vehicle weight. The weight differences, in this case, are misleading because of the penalty incurred in installing the systems on a non-optimized vehicle.

Contrails

12. Adverse weather capability differences between conventional landing gear and air cushion or air bag skid systems are largely related to runway surface conditions. A vehicle with conventional landing gear is more limited by surface water, mud, slush, ice and snow. A requirement for decrabbing in crosswind landings may also be a restriction with conventional gear.

13. Tow vehicles for movement of vehicles on the ground appears to be the simplest, most reliable method. Therefore, ground equipment differences were largely between those systems requiring arrestment and those relying on ground friction. Overall facility costs were lower for vehicles with an effective suction braking system than for those with arrestment. The vehicle with landing gear also requires a prepared surface or landing mats.

SECTION VI RECOMMENDATIONS

1. The high speed aspects of recovery of RPVs with an air cushion system requires further investigation. Integration of the air cushion system with the air vehicle design is required to determine overall system performance.
2. The relationship between lubrication flow and sliding friction should be better defined, based on experiment.
3. Further development of the program EASY elastic trunk model is necessary to make it an effective preliminary design tool.
4. Expansion of the air bag skid program EASY model should be done to include the capability for analysis of trunk shapes other than circular cross section.
5. The results of this study show that RPV recovery is a feasible application for air cushion technology. This study, however, was directed at integration of the recovery system into an existing airframe design. This approach leads to a non optimized system. Also, a wide variety of configurations were investigated so that sufficient depth of analysis was not made on any one concept. Therefore, it is recommended that a thorough study be made of an air cushion system integrated into a mission optimized air vehicle. This study should include dynamic simulation and performance analysis.

REFERENCES

1. Advanced RPV System Trade Study Reports, D180-18906-1, The Boeing Company, February 17, 1976.
2. ARPV System/Subsystem Summary Report, C76-1331/034C, Rockwell International Corporation, April 25, 1976.
3. Wahi, M. K., et al, EASY-ACLS Dynamic Analysis, Preliminary Draft, Boeing Aerospace Company, June 1978.
4. USAF Stability and Control DATCOM, McDonnell Douglas Corporation, April 1978.
5. MIL-A-8863A, Airplane Strength and Rigidity Ground Loads for Navy Procured Airplanes, July 12, 1974.
6. Vaughan, J. C., et al, "Laboratory Tests of Air Cushion Recovery System for the Jindivik Aircraft", AFFDL-TR-74-64, April 1974.
7. Kunstadt, Ernest, "Study of Reverse Flow Characteristics of a Tip Fan and an Ejector", AFFDL-TR-73-73, AD 770080, October 1973.
8. Propulsion Simulation Equipment for Wind Tunnel Testing, Product Catalog, Tech Development, Inc.
9. 1979 Independent Research and Development Program, D1-8269-2, Page 2-734, Boeing Aerospace Company, March 1979.
10. Lloyd, A. J. P., et al, "Integration of Air Cushion Landing System Technology Into the Jindivik Remotely Piloted Vehicle", AFFDL-TR-77-21, Boeing Aerospace Company, March 1978.